

https://dspace.org/

An analysis of the physiological mechanisms for the uptake, accumulation and excretion of gold by Tamarix usneoides E. Mey ex. Bunge

Wilson, Hayden Thorburn

2020
https://hdl.handle.net/10539/32001

Downloaded from a DSpace repository. https://dspace.org/

An analysis of the physiological mechanisms for the uptake, accumulation and excretion of gold by *Tamarix usneoides* E. Mey ex. Bunge.

Hayden Thorburn Wilson

Degree of Doctor of Philosophy:

A thesis submitted to the Faculty of Science, University of the Witwatersrand, Johannesburg, in fulfilment of the requirements for the degree Doctor of Philosophy.

25 October 2019 Johannesburg

Declaration

I declare that this thesis is my own, unaided work. It is being submitted for the Degree of Doctor of Philosophy at the University of the Witwatersrand, Johannesburg. It has not been submitted before for any degree or examination at any other University.



_____

(Signature of candidate)

25th day of October 2019 at 9.30 AM

Abstract

Tamarix usneoides E. Mey ex Bunge is an exo-rectretohalophyte riparian tree species that is endemic to arid to semi-arid regions in southern Africa. There has been considerable interest in the genus *Tamarix* for its potential for use in erosion control and on environmental rehabilitation sites as it is capable of tolerating a wide range of environmental conditions including fire, varying temperature ranges, saline water, extreme pH and elevated metal salts. The species hyper-accumulates some chloride and sulphate salts and a range of elements have been documented at elevated concentrations in its tissues. This species, as well as *T. usneoides* X *ramosissima* hybrids have been planted on gold bearing tailings storage facilities as well as sites contaminated with gold tailings on the Witwatersrand Highveld in order to provide dust control measures and phyto-stabilise the tailings facilities. Prior studies have detected trace quantities of gold in the foliar tissue of *T. usneoides* and there is interest in the accumulation of gold within the foliar tissue of *T. usneoides*, as the species is used in phytoremediation of areas contaminated by mining and recovery of gold from contaminated areas could potentially offset the remediation costs. This study aimed to investigate the physiological processes that allow *T. usneoides* to accumulate gold and other elements within the various tissues of the plant and determine the potential for its use in the recovery of gold from contaminated sites. This was achieved in four separate studies, each of which explored a different aspect of the process of the accumulation of gold and other elements. The *in vitro* chapter investigated how variables such as gold chemical form, concentration and rhizosphere pH could potentially affect uptake in *Tamarix* plantlets grown in a liquid media that was dosed with different gold compounds at a range of concentrations and pHs. The *in-situ* study used plants grown on a gold tailings storage facility in order to localise elemental accumulation within specific tissues as well as to identify how rhizosphere elemental concentrations affect elemental uptake, translocation and accumulation. A microstructural analysis of the salt glands was performed in order to elucidate possible excretion mechanisms for metal salts. An elemental mapping exercise was performed on *in vitro* material that exhibited the highest gold accumulation values in order to detect which tissues are involved in gold accumulation and relate those findings to the behaviour of other detected elements.

The findings showed that *T. usneoides* is capable of accumulating gold *in vitro* and that the media pH and gold concentration as well as gold chemical form did affect uptake. The highest concentration of gold in the root tissue was associated with gold chloride trials and the highest concentration in shoot tissue was associated with gold potassium cyanide trials. pH of the growth medium did not affect cutting growth, nor did it affect gold uptake into roots but it did affect gold uptake into shoots, where a lower pH limited gold bioconcentration. In contrast, 5-year old trees grown *in-situ* on a gold and uranium tailings storage facility showed very low gold concentrations within root, stem or leaf tissue. It is likely that this was due to relatively low gold concentrations in the tailings and low gold bio-availability due to the site-specific geochemical characteristics. The *in-situ* study demonstrated that *T. usneoides* regulates elemental concentrations in tissue, with a number of elements remaining bound to the root epidermis and root cortex tissue, while elements that are accumulated are transported to leaf tissue and do not remain bound in the woody biomass. Additionally, an

ameliorative effect was observed where tailings samples collected from locations with no trees had a lower pH than areas with trees, suggesting that *T. usneoides* regulates the conditions of the rhizosphere, which also affects elemental mobility. Studies into the microstructure of the salt glands of the species showed a number of structural adaptations that allowed for the rapid excretion of solutes from the plant. These included adaptations to keep those solutes isolated from the surrounding tissue by transporting them in micro-vesicles and complexing them with polyphenolic compounds. Tissue elemental mapping using wavelength-dispersive spectroscopy illustrated that accumulated elements are partitioned, with chlorine being ubiquitous within tissue while elements such as sodium, calcium and sulphur accumulate within specific cells within the stem mesophyll tissue as well as within the cells containing flocculated polyphenolic compounds. Elemental mapping for gold showed that it followed a similar trend as the accumulation of other lighter elements, albeit at a significantly lower concentration.

The findings of this study show that while *T. usneoides* is capable of accumulating gold when it is supplied in a form that is bioavailable for uptake, site geochemical characteristics will determine the applicability of the species for the recovery of gold from those areas. Thus, the interaction between *T. usneoides* and the rhizosphere of sites with differing geochemical characteristics warrant additional study. Further studies should also investigate potential ways of increasing gold bioavailability through soil amelioration. The ultrastructural studies and tissue elemental mapping show that *T. usneoides* can tolerate the elevated solute concentrations within its tissues through a variety of different means, providing insight into the potential mechanisms utilised by other recretohalophyte species to maintain tissue homeostasis.

To my high school biology teacher, Mrs Christine Almeida. She gave me the confidence to question the world.

Acknowledgements

First and foremost, I would like to thank Professor David Mycock. Without his tireless support and endless patience and wisdom this work would never have been completed. I would also like to thank Ms Isabel Weiersbye for conceptualising the initial parts of this study, sourcing funding, wrangling work forces to assist with field work and providing a significant amount of support in the forms of elemental analysis and sample preparation protocols as well as providing laboratory space to work, store and analyse samples. I would also like to thank Professor Alexander Ziegler for providing training and use of the analytical equipment at the University of the Witwatersrand Microscopy and Microanalysis unit and Mr Jacques Gerber and Dr Deran Reddy for their assistance, advice and good humour when dealing with recalcitrant materials and students. I also must extend my gratitude to the technicians Bruce McLeroth (Red Earth), Innocent Rabohale and Rose Poultney (University of the Witwatersrand Ecological Engineering and Phytoremediation Program) and Riana Rossouw of CAF Stellenbosch for their assistance in substrate sampling and sample elemental analyses.

Finally, I would like to thank my wife Miranda Wilson for her tireless support, patience and optimism.

This study was financially supported by the Ecological Engineering and Phytotechnology Programme (EEPP) at the University of the Witwatersrand; the Department of Trade and Industry and National Research Foundation of South Africa's Technology for Human Resources for Industry Programme (THRIP) award no. TP13080525596 (E.T.F. Witkowski and I.M. Weiersbye) and AngloGold Ashanti Limited South Africa.

Contents

1. Introduction 1-1

1.1. Literature Review 1-7

Plant metal tolerance strategies 1-8

Bioavailability and uptake of metals 1-10

Ion translocation and detoxification 1-13

Halophytes and their specific adaptations 1-14

Plant glandular structures and mechanisms for salt excretion 1-16

Gold Accumulation by plants 1-20

In-situ remediation of contaminated soils using plants 1-23

1.2. Aims and Objectives 1-27

1.3. References 1-28

2. *In vitro* growth and accumulation of gold within tissues of *Tamarix usneoides* (southern African salt cedar, Tamaricaceae). 2-1

2.1. Abstract 2-1

2.2. Introduction 2-2

2.3. Methods 2-5

Material collection and mother stock propagation 2-5

Propagation of *in vitro* material 2-5

Gold uptake and translocation by *Tamarix usneoides* explants *in vitro* 2-6

Growth measurements and analysis of gold 2-6

Verification of gold accumulation *in planta* 2-7

Data processing and statistical analysis 2-8

2.4. Results 2-10

Verification of gold accumulation *in planta* 2-10

Growth and gold accumulation of *in vitro* material 2-14

2.5. Discussion 2-20

2.6. Summary & Conclusions 2-26

2.7. Acknowledgements 2-27

2.8. References 2-28

3. The accumulation of gold and other elements by *Tamarix usneoides* trees from gold and uranium tailings 3-1

3.1. Abstract 3-1
3.2. Introduction 3-2
3.3. Methodology 3-4
Study site history, characterisation, preparation and plant selection 3-4
Material collection and preparation 3-7
Data analysis 3-11
3.4. Results and Discussion 3-12
Site chemical characteristics 3-12
Plant elemental uptake 3-16
Solute accumulation in *Tamarix usneoides* 3-30
3.5. Conclusion 3-33
3.6. Acknowledgements 3-35
This study was supported by AngloGold Ashanti and the Technology for Human Resources for Industry Programme (THRIP) award no. TP13080525596 from the Department of Trade and Industry and the National Research Foundation of South Africa to I.M. Weiersbye and E.T.F. Witkowski.References 3-35
3.7. References 3-35
4. The salt glands of *Tamarix usneoides* E. Mey. ex Bunge (South African Salt Cedar) 4-1
4.1. Abstract 4-1
4.2. Introduction 4-2
4.3. Methods 4-3
Plant identification and provenance 4-3
Propagation of mother stock material 4-3
Propagation of *in vitro* material for microscopy 4-4
Material preparation for light and electron microscopy 4-4
Light microscopy 4-5
Transmission electron microscopy 4-5
Scanning Electron Microscopy 4-6
4.4. Results 4-6
Leaf structure and mechanisms for salt excretion 4-6
Microstructure of the salt excretory apparatus 4-8
4.5. Discussion 4-13
Salt excretion by the leaves of *Tamarix usneoides* 4-13
4.6. Conclusions 4-20
4.7. Acknowledgements 4-21

4.8. References 4-22
5. Ion uptake and compartmentalisation in the leaves of the recretohalophyte *Tamarix usneoides* 5-1
5.1. Abstract 5-1
5.2. Introduction 5-2
5.3. Methods 5-7
Propagation of *in vitro* material 5-7
Dosing of *in vitro* plantlets with Au 5-7
Analytical Microscopy 5-8
5.4. Results and Discussion 5-10
Material Quality as a result of processing for microscopy. 5-10
Description of the Root, Stem and Leaf Structure of *T. usneoides* 5-11
Root elemental uptake. 5-13
Shoot tissue elemental accumulation and transfer 5-18
Tissue elemental transfer 5-25
5.5. Conclusion 5-28
5.6. Acknowledgements 5-29
5.7. References 5-30
6. Salinity tolerance, metal accumulation and gold phytoextraction by *Tamarix usneoides* 6-1
6.1. Introduction 6-1
6.2. A model for ion transfer and elemental tolerance in *T. usneoides* 6-2
6.3. Ecophysiological reasons for ionic stress tolerance in *Tamarix usneoides* 6-2
6.4. Gold accumulation within the tissues of *T. usneoides* 6-5
6.5. Conclusion 6-8
6.6. References 6-10
Appendices 1
Appendix A – Supplementary data for chapter 3 1
Appendix B – Supplementary data for chapter 4 11

List of Figures

Figure 1: Gold Deposits of the Witwatersrand basin (CJ Vorster, 2000) 1-3
Figure 2: Salt excretion by *Tamarix usneoides* growing on a saline watercourse at Goodhouse in the province of the Northern Cape, South Africa 1-20
Figure 3: Gold pourbaix diagram (Mortier, 2006).....1-21
Figure 4: Gold accumulation within shoot tissue of *T. usneoides* plantlets grown in Murashige and Skoog medium enriched with 25mg/kg gold thiosulphate at pH 5.6, detected using WDS. Count data is on a scale of 0-3 where counts of 3 indicate higher gold concentrations Arrow shows areas of higher elemental accumulation. 2-13
Figure 5 : Boxplots of tissue gold concentration (mg/kg), percentage recovery from medium, tissue gold bioconcentration factor and translocation factor by gold compound treatment for root and shoot tissue.....2-18
Figure 6: Overview of sample point locations and typical tailings particle size distribution.....3-6
Figure 7: Examples of Stems (A) Twigs (B), Micro-twigs (C), and Leaf shoots biomass collected from selected trees growing *in-situ* trials on the Mponeng tailings storage facility. 3-9
Figure 8: Dendrogram of elemental groupings based on their concentration and translocation factors. The dendrogram was generated using hierarchical clustering analysis (Wards method) to generate a hierarchy of similarity between different elements concentration and translocation factors. Elements with similar groupings for translocation and concentration are likely to have similar physiological response by the plant. As such this dendrogram can be used to determine and relate patterns of uptake for multiple elements. 3-18
Figure 9: Dendrogram showing tissue groupings for tissue elemental concentration (mg/kg) and the translocation factor (%) derived from multi-factoral unsupervised hierarchical cluster analysis (Wards method) to determine similarities in elemental concentrations and translocation for the different tissue types.. 3-29
Figure 10 : A) *Tamarix usneoides* stem section showing numerous salt patches from the underlying glands (Sg) situated on small scale like leaves. B) Scanning electron micrograph of the surface of a *Tamarix usneoides* leaf showing salt glands situated within epidermal crypts (Sg) and numerous stomata (Sto) evenly distributed across the leaf surface. 4-7
Figure 11: A) Cross section showing how the salt glands (SG) on the adaxial surface of a *Tamarix usneoides* leaf are situated in sunken epidermal crypts and are in close proximity to vascular bundles (VB). B) Cross section through a *Tamarix* salt gland showing basal collecting cells (Bcc) located beneath the stack of excretory cells (Ec) which are surrounded by a specialised secondary cell wall (Scw), This specialised wall is absent at the junction between the basal collecting cell and the lowest excretory cell, this region is often referred to as the transfusion site (Ts).....4-8
Figure 12: Transmission electron micrographs showing, A) transverse section through a *Tamarix usneoides* salt gland. Note the predominance of plasmodesmata (Pl) between the basal collecting cell (Bcc) and the first excretory cell (Cell 1). The secondary thickening surrounding the excretory cell is clearly defined (Scw). Nucleus (N), Nucleolus (Nu), Secondary Cell wall (Scw), Vesicles (V) and Interfacial apparatus (Ia) are clearly visible. B) Cross section through a basal collecting cell (Bcc) and surrounding mesophyll tissue (Mc) and salt gland (Cells 1-3) showing chloroplasts (Chl) and mitochondria (M) as well as large vacuoles (Va) within the collecting cell, plasmodesmata (Pl) at the

transfer site and numerous vesicles (V) and predominant nuclei (N) within the basal excretory cells. C) The transfusion site between the basal collecting cell (Bcc) and the first excretory cell (Cell 1) is characterised by numerous plasmodesmata (Pl). The secondary cell wall of the first excretory cell is subtended by interfacial apparatus (Ia). The vacuoles of the basal cells contain what are suggested to be flocculated tannin strands (Fts). D) The transfusion site between the basal cell (Bcc) and first excretory cell (Cell 1), showing vesicles (V) and numerous plasmodesmata (Pl). 4-9
Figure 13: Transmission electron micrographs showing: A.) Cell wall of the basal excretory cell showing interfacial apparatus consisting of budding vesicles (v), Golgi (Go), mitochondria (M) and rough endoplasmic reticulum (Rer) in close proximity to the plasmodesmata (Pl) of the transfer site. Larger vesicles (V) as well as cell wall protuberances (Pr) are present within cell 2. B.) The interfacial apparatus consisting of rough endoplasmic reticulum (Rer), mitochondria (M) and vesicles (V) characterise the first excretory cell (Cell 1) of the stack of cells within the gland and the second excretory cell (Cell 2) is characterised by numerous cell wall protuberances (Pr) as well as larger vesicles (V). C.) Apical excretory cell (Cell 3) of a *T. usneoides* salt gland showing cell protuberances (Pr), rough endoplasmic reticulum, (Rer), vesicles and Golgi (Go) 4-12
Figure 14: Cross section through *T. usneoides* tissues collected from material grown *in vitro* in 1/4 strength MS at a pH of 5.6 and dosed with AuCl at a concentration of 25mg/kg Au. A.) Root Tissue Showing: (E) endodermis, (V) Vascular tissue, (C) Cortex tissue. B.) : vaginate leaf showing: Palisade mesophyll (Pm), Spongy mesophyll tissue (Smt), salt glands (Sg), Vascular bundle tissue (Vbt), Flocculated polyphenolic compounds (Flph), Stomata (Sto) and Polyphenolic compounds (Ph). C.) Cross section through two parenchyma cells showing flocculated tannins (Ft) and disperse tannins (dt). D.) Cross section through a Sessile leaf and stem showing Showing salt glands (Sg), Epidermal tissue (Et), Mesophyll tissue (Mt), Vascular tissue (Vt), Vascular bundles (Vb), Parenchyma tissue (Pt) and stomata (Sto). E.) median section of a sessile leaf showing stomata (Sto), Epidermal tissue (Ep), Single Vascular bundle (Vb), Spongy mesophyll tissue (Smt) and Salt glands (Sg). 5-15
Figure 15: SEM images and 2 EDS spectra of *in vitro T. usneoides* root tissue from material grown in ¼ strength MS and treated with 25mg/kg gold chloride 5-16
Figure 16: Cross Section (A) through root tissue from of explants grown in gold chloride at a concentration of 25mg/kg showing Vascular bundles (vb), Casparian Strip (Cs), Cortex (Cor) and Epidermis. Overlaid with WDS elemental maps and count values for B) Chlorine C) Gold D) Sodium. 5-17
Figure 17: Back scattered electron SEM image (A) showing excreted sulphur (S) and WDS elemental Maps for B.) Cl, C.) Au and D.) S for a stem section from a *T. usneoides* plantlet treated with gold chloride at a concentration of 25 mg/kg 5-18
Figure 18: Cross section through a portion of stem (epidermis and subtending parenchyma tissue) (St) and leaf tissue (L) from a *T. usneoides* plantlet grown in a solution of gold thiosulphate at a concentration of 25mg/kg overlaid with WDS elemental maps and counts. A.) Sulphur, B.) Sodium, C.) Gold and D.) Chlorine. 5-21
Figure 19: : Cross section througha stem showing Parenchyma tissue (P) with flocculated polyphenolic compounds (Fl) Stem Vascular tissue (Vb) and stem epidermis (Ep) from a *Tamarix usneoides* plantlet grown in a solution of gold thiosulphate dosed to a concentration of 25mg/kg Au, overlaid with WDS elemental maps and counts for A.) sulphur B.) Chlorine, C.) Gold and D.) Sodium. 5-22
Figure 20: A torn cross section through a vaginate *Tamarix usneoides* leaf from a plantlet grown *in vitro* dosed with Gold Thiosulphate to a concentration of 25mg/kg showing Bascular bundles (Vb),

Salt gland (Sg), Epidermal tissue (Ep), overlaid with WDS elemental maps and counts for A.) Sulphur, B.) Sodium, C.) Gold and D.) Chlorine (1) Evidence of elemental exclusion where sulphur is accumulated but sodium is excluded from cells with flocculated polyphenolic compounds (Fl) ..5-23
Figure 21: Cross section through a *Tamarix usneoides* leaf showing a salt gland (Sg), Vascular bundles (Vb) and surrounding mesophyll tissue containing flocculated tannins (Fl) from a plantlet grown *in vitro* in a ¼ strenghtb Murashige and Skoog gowth medium solution spiked with gold chloride at a concentration of 25mg/kg, overlaid with WDS elemental maps and counts for A.) Calcium, B.) Sodium, C.) Gold and D.) Chlorine.....5-24
Figure 22: Model of proposed pathways for ion transport from the rhizosphere to the leaf surface. The components of the proposed pathway are: 1) rhizosphere 2) Root Epidermis 3) Root Cortex 4) Casparian strip 5) Root Vascular Tissue 6) Transpirational pull 7) Leaf Vascular tissue Tissue 8) Parenchyma Tissue, 9a) Flocculated Polyphenol, 9b) Dispersed polyphenols 10) Basal Collecting Cells 11) Salt Gland 12) Leaf surface. The pathways are A.) Yellow- Apoplastic transport within the root cortex tissue, Green – Loading of ions into the cortex via active transport Red Intercellular transport in the cortex via a coupled apoplastic and symplastic transport path Blue – Ion transportfrom the cortex tissue into the vascular tissue past the Casparian strip. B) Yellow – Transportation up the vascular tissue via transpirational pull. C) Yellow- Apoplastic transport from the vascular bundles of the leaf to the salt gland Blue- Symplastic transport utilising plasmodemata and vesicle transport Red- Coupled apoplastic-symplastic transportation Green – Ion Sequestration within parenchyma tissue containing flocculated and disperse polyphenolics..... **Error! Bookmark not defined.**
Figure 23: Optimal number of clusters for the elemental concentration dendrogram 22
Figure 24: Optimal number of clusters for the elemental Translocation factor dendrogram 22

List of tables

Table 1: Summary statistics for the measured variables for each tissue by gold compound type and media gold gold compound concentration.....2-11

Table 2: Summary Statistics for growth parameters measured for *T. usneoides* plantlets grown *in vitro* at 3 different pH values.....2-15

Table 3: The effect of pH on gold concentration in tissue (Tis conc) of *Tamarix usneoides* plantlets grown *in vitro* by tissue gold concentration, gold percentage recovery (Rec) , gold bioconcentration (Bioconc) and gold translocation (Trans) per tissue type. 2-15

Table 4: Mean plantlet root length, root number and degree of root branching after a two week treatment period with one of three gold compounds.....2-16

Table 5: *Tamarix usneoides* growth at different gold compound dosages.....2-16

Table 6: Dunns pairwise comparison p-values showing the compounds which had significant differences for each of the measured variables for each tissue and medium gold compound concentration.....2-17

Table 7: Mean and p-value for pH, EC and Eh for each tailings sample depth collected from the control pits and sample pits from the Mponeng Tailings facility 3-14

Table 8: Mean Concentration for selected elements for control and sample pits, mean elemental concentration for sample pit depths and p-values for statistical measures 3-15

Table 9: Median Concentration values (mg/kg) for samples grouped into tailings, aboveground and belowground biomass categories 3-18

Table 10: The median elemental concentration (mg/kg) and median translocation factors for belowground plant tissues of *T.usneoides* collected from the Mponeng Tailings facility. Associated p values are also presented. 3-19

Table 11: Median elemental concentrations (mg/kg) and median translocation factors for aboveground *T. usneoides* tissues collected from the Mponeng Tailings facility. The associated p values are also presented. 3-25

Table 12: Median elemental concentration ratio and p-value from Kruskall - Wallis test for tissue samples collected from trees harvested from the Mponeng tailings facility 3-29

Table 13: Murashige and Skoog Basal growth media constituents modified to include gold potassium cyanide, gold chloride and gold thiosulphate at a concentration of 50mg/kg gold 1

Table 14: % gold recovery from CRM and sample material spiked with gold at set concentrations. 2

Table 15: Normality test values for root and shoot tissue Au concentration for *T. usneoides* plantlets grown *in vitro* 2

Table 16: Kruskall Wallis tests for Tissue Concentration, Gold Percentage recovery and bioconcentration per Tissue type for *T. usneoides* plantlets grown *in vitro* and spikes with 3 different gold compounds..... 2

Table 17: Kruskall wallis test results for tissue gold concentration, bioconcentration and gold recovery by tissue type and treatment concentration for *T. usneoides* plantlets grown *in vitro* in a media solution spiked with additional gold compounds 3

Table 18: Root Tissue Au Concentration (mg/kg) by pH, Gold Compound and Media gold Concentration 4

Table 19: Root Tissue Au Recovery % by pH, Gold Compound and Media gold Concentration 5

Table 20: Root Tissue Au Bioconcentration factor by pH, Gold Compound and Media gold Concentration 6

Table 21: Shoot Tissue Au Concentration (mg/kg) by pH, Gold Compound and Media gold Concentration 7

Table 22: Shoot Tissue Au Recovery % by pH, Gold Compound and Media gold Concentration 8

Table 23: Shoot Tissue Au Bioconcentration factor by pH, Gold Compound and Media gold Concentration 9

Table 24: Shoot Tissue Au Translocation Factor by pH, Gold Compound and Media gold Concentration 10

Table 25: Percentage recovery for selected elements from tailings certified reference material as analysed using the XEPOS XRF 11

Table 26: Percentage recovery of selected elements from biomass certified reference material as analysed using the XEPOS XRF 11

Table 27: Summary Statistics for pH, EC and Eh for tailings samples collected from the control pits and sample pits from the Mponeng Tailings facility 11

Table 28: Summary statistics for pH, EC and Eh at 6 different sampling depths from the sample pits located on the Mponeng tailings facility 12

Table 29: Summary statistics for elemental concentration (mg/kg) for tailings samples collected at different depths from control and sample pits on the mponeng tailings facility 12

Table 30: Summary statistics for elemental concentration in tissue samples from trees harvested from the Mponeng tailings facility 17

Table 31: Comparison of mean Gold concentration (mg/kg) between Control and Sample pits at 6 different depths 20

Table 32: Mean Au concentration per tissue type 20

Table 33: comparison between mean elemental concentrations (mg/kg) for Control and Sample pits 20

Table 34: Summary statistics for elemental ratios derived from tissue elemental concentration (mg/kg) from trees harvested from the Mponeng tailings facility 21

Structure of the Thesis

This thesis is presented as four data chapters associated with overarching introductory and concluding chapters. The first data chapter investigates the *in vitro* accumulation of gold. The second data chapter explores the potential for using *T. usneoides* for the recovery of gold and other elements from trees grown on the surface of a South African tailings storage facility and sought to identify which tissues exhibit elevated elemental concentrations. The third data chapter describes the salt gland microstructure and hypothesises about potential uses for the structural adaptations present within the salt glands of *T. usneoides.* This chapter was published in the International Journal of Phytoremediation and as such the chapter has been included in this thesis as it was published (https://doi.org/10.1080/15226514.2016.1244163). The fourth chapter mapped elemental localisation within different tissue types using a range of analytical microscopy techniques.

Each of the data chapters have been written in scientific manuscript format, *viz*. they each have their own Introduction, Methodology, Results, Discussion and Reference sections. Preceding these data chapters is a contextualising introduction and literature review which provides the broader perspective and rationale for the research. The final chapter summarises the findings and explores the implications of the research. Appendices for the entire thesis are also provided.

The authors mentioned in each of the preceding chapters played the following roles and their percentage contribution to the final project can be summarised as follows:

H.T Wilson – Primary author, conducted the research and wrote the manuscript (75%)
Prof D.J. Mycock – Supervisor, reviewed the manuscript and provided laboratory facilities. (12.5%)
I.M. Weiersbye – Provided initial project concept (investigate gold accumulation in *T. usneoides*) and provided project funding and advised on methodologies and performed project review (12.5%)

The first data chapter entitled *In vitro* growth and accumulation of gold within tissues of *Tamarix usneoides* (southern African salt cedar, Tamaricaceae). includes Anthony M Mader as a third author as his Honours project provided in vitro material grown at a pH of 4.6 which was used in this study. As such his contribution to that paper constitutes 10% of that paper.

1. Introduction

The accumulation and tolerance of excess elements in plant species, in particular metal accumulation, is an aspect of plant science that is widely studied (Baker, 1981; Krämer, 2010). This is because plants occupy the primary trophic level and as such act as a gateway for the movement of elements into the wider ecosystem (Devkota & Schmidt 2000; Judy *et al.*, 2011). Understanding the mechanisms which allow plants to move elements from the soil environment into their aboveground biomass can thus contribute to a number of plant-based technologies, for example, improved nutrition of crops and the limitation of the movement of undesirable elements into the broader ecosystem (Devkota & Schmidt, 2000). Plants with the correct suite of characteristics (tolerance, growth rates, rooting depths) can be utilised in programmes designed to prevent the spread of pollutants from industrial and mine sites as well as act as *in-situ* mechanisms for contaminant removal (Lamb *et al.,* 2001) using a suite of techniques collectively termed phytotechnologies (Gardea-Torresdey, *et al.,* 2005). There is also interest in the use of plant elemental accumulation for the purposes of bio-mining and mineral exploration (Dunn, 2007; Reeves, 2003; Yang *et al.*, 2002; Brooks, 1998).

Gold accumulation by plants has been documented in several species. Some of the earliest records are from 1824 where it was found that wood ash from English oak trees (*Quercus robur)* contained gold in concentrations ranging between 0.06 and 0.6 ppb dry mass (Malte-Brun, 1824). Subsequently, several other species including Douglas Fir (*Pseudotsuga menziesil*), Wormwood (*Artemisia absinthium*) and honeysuckle (*Lonicera* sp.) were found to accumulate gold at concentrations ranging between 10-20 ppb dry mass (Anderson, *et al.*, 1999). Studies by Lintern *et al* (2013) noted that *Eucalyptus* species growing on gold

containing ore bodies are capable of accumulating gold in concentrations up to 80 ppb dry mass. There have also been a number of studies investigating gold nanoparticle synthesis within live plants and by dead plant biomass (Gardea-Torresdey *et al.,* 2002; Sharma *et al.*, 2007; Navarro *et al*., 2008; Starnes *et al.*, 2010; Arora *et al.,* 2012; Zhu *et al.*, 2012; Anderson *et al.*, 2013; Shukla *et al.*, 2015; Li *et al.*, 2016; Plotnikov *et al.*, 2017; Dykman and Shchyogolev, 2018). For example, in Alfalfa and *Sesbania* plants grown in an $AuCl_4$ enriched substrate, the Au(III) was reduced into Au(0) nanoparticles with a mean size of 6 to 20nm (Sharma *et al.*, 2007; Starnes *et al.*, 2010). Gold nanoparticles are of commercial value as they are highly effective for processes such as catalysis, as well as for drug delivery and a number of other medical applications (Fricker, 1996). As a result of the increasing use of nano-technologies, there has been a consequent increase in environmental exposure to nanoparticles and there has been considerable interest in the effects of nanoparticle accumulation on plant growth (Dykman and Shchyogolev 2018). Studies by Zhu *et al.*, 2012 showed that in addition to being able to reduce gold in solution into gold nanoparticles, plants have the ability to accumulate gold directly as gold nanoparticles.

Within a South African context, there is considerable interest in the use of plants for the recovery of gold and other elements from contaminated environments. The Witwatersrand basin is a geological formation in South Africa that spans the provinces of Gauteng, Freestate and the North Western province (Figure 1). Gold mined from the Witwatersrand basin accounts for approximately 50% of the gold ever mined globally and still is considered as one of the largest gold reserves in the world (Whitfield, 2006). The Witwatersrand basins consist of reef horizons which are associated with high concentrations of heavier elements such as gold, uranium, silver and iridium as well as significant quantities of iron and sulphur (Pretorius, 1976), this has led to significant exploitation of the mineral resources within the region.

Historically, gold extraction processes were not efficient, resulting in mine tailings which contain gold in low concentrations (0.2- 0.5 g of gold per ton of tailings) (Gold Fields Ltd, June 2009 Quarterly Report, Aug. 6, 2009; Naicker *et al.*, 2003, Mphephu, 2004).

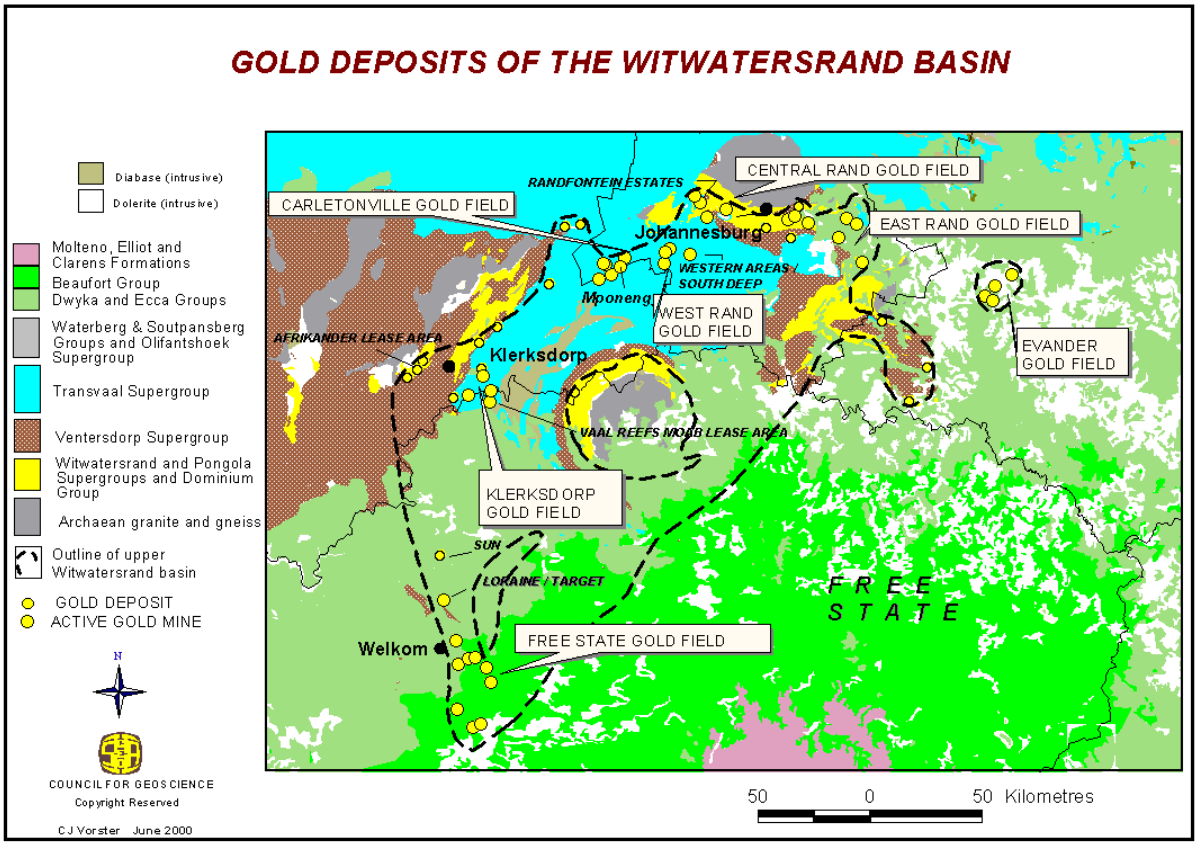

Figure 1: Gold Deposits of the Witwatersrand basin (CJ Vorster, 2000)

When the South African Tailings Storage Facilities (TSFs) were first built, there were no legislative requirements to have them located on appropriate soils or designed in such a way as to minimise the generation and drainage of leachate (e.g. physical liners and evapotranspiration covers) and this has resulted in the emanation of contaminated leachate from the TSFs into shallow aquifers (Tutu *et al.*, 2008). Frequent failures of TSFs and associated spillages (~64% of TSFs have failed in Ekurhuleni, South Africa alone between 1930 and 2004 (Sutton *et al.*, 2006)) and subsequent transport of the tailings into the environment via runoff and mass movement have led to significant amounts of gold along with other

metals and contaminants being dispersed into the environment (Tutu *et al.*, 2008). Additionally, the gold bearing ore of the various reef horizons of the Witwatersrand basin contain sulphide minerals such as iron pyrite and arsenopyrite (Pretorius, 1976). The gold tailings contain, on average, two percent sulphur, and based on the tonnage of tailings in the 1990's, it was estimated that there were approximately 30 000 000 tonnes of sulphur in TSFs in the Witwatersrand basin (Weiersbye and Witkowski, 1998). Iron pyrite, on exposure to air, oxygenated water and combined with the action of sulphur-utilising bacteria (*Thiobacillus* sp.), oxidises and releases sulphuric acid and iron. As a consequence of acid rock drainage (ARD) and the strongly oxidizing conditions, there is a lowering of pH and concomitant mobilisation of metals and metalloids such as As, Cu, Cr, Ni, Pb, Co Zn, S, Na, Ca, Mg, Mn and U contained in the tailings and contaminated soils (Galan *et al.,* 2003, Naicker *et al.*, 2003, Tutu *et al*., 2008). Oxidation of tailings generally occurs rapidly at the surface of the TSF and more slowly deeper within the tailings facility as oxidation depth is limited by the depth of infiltration by oxygenated water and aerobic bacteria (Kempe, 1983). Thus, exposure of TSFs or spilled tailings to oxygenated water through processes such as hydraulic sluicing, erosion or mass movement results in the rapid formation of ARD, with an ensuing increased rate of contaminant spread, often leading to contaminated water percolating through the soil profile into aquifers (Mphephu, 2004; Tutu *et al.*, 2005; Tutu *et al*., 2008). When the TSF's are situated on rock types such as limestone and dolomite, ARD can be neutralised, resulting in acid neutral drainage (AND) at varying distances from the ARD point source. However, AND also contains high concentrations of metal sulphates and other salts (Tutu *et al*., 2008). In the presence of calcium, sodium and magnesium solubilised from the host rocks in such situations, the excess sulphates can precipitate as gypsum (calcium sulphate) and other

minerals (Tutu *et al*., 2011). Concentrations of contaminants such as Co, Ni and Zn range from 2000 to 5000 mg/kg in the salt crusts associated with AND (Naicker *et al.*, 2003).

Within regions that are impacted by mining, drainage lines and shallow depressions or "sink" areas present potentially hazardous locations due to the accumulation in them of contaminated materials carried via surface runoff and the efflux of contaminated shallow groundwater plumes (Coetzee *et al.*, 2002). The elements within the contaminated materials bind to organic compounds, resulting in high concentrations of metals and other elements within these sites (Coetzee *et al.*, 2002; Sheoran & Sheoran, 2006). In South Africa these polluted sinks, most commonly *Phragmites australis* reed-beds, represent a source of the precious metal (Sheoran and Sheoran, 2006), and thus there is a need for an effective mechanism for gold recovery from these environments as well as their decontamination (Winde and Stoch, 2010).

Current methods for the recovery of residual gold from tailings spillages and polluted soils involves excavating the gold bearing material, and reprocessing it through the metallurgical plant for metal recovery (Muir, *et al*., 2004, Golder report, 2008). The problem with this approach is that the process of excavation, transport to the metallurgical plant for gold screening and subsequent redepositing of the screenings is very costly. These costs are compounded by the large amounts of organic matter present in the material which compromises the metallurgical process. Additional problems are: (a) it is illegal in South Africa to disturb the sediments of any natural wetland, and (b) disturbance of the sediments allows for the oxidation and leaching of some contaminants that were previously precipitated or bound in the sediments, resulting in further downstream contamination (Tutu *et al.*, 2005, 2008; McCarthy & Venter, 2006). In South Africa, many contaminated sites that contain high

gold grades are the focus of illegal gold recovery by artisanal miners. This has the potential to cause considerable downstream contamination, not only from the consequent release of contaminants bound within the sediments but also due to the unsafe practices utilised by the artisanal miners in the gold extraction process (Walters *et al.*, 2011, Mallo, 2012). Thus, in order to minimise the potential release of bound contaminants during the rehabilitation of these areas, there is a requirement for a technology that allows for the *in-situ* recovery of gold and other contaminant elements from old tailings spillages and TSF footprints.

Tamarix usneoides E. Mey. ex Bunge (South African Salt Cedar, *Tamaricaceae*) is a halophyte riparian tree species indigenous to Southern Africa (Baum, 1978). Members of the genus *Tamarix* are adapted to highly saline, wet environments e.g. salt pans, estuaries and desert riparian zones (Baum 1978). These environments are similar to those found on some mining facilities and *T. usneoides*, *T. ramosissima, T. chinensis, T. aphylla* and hybrids have been documented as growing on gold mine tailings (Weiersbye and Witkowski, 1998; Weiersbye *et al*., 2006, Mayonde *et al.*, 2015). *Tamarix usneoides* is also capable of hyper-accumulating sulphur and other elements from acid mine drainage and mine waste, and as such is utilised for the phytoremediation of affected soils and groundwater on South African gold and platinum mines (the Mine Woodlands Project, Dye & Weiersbye, 2010; I.M. Weiersbye, 2005; unpublished data; Weiersbye 2007; Dye *et al.*, 2008). As an exo-rectohalophyte *T. usneoides* maintains homeostasis through the excretion of excess Na^+ and Cl^- ions from specialised salt glands known as vesiculated trichomes in the form of halite and gypsum (Dennis, 2008; Wilson *et al.*, 2017), effectively maintaining both osmotic pressure and ion balances within the cells. A range of other elements (including metals and metalloids) such as Mg, S, Ca, K, Co, Cu, Cd, As, Se, Zn, Mn, Au, and U have been detected in the leaves and shoots of *T. usneoides*

and *T. ramosissima X usneoides hybrids* at concentrations exceeding ambient geochemical backgrounds (Dennis, 2008; I.M. Weiersbye, unpublished data).

Thus, there is potential for *Tamarix* species, including *T. usneoides,* to be used for the concentration *in planta* or in the rhizosphere, and recovery of gold and other elements from contaminated environments. However, the potential viability of gold accumulation and recovery, as well as the physiological mechanisms involved in solute uptake and processing need to be further explored.

1.1. Literature Review

Metal nutrient acquisition and accumulation by plants is a well-documented phenomenon. Agriculturalists in the mid 1800's realised that a number of plants in intensively farmed fields benefitted from the addition of potash (a generic term for any mineral which contains potassium) (Dyer, 1894). The first use of plant accumulation of metals other than the recognised macronutrients (Nitrogen, Phosphorous, Potassium, Sulphur, Calcium and Magnesium) and micro-nutrients (Iron, Molybdenum, Boron, Copper, Manganese, Sodium, Zinc, Nickel, Chlorine, Cobalt, Aluminium, Silicon, Vanadium and Selenium) was in 1947, when it was found that plants could be used as indicators for zinc. This in turn led to the development of the field of biogeochemical prospecting which today is extensively used for mineral exploration (Dunn, 2007). Subsequent to the use of indicator species in biogeochemical prospecting, a host of related technologies called phyto-technologies, have been developed. These have explored the use of plants as novel 'mechanisms' for extracting metals and contaminants from soils without disturbing the soil profiles or interrupting

ecological processes (Pilon-Smits, 2005). *In-situ* removal of contaminants is often not sufficient to prevent the spread or further contamination of an area, thus there are a number of related and supplementary phyto-technologies used for the control of groundwater recharge, dust control, *in-situ* stabilisation and other approaches (USEPA, 2009). Phyto-extraction and bio-mining are phyto-technologies that are primarily concerned with the removal of contaminants or precious metals from soils (Brooks and Robinson, 1998).

The ability of plants to tolerate and accumulate non-nutrient elements is largely dependent on an inherent tolerance to the element in question as well as the bioavailability of the element (Yang *et al*., 2005). Metal bioavailability is dependent on factors such as electroconductivity, soil saturation and pH (Lasat, 2000), while plant tolerance is determined by the physiological strategies used by the species to survive under conditions of elevated metal concentration (Clemens, 2006).

PLANT METAL TOLERANCE STRATEGIES

Metallophytes are plants which are able to grow and complete their life-cycle in metal-rich environments, and may exhibit three general responses as a result of their underlying tolerance. Firstly, there are the “accumulators”, which accumulate metals in their above-ground biomass to concentrations that are above geochemical background concentrations. Secondly, there are “indicators” where metal uptake by the plant results in internal metal concentrations which reflect the available metal concentrations of the soil, and finally, there are the “excluders” where metal concentrations in tissue are maintained at lower concentrations than the ambient substrate concentrations, until substrate available metal

concentrations exceed a critical threshold and unrestricted uptake occurs, usually resulting in plant death (Baker, 1981).

It was hypothesized by Boyd *et al.*, 2002 that one of the reasons why some plants accumulate significant quantities of metals is because elevated metal concentrations act as elemental defences against generalist herbivores and pathogens (Boyd *et al.*, 2002). It has also been theorised that the accumulation of metals within the plant is a mechanism that allows the plant to cope with high concentrations of metals within the rooting zone, as the removal of metals and subsequent sequestration within woody tissue prevents ion competition at the ion specific transporter proteins within the membranes of the cells of the roots (Boyd & Martens, 1992).

An early formal description of plant hyperaccumulation of metals was documented in *Alyssum bertolonii* by Minguzzi & Vergnano in 1947, who found that the species accumulated nickel to a concentration of 12 200 µg/g in the leaves (*loc. sit.,* Brooks and Radford, 1978). Subsequently, a metal hyperaccumulator was formally defined as a plant which accumulates metals in its tissues at concentrations significantly higher than other non-accumulating plants growing under similar conditions (Brooks, 1998). In order for a plant to accumulate metals above ground there need to be three biological adaptations, namely: one which allows the plant to actively take up a particular metal to concentrations above those in the substrate; a second to translocate the metal from root to shoot; and a third which prevents the plant from suffering detrimental effects of metal toxicity associated with the high metal concentrations (Baker, 1981).

Plants which naturally occur on serpentine and calamine soils are of interest as these plants have the ability to tolerate high concentrations of metals such as magnesium and first transition series metals (vanadium, titanium, chrome, manganese, cobalt, nickel, and iron) which are characteristic of those soils (Brooks, 1998, Brady, *et al.*, 2005). In these plants, tolerance is achieved by either excluding the metal from being taken up by the plant roots or by having physiological adaptations which prevent metal toxicity (Clemens, 2006). Through a series of inter- and intra-specific crosses it has been shown that plant hyper tolerance and plant hyperaccumulation of metals are independent characteristics and that the genes which control for tolerance of one metal do not necessarily control for tolerance of others (Bert *et al.*, 2003). Metal accumulation has been documented in over 450 species, a number of which are unrelated, implying that metal accumulation has a polyphyletic origin (Macnair, 2003). Studies comparing the gene expression between a closely related accumulator and a non-accumulator showed that the genes which controlled for metal tolerance and accumulation were not novel but merely an up-regulation of the genes involved in the production of metal ligands and metal-ligand complex transporters (Talke *et al*., 2006).

BIOAVAILABILITY AND UPTAKE OF METALS

The ability of plants to accumulate non-nutrient metals in the shoot is dependent on the ability to absorb, translocate the metals and finally to detoxify and/or sequestrate the metals in question (Yang *et al*., 2005). In order for plants to take up metals they need to be in a form that is bioavailable and bio-accessible (i.e. accessible to roots). Bioavailable metals occur as free ions or soluble metal complexes, or they are adsorbed to the soil constituents at ion exchange sites (Lasat, 2000). Metal absorption by plants is also dependent on a number of soil characteristics, for example, many metal cations (positively charged ions) are bound to

negatively-charged organic or clay particles at ion-exchange sites within the soil. However, when there is a lowering of the soil pH, there is increased competition between H^+ ions and the metal cations at the soil binding sites, resulting in the less strongly bound metal cations being liberated and going into solution (Lasat, 2000). Plants have evolved several strategies to increase the bio-availability of required nutrients. Strategies include acidifying the rhizosphere through the action of plasma membrane-localized proton pumps as well as through the secretion of chelating agents such as low-molecular weight (LMW) compounds (Krämer *et al.*, 2007; Clemens, 2006). Likewise, rhizosphere and root colonising bacteria and mycorrhizal fungi catalyse redox transformations with ions such as Pb^{2+}, Hg^{2+}, Au^{3+}, $Te^{4+}$and Ag^+ and these facilitate plant metal uptake by increasing the effective surface area of the root (Heggo *et al.,* 1990; Yang *et al.*, 2005). It has also been found that rhizosphere elemental composition affects elemental uptake, for example, an increase in rhizosphere calcium concentrations resulted in a decrease in uranium ion accumulation in *Brassica juncea* (EL Hayek *et al.*, 2018).

Regardless of the effective area for absorption by the root, movement of metal ions from the soil matrix into the cytoplasm of the plant cells is reliant on transportation past the phospholipid bilayer of the cell membranes, which is impermeable to charged elements (Lasat, 2000). Thus, in order for a plant to accumulate a particular metal, there needs to be a specific channel through the cellular membranes, which allow the metals into the cytoplasm. This can occur via ion transporters or ion channels within the cell membrane and there is evidence that endocytosis may also occur (Rigal *et al.,* 2015) However, despite the specificity of the binding sites on the plasma membranes, certain transporter proteins are unable to differentiate between particular essential and non-essential metals (Krämer, 2007). Metal ions are required for many cellular processes due to their chemical properties for example,

redox–activity under physiological conditions (i.e. Cu, Fe, among others) and Lewis acid strength (i.e. Zn, among others) (Halliwell & Gutteridge, 1990). Thus, there is a need for a specific mechanism for the active uptake of metal ions (Krämer, 2007). However, a high concentration of metal ions present within the cell can result in uncontrolled, high-affinity bonding to various functional groups (e.g. those associated with lipids, nucleic acids and proteins). This can result in damage and inactivation of the functional groups/biomolecules as well as disruption of cell signalling mechanisms through the displacement of Ca^{2+} ions (in particular) by other metal cations (Clemens, 2006). Accidental uptake of the incorrect metal ions can also occur, where transporter proteins within plant root cell membranes are unable to distinguish between some nutrients and potentially toxic metals or metalloids with no nutrient properties – e.g. plants substitute uptake of Se for S when Se is readily available (Sors, *et al*., 2005). Similarly, it has been shown that some ions can displace other ions from downstream in the Irving–Williams series from their specific binding sites (i.e. Zn^{2+}> Cu^{+}> Cu^{2+}> Ni^{2+}> Co^{2+}> Fe^{2+}>Mn^{2+}>Mg^{2+} > Ca^{2+}) (Krämer *et al.*, 2007). Thus, there is a high potential for associated toxicity and nutrient deficiencies to occur. Toxicity and nutrient deficiencies occur via processes such as ion competition at the root level, where the channels for nutrient absorption are blocked by the non-biologically relevant ion resulting in nutrient deficiencies within the plant. Nutrient deficiencies can also lead to uncontrolled uptake of ions of similar valence, resulting in oxidative stress (Clemens, 2006). Conversely, it has been shown that cadmium ions utilise the same cellular pathways as calcium ions and that increasing the amount of available calcium reduces the toxic effects associated with cadmium (Dalton *et al*., 2005). Similarly, it has been shown that the metalloids arsenic and selenium enter the cells of plants via the uptake systems for phosphates and sulphates (Clemens, 2006).

ION TRANSLOCATION AND DETOXIFICATION

The transportation of non-essential metal ions within the plant occurs via similar pathways to the transportation of essential nutrient metal ions (Macnair, 2003). Metals are initially (generally) transported within the apoplast of the plant root cortex and subsequently across the plasmalemma at the endodermis (Lasat *et al.*, 1996). Metal ions that enter the endodermal cells via transporter proteins move via simple diffusion, or alternatively they are complexed with cytosolic chelators such as histidine, and transported to neighbouring cells via the plasmodesmata and ultimately, they are actively moved into the xylem of the plant (Clemens, 2006). Within the xylem they are then transported up the stem via transpirational pull and unloaded into the symplasm of the aerial tissues. Here the non-essential ions are either detoxified by organic ligands (e.g. polyphenolics) or loaded into specific tissues which are then allowed to senesce (Clemens *et al.*, 2002). The suite of ligands used in metal detoxification varies with the age of the plant as well as a number of environmental variables, but can include compounds such as histidine, nicotianamine, glutathione, other organic acids and phyto-chelatins (Clemens *et al.*, 2002).

Adaptations to prevent metal toxicity within the cell include mechanisms to collect excess metal ions and a storage area to sequestrate metal ions so that they are not biologically available. Areas for metal sequestration can be specific tissues or apoplast structures such as cell walls (Clemens, 2007). An increase in the concentration of metal ions can result in oxidative stress, which at the whole plant level is characterised by blackening of roots, reduction in root growth and development of necrotic spots on the surface of the leaves (van der Zaal *et al*., 1999, Gonzalez *et al*., 1998). Many plants reduce the effects of metal toxicity through the production of phytochelatins (PCs) and other sulphur-containing compounds (e.g. amino acids and polypeptides) which have high metal bonding affinities and are

responsible for transporting the metal ions to the vacuole (Ernst *et al.*, 2008). For instance, with iron tolerance, a specific multimeric protein (a complex protein containing discrete subunits) with a high storage capacity for iron called ferritin is produced when the plant experiences iron stress (Pich *et al.*, 2001).

One of the strategies used by some plants to tolerate high ion concentrations in the rooting zone or in the plant tissues themselves is to absorb and remove the ions, thus preventing a toxic build up within the cytoplasm of the cells. This can be achieved by loading specific tissues (such as bark or leaves) with metal ions and then allowing that structure to senesce (Scholander *et al.*, 1962). Some trees, such as the mangrove *Avicennia marina,* concentrate excess Na and Cl within leaves which are then shed, essentially hyperaccumulating as well as excreting excess metals (Mycock, Frankland and Berjak, 1985, Mertens, *et al.*, 2006). Other plants, such as the recretohalophytes, have specialised glandular structures for the excretion of excess ions from within the plant (Ding *et al.*, 2010). These glands/salt bladders are often capable of excreting a wide range of excess ions, for example, the exo-recretohalophyte tree *T. aphylla* excreted beryllium, manganese, copper, zinc and molybdenum ions (Berry, 1970).

HALOPHYTES AND THEIR SPECIFIC ADAPTATIONS

Halophytes are defined as plants which are able to tolerate high levels of sodium chloride (NaCl) and complete their life cycles under elevated salinities in their growth environment (Flowers *et al*., 1977, Flowers *et al*., 2008). Increased Na^+ concentration in cellular cytoplasm is toxic to plants due to competition between Na^+ and K^+ ions (Kramer, 1983). As a result of this toxicity, halophytes have developed a series of adaptations to either exclude Na^+ at the root level or to excrete excess Na^+ ions from specialised glands (Figure 2), preventing Na^+ from competing with K^+ ions within the cytosol and maintaining homeostasis (Kramer, 1983).

Examples of halophyte plants are mangroves (e.g. *Avicennia marina*), common ironwood (*Casuarina equisitifolia*) and the South African Salt Cedar (*Tamarix usneoides*). One of the primary features of halophytes is that their uptake of K^+ ions is not affected by competition with Na^+ ions in the soil, (Kramer, 1983). The reason for this, is the ion discrimination by the transport protein `high affinity potassium transporter two' (HKT2), which has the ability to transport both K^+ and Na^+, but preferentially transports K^+ ions before Na^+ ions into the root cells (Kronzucker & Britto, 2011). Other candidates for Na^+ uptake are ion transporters such as Na^+/ H^+ (NHX) transporters which have been documented in the uptake of monovalent cations such as Li^+, Rb^+ and K^+. A further method for transportation is through the use of cation-chloride co-transporters, which can transport Na^+ and Cl^- electro-neutrally (Kronzukker and Britto, 2011).

Prevention of Na^+ and Cl^- toxicity is likely to occur by direct compartmentalisation of the potentially toxic ions within vesicles derived from the endoplasmic reticulum (ER), from which the ions can either be secreted back into the soil or be transported to vacuoles in storage tissue (Kramer, 1983; Kronzukker and Britto, 2011; Flowers *et al*., 2019). Energy dispersive X-ray microanalysis of tissues has shown that the ionic content of the xylem sap can be controlled during upward transport toward the shoot. For example, in *Phaseolus,* Na^+ accumulates in the proximal part of the shoot and in lower parts of the stem. Sites where salt sequestration occurs were seen to be characterised by rough endoplasmic reticulum and numerous mitochondria. Energy dispersive X-ray micro-analysis of these regions showed that the excess Na^+ in the xylem sap is swapped for K^+ and the Na^+ is secreted or sequestered (Kramer, 1977). It is further hypothesised that secondary metabolites play a role in salinity

tolerance, where salt-tolerant clones showed elevated levels of soluble phenolics, anthocyanins and flavones (Wahid and Ghazanfar, 2006).

As a recretohalophyte, *T. usneoides* has several adaptations which allow it to tolerate the highly saline riverbeds which are characteristic of the arid environment in which it is found. These include vesiculated trichomes which cover the surfaces of its small scale-like leaves (Wilson *et al.*, 2017) (Figure 2). Salt glands of other members of the genus *Tamarix* have been documented to excrete salts at a very high rate (Hagemeyer, 1988), implying that there are efficient mechanisms within the plant which allow for the uptake, translocation and subsequent excretion of excess salts. These mechanisms are of interest as the vesiculated trichomes of *Tamarix* have been documented by Manousaki *et al*. (2007) to excrete a range of other ions. Thus, an understanding of the mechanisms involved in the excretion of salts by *T. usneoides* could provide a model for the transportation and excretion of other metal ions as well as metal complexes.

PLANT GLANDULAR STRUCTURES AND MECHANISMS FOR SALT EXCRETION

The cellular mechanisms utilised by plants for the secretion and excretion of specific substances require a number of physiological adaptations to the cells that are involved in the process of transporting, concentrating and excreting the substance from the cytoplasm (Ding *et al.*, 2010). This is due to the fact that the substances that are excreted are processed against the concentration gradient found within the cells, i.e. the concentration of a substance that is being excreted/secreted tends to be far higher in the secretion than that of the cytoplasm of the cells of the surrounding tissue. Hence, plants glands are characterised by specific physiological adaptations that allow for the transportation of concentrated substances within

the cytoplasm and also prevent the movement of excreted substances back into the plant tissues (Thomson *et al.*, 1985).

Plant glandular structures can be differentiated according to their function. For instance, nectaries and salt glands each have distinctive mechanisms by which they function. However, there are similarities between the two. These similarities lie in the apparatus involved in the packaging and processing of the substances to be secreted (i.e. the endomembrane system *viz*. endoplasmic reticulum and Golgi bodies) as well as in the provision of energy for the transport and secretion/excretion of the substances. Hence, it is possible to draw analogies between the structure and function of different glandular structures despite the fact that they excrete different substances (Fahn, 1988).

Salt glands are characterised by having complex structures and many of these structures achieve very high rates of excretion (Flowers *et al.,* 2019). This may be due to the fact that the excretion of excess salts is a process whereby the plant is removing a potentially toxic substance. Excretion rates that are achieved by the plant are often dramatically higher than the rate of uptake by the roots (Lutge, 1993), ensuring that there is no accumulation of excess salts within the plant which would in turn disrupt other metabolic processes (Ksouri, *et al.*, 2007).

Due to the fact that concentrated salts affect cellular processes, there needs to be a mechanism which allows for the transportation of these salts to the site of excretion without affecting basic cellular processes. Ion movement from the rhizosphere to the xylem tissue of the roots occurs via apoplastic and symplastic processes, where ions are transported via the epidermis, exodermis, cortex, and finally via the endodermis (Steudle & Peterson, 1998). Ion selection primarily occurs at the endodermis, as the Casparian strip limits apoplastic transport

forcing ions to be transported symplastically via ion specific transporters located within the endodermal tissue (Bao *et al*., 2019). Halophyte plants are characterised by Casparian strips that are frequently in excess of three times wider than those documented in glycophytes (Peng *et al.*, 2004). Ding *et al*., 2010 proposed that the pathway by which salts are accumulated and transported to aboveground biomass prior to excretion occurs as follows: salts move via the apoplast until the endodermis where they are moved into the symplasm and transported to the xylem vessels. From the xylem they are either deposited in woody tissue where they are inert or they move via transpirational pull to the leaf. From the xylem vessels of the leaf there are two pathways that can be followed. The more energy-expensive method is where the excess salts from the xylem are directly parcelled into sub-cellular vesicles by endocytosis and then transported across the cell to the plasmalemma, whereupon the vesicle fuses with the cell membrane, expelling the salts from the cell (exocytosis) into the apoplast where they travel to plasmodesmata which then channel the salts into the adjacent cell where the process is repeated (an alternative to the exocytosis theory is where the endoplasmic reticulum traverses the plasmodesmata into a neighbouring cell as suggested by White and Barton 2011). This allows the excess salts to be transported from cell to cell within the tissues of the plant and ultimately to the site of salt excretion (Ding *et al.*, 2010). The second pathway utilised by plants is to off-load the excess ions into the apoplast whereupon the excess ions move along a concentration gradient toward the site of excretion. The concentration gradient is maintained by the rapid rates of excretion from the salt gland. Once at the salt gland, the excess ions move into the symplasm of the salt gland and are sequestered into micro-vesicle structures and actively excreted to the outer surface of the plant (Thomson *et al*., 1985).

According to Ding *et al.* (2010) in the salt gland, excretion occurs by direct sequestration of excess ions into micro-vesicles which are then transported to the plasmalemma, whereupon they fuse, releasing the ions contained in the micro-vesicle into the extracellular space. Alternatively, the micro-vesicles form “junctional complexes” where the channels on both the micro-vesicle membrane and the cell plasmalemma line up, allowing passage of solutes from the vesicle to the exterior of the cell (Ding *et al.*, 2010). It has been documented in certain halophytic species that there is a range of excess cations excreted from the specialised salt glands (Kadukova *et al*., 2008). This implies that the cellular mechanism for the removal of excess ions is not Na^+ specific but may be used as a method to maintain homeostasis for a number of potentially detrimental ions. Thus, in a study to determine sites of metal accumulation and excretion, it is prudent to begin the study at the cells which immediately surround structures involved in the excretion of excess salts. In the genus *Tamarix*, these are known as vesiculated trichomes and serve as the primary mechanism for the excretion of excess salts (Berry, 1970).



Figure 2: Salt excretion by *Tamarix usneoides* growing on a saline watercourse at Goodhouse in the province of the Northern Cape, South Africa

GOLD ACCUMULATION BY PLANTS

Gold is considered a "noble metal" and is largely unreactive unless conditions are highly acidic (Figure 3). However, studies have shown that the action of certain groups of microbes are capable of mobilising gold either as gold cyanide, gold thiosulphate or gold chloride complexes (Reith *et al*., 2007). Plant uptake and accumulation of gold tends to be limited, partly due to the fact that gold is not an element required for cellular process and because the unreactive nature of gold limits its potential to be mobilised within the rhizosphere (Figure 3). As such, the mean gold uptake by plants is only 10 ng/kg (Anderson *et al.*, 1999), an amount that is too low for it to be economically viable for plants to be used in the phyto-extraction of gold. However, it is possible to induce gold hyperaccumulation in plants through the addition of chelating agents (Anderson, *et al*., 2005). Additionally, cyanide in the soil (a

by-product of root wounding and the decomposition of leaf litter) can solubilise gold within the soil and allow for uptake. Ten times more gold has been found in cyanogenic plants when compared with similar non-cyanogenic species (Girling & Peterson, 1980). In northern Australia it was found that *Triodia pungens, Melaleuca lasiandra* and *Acacia bivenosa* showed elevated gold concentrations within their above-ground biomass which was associated with surface projections of gold bearing rock (Reid *et al.,* 2008) and in western Australia a *Eucalyptus* species growing over a shallow ore body accumulated gold nanoparticles within its leafy biomass (Lintern *et al.,* 2013).

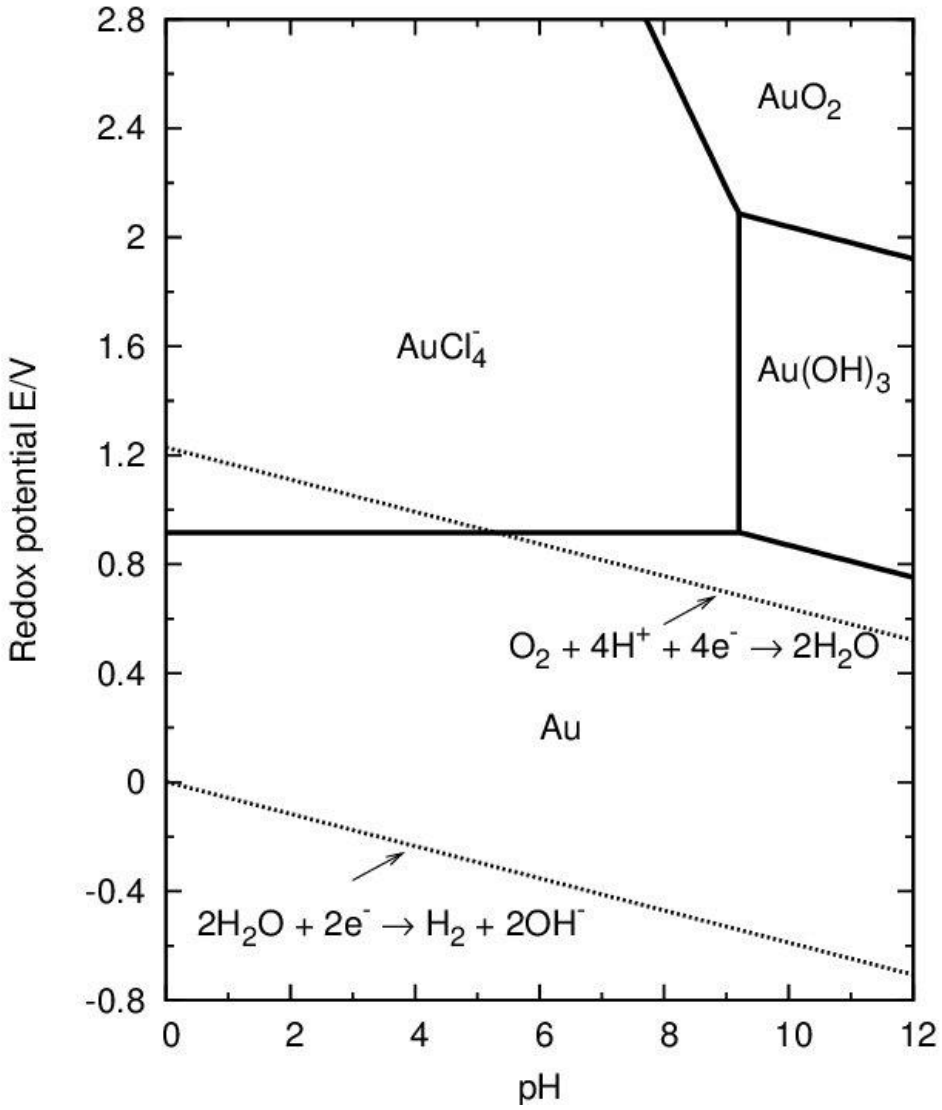

Figure 3: Gold pourbaix diagram (Mortier, 2006)

Studies by Girling & Peterson 1980 showed that gold availability to the plant for uptake is strongly dependent on the chemical form of the gold. Gold potassium cyanide showed the highest concentrations within the root of *Phacelia sericea* (3857 mg/kg) and had the highest translocation from root to shoot (shoot concentration was 87.3 mg/kg). Gold bromide and gold chloride were both accumulated to a similar degree, while gold thiosulphate showed the least uptake (458 mg/kg in root, 6.5 mg/kg in shoot) (Girling & Peterson, 1980). The pH of the soil also affects gold uptake, where lower pH resulted in higher uptake from the medium to the roots. However, gold translocation from root to shoot was not affected by pH (Anderson, *et al.*, 2005). Addition of soil ameliorants such as sodium cyanide, ammonium thiocyanate, or sodium thiosulfate increase gold bioavailability (Anderson *et al.*, 2013) and consequently there has been considerable interest in the application of these lixiviants in gold phytomining (Anderson *et al.*, 1999; Anderson *et al.*, 2005). In addition to being able to accumulate gold in ionic form, some studies have reported direct gold nanoparticle accumulation by plants, but pore size of the plant cell wall limits the size of nanoparticles that can potentially enter the plant (Navarro *et al.*, 2008). There has also been very little study in to the mechanism whereby nanoparticles enter the cell (Dykman and Shchyogolev, 2018). However, research into the accumulation of gold nanoparticle ligand complexes have shown that the uptake of the nanoparticle ligand complexes occurs via endocytosis (Li *et al.*, 2016). Their subsequent translocation is strongly affected by the size and surface charge of the gold nanoparticle, where positively charged nanoparticles remain within root tissue, while negatively charged nanoparticles are transported to stem and leaf tissue (Zhu *et al.*, 2012). Studies into the biological effects of gold nano-particles on plant growth have produced contradictory results. Plotnikov *et al.*, 2017 dosed winter barley with gold nano-particles of 10nm in size at

concentrations ranging from 1-10ug/l and showed that there was a dosage related suppression in root and leaf growth. In contrast, Arora *et al.* (2012) showed an increase in leaf size, increased stem length and diameter, as well as improved productivity in *Brassica juncea* after foliar application of gold nanoparticles.

There have been numerous studies into plant mediated nanoparticle synthesis (Anderson *et al.*, 2013), with evidence suggesting that some plants accumulate gold in ionic form and then reduce the accumulated Au ions *in planta* into nanoparticles. There is speculation that this occurs as a protective mechanism to limit the effects of harmful Au ions (Shukla *et al.*, 2015).

IN-SITU REMEDIATION OF CONTAMINATED SOILS USING PLANTS

Anthropogenic activities such as construction, mining, agriculture and industrial spills have significantly impacted soils globally (Kuppusamy *et al.*, 2016). Due to their nature, contaminant metals and metalloids do not biodegrade and so accumulate and bio magnify in ecosystems (Judy *et al.*, 2011). Due to the diffuse nature of such contaminants, effective remediation of contaminated material requires that large volumes of material are treated and the contaminant removed or rendered bio-unavailable (Pilon-Smits, 2005). *Ex situ* remediation techniques for contaminated soils typically consist of excavation of material and subsequent transportation to another location for decontamination (Kuppusamy *et al.*, 2016). This process is costly due to the machine time and man hours required and there is additional risk to other environments and personnel due to potential exposure to the contaminated material during its excavation and transportation (Kuppusamy *et al.*, 2016) as well as potential remobilisation of contaminants bound in the soils (Tutu *et al.*, 2008). Contaminated ground water is typically remediated using techniques such as 'pump and treat', where the contaminated groundwater is removed via a series of wells or boreholes and then the water

is treated using a range of techniques such as filtration through activated carbon, ion exchange membranes or artificial wetlands (Pavel and Gavrilescu, 2008). Studies by the United States Environmental Protection Agency have shown that the majority of pump and treat treatments require long time frames to meet the remediation goals (USEPA 1996).

In-situ technologies are thus an attractive alternative to *ex situ* remediation techniques as the cost of bulk material transport and personnel/ environmental exposure to the contaminant material is limited. A suite of techniques which utilise the biochemical traits of plants have been successfully used for *in-situ* remediation (Sarwar *et al.*, 2017). Phytoremediation is an umbrella term which is used to describe the group of separate related technologies. These include soil stabilisation, hydraulic control, rhizofiltration, phytostabilisation, phytovolatilisation and phytoextraction (Brooks 1998). Many remediation projects (for example the mine woodlands project, Dye & Weiersbye, 2010) utilise a variety of these technologies in order to achieve a specific end goal. For instance, a combination of hydraulic control and phytostabilisation can be utilised to decrease the rate of or prevent contaminated groundwater plumes, as the action of plants which maintain a high evapotranspiration rate utilises available water, while other plants which adjust the rhizosphere chemistry immobilise elements which may be in solution within the contaminant plume (Mendez & Maier, 2007).

A detailed understanding of how a plant species ameliorates the growing conditions of its rhizosphere as well as understanding the complex relationships that exist in a sites geochemistry is important for achieving a remediation project's end goals (Jung, 2008). Some plants are capable of fulfilling multiple roles within a remediation project. For instance, *Searsia lancea* is an accumulator of sulphur and chlorine, a stabiliser for aluminium, iron and chrome and maintains a high-water use (Joubert, 2018).

Phytoextraction technology is aimed at the physical removal of contaminants from the rhizosphere. Traditionally, the use of hyperaccumulating plant species was of key interest as these plants naturally accumulate specific elements to significant concentrations within their aboveground biomass (Anderson *et al*., 2005). However, the applicability of such species is often limited by shallow root systems (for example *Brassica juncea*), slow growth rates, or they are not be able to accumulate the suite of elements that need to be removed from a particular area (Sarwar *et al*., 2017). In recent years, an approach to this problem was to induce hyperaccumulation in a non-accumulator species. This can be achieved either through the use of microbiota, or lixiviants in order to increase the mobility of elements within the rhizosphere (Anderson *et al.*, 2005). This allows the non-accumulator species with the correct suite of physical characteristics such as fast growth rates or deep root systems, to accumulate an appreciable amount of a contaminant in their aboveground biomass (Sarwar *et al*., 2017). The disadvantages to this technique include the possibility of increased contaminant spread due to increased metal mobility as well a possibility of plant death as a result of the toxicity associated with the elevated contaminant concentrations within aerial tissues of the plant (Nowack *et al.*, 2006).

At the University of the Witwatersrand in Johannesburg, South Africa, the Ecological Engineering and Phytotechnology Programme encompasses both the development, and the on-site implementation, of methodologies to re-value mine wastes, land and water damaged through industrial activities in sub-Saharan Africa. Part of that goal is investigating *T. usneoides* ability to tolerate conditions such as those found on mine sites and its ability to accumulate a wide range of contaminants associated with acid mine drainage. In this regard a better understanding of the underlying biology of the species is fundamental. The present research forms part of that endeavour.

1.2. Aims and Objectives

The aim of this study was to investigate gold accumulation in *T. usneoides* in relation to elemental uptake, transportation and excretion processes. This was achieved through the following objectives:

1.) Determine if *T. usneoides* is capable of accumulating gold *in vitro* and to investigate *in vitro* whether the form of gold compound supplied, gold concentration and growth medium pH affected the growth of *T. usneoides* as well as gold uptake into root tissue and its translocation to shoot tissue.

2.) Determine the potential for *T. usneoides* to be used as an *in-situ* mechanism for the extraction of residual gold and other elements from a gold tailings storage facility where gold extraction occurred via the cyanidation process.

3.) Describe the microstructure of *T. usneoides* salt glands in order to elucidate possible excretion mechanisms for metal salts.

4.) Determine the cellular mechanisms and pathways used by *T. usneoides* to process and excrete excess solutes.

1.3. References

Anderson C. W. N., Bhatti S. M., Gardea-Torresdey J. & Parsons J. (2013). *In vivo* effect of copper and silver on synthesis of gold nanoparticles inside living plants. *ACS Sustainable Chemistry & Engineering*, 1(6), 640-648.

Anderson C. W. N., Brooks R. R., Chiarucci A., LaCoste C. J., Leblanc M., Robinson B. H., Simcock R. and Stewart R. B. (1999). Phytomining for nickel, thallium and gold. *Journal of Geochemical Exploration*, 67(1), 407-415.

Anderson C. W. N., Moreno F. & Meech, J. (2005). A field demonstration of gold phytoextraction technology., *Minerals Engineering*, 18 (4), 385-392.

Arora S., Sharma P., Kumar S., Nayan R., Khanna P. K., & Zaidi M. G. H. (2012). Gold-nanoparticle induced enhancement in growth and seed yield of *Brassica juncea*. *Plant growth regulation*, 66(3), 303-310.

Baker A. J. (1981). Accumulators and excluders - strategies in the response of plants to heavy metals. *Journal of plant nutrition*, 3(1-4), 643-654.

Bao Z., Bai J., Cui H., & Gong C. (2019). A missing link in radial ion transport: ion transporters in the endodermis. *Frontiers in Plant Science*, *10*.

Baum B.R. (1978). The genus *Tamarix*. Jerusalem, The Israeli Academy of Sciences and Humanities.

Berry W.L. (1970). Characteristics of salts excreted by *Tamarix aphylla. American Journal of Botany,* 57(10), 1226-1230.

Bert V., Meerts P., Saumitou-Laprade P., Salis P., Gruber W. & Verbruggen, N. (2003). Genetic basis of Cd tolerance and hyperaccumulation in *Arabidopsis helleri. Plant and Soil*, 249(1), 9-18.

Boyd R. S., & Martens S.N. (1992). The *raison d' etre* for metal hyperaccumulation by plants. In A. J. M. Baker, J. Proctor, and R.D. Reeves [eds.], The ecology of ultramafic (serpentine) soils, 279–289.

Boyd R.S., Davis M.A., Wall M.A. & Balkwill K. (2002). Nickel defends the South African hyperaccumulator *Senecio coronatus* (Asteraceae) against *Helix aspersa* (Mollusca: Pulmonidae). *Chemoecology*, 12, 91–97.

Brady K. U., Kruckeberg A. R., & Bradshaw Jr H. D. (2005). Evolutionary ecology of plant adaptation to serpentine soils. *Annual Review of Ecology, Evolution, and Systematics*, 243-266.

Brooks R. R. & Radford C. C. (1978). Nickel accumulation by European species of the genus *Alyssum*. *Proceedings of the Royal Society of London*, 200 (1139), 217-224.

Brooks R.R. (1998). General Introduction. In: R.R. Brooks (Ed), Plants that hyperaccumulate heavy metals: their role in phytoremediation, microbiology, archaeology, mineral exploration and phytomining. CAB International: Wallingford, England, pp. 1–12.

Brooks R. R., & Robinson B. H. (1998). The potential use of hyperaccumulators and other plants for phytomining. Plants that hyperaccumulate heavy metals—their role in phytoremediation, microbiology, archeology, *mineral exploration, and phytomining*. Cambridge: CAB International (1998): 327-356.

Clemens S., Palmgren M.G. & Krämer U. (2002). A long way ahead: understanding and engineering plant metal accumulation. *Trends in plant science*, 7(7), 309-315

Clemens S. (2006). Toxic metal accumulation, responses to exposure and mechanisms of tolerance in plants. *Biochimie*, 88, 1707–1719.

Coetzee H., Wade P., & Winde F. (2002). Reliance on existing wetlands for pollution control around the Witwatersrand gold/uranium mines of South Africa-Are they sufficient? In *Uranium in the aquatic environment* (pp. 59-64). Springer, Berlin, Heidelberg.

Dalton T.P., He L., Wang B., Miller M.L., Jin L., Stringer K.F., Chang X., Baxter C.S., & Nebert D.W. (2005). Identification of mouse SLC39A8 as the transporter responsible for cadmium-induced toxicity in the testis. *Proceedings of the Natural Academy of Science USA*, 102, 3401–3406.

Dennis A.M. (2008). Salt glands and elemental concentrations in leaves of *Tamarix usneoides* E. Mey ex Bunge (Tamaricaceae) grown on seepage from Highveld gold mines. unpublished Honours Project.

Devkota B. & Schmidt G. H. (2000). Accumulation of heavy metals in food plants and grasshoppers from the Taigetos Mountains, Greece. *Agriculture, ecosystems & environment*, 78(1), 85-91.

Ding F., Yang J.C., Yuan F., & Wang B.S. (2010). Progress in mechanism of salt excretion in recretohalopytes. *Frontlines of Biology*, 5(2), 164–170.

Dunn C.E., (2007). Biogeochemistry in mineral exploration. *Handbook of Exploration and Environmental Geochemistry*, Elsevier publishing.

Dye P. & Weiersbye I.M. (2010). The Mine Woodlands Project in the Witwatersrand Basin, South Africa: research strategy and progress. *Mine Water & Innovative Thinking*. 471-475.

Dye P.J., Jarmain C., le Maitre D., Everson C.S., Gush M. & Clulow A. (2008) Modelling vegetation water use for general application in different categories of vegetation. *Report to the Water Research Commission*.

Dyer B. (1894). On the analytical determination of probably available “mineral” plant food in soils. *Journal of the Chemical Society, Transactions*, 65, 115-167.

Dykman L. A. & Shchyogolev S. Y. (2018). The effect of Gold and Silver Nanoparticles on Plant Growth and Development. In: Y. Saylor and V. Irby [Eds] *Metal Nanoparticles*, 2018, Nova Science Publishers, Inc. pp 263 – 300

El Hayek E., Torres C., Rodriguez-Freire L., Blake J.M., De Vore C.L., Brearley A.J., Spilde M.N., Cabaniss S., Al A.M.S. & Cerrato, J.M., (2018). Effect of Calcium on the Bioavailability of Dissolved Uranium (VI) in Plant Roots under Circumneutral pH. *Environmental science & technology*, 52(22), 13089-13098

Ernst W.H.O., Krauss G.J., Verkleij J.A.C & Wesenberg J. (2008). Interaction of heavy metals with the sulphur metabolism in angiosperms from an ecological point of view. *Plant, Cell and Environment*, 31, 123–143.

Fahn A. (1988). Tansley Review No. 14 Secretory tissues in vascular plants. *New Phytologist*, 108, (3), 229-257.

Flowers, T. J., Glenn, E. P., & Volkov, V. (2019). Could vesicular transport of Na^+ and Cl^-be a feature of salt tolerance in halophytes?. *Annals of botany*, 123(1), 1-18.

Fricker F.P. (1996). Medical Uses of Gold Compounds: Past, Present and Future. *Gold Bulletin*, 29,2.

Galan, E. Gomez-Ariza, J.L., Gonzalez, I. Fernandez-Caliani, J.C. Morales, I. & Giraldez, I. (2003). Heavy metal partitioning in river sediments severely polluted by acid mine drainage in the Iberian Pyrite Belt, *Applied Geochemistry*, 18, 409–421.

Gardea-Torresdey J.L., Parsons J.G., Gomez E., Peralta-Videa J., Troiani H.E., Santiago P., Jose & Yacaman M. (2002). Formation and growth of Au nanoparticles inside live alfalfa plants. *Nano Letters*, 2, 397–401.

Gardea-Torresdey J. L., Peralta-Videa J. R., De La Rosa G. & Parsons J. G. (2005). Phytoremediation of heavy metals and study of the metal coordination by X-ray absorption spectroscopy. *Coordination chemistry reviews*, 249(17-18), 1797-1810.

Girling C.A. & Peterson P.J. (1980). Gold in plants. *Gold Bulletin*, 13, 4, 151-157.

Gold Fields Ltd, June 2009 Quarterly Report, Aug. 6, 2009

Golder & Associates, Rand Uranium, (2008). Environmental Impact Assessment for Rand Uranium's proposed re-processing of tailings for gold and uranium extraction in the Randfontein/Westonaria Region, Document no. 2, DEAT Reference No.: 12/12/20/1285, Golder Report No 8788-8175-23.

González A., Steffen K.L. & Lynch J.P. (1998). Light and Excess Manganese: Implications for Oxidative Stress in Common Bean, *Plant Physiology*, 118(2), 493-504.

Hagemeyer J., & Waisel Y. (1988). Excretion of ions (Cd^{2+}, Li^{+}, Na^{+} and Cl^{-}) by *Tamarix aphylla. Physiologia Plantarum*, 73(4), 541-546.

Halliwell B. & Gutteridge J.M.C. (1990). Role of free radicals and catalytic metal ions in human disease—an overview. *Methods Enzymology*, 186, 1– 85.

Heggo A., Angle J.S. & Chaney R.L. (1990). Effects of vesicular-arbuscular mycorrhizal fungi on heavy metal uptake by soybeans. *Soil Biology and Biochemistry*, 22(6), 865-869.

Joubert M. K. (2018) Contaminant fate in *Searsia Lancea* woodlands on acid mine drainage in the Witwatersrand Basin Goldfields. (MSc Dissertation, University of the Witwatersrand).

Judy J. D., Unrine J. M. & Bertsch P. M. (2010). Evidence for biomagnification of gold nanoparticles within a terrestrial food chain. *Environmental science & technology*, 45(2), 776-781.

Jung M. C. (2008). Heavy metal concentrations in soils and factors affecting metal uptake by plants in the vicinity of a Korean Cu-W mine. *Sensors*, *8*(4), 2413-2423.

Kadukova J., Manousaki E. & Kalogerakis N. (2008). Pb and Cd accumulation and phyto-excretion by salt cedar (*Tamarix smyrnensis* Bunge). *International Journal of Phytoremediation*, 10(1), 31-46.

Kempe J.O. (1983). Review of the water problems and control strategies in the South African mining industry. *Water science and technology*, 15(2), 27-58.

Kramer D., Läuchli A., Yeo A. R. & Gullasch J. (1977). Transfer cells in roots of *Phaseolus coccineus*: ultrastructure and possible function in exclusion of sodium from the shoot. *Annals of Botany*, 41(5), 1031-1040.

Kramer D. (1983) Genetically determined adaptations in roots to nutritional stress: correlation of structure and function. *Plant and Soil*, 72,167-173.

Krämer U., Talke I.N. & Hanikenne M. (2007). Transition metal transport. *FEBS Letters*, 581, (12-25), 2263-2272.

Krämer U. (2010). Metal hyperaccumulation in plants. *Annual review of plant biology*, 61, 517-534.

Kronsukker H.J. & Britto D.T. (2011). Sodium transport in plants: a critical review. *New Phytologist*, 189, 54–81.

Ksouri R., Megdiche W., Debez A., Falleh H., Grignon C. & Abdelly C. (2007). Salinity effects on polyphenol content and antioxidant activities in leaves of the halophyte *Cakile maritima*. *Plant Physiology and Biochemistry*, 45, 244-249.

Kuppusamy S., Palanisami T., Megharaj M., Venkateswarlu K., & Naidu R. (2016*). In-situ* remediation approaches for the management of contaminated sites: a comprehensive overview. In *Reviews of Environmental Contamination and Toxicology,* Volume 236 (pp. 1-115). Springer, Cham.

Lamb A.E., Anderson C.W.N & Haverkamp R.G., (2001). The induced accumulation of gold in the plants *Brassica juncea, Berkheya coddii* and chickory. *Chemistry in New Zealand*, 34-36.

Lasat M.M., Baker A.J.M, & Kochian L.V. (1996). Physiological characterization of root Zn^{2+} absorption and translocation to shoots in Zn hyperaccumulator and nonaccumulator species of *Thlaspi*. *Plant Physiology*, 112,1715-1722.

Lasat M.M. (2000). Phytoextraction of metals from contaminated soil: A review of plant/soil/metal interaction and assessment of pertinent agronomic issues. *Journal of Hazardous Substance Research*, 2, 5-1.

Li H., Ye X., Guo X., Geng Z., & Wang G. (2016). Effects of surface ligands on the uptake and transport of gold nanoparticles in rice and tomato. *Journal of hazardous materials*, 314, 188-196.

Lintern M., Anand R., Ryan C. & Paterson D. (2013). Natural gold particles in *Eucalyptus* leaves and their relevance to exploration for buried gold deposits. *Nature Communications*, 4, 2274.

Luttge U. (1993). Plant cell membranes and salinity: structural, biochemical and biophysical changes. *Revista brasileira de fisiología vegetal*, 5(2), 217-224.

Macnair M. R. (2003). The hyperaccumulation of metals by plants. *Advances in Botanical Research*, 40, 63-105.

Mendez M. O., & Maier R. M. (2007). Phytostabilization of mine tailings in arid and semiarid environments — an emerging remediation technology. *Environmental health perspectives*, *116*(3), 278-283.

Mallo S. J. (2012). Mitigating the activities of artisanal and small-scale miners in Africa: challenges for engineering and technological institutions. *International Journal of Modern Engineering Research*, 2(6), 4714-4725.

Manousaki E., Kadukova J., Papadantonakis N. & Kalogerakis N. (2007). Phytoextraction and phytoexcretion of Cd by the leaves of *Tamarix smyrnensis* growing on contaminated non-saline and saline soils. *Environmental Research*, 31, 326-332.

Mayonde S. G., Cron G. V., Gaskin J. F. & Byrne M. J. (2015). Evidence of *Tamarix* hybrids in South Africa, as inferred by nuclear ITS and plastid trnS–trnG DNA sequences. *South African journal of botany*, 96, 122-131.

McCarthy T. S., Venter J. S. (2006). Increasing pollution levels on the Witwatersrand recorded in the peat deposits of the Klip River wetland. *South African Journal of Science*, 102.

Mertens J., Vervaeke P., Meers E., & Tack F. M. (2006). Seasonal changes of metals in willow (*Salix* sp.) stands for phytoremediation on dredged sediment. *Environmental science & technology*, 40(6), 1962-1968.

Mortier T. (2006). An experimental study on the preparation of gold nanoparticles and their properties.

Mphephu N. F. (2004). Geotechnical environmental evaluation of mining impacts on the Central Rand. PhD Thesis submitted to the University of the Witwatersrand, Johannesburg.

Muir D. M. & Aylmore M. G. (2004). Thiosulphate as an alternative to cyanide for gold processing–issues and impediments. *Mineral Processing and Extractive Metallurgy*, 113(1), 2-12.

Mycock D.J., Frankland C.A. & Berjak P. (1985). Some effects of fluoride on the establishment and growth of propagules of *Bruguiera gymnorrhiza* and *Avicennia marina*. *South African Journal of Botany*, 51, 439-447.

Naicker K. Cukrowska E. & McCarthy T.S. (2003). Acid mine drainage arising from gold mining activity in Johannesburg, South Africa and environs, *Environmental Pollution*, 122, 29–40.

Navarro E., Baun A., Behra R., Hartmann N.B., Filser J., Miao A.J., Quigg A., Santschi P.H. and Sigg L., (2008). Environmental behaviour and ecotoxicity of engineered nanoparticles to algae, plants, and fungi. *Ecotoxicology*, 17(5), pp.372-386.

Nowack B., Schulin R., & Robinson B. H. (2006). Critical assessment of chelant-enhanced metal phytoextraction. *Environmental Science & Technology*, 40(17), 5225-5232.

Peng Y.H., Zhu Y.F., Mao Y.Q., Wang S.M., Su W.A., & Tang Z.C. (2004). Alkali grass resists salt stress through high [K^+] and an endodermis barrier to Na^+. *Journal of Experimental Botany*, 55, 939–949.

Pich A., Manteuffel R., Hillmer S., Scholz G., & Schmidt W. (2001). Fe homeostasis in plant cells: does nicotianamine play multiple roles in the regulation of cytoplasmic Fe concentration? *Planta*, 213(6), 967-976.

Pilon-Smits E. (2005). Phytoremediation. *Annual Review of Plant Biology*, 56, 15–39.

Plotnikov VK, Salfetnikov, AA, Golubev, AA, Dykman, LA. (2017). Effect of gold nanoparticles on seeds germination of winter barley. *Scientific Journal of KubSAU*, 127, 295-307

Pretorius, D. A. (1976). The nature of the Witwatersrand gold-uranium deposits. *Handbook of stratabound and stratiform ore deposits*, 29-88.

Reeves R.D. (2003). Tropical hyperaccumulators of metals and their potential for phytoextraction, *Plant and Soil*, 249, 57–65.

Reid N., Hill S. M. & Lewis D. M. (2008). *Spinifex* biogeochemical expressions of buried gold mineralisation: the great mineral exploration penetrator of transported regolith. *Applied Geochemistry*, 23(1), 76-84.

Rigal, A., Doyle, S. M., & Robert, S. (2015). Live cell imaging of FM4-64, a tool for tracing the endocytic pathways in Arabidopsis root cells. In *Plant Cell Expansion* (pp. 93-103). Humana Press, New York, NY.

Reith F., Lengke M. F., Falconer D., Craw D., & Southam G. (2007). The geomicrobiology of gold. The ISME Journal, 1(7), 567.

Sarwar N., Imran M., Shaheen M. R., Ishaque W., Kamran M. A., Matloob A. & Hussain S. (2017). Phytoremediation strategies for soils contaminated with heavy metals: Modifications and future perspectives. Chemosphere, 171, 710-721.

Scholander P. F., Hammel H. T., Hemmingsen E., & Garey W. (1962). Salt balance in mangroves. *Plant Physiology*, 37 (6), 722–729.

Sharma N. C., Sahi S. V., Nath S., Parsons J. G., Gardea-Torresdey J. L. & Pal T. (2007). Synthesis of plant-mediated gold nanoparticles and catalytic role of biomatrix-embedded nanomaterials. *Environmental Science and Technology*, 41, 5137–5142.

Sheoran A. S., Sheoran V., (2006). Heavy metal removal mechanism of acid mine drainage in wetlands: a critical review. *Minerals Engineering*, 19(2), 105-116.

Shukla D., Krishnamurthy S., & Sahi S. V. (2015). Microarray analysis of *Arabidopsis* under gold exposure to identify putative genes involved in the synthesis of gold nanoparticles (AuNPs). *Genomics data*, 3, 100-102.

Sors T., Ellis D. & Salt D. (2005). Selenium uptake, translocation, assimilation and metabolic fate in plants. *Photosynthesis Research*, 86, 373–389.

Starnes D., Jain A. & Sahi S.V. (2010). *In planta* engineering of gold nanoparticles of desirable geometries by modulating growth conditions: an environment-friendly approach. *Environmental Science and Technology*, 44, 7110–7115.

Steudle E., & Peterson C. (1998). How does water get through roots? *Journal of Experimental Botany,* 322, 775–788.

Sutton M.W., Weiersbye I.M., Galpin J.S & Heller D. (2006). GIS-based history of gold mining and risk assessment of post-mining land-uses on the Witwatersrand Basin of South Africa. In Fourie, A.B. & Tibbett, M. (eds.). *Proceedings of the 1st International Seminar on Mine Closure, Australian Centre for Geomechanics*, Perth.

Talke I., Hanikenne M. & Krämer U. (2006). Zinc dependent global transcriptional control, transcriptional de-regulation and higher gene copy number for genes in metal homeostasis of the hyperaccumulator *Arabidopsis halleri. Plant Physiology*, 142, 148–167.

Thomson W. W. & Platt-Aloia K. (1985). The ultrastructure of the plasmodesmata of the salt glands of *Tamarix* as revealed by transmission and freeze-fracture electron microscopy. *Protoplasma,* 125(1-2), 13-23.

Tutu H., McCarthy T.S. & Cukrowska E. (2008). The chemical characteristics of acid mine drainage with particular reference to sources, distribution and remediation: The Witwatersrand Basin, South Africa as a case study. *Applied Geochemistry*, 23 (12), 3666-3684.

Tutu H., Camden-Smith B., Cukrowska E. M., Bakatula E. N., Weiersbye I. M. & Sutton M. S. (2011). Mineral efflorescent crusts as sources of pollution in gold mining environments in the Witwatersrand Basin. Mine Water – Managing the Challenges", *IMWA 2011*.

Tutu H., Cukrowska E. M., Dohnal V., & Havel J. (2005). Application of artificial neural networks for classification of uranium distribution in the Central Rand goldfield, South Africa. *Environmental Modeling & Assessment*, 10(2), 143-152.

van der Zaal B. J., Neuteboom L. W., Pinas J. E., Chardonnens A. N., Schat H., Verkleij J. A. & Hooykaas P. J. (1999). Overexpression of a novel *Arabidopsis* gene related to putative

zinc-transporter genes from animals can lead to enhanced zinc resistance and accumulation. *Plant Physiology*, 119(3), 1047-1056.

Vorster C.J. (2000). Gold Deposits of the Witwatersrand Basin, *Council for Geosciences South Africa* http://www.geoscience.org.za/images/Maps/golddeposits.gif

Wahid A., & Ghazanfar A. (2006). Possible involvement of some secondary metabolites in salt tolerance of sugarcane. *Journal of Plant Physiology*, 163(7), 723-730.

Walters C. R., Somerset V. S., Leaner J. J. & Nel J. M. (2011). A review of mercury pollution in South Africa: current status. *Journal of Environmental Science and Health*, Part A, 46(10), 1129-1137.

Weiersbye I.M. (2007). Global review and cost comparison of conventional and phyto-technologies for mine closure. Plenary paper in A.B. Fourie, M. Tibbett and J. Wiertz (eds), *Mine Closure 2007 - Proceedings of the 2nd International Seminar*, Santiago, Chile. Publ. Australian Centre for Geomechanics and the University of Western Australia, Perth, ISBN 978-0-9804 185-0-7, pp 13-31

Weiersbye I.M. & Witkowski (1998). The structure, diversity and persistence of naturally-colonizing and introduced vegetation on gold tailings and tailings-polluted soils. *Plant Ecology & Conservation*, 8, 224.

Weiersbye I.M., Witkowski E. T. F. & Reichardt M., (2006). Floristic composition of gold and uranium tailings dams, and adjacent polluted areas, on South Africa's deep-level mines. *Bothalia*, 36(1), 101-127.

White R. G. & Barton D. A. (2011). The cytoskeleton in plasmodesmata: a role in intercellular transport? *Journal of experimental botany*, *62*(15), 5249-5266.

Norman N. & Whitfield G. (2006) ''Geological Journeys''. p. 38-49, 60–61. Struik Publishers, Cape Town.

Wilson H., Mycock D., & Weiersbye I. M. (2017). The salt glands of *Tamarix usneoides* E. Mey. ex Bunge (South African Salt Cedar). *International journal of phytoremediation*, 19(6), 587-595.

Winde F. & Stoch E. J. (2010). Threats and opportunities for post-closure development in dolomitic gold mining areas of the West Rand and Far West Rand (South Africa)–a hydraulic view Part 1: Mining legacy and future threats. *Water SA*, 36(1).

Yang M. J., Yang X. E. & Volker R. (2002). Growth and nutrient composition of *Elsholtzia splendens Nakai* under copper toxicity. *Journal of Plant Nutrition*, 25(7), 1359 - 1375.

Yang X., Feng Y., He Z. & Stoffella P.J. (2005). Molecular mechanisms of heavy metal hyperaccumulation and phytoremediation. *Journal of Trace Elements in Medicine and Biology*, 18, 339–353.

Zhu Z. J., Wang H., Yan B., Zheng H., Jiang Y., Miranda O.R., Rotello V.M., Xing B. & Vachet R.W., (2012). Effect of surface charge on the uptake and distribution of gold nanoparticles in four plant species. *Environmental science & technology*, 46(22), 12391-12398.

2. *In vitro* growth and accumulation of gold within tissues of *Tamarix usneoides* (southern African salt cedar, Tamaricaceae).

Hayden T. Wilson, David J. Mycock, Anthony Mader and Isabel M. Weiersbye

University of the Witwatersrand, Johannesburg, Faculty of Science, School of Animal, Plant and Environmental Sciences, +27 (11) 717 6403, Private Bag 3 Wits 2050, South Africa.

Hayden.Wilson@students.wits.ac.za, David.Mycock@wits.ac.za, anthonymader91@hotmail.com, Isabel.Weiersbye@wits.ac.za

The following chapter is in scientific manuscript format, as such there is some repetition of contextualising information and background information.

2.1. Abstract

Tamarix usneoides E. Mey ex Bunge is a halophyte riparian tree species indigenous to south western Africa that has been introduced to parks as well as gold, uranium, platinum and copper mines in southern Africa. Previous studies have identified a range of elements, including gold, within the roots and leaves of *T. usneoides* and *T. ramossisima X usneoides* species. This study investigated if *T. usneoides* explants grown *in vitro* are capable of gold accumulation and determined whether factors such as gold chemical form, concentration and growth medium pH affect explant growth, uptake and gold tissue allocation. Three forms of gold were tested (gold chloride, gold potassium cyanide and gold sodium thiosulphate) at doses of 0.5 to 50 mg/kg gold in liquid nutrient media under controlled environmental conditions. Based on organ concentrations, gold bioavailability to *T. usneoides* was in the order of gold potassium cyanide > gold chloride > gold sodium thiosulphate, and accumulation followed a linear pattern in relation to substrate.

The highest concentration of gold associated with the root tissue (8093 mg/kg) occurred at a dose of 50 mg/kg gold chloride whereas the highest concentration in shoot tissue (219 mg/kg) occurred at a dose of 50 mg/kg gold potassium cyanide. These concentrations of gold in *Tamarix* root and shoot are well above those found in gold tailings spills and ore bodies (generally in the range of 0.2 to 10 mg/kg). Explants showed toxicity symptoms from 25mg/kg media gold concentration for the gold potassium cyanide trials, while the gold sodium thiosulphate and gold chloride trials showed no evidence of growth depression or toxicity. pH of the growth medium did not affect explant growth, nor gold uptake into roots but did affect gold translocation into shoots, where a lower pH of 4.6 limited gold percentage recovery when compared to pH 5.6 and 7.6. These results demonstrate that *T. usneoides* can hyperaccumulate gold from a range of compounds in liquid media under suitable conditions, and imply that there is a possibility that *T. usneoides* could be used for the *in-situ* extraction of gold from metallurgical effluents or spillages.

Keywords.

Gold, phytomining, tissue culture, hyperaccumulation.

2.2.Introduction

Historically, gold extraction processes were not efficient and, as a result, some mine tailings in South Africa contain gold in low concentrations (0.2- 0.5 mg/kg) (Naicker *et al.* 2003, Mphephu, 2004). In South Africa, most rock containing gold is associated with sulphide minerals such as iron pyrite and arsenopyrite and it is estimated that gold tailings contain, on average, two percent sulphur (Weiersbye and Witkowski, 1998). Sulphide minerals, on exposure to air, oxygenated water and the action of sulphur-utilising bacteria (Thiobacillus spp.), oxidise with the consequent release of sulphuric acid and associated metals, resulting in so called acid mine drainage(AMD) (Akcil and Koldas 2006). Consequently there is a lowering of pH and concomitant mobilisation of metals and metalloids contained in the tailings and contaminated soils (Galan *et al.* 2003, Naicker *et al.* 2003, Tutu *et al.* 2008).

Frequent failures of Tailings Storage Facilities (TSF) as well as metallurgical plant and sewerage effluent spillages, TSF erosion and movement in solution in AMD, have led to significant amounts of gold along with other metals and contaminants being dispersed into the environment (Sutton *et al*., 2006, Tutu *et al.*, 2008). The contaminants associated with these pollution sources typically accumulate in shallow depressions or “sink” areas such as wetlands, pans and drainage lines (Coetzee *et al.*, 2002, Sheoran & Sheoran 2006).

These polluted sinks represent a source of the precious metal and despite the low

concentrations, associated with such deposits, it is still economically viable to re-mine them for extraction of gold (I.M. Weiersbye, *pers comm*). Current methods for gold recovery from old tailings spillages and polluted soils consist of excavating the material, and reprocessing it through the metallurgical plant for gold recovery (Muir & Aylmore 2004). However, a major limitation to the recovery of gold from old spillages is the presence of organic matter from decayed vegetation, which compromises the metallurgical extraction process. An additional problem with this approach is that disturbance of the sediments in these polluted sinks allows for the oxidation and leaching of contaminants that were previously precipitated or bound in the sediments, resulting in the subsequent re-release of these contaminants into the environment (Tutu *et al.,* 2005, 2008; McCarthy & Venter 2006). Thus there is a requirement for an *in-situ* technology that allows for the extraction and removal of salts and metals from the impacted sediments, while also reducing the rate of contaminant spread through hydraulic control.

The existence of free gold ions has been shown to be thermodynamically unfavourable as the standard redox potentials of Au^{+} (1.68 V) and Au^{3+} (1.50 V) exceed that of water (1.23 V) (Boyle 1979; Vlassopoulos and Wood 1990). However, studies have shown that the action of plants as well as certain fungi and bacteria are capable of oxidising gold into gold complexes (Reith *et al*., 2007, Maluckov 2015). Studies into microbially assisted gold oxidation have shown that depending on the site geochemical characteristics, microbially induced gold complexes will be in the form of gold cyanide where organic matter is available, gold chloride in arid saline environments and gold thiosulphate in acid environments (Southam *et al.*, 2009). These chemical forms of gold are of interest as they are biologically available to plants for accumulation, where gold complexes present within the plants rhizosphere are accumulated,

either bound to root tissue or translocated into aboveground biomass (Anderson *et al.,* 1999).

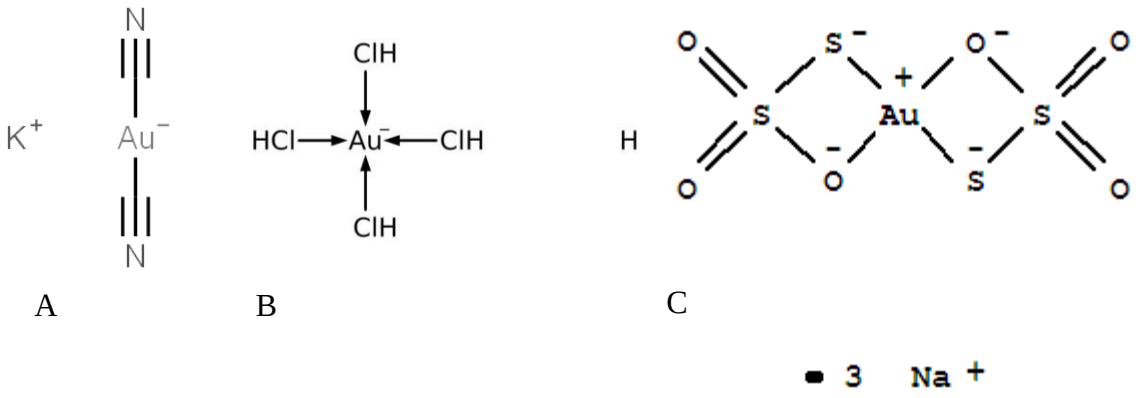

Figure 4: Diagram showing the structure of the gold complexes in solution for A.) Gold Potassium Cyanide, B.) Gold Chloride and C.) Gold Sodium Thiosulphate

Tamarix usneoides E. Mey. ex Bunge (South African Salt Cedar, Tamaricaceae) is a riparian halophyte tree species indigenous to the western regions of southern Africa, which inhabits saline, wet environments such as salt pans and riparian zones (Baum 1978). In saline environments, plants from the genus *Tamarix* such as *T. usneoides* excrete excess ions from specialised glands on the surface of their leaves known as vesiculated trichomes (Thomson *et al.,* 1969, Wilson *et al.*, 2017). Initial studies into the content of root and shoot tissues of *T. usneoides,* detected a range of elements including lithium, sodium, magnesium, sulphur, chlorine, potassium, calcium, manganese, cadmium, nickel, cobalt, copper, molybdenum, arsenic, selenium, zinc, gold, lead and uranium at concentrations that exceed substrate or ambient geological background concentrations (Dennis 2008, Weiersbye *unpublished data*). Due to its salinity tolerance and ability to extract a range of contaminant ions from acid mine drainage, *T. usneoides* is being utilised for the phytoremediation of affected soils and groundwater on Witwatersrand Basin gold mines (the Mine Woodlands Project (Dye *et al.,* 2018)).

This study describes an *in vitro* plant-based approach to gold recovery from solution, and the optima achieved under non-limiting conditions for growth and gold bioavailability by investigating if gold chemical species, concentration and growth medium pH affects gold uptake and translocation *in planta*.

2.3. Methods

MATERIAL COLLECTION AND MOTHER STOCK PROPAGATION

The results from a genetic survey of the populations of *Tamarix* in South Africa (Mayonde *et al.*, 2015) were used to select verified *T. usneoides* trees for the present study. Stem sections of 15cm in length and diameter of 0.8-1.2cm were collected from green apical branches. The stem sections were then treated with Copper oxychloride, 8.5 g/l prior to transportation to the greenhouse. The stem sections were planted 10cm deep in 750 ml plastic planting bags containing 1:4 parts potting compost and washed river sand. Cuttings were then established within a glass greenhouse experiencing temperatures in the range of 15-30 ^{o}C and overhead irrigation with potable chlorinated water (10 minutes every 8 hours). Cutting maintenance consisted of weeding, treatment with Benlate 500WP (5 ml/l) (active ingredient, benzimidazole [500 g.kg^{-1}]) or Previcure (1 ml/l) (active ingredient, propamocarb) every 4 weeks and fertilisation with Nitrosol® (3.33 ml/l) every 6 weeks.

PROPAGATION OF *IN VITRO* MATERIAL

400 three cm long apical shoots were harvested from the greenhouse cuttings. Working within a laminar flow bench, the apical shoots were surface decontaminated in 2% sodium hypochlorite for 15 minutes and rinsed in sterilised deionised water (MilliQ). The shoots were

added to 10ml borosilicate growth vials containing 2ml of sterilised quarter strength Murashige and Skoog (1962)(MS) growth medium buffered to one of three different pHs (4.8, 5.6 or 7.6) with NaOH. Vials were incubated in a growth chamber at a constant temperature of 25°C and photoperiod of 16L/8D hours supplied by fluorescent lights producing approximately 2000 lumens of output. Only explants that exhibited no tissue browning or phenolic production were selected for the subsequent gold treatments.

GOLD UPTAKE AND TRANSLOCATION BY *TAMARIX USNEOIDES* EXPLANTS *IN VITRO*

Working aseptically, four clones of 36 six week old explants each were transferred to sterilised 10ml borosilicate growth vials containing 2ml of quarter strength MS liquid basal growth medium buffered to a pH of 4.8, 5.6 and 7.6. Each of the vials was dosed with one of three gold compounds (gold (III) chloride ($HAuCl_4$), gold sodium thiosulphate ($Na_3Au(S_2O_3)^{2}\cdot 2H_2O$) and gold potassium cyanide (C_2AuKN_2), resulting in final Au concentrations of: 0.5mg/kg, 5mg/kg, 25mg/kg and 50mg/kg (Quarter strength MS used to prevent ion toxicity, See appendix A Table 13 for calculations on tissue culture media ion concentrations). This resulted in a total of 144 plantlets being grown for this experiment (3 Ph treatments X 3 Gold Compound types X 4 Gold concentrations x 4 Clonal Replicates). The vials were agitated every 3 days by gently swirling for 5 seconds. Explant position within the growth chamber was randomised every 3 days. Explants were incubated under growth chamber conditions for 2 weeks prior to harvest.

GROWTH MEASUREMENTS AND ANALYSIS OF GOLD

Weekly measurements of the length of the root, number of roots, number of root branches, shoot length of the longest shoot and the number of shoots on each of the explants were taken for the duration that the plantlets were grown *in vitro*.

The explants were harvested at 8 weeks (14 days after gold treatment) and separated immediately into shoots and roots. Shoot tissue was not rinsed (to avoid loss of any exudate from salt glands). Root tissue was rinsed in sterilised deionised water (MilliQ) to remove culture medium without dislodging any Au bound on the surface of the roots. Root and shoot tissue were lyophilised for three days at -85 ^{o}C (Labconco FreeZone 4.5l freeze dry system). Dry mass was then determined by weighing the tissue using a 5-place balance.

The samples were digested under closed microwave conditions in 5 ml HNO_3 and 2 ml of HCl (Wu *et al.*, 1997) optimised by the Central Analytical Facility, University of Stellenbosch, South Africa, specifically for small samples. The digestion was subsequently diluted to a volume of 50 ml with de-ionised water. The samples were then assayed for gold using inductively coupled plasma mass spectrometry (ICP-MS), calibrated with multi-elemental standards and corrected with digestion blank solutions, alongside gold spiked (0.014 and 0.14 mg/kg) certified reference material (National Bureau of Standards Orchard Leaf No. 1571) (see Appendix A Table 14 for the recovery % from the spiked CRM samples). Gold concentration on a dry mass basis (mg/kg) was calculated using the analytical dilution factor (derived from sample mass and total analytical volume).

VERIFICATION OF GOLD ACCUMULATION *IN PLANTA*

3 leaf samples from plantlets grown in media consisting of 50ppm Au at pH 5.6 from each gold compound treatment were selected for verification of gold accumulation *in planta*. Selected samples of *in vitro* material were fixed overnight at room temperature (20 – 25 ^{o}C) in 2 % gluteraldehyde in a 0.05 M sodium phosphate buffer, pH 7.2, followed by rinsing four times in the buffer, post-fixation for two hours in 2 % OsO_4 and a subsequent rinsing four times in buffer. The material was then dehydrated through a 10, 25 and 50 % graded ethanol

series. The material was then rinsed in 75 % ethanol and passed through four sequential dehydrations of 15 minutes each, starting with two in 100 % ethanol and then two in propylene oxide.

The tissue was then infiltrated in a solution consisting of 50 % Spurr epoxy resin (Spurr, 1969) and propylene oxide for 4-5 hours. This mixture was then replaced with pure resin and allowed to infiltrate for 14 hours. The samples were then placed in resin trays and polymerised at 70 ^{o}C for 8-12 hours.

Samples were sectioned to a thickness of 5 µm, placed on glass slides and carbon coated to a thickness of 10nm layer using an EMITECH K550 X sputter coater. Elemental analysis consisted of first collecting photographs using the optical microscope built into the CAMECA SX5-FE EPMA, followed by elemental mapping of areas of interest using wavelength dispersive spectroscopy (WDS). Areas of interest included the areas surrounding the salt glands of the leaf as gold was previously detected within the excreta of *T. usneoides* (Dennis, 2008) and as such it is likely that gold that is accumulated prior to excretion would likely be in the tissue immediately surrounding the salt gland.

DATA PROCESSING AND STATISTICAL ANALYSIS

Differences in mass and explant growth were determined using a combination of statistical analytical procedures.

Percentage recovery was calculated as follows (Jiang *et al.*, 2015):

Amount of gold (g) in tissue / amount (g) of gold in media x 100 ***(1)***

Bioconcentration Factors (BCF) for gold were calculated for the whole plantlet, root and shoot, where a BCF of >1.0 indicates gold accumulation *in planta* from the media (Raskin *et al.*, 1994):

BCF = concentration of gold in plant, root or shoot / concentration of gold in media x 100 (2)

Translocation Factors (TF) for gold were calculated for shoot tissue, where a TF of > 1.0 indicates gold accumulation by the shoot (Raskin *et al.*, 1994):

TF = concentration of gold in shoot (mg/kg) / concentration of gold in root (mg/kg) x 100 (3)

The data were checked for normality using a Shapiro-Wilk test (Shapiro & Wilk, 1965). As the data was skewed, a Kruskal-Wallis (1962) test was used to determine the effect of gold dose and pH treatment on plantlet dimensions, gold concentration, BCF and TF. Multiple pairwise comparisons (Dunn, 1961) were used to identify where differences occurred and to determine relationships between treatments. Kruskall-wallis tests showed no differences in the pH trials, so data from those trials were combined and all summaries and statistics reported here are for the combined pH trials.

2.4. Results

VERIFICATION OF GOLD ACCUMULATION *IN PLANTA*

Wavelength dispersive spectroscopy showed that when grown *in vitro, T. usneoides* is capable of accumulating gold into root tissue and subsequently translocating it to shoot tissue (Figure 5). The highest median concentrations were found in root tissue which had been treated with gold chloride at a concentration of 50mg/kg, while the highest shoot concentration was associated with the 50mg/kg gold cyanide treatment (Table 1). Gold percentage recovery values ranged between 2% and 29%, with the highest percentage recovery values in root tissue treated with gold cyanide, while for shoot tissue the highest percentage recovery values were associated with the 0.5mg/kg gold chloride treatment. Bioconcentration factors were highest in root tissue, with the highest being in the roots of the 25mg/kg gold chloride treatment, while conversely the highest median bioconcentration factor in shoot tissue was associated with the gold thiosulphate treatment at 0.5mg/kg. Translocation factors also varied with gold compound type, with gold potassium cyanide at 50mg/kg having the highest median gold translocation factors (Table 1).

Table 1: Summary statistics for the measured variables for each tissue by gold compound type and media gold compound concentration.

Measure	Au compound	Tissue type	0 mg/kg	0.5 mg/kg	5 mg/kg	25 mg/kg	50 mg/kg
Tissue Au concentration (mg/kg)	Au_Cl	n		14	13	6	15
		Root		106.27 ±±79.76	692.35± 1784.09	8242.29± 5611.14	8903.97± 9146.96
		Shoot		3.38 ± 1.62	14.77 + 5.6	96.07 + 106.36	105.87 + 56.04
	Au_CN	n		15	16	6	14
		Root		94.52 ± 79.23	627.87 ± 876.12	1612.56 ± 2397.96	2084.76 ± 1861.22
		Shoot		3.23 ± 2.69	28.12 ± 19.67	160.39 ± 36.32	269.87 ± 163.56
	Au_S2O3	n		15	14	6	14
		Root		92.70 ± 119.69	738.76 ± 722.19	1627.92 ± 2017.64	4577.03 ± 3709.98
		Shoot		3.8 ± 2.35	16.67 ± 17.82	109.3 ± 56.01	75.88 ± 118.78
	None	n	9				
		Root	1.26 ± 3.33				
		Shoot	0.33 ± 0.79				
% gold recovered from medium	Au_Cl	n		14	13	6	15
		Root		22.81 ± 11.11	20.95 ± 12.11	24.90 ± 10.19	25.82 ± 13.22
		Shoot		9.77 ± 5.6	2.91 ± 3.04	8.12 ± 5.14	2.71 ± 1.44
	Au_CN	n		15	16	6	14
		Root		28.36 ± 18.13	29.68 ± 19.41	4.39 ± 4.79	5.49 ± 12.64
		Shoot		9.76 ± 7.36	7.35 ± 3.05	7.71 ± 1.91	6.22 ± 3.34
	Au_S2O3	n		15	14	6	14
		Root		23.20 ± 18.13	10.26 ± 24.26	5.06 ± 3.88	8.68 ± 20.42
		Shoot		9.68 ± 10.44	4.24 ± 4.39	4.04 ± 4.19	2.08 ± 2.93
	None	n	9				
		Root	0				
		Shoot	0				

Bioconcentration factor (%)	Au_Cl	n	14	13	6	15
		Root	21254.03 ± 15952.8	13847.00 ± 35681.85	32969.18 ± 22444.56	17807.94 ± 18293.93
		Shoot	675.32 ± 323.97	295.57 ± 112.16	384.29 ± 425.46	211.75 ± 112.08
	Au_CN	n	15	16	6	14
		Root	18904.37 ± 15845.03	12557.53 ± 17522.56	6450.25 ± 9591.87	4169.52 ± 3722.44
		Shoot	646.28 ± 538.04	562.4 ± 393.57	641.58 ± 145.3	539.75 ± 327.13
	Au_S2O3	n	15	14	6	14
		Root	18540.54 ± 23937.23	14775.32 ± 14443.99	6511.70 ± 8070.58	9154.06 ± 7419.96
		Shoot	759.95 ± 469.15	333.4 ± 356.46	437.21 ± 224.05	151.77 ± 237.57
	None	n	9			
		Root	0			
		Shoot	0			
Translocation factor (%)	AuCl	n	14	13	6	15
		median	3.6 ± 2.03	1.87 ± 1.74	2.47 ± 1.42	0.79 ± 1.3
	AuCN	n	15	16	6	14
		median	3.68 + 3.33	3.89 ± 2.54	9.37 ± 3.58	14.43 ± 9.93
	Au_S2O3	n	15	14	6	14
		median	5.46 ± 9.43	2.74 ± 4.8	6.3 ± 2.02	2.62 ± 1.57
	None	n	9			
		median	29.87 ± 11.32			

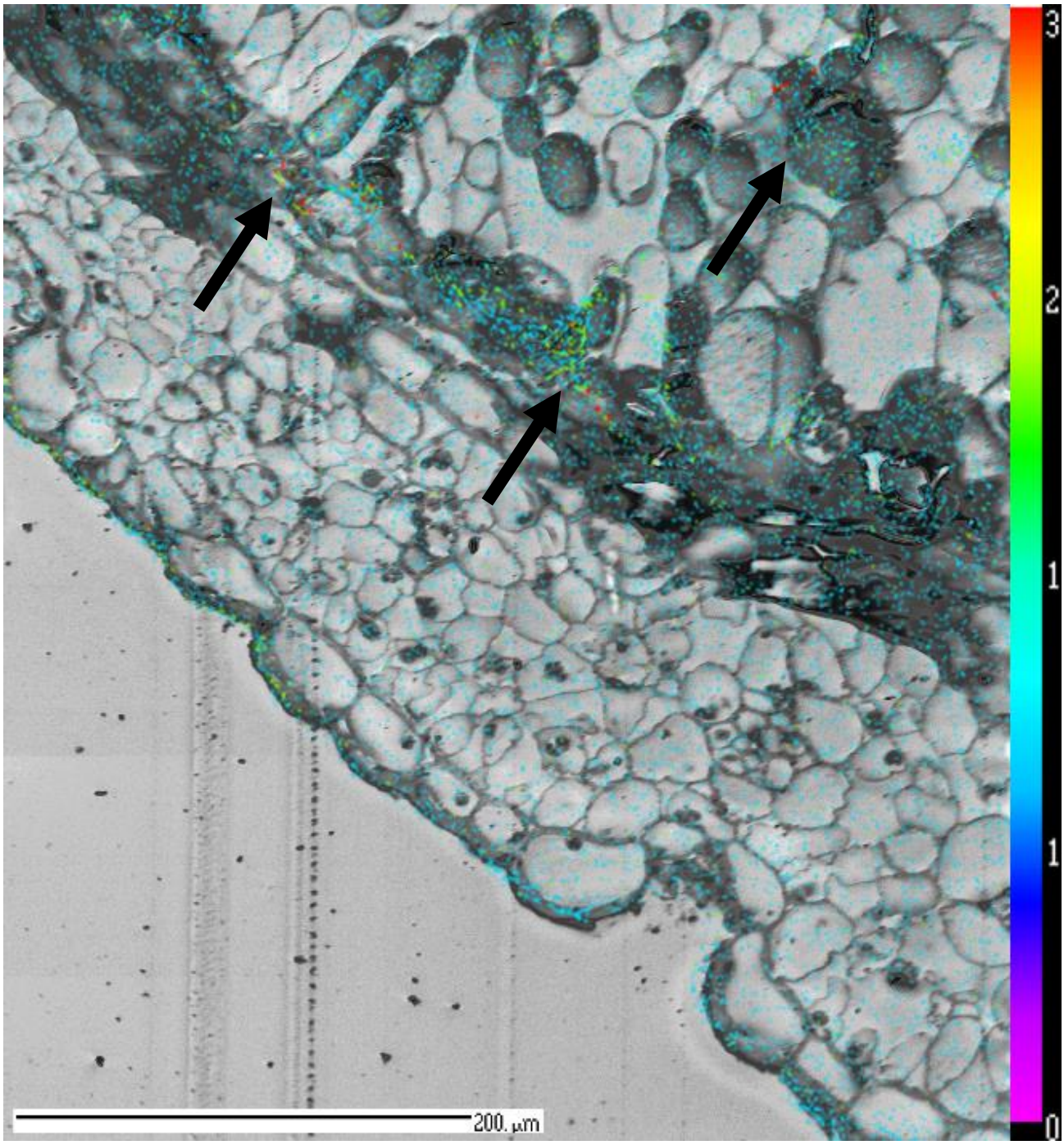

Figure 5: Gold accumulation within shoot tissue of *T. usneoides* plantlets grown in Murashige and Skoog medium enriched with 25mg/kg gold thiosulphate at pH 5.6, detected using WDS. Count data is on a scale of 0-3 where counts of 3 indicate higher gold concentrations Arrow shows areas of higher elemental accumulation.

GROWTH AND GOLD ACCUMULATION OF *IN VITRO* MATERIAL

Data from the combined results of the gold compound and concentration trials showed that the pH of the growth medium had no discernible effect on the growth and development of *T. usneoides in vitro,* with the exception of degree of root branching where there were significantly fewer branches in the treatments with a growth medium pH of 7.6 (Table 2). Additionally, pH had no effect on gold uptake and accumulation (Table 3)

The combined results of the pH trials showed that gold compound type had little effect on the growth of the *in vitro* material(Table 4). However, gold compound concentration had an effect, where plantlets dosed with 0.5 mg/kg gold had a higher degree of root branching than the more concentrated treatments, while in contrast, the plantlets dosed with a growth medium concentration of 50 mg/kg gold had increased the number of shoots when compared to the plantlets which received lower doses of gold in their growth medium (Table 5) .

Table 2: Summary Statistics for growth parameters measured for *T. usneoides* plantlets grown *in vitro* at 3 different pH values

	pH				Multiple pairwise comparisons			
	4.6	**5.6**	**7.6**	**p-value**				**p-value**
Mean shoot length (mm) per plantlet	46	45.5	39	0.27	5.6	-	4.6	0.83
					7.6	-	4.6	0.25
					7.6	-	5.6	0.58
Mean number of shoots per plantlet	17	17	16	0.26	5.6	-	4.6	0.40
					7.6	-	4.6	0.28
					7.6	-	5.6	0.97
Mean number of roots per plantlet	3	4	3	0.46	5.6	-	4.6	0.51
					7.6	-	4.6	0.55
					7.6	-	5.6	0.99
Mean root length per plantlet	49	61	54	0.13	5.6	-	4.6	0.13
					7.6	-	4.6	0.34
					7.6	-	5.6	0.86
Mean number of root branches per plantlet	36	38	28	0.01	5.6	-	4.6	0.43
					7.6	-	4.6	0.22
					7.6	-	5.6	**0.01**

Table 3: The effect of pH on gold concentration in tissue (Tis conc) of *Tamarix usneoides* plantlets grown *in vitro* by tissue gold concentration, gold percentage recovery (Rec) , gold bioconcentration (Bioconc) and gold translocation (Trans) per tissue type.

Tissue	Test	chi-squared	p-value
Root	Tis_conc by pH	0.18166	0.9132
Root	Rec by pH	3.8431	0.1464
Root	Bioconc by pH	1.0613	0.5882
Shoot	Tis_conc by pH	2.0491	0.3589
Shoot	Rec by pH	4.1803	0.1237
Shoot	Bioconc by pH	0.25307	0.8811
Shoot	Trans by pH	1.0356	0.5958

Table 4: Mean plantlet root length, root number and degree of root branching after a two-week treatment period with one of three gold compounds.

	Plantlet Treatment				
	$HAuCl_4$	C_2AuKN_2	$Na_3Au(S_2O_3)_2 \cdot 2H_2O$	Control	**p-value**
Mean shoot length (mm)	56.5	54	55	49	0.8866
Mean number of roots	3	4	3	3	0.2551
Mean root branching	32	37	33	30	0.3211

Table 5: *Tamarix usneoides* growth at different gold compound dosages

Gold Concentration	0 mg/kg	0.5 mg/kg	5 mg/kg	50 mg/kg	p-value
Shoot length (mm)	36	46.5	45	46.5	0.20
Number of shoots	15	17	15.5	19	**0.05**
Root length	49	54.5	56.5	56.5	0.78
Number of roots	3	4	3	3	**0.04**
Root branching	30	33	32	40	0.31

The concentration of gold in the medium affected uptake with the lower gold treatment concentrations, resulting in higher percentage recovery values (Table 1; Figure 6). Similarly, bioconcentration factors were typically higher when the material was treated with lower gold concentrations (Figure 6; Table 1; Table 6). However, the actual gold concentration in the tissues showed the opposite trend, where the higher concentration gold treatments resulted in a higher uptake by the roots and shoots (compare the 0.5mg/kg trial Au tissue concentration =9.79mg/kg with the 50mg/kg trial Au tissue concentration =550mg/kg; Figure 6; Table 6).

Table 6: Dunns pairwise comparison p-values showing the compounds which had significant differences for each of the measured variables for each tissue and medium gold compound concentration.

Tissue	Variable	Comparison	0.5 mg/kg	5 mg/kg	25 mg/kg	50 mg/kg
Root	Tissue Au concentration (mg/kg)	Au_Cl - Au_CN	1	1	0.10	**0.001**
		Au_Cl - Au_S2O3	1	1	**0.04**	0.27
		Au_CN - Au_S2O3	1	1	1	0.22
	Tissue Au % recovery	Au_Cl - Au_CN	1	0.57	**0.007**	**0.005**
		Au_Cl - Au_S2O3	1	0.27	**0.01**	0.10
		Au_CN - Au_S2O3	0.93	**0.005**	1	0.98
	Tissue Au bioconcentration factor	Au_Cl - Au_CN	1	1	0.10	**0.001**
		Au_Cl - Au_S2O3	1	1	**0.04**	0.27
		Au_CN - Au_S2O3	1	1	1	0.22
Shoot	Tissue Au concentration (mg/kg)	Au_Cl - Au_CN	1	**0.03**	1	**0.001**
		Au_Cl - Au_S2O3	0.65	0.85	1	1
		Au_CN - Au_S2O3	0.53	0.40	0.91	**0.0003**
	Tissue Au % recovery	Au_Cl - Au_CN	1	**0.02**	1	**0.04**
		Au_Cl - Au_S2O3	1	1	0.83	1
		Au_CN - Au_S2O3	1	0.058	0.39	**0.005**
	Tissue Au bioconcentration factor	Au_Cl - Au_CN	1	**0.03**	1	**0.001**
		Au_Cl - Au_S2O3	0.65	0.85	1	1
		Au_CN - Au_S2O3	0.53	0.40	0.91	**0.0003**
	Tissue Au translocation factor	Au_Cl - Au_CN	1	0.09	**0.01**	**9.63E-07**
		Au_Cl - Au_S2O3	0.89	1	0.06	**3.57E-01**
		Au_CN - Au_S2O3	0.95	0.59	1	**1.44E-03**

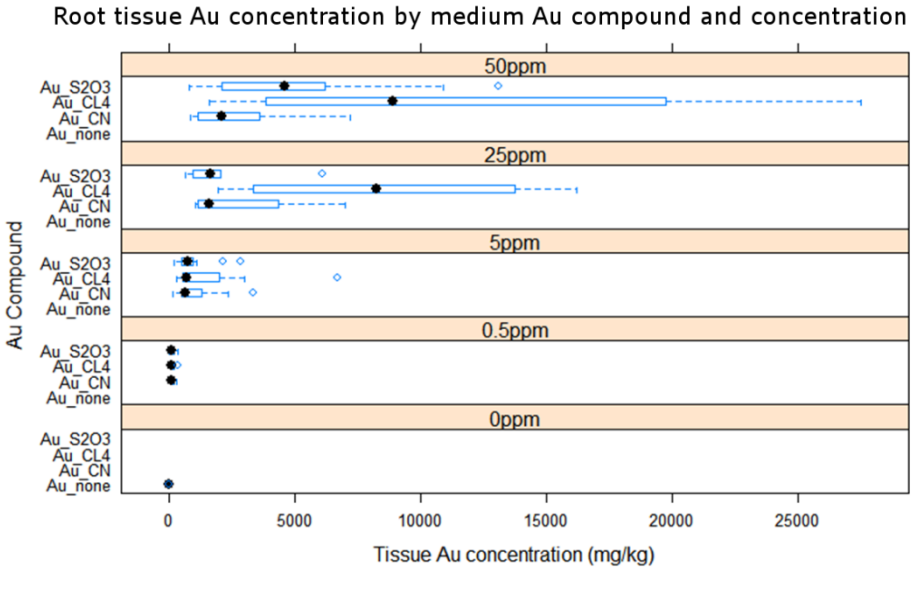

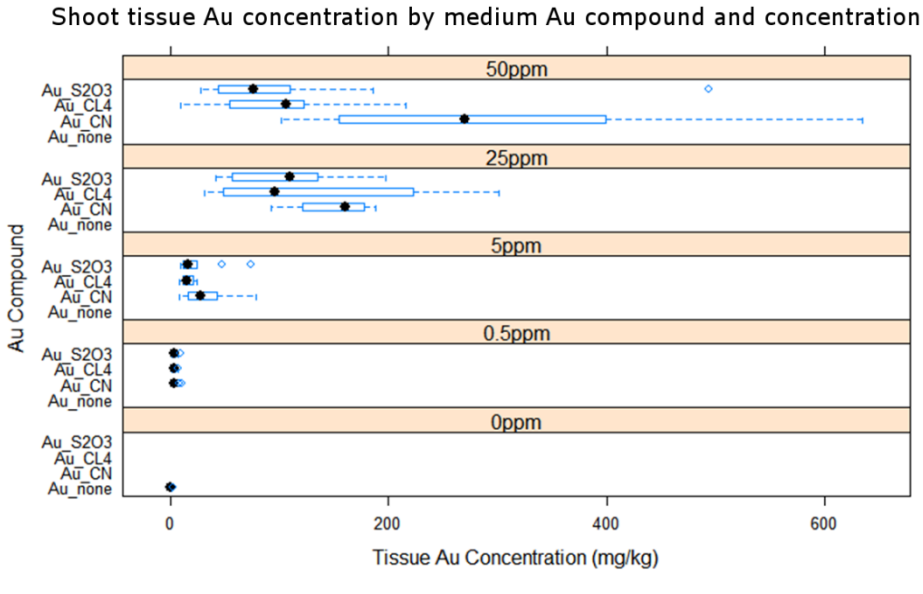

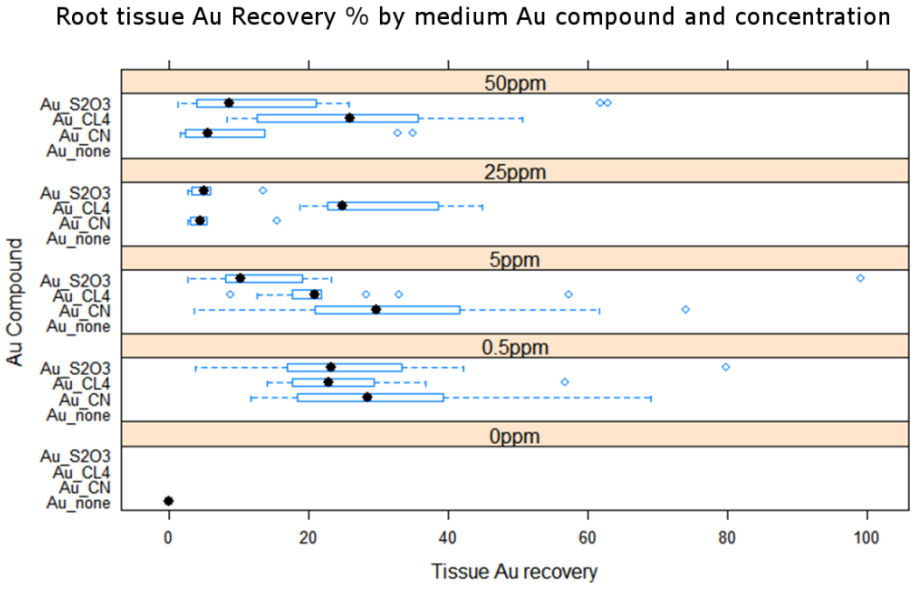

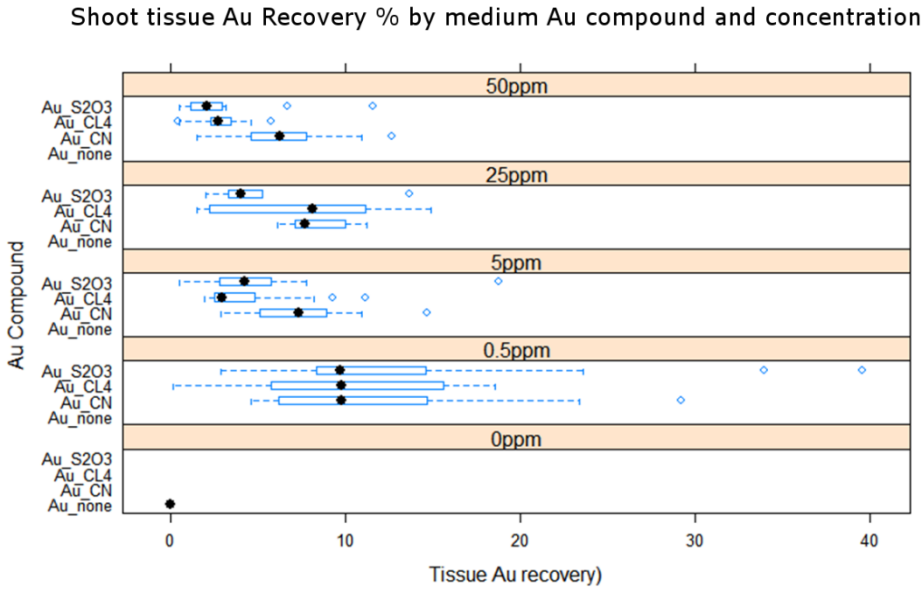

Root tissue Au bioconcentration by medium Au compound and concentration

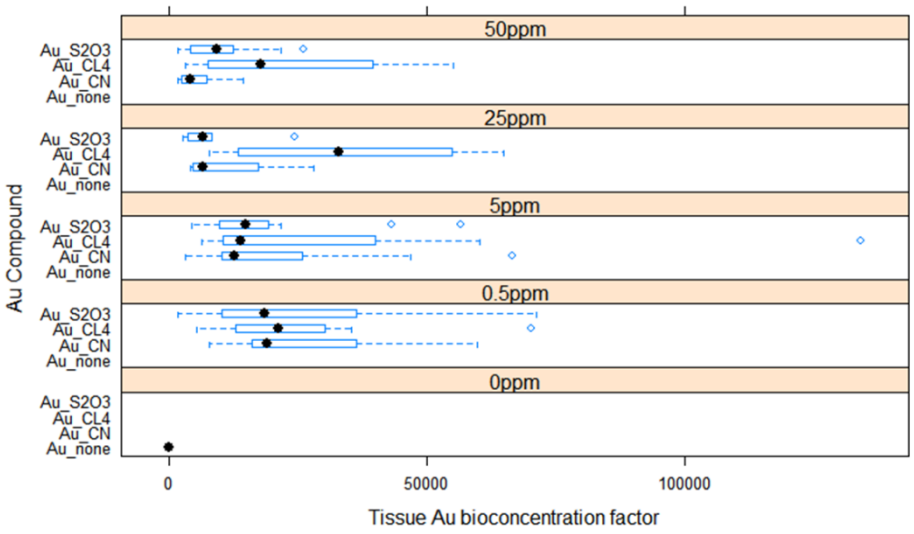

Shoot tissue Au bioconcentration by medium Au compound and concentration

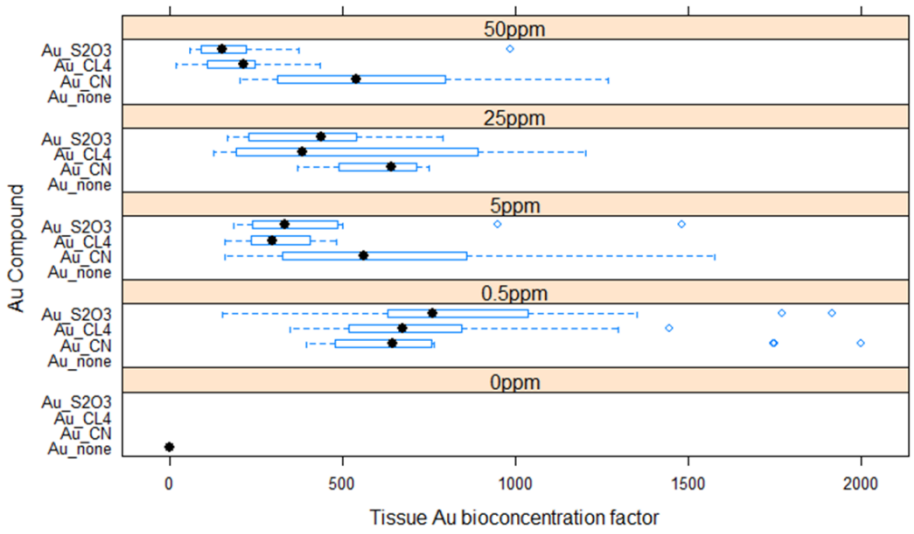

Shoot tissue Au translocation factor by medium Au compound and concentration

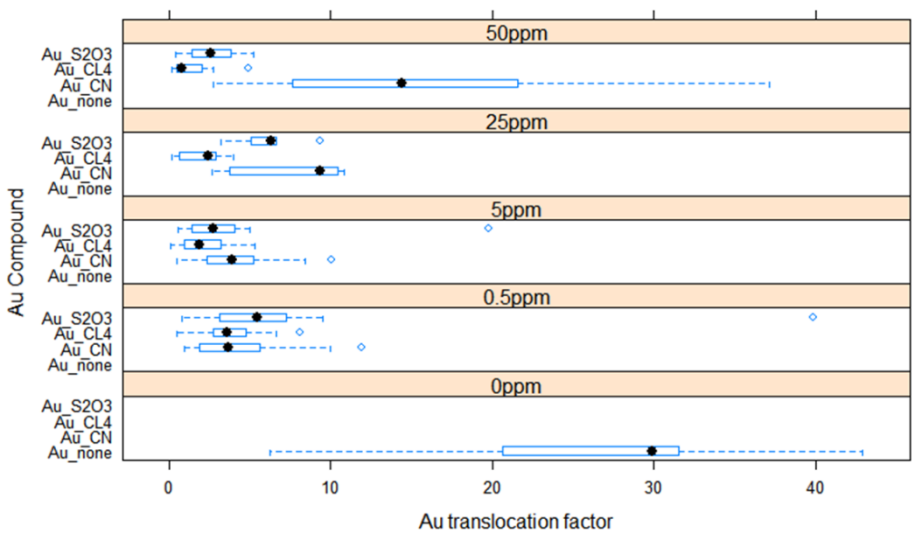

Figure 6 : Boxplots of tissue gold concentration (mg/kg), percentage recovery from medium, tissue gold bioconcentration factor and translocation factor by gold compound treatment for root and shoot tissue

The explant tissue response to the different gold compounds also varied. In root tissue, differences were found between the gold sodium thiosulphate and gold chloride treatments (p-value= 0.003), with higher concentrations of gold in the gold chloride treatment (Figure 6, Table 1). The gold concentration in the root tissue increased as the concentration of supplied gold increased (Figure 6). No differences were found between the different gold compounds at 0.5mg/kg or 5 mg/kg. However, at 50 mg/kg the material grown in the gold chloride trial accumulated significantly more gold (8903 mg/kg) than the gold potassium cyanide trial (2084 mg/kg) (p-value = 0.0022; Figure 6; Table 1; Table 6). Gold percentage recovery values decreased with increased gold concentrations for gold potassium cyanide (0.5mg/kg trial percentage recovery =39.49%; 50mg/kg trial percentage recovery =8.97%; p-value < 0.0001) and gold sodium thiosulphate treatments (0.5mg/kg trial percentage recovery =35.45%; 50mg/kg trial percentage recovery =11.17%; p-value= 0.01) but remained relatively stable for the gold chloride treatment (0.5mg/kg trial percentage recovery =29.11%; 50mg/kg trial percentage recovery =28.15%; p-value= 1, Figure 6; Table 1; Table 6).

Gold concentration within the shoot tissue increased with an increase in the concentration of the supplied gold compound (Table 1; Table 6). No differences were found for the shoot gold concentration for the 0.5 and 5 mg/kg gold concentration trials, however there were differences between them and the 50mg/kg trial (Table 1). At 0.5 mg/kg and 5 mg/kg there were no differences between the different gold compound concentrations, however at 50 mg/kg there were significant differences between the gold cyanide trials (219.38 mg/kg) and gold chloride (105.8 mg/kg) and gold sodium thiosulphate (84.18 mg/kg), where the gold cyanide trial showed significantly elevated concentrations (Table 1; Table 6). Percentage gold recovery from shoot tissues showed a similar trend, however the translocation factors were

significantly different between the three gold compounds (p-value<0.0001) (Table 6; Table 6; Figure 6). Gold percentage recovery in shoot tissue decreased with an increase in applied gold concentration (Table 1; Figure 6). No significant differences were found for the gold bioaccumulation values at 0.5mg/kg. However, at 5 and 50mg/kg, the gold potassium cyanide treatment showed higher percentage recovery values than the gold sodium thiosulphate and the gold chloride treatments (5mg/kg trial, $HAuCl_4$= 4.23%; C_2AuKN_2= 7.98%; $Na_3Au(S_2O_3)2{\cdot}2H_2O$= 5.53%; p-value = 0.0431and 50mg/kg trial, $HAuCl_4$= 3.26%; C_2AuKN_2= 6.57%; $Na_3Au(S_2O_3)_2{\cdot}2H_2O$= 3.99%; p-value = 0.0132) (Table 6).

In terms of explant response to the different gold treatments within the culture medium, only the material growing in the presence of gold potassium cyanide showed any signs of stress, where some explants growing in the 5mg/kg treatment began to exhibit tip wilt and leaf senesce within 2 weeks of applying the treatment. In the 50mg/kg gold cyanide treatment there was almost complete senescence, shoots were wilted and the growth medium was discoloured, possibly by the release of phenolic compounds from the plant tissues.

2.5. Discussion

Studies into the exposure of plant material to gold in aqueous solution have shown that the gold typically occurs as an Au(0) colloid, as an aurous [Au(I)] or as an auric [Au(III)] complex. Au^+ and Au^{3+} redox potentials exceed that of water and so the formation of free gold ions is thermodynamically unfavourable (Boyle, 1979). In this study, it is likely that the gold in solution was in the form of $[Au(CN)_2]^-$, $[AuCL_4]^-$, $[AuCl_3(OH)]^-$, $[Au(CN)]^{2-}$ and $[Au(S_2O_3)_2]^{3-}$ anions (Habashi, 1967, Lengke *et al.*, 2006, Southam *et al.*, 2009) or as aqueous gold(I/III)

thiosulphate, cyanide and chloride complexes (Boyle 1979; Vlassopoulos and Wood 1990; Vlassopoulos *et al.,* 1990).

The highest median concentration of gold in shoot tissue was 269mg/kg (269mg/kg), which is well above the threshold for gold hyperaccumulation defined as 1mg/kg under field conditions (Anderson *et al.*, 1999, Table 1). The gold concentration in shoot tissue was significantly lower than the concentration within root tissue for all the trials. This implied that there are mechanisms in place to restrict the translocation of gold from root to shoot, thus limiting the uptake of potentially harmful ions. However, observations of senescence at higher concentrations implied that these mechanisms were not totally effective and that excess ion concentrations could still induce toxicity. Alternatively, the observations of low gold concentrations in shoot tissue relative to the root tissue could be due to gold forming a precipitate on the surface of the roots, with comparatively little being absorbed into the plant (Taylor *et al.*, 2014).

The gold sodium thiosulphate and gold potassium cyanide trials exhibited an inverse relationship between the growth medium gold concentration, the bioconcentration factor and the percentage gold recovered in root tissue (Figure 6). While for the gold chloride treatment the percentage recovery and bioconcentration factors remained relatively constant across the gold concentration range. This suggested that the accumulation of gold either on or into the root tissue was being restricted by a physiological process: if the gold were accumulating on the roots as a precipitate there would be a direct relationship between gold concentration in the medium and the percentage gold recovered and gold bioconcentration factors; as an increase in medium gold concentration would result in an increase in the relative amount of

gold that precipitated onto the surface of the root. However, this was not observed, which implied that there is/are some other factors which cause the relative amount of gold accumulated by the plant to be limited at higher concentrations. Additionally, the gold chloride bioconcentration factors and percentage recovery values remained relatively stable despite the increased amount of gold in the media (Table 1; Figure 6). If this was due to the toxic effects of gold accumulation on gold uptake (Rodriguez *et al*., 2007) then the gold bioconcentration factor and gold percentage recovery values would follow a similar trend for all three of the gold compounds. But this did not occur, which implied that there are differential processes for gold accumulation in *T. usneoides* which vary depending on the gold compound present within the medium.

There is little evidence on the mechanisms by which gold ions enter *in planta*. Authors Gardea-torresdey *et al.*, 2002 and Avellan *et al.*, 2017 have shown that there is gold accumulation in root tissue when it is supplied in the form of nanoparticles, however there are few reports on the mechanisms by which plants absorb gold (either in ionic form or in the form of nanoparticles) from the rhizosphere (Avellan *et al.*, 2017) From the studies into the accumulation of gold nanoparticle ligand complexes it appears that the uptake of the nanoparticle ligand complexes occurs via endocytosis (Li *et al.*, 2016). When the gold compounds used in this study go into solution they do not dissociate into gold ions but rather as $[Au(CN)_2]^-$, $[Au(S_2O_3)_2]^{3-}$ and $[AuCl_4]^-$ anions. It is likely that the gold complex ions are either reduced to Au(0) nanoparticles before being accumulated or that the gold complex ions are accumulated directly. The chemistry of gold nanoparticles is complex and the coordination chemistry is poorly understood (Toma *et al.,* 2010). It is known that gold nanoparticles exhibit incomplete valence and as a result, the external sites on the surface of the gold nanoparticle

are capable of interacting with ligands (Toma *et al.,* 2010). This allows for the surface of the gold nanoparticles to be charged and Avellan *et al.*, 2017 have shown that the surface charge of gold nano-particles plays a fundamental role in their uptake behaviour. Positively charged gold nanoparticles caused an increase in mucilage production at the root cap of *Arabidopsis thaliana* and were bound to the mucilage, while negatively charged gold nanoparticles did not induce the same phenomenon and were able to translocate into the apoplast of the tissue. If the negatively charged gold complex ions are absorbed by the plant directly, their transport *in planta* would need to be mediated by the action of anion channels in the membranes of the cells of the root tissue. For example, this could be achieved via active H^+/anion transport channels as the rhizosphere – root tissue pH gradient favours the efflux of anions through channels due to the steep gradient of the anionic species (Kollist *et al*., 2011). This is also true if *T. usneoides* were to accumulate gold as $[Au(CN)_2]^-$, $[Au(S_2O_3)_2]^{3-}$ and $[AuCl_4]^-$ anions. In this regard there is experimental evidence that there was higher gold accumulation rates in the roots of *Brassicica juncea* at lower pH's (Bali *et al.*, 2010) and that lower pH increases gold uptake (Girling & Peterson, 1980), however this phenomenon was not recorded in this study as there was no difference between the different pH treatments for any of the compounds (Table 2, Table 3). This may be because *T. usneoides,* like other species (Marschner, 1995) has the ability to simply adjust the pH of the soils immediately surrounding the roots to a pH that is best suited for nutrient uptake and growth.

The fact that *T. usneoides* is a recretohalophyte can help to explain the higher root gold concentrations associated with the gold chloride trial (Wilson *et al*., 2017). Halophytes typically have adaptations which allow for the active uptake and transport of chloride ions (for instance cation – chloride co-transporters and others, see Flowers and Colmer, 2008). It is thus

feasible that the accumulation of gold chloride ions occurs via the chloride exchange channels in the root cell membranes. It is also possible that the processing mechanisms for the excretion of chlorides are used in the uptake and excretion of gold chloride, while the gold thiosulphate and gold potassium cyanide treatments were less efficient at entering the root translocation system, thus resulting in their diminished uptake.

WDS imaging confirmed the presence of gold in shoot tissue of *T. usneoides* (Figure 5). The gold accumulation in shoot tissue exhibited a similar trend to root tissue in that there was a direct linear relationship between growth medium gold concentration and shoot tissue gold concentration and an inverse relationship for the shoot tissue bioconcentration factor and percentage recovery values (Figure 6). Unlike in root tissue where the gold concentrations within the gold potassium cyanide treatments were significantly higher than the other compounds but it did exhibit the same inverse relationship with medium gold concentration and bioconcentration factors and the percentage recovery values. This was a significant finding because it suggests that the gold that is accumulated is not simply reduced to Au(0) but retains some physical properties that differentiate the compounds . If the gold compounds were reduced in the roots to Au(0) prior to translocation to shoot tissue, there wouldn't be the observed differential translocation of the different gold compounds unless the Au(0) which forms as a result from the reductions of the different gold compounds has distinct chemical properties such as those that gold nano-particles are reported to exhibit (Avellan *et al.*, 2017)

Studies by Girling & Peterson, 1980 showed that cyanogenic tree species (i.e. trees which secrete cyanide ions from their roots) have significantly higher quantities of gold within their

shoot tissue than similar non-cyanogenic species. Many plant species are tolerant to hydrogen cyanide and metal cyanide complexes as hydrogen cyanide is a by-product of the synthesis of the hormone ethylene (Yip and Yang, 1998). Plants synthesise cyanide to deter herbivory and in a few species provide a source of nitrogen for seed germination (Seigler, 1991). Cyanogenic tree species are tolerant to metal-cyanide complexes until a particular threshold is exceeded and then death occurs (Ebbs, 2004). The present gold potassium cyanide trial did exhibit additional signs of stress, with higher rates of senescence, media browning and death. Although none of those plants were analysed for gold accumulation in their tissues, it is possible that of the plants that did survive the dosage with gold potassium cyanide, there was unrestricted uptake at concentrations above 25mg/kg as a result of the breakdown in the physiological processes that mitigate cyanide toxicity. However, it is unlikely that this was the case as the bioconcentration factors and percentage recovery values remained relatively constant across the dosage range. It is more likely that the gold cyanide complexes were transported in a fashion which rendered them non-toxic. This could include transportation via metal-chelate transporters (Clemens, 2006), or other intracellular processes such as via vacuoles as suggested by Flowers *et al.*, 2018.

The fact that gold cyanide resulted in higher gold uptake in shoot tissue is significant as cyanide is used in the extraction of gold from crushed gold bearing ore (Vorster & Flatman, 2001). After extraction the gold bearing tailings are treated to remove the excess cyanide and deposited onto the tailings facility (Ackil, 2002). The International Cyanide Management Institute guidelines (Gibbons, 2005) for the emission of cyanide into the environment, limits the emission of cyanide to less than 50mg/kg. The use of *T. usneoides* for gold phytoextraction on sites with potentially high cyanide concentrations needs to be further studied as the

present *in vitro* results do not reflect the conditions found in wetlands, TSF footprints or historical tailings spills, where the cyanide may be bound to form weak acid dissociable or strong acid dissociable complexes and so would not necessarily be bioavailable (Ebbs, 2004).

2.6.Summary & Conclusions

Tamarix usneoides proved capable of accumulating gold to concentrations that are well above the threshold for gold hyperaccumulation. This indicated that the gold compounds provided *in vitro* could release gold in a form that was available to the plant for uptake. Gold chemical form did affect uptake and translocation, with gold potassium cyanide resulting in the highest mean gold concentration within shoot tissue and gold chloride resulting in the highest mean gold concentration associated with root tissue. Gold accumulation was also affected by supplied gold concentration, where higher gold concentrations within the rooting zone resulted in higher translocation to shoot tissue, however there was evidence that the efficiency with which the plants accumulated gold decreased as concentration increased. Thus it is likely that there is a maximum rate at which *T. usneoides* can accumulate gold regardless of the gold concentration within the rooting zone. The differential processes for gold assimilation on/into root tissue and the differences between the gold potassium cyanide trials and the gold chloride and gold sodium thiosulphate trials in shoot tissue is compulsive evidence that the gold that is translocated to aerial parts of the plant tissue are chemically different from each other and additional research should be performed in order to determine if this is due to changes in elemental composition or if it is due to varying properties associated with the reduction of the gold compounds to gold nano-particles.

Further research should include studies on the kinetics of gold surface binding, reduction, assimilation, translocation and accumulation by *T. usneoides.*

2.7. Acknowledgements

This study forms part of the doctoral research of the first author, and was funded by the Department of Trade and Industry (the DTI) and the National Research Foundation (NRF) of South Africa Technology for Human Resources for Industry Programme (THRIP) awards TP13080525596 and TP2010072200029 to I.M. Weiersbye and E.T.F. Witkowski, and AngloGold Ashanti Limited South Africa (Metallurgy and Environmental Management Department)

2.8. References

Akcil A. (2002). First application of cyanidation process in Turkish gold mining and its environmental impacts. *Minerals Engineering*, 15(9), 695-699.

Akcil A., & Koldas S. (2006). Acid Mine Drainage (AMD): causes, treatment and case studies. *Journal of cleaner production*, 14(12-13), 1139-1145.

Anderson C. W. N., Brooks R. R., Chiarucci A., LaCoste C. J., Leblanc M., Robinson B. H. & Stewart R. B. (1999). Phytomining for nickel, thallium and gold. *Journal of Geochemical Exploration*, 67(1-3), 407-415.

Avellan A., Schwab F., Masion A., Chaurand P., Borschneck D., Vidal V., Rose J., Santaella C. & Levard C., (2017). Nanoparticle uptake in plants: gold nanomaterial localized in roots of *Arabidopsis thaliana* by X-ray computed nanotomography and hyperspectral imaging*. Environmental science & technology*, 51(15), 8682-8691.

Baker A. J. (1981). Accumulators and excluders-strategies in the response of plants to heavy metals. *Journal of plant nutrition*, 3(1-4), 643-654.

Bali R., Siegele R., & Harris A. T. (2010). Phytoextraction of Au: uptake, accumulation and cellular distribution in *Medicago sativa* and *Brassica juncea*. *Chemical Engineering Journal*, 156(2), 286-297.

Baum B.R. (1978). The genus *Tamarix*. Jerusalem, The Israeli Academy of Sciences and Humanities.

Boyle R. W. (1979). The geochemistry of gold and its deposits. *Geological Survey of Canada. Bulletin*, 280, 584.

Clemens S. (2006). Toxic metal accumulation, responses to exposure and mechanisms of tolerance in plants. *Biochimie*, 88(11), 1707-1719.

Coetzee H., Wade P., & Winde F. (2002). Reliance on existing wetlands for pollution control around the Witwatersrand gold/uranium mines of South Africa-Are they sufficient? In *Uranium in the aquatic environment* (pp. 59-64). Springer, Berlin, Heidelberg.

Dunn O. J. (1961). Multiple comparisons among means. *Journal of the American statistical association,* 56(293), 52-64.

Dye P. J., Jarmain C., Clulow A. D., Everson C. S., Mengistu M. G., & Weiersbye I. M. (2018). Evapotranspiration from mine-affected riparian sites along the Vaal River in central South Africa. *South African Geographical Journal*, 100(1), 62-81.

Ebbs S. (2004). Biological degradation of cyanide compounds. *Current opinion in Biotechnology*, 15(3), 231-236.

Flowers T. J., & Colmer T. D. (2008). Salinity tolerance in halophytes. *New Phytologist*, 179(4), 945-963.

Flowers T. J., Glenn E. P. & Volkov,V. (2018). Could vesicular transport of Na^+ and Cl^- be a feature of salt tolerance in halophytes? *Annals of botany*, 123(1), 1-18.

Galán E., Gómez-Ariza J. L., González I., Fernández-Caliani J. C., Morales E., & Giráldez I. (2003). Heavy metal partitioning in river sediments severely polluted by acid mine drainage in the Iberian Pyrite Belt. *Applied Geochemistry*, 18(3), 409-421.

Gardea-Torresdey J.L., Parsons J.G., Gomez E., Peralta-Videa J., Troiani H.E., Santiago P., Jose & Yacaman M. (2002). Formation and growth of Au nanoparticles inside live alfalfa plants*. Nano Letters*, 2, 397–401.

Gibbons T., (2005) International cyanide management code. *Advances in Gold Ore Processing*. Elsevier, Amsterdam, 182-200.

Girling C. A., & Peterson P. J. (1980). Gold in plants. *Gold bulletin*, 13(4), 151-157.

Habashi F. (1967). Kinetics and mechanism of gold and silver dissolution in cyanide solution. *Montana College of Mineral Science and Technology.*

Jiang Y., Lei M., Duan L. & Longhurst P. (2015). Integrating phytoremediation with biomass valorisation and critical element recovery: a UK contaminated land perspective. *Biomass and Bioenergy*, 83, 328-339.

Kollist H., Jossier M., Laanemets K., & Thomine S. (2011). Anion channels in plant cells. *The FEBS journal*, 278(22), 4277-4292.

Kruskal W. H., & Wallis W. A. (1952). Use of ranks in one-criterion variance analysis. *Journal of the American statistical Association*, 47(260), 583-621.

Li H., Ye, X., Guo X., Geng Z., & Wang G. (2016). Effects of surface ligands on the uptake and transport of gold nanoparticles in rice and tomato. *Journal of hazardous materials*, 314, 188-196.

Lengke M. F., Ravel B., Fleet M. E., Wanger G., Gordon R. A. & Southam G. (2006). Mechanisms of gold bioaccumulation by filamentous cyanobacteria from gold(III)−chloride complex. *Environmental science & technology*, 40(20), 6304-6309.

Maluckov B.S. (2015). Bioassisted phytomining of gold. *JOM*, 67(5), pp.1075-1078.

Marschner H. (1995) Mineral nutrition of higher plants. second edition. 889pp. London: Academic Press

Mayonde S. G., Cron G. V., Gaskin J. F. & Byrne M. J. (2015). Evidence of *Tamarix* hybrids in South Africa, as inferred by nuclear ITS and plastid trnS–trnG DNA sequences. *South African Journal of Botany*, 96, 122-131.

McCarthy T. S., & Venter J. S. (2006). Increasing pollution levels on the Witwatersrand recorded in the peat deposits of the Klip River wetland. *South African Journal of Science*, 102(1), 27-34.

Mphephu N. F. (2004) Geotechnical environmental evaluation of mining impacts on the Central Rand. PhD Thesis submitted to the University of the Witwatersrand, Johannesburg.

Muir D. M., & Aylmore M. G. (2004). Thiosulphate as an alternative to cyanide for gold processing–issues and impediments. *Mineral Processing and Extractive Metallurgy*, 113(1), 2-12.

Murashige T., & Skoog F. (1962). A revised medium for rapid growth and bio assays with tobacco tissue cultures. *Physiologia plantarum,* 15(3), 473-497.

Naicker K., Cukrowska E. & McCarthy T. S. (2003). Acid mine drainage arising from gold mining activity in Johannesburg, South Africa and environs. *Environmental pollution*, 122(1), 29-40.

Raskin I., Kumar P. N., Dushenkov S., & Salt D. E. (1994). Bioconcentration of heavy metals by plants. *Current Opinion in biotechnology*, 5(3), 285-290.

Reith F., Lengke M. F., Falconer D., Craw D., & Southam G. (2007). The geomicrobiology of gold. *The ISME Journal,* 1(7), 567.

Rodriguez E., Parsons J. G., Peralta-Videa J. R., Cruz-Jimenez G., Romero-Gonzalez J., Sanchez-Salcido B. E., Saupe G. B., Duarte-Gardea M. and Gardea-Torresdey J. L. (2007) Potential of *Chilopsis linearis* for gold phytomining: Using XAS to determine gold

reduction and nanoparticle formation within plant tissues. *International Journal of Phytoremediation* 9(1-3): 133-147.

Seigler, D. S. (1991). Cyanide and cyanogenic glycosides. GS Rosenthal & MR Berenbaum, 35-77.

Shapiro, S. S. & Wilk, M. B. (1965). An analysis of variance test for normality (complete samples). *Biometrika*, 52(3/4), 591-611.

Sheoran A. S., & Sheoran V. (2006). Heavy metal removal mechanism of acid mine drainage in wetlands: a critical review. *Minerals engineering*, 19(2), 105-116.

Southam G., Lengke M. F., Fairbrother L., & Reith F. (2009). The biogeochemistry of gold. *Elements*, 5(5), 303-307

Spurr A. R. (1969). A low-viscosity epoxy resin embedding medium for electron microscopy. *Journal of ultrastructure research*, 26(1-2), 31-43.

Sutton M.W., Weiersbye I.M., Galpi, J.S & Heller D. (2006). GIS-based history of gold mining and risk assessment of post-mining land-uses on the Witwatersrand Basin of South Africa. In Fourie, A.B. & Tibbett, M. (eds.). *Proceedings of the 1st International Seminar on Mine Closure*, Australian Centre for Geomechanics, Perth.

Taylor A. F., Rylott E. L., Anderson C. W., & Bruce N. C. (2014). Investigating the toxicity, uptake, nanoparticle formation and genetic response of plants to gold. *PLOS one*, 9(4), e93793.

Thomson W. W., Berry W. L. & Liu L. L. (1969). Localization and secretion of salt by the salt glands of *Tamarix* aphylla. *Proceedings of the National Academy of Sciences*, *63*(2), 310-317.

Toma H. E., Zamarion V. M., Toma S. H., & Araki K. (2010). The coordination chemistry at gold nanoparticles. *Journal of the Brazilian Chemical Society*, 21(7), 1158-1176.

Tutu H., Cukrowska E. M., Dohnal V., & Havel J. (2005). Application of artificial neural networks for classification of uranium distribution in the Central Rand goldfield, South Africa*. Environmental Modeling & Assessment*, 10(2), 143-152.

Tutu H., McCarthy T. S., & Cukrowska E. (2008). The chemical characteristics of acid mine drainage with particular reference to sources, distribution and remediation: The Witwatersrand Basin, South Africa as a case study. *Applied Geochemistry*, 23(12), 3666-3684.

Vlassopoulos D., & Wood S. A. (1990). Gold speciation in natural waters: I. Solubility and hydrolysis reactions of gold in aqueous solution. *Geochimica et Cosmochimica Acta*, 54(1), 3-12.

Vorster B. J. & Flatman S. R., 2001. Cyanide control in the metallurgical process of gold extraction in AngloGold (SA). *Journal of the South African Institute of Mining and Metallurgy*, 101(7), 359-365.

Weiersbye I. M., & Witkowski E. T. F. (1998). The structure, diversity and persistence of naturally-colonizing and introduced vegetation on gold tailings and tailings-polluted soils. *Plant Ecology & Conservation Series*, (8), 224.

Wilson H., Mycock D., & Weiersbye I. M. (2017). The salt glands of *Tamarix usneoides* E. Mey. ex Bunge (South African Salt Cedar). *International journal of phytoremediation*, 19(6), 587-595.

Wu S., Feng X., & Wittmeier A. (1997). Microwave digestion of plant and grain reference materials in nitric acid or a mixture of nitric acid or a mixture of nitric acid and hydrogen peroxide for the determination of multi-elements by inductively coupled plasma mass spectrometry. *Journal of Analytical Atomic Spectrometry*, 12(8), 797-806.

Yip W. K., & Yang S. F. (1998). Ethylene biosynthesis in relation to cyanide metabolism. *Botanical Bulletin of Academia Sinica*, 39.

3. The accumulation of gold and other elements by *Tamarix usneoides* trees from gold and uranium tailings

Hayden T. Wilson, David J. Mycock and Isabel M. Weiersbye
University of the Witwatersrand, Johannesburg, Faculty of Science, School of Animal, Plant and Environmental Sciences, +27 (11) 717 6403, Private Bag 3 Wits 2050, South Africa.
Hayden.Wilson@students.wits.ac.za, David.Mycock@wits.ac.za, Isabel.Weiersbye@wits.ac.za

The following chapter is in scientific manuscript format, as such there is some repetition of contextualising information and background information that was included in previous chapters.

3.1. Abstract

Historical spillages from tailings storage facilities as well as contaminated groundwater plumes from old and tailings storage facilities present a significant source of contamination in South Africa. Attempts to rehabilitate such areas are often costly, legislatively prohibited or significantly disrupt the typical ecosystem function of the rehabilitated area. Thus, there is a requirement for an *in-situ* mechanism for contaminant removal that is cost effective and does not disrupt ecosystem function. Members of the genus *Tamarix* have the ability to accumulate a wide range of elements from the environments they inhabit and *in vitro* trials have shown that *Tamarix usneoides* plantlets can potentially accumulate significant quantities of gold if the gold is bio-available (Wilson, 2019 manuscript, previous chapter of this thesis). Consequently, there is potential for *T. usneoides* to be used for the *in-situ* removal of a range of elements from tailings storage facilities and historical tailing spills, with recovered gold being used to offset the remediation costs. This study aimed to determine if *T. usneoides* is capable of accumulating gold *in-situ* from a tailings storage facility, as well as determine if *T. usneoides* has an ameliorative effect on the tailings, potentially adjusting elemental mobility within the rhizosphere. Additionally, the study aimed to determine the elemental concentrations of different tissue types in order to better understand the mechanisms and processes involved in elemental accumulation. It was found that *T. usneoides* plants grown on a tailings storage facility do not accumulate significant quantities of gold in biomass, however, a range of other elements were accumulated in specific tissues at concentrations that exceeded rhizosphere concentrations. Additionally, there was significant evidence of the ameliorative effect that the trees had on the tailings, where samples taken from control pits with no trees had significantly lower pH values than the samples that were harvested from the pits where trees were growing. This suggests that *T. usneoides* could potentially be used for phytostabilisation in addition to its established role as a sulphate and chloride salt accumulator as raising rhizosphere pH significantly reduces elemental mobility.

Keywords.

Gold, phytomining, remediation, hyperaccumulation.

3.2.Introduction

In South Africa, most rock containing gold is associated with sulphide minerals such as iron pyrite and arsenopyrite (Naicker *et al.*, 2003). Gold mine tailings contain, on average, two percent sulphur and it was estimated that there were approximately 30 000 000 tonnes of sulphur in tailings storage facilities (TSFs) in the Witwatersrand basin (Weiersbye and Witkowski, 1998). In South Africa, TSF's are a significant source of pollution. When these facilities were first built, there were no legislative requirements to have them located on appropriate soils and designed in such a way as to minimise the generation and drainage of leachate (e.g. physical liners and evapotranspiration covers). The leachate is contaminated by the oxidation of sulphate bearing minerals and the concomitant generation of acid mine drainage (Tutu *et al*., 2008). This has resulted in the movement of contaminated leachate into surrounding soils and waterways (Naicker *et al.*, 2003). Some metal contaminants within the leachate have become concentrated in the receiving `sink' areas, such as wetlands, where they are bound to organic compounds (Sheoran & Sheoran, 2006). As conventional processes to reclaim elements from such substrata are expensive (Kuppusamy *et al.*, 2016) and require a different metallurgical process, there is a requirement for an *in-situ* technology that allows for the extraction and removal of salts and metals from the impacted sediments and at their source.

Phytotechnologies represent a relatively low-cost alternative to conventional *ex situ* remediation techniques (Kuppusamy *et al.*, 2016). Phytomining is an extractive process whereby accumulator plants are utilised to extract valuable elements from polluted soils (Chaney *et al*., 2007) or shallow ore bodies with minimal disturbance to soil profile or function

(Lintern *et al*., 2013). However, due to the mechanisms involved in plant metal uptake, plants are generally unable to accumulate metals that are not bio-available and this limits the range of elements that are suitable for phyto-mining (McGrath *et al*., 2003). Application of metal chelating agents can potentially increase elemental mobility and in this regard studies by Anderson *et al.*, 1999 have shown that soil treatment with ammonium thiocyanate induced gold accumulation in *Brassica juncea*. Non-induced gold accumulation has been observed in several species, including eucalyptus growing on gold enriched ore bodies (Girling & Peterson, 1980; Lintern *et al.*, 2013) and there has been studies on gold nano-particle accumulation in species such as *Medicago sativa* and *Brassica juncea* (Gardea-Torresdey *et al.*, 2002, Marshall *et al*., 2007).

Tamarix usneoides E. Mey. ex Bunge (South African Salt Cedar, Tamaricaceae) and *T. usneoides x ramossisima* hybrids grow readily on tailings facilities (Weiersbye *et al*., 2006) and colonise areas that have elevated concentrations of sulphate and chloride salts. Due to these characteristics, there has been considerable interest in the use of *T. usneoides* as a vegetative cover on TSF's (Dye *et al.,* 2008) for the phytoremediation of affected soils and groundwater on Witwatersrand Basin gold mines (The Mine Woodlands Project, Weiersbye *et al.* 2006).

In vitro uptake trials (Wilson *et al.,* 2019, manuscript; Chapter 2 of this thesis) showed that *T. usneoides* accumulated significant quantities of gold when the gold was supplied in a form that was bio-available for uptake. As a result of those findings and the findings of elemental accumulation in *Tamarix* by other authors (Thomson *et al.* 1969, Kleinkopf and Wallace 1974; Hagemeyer and Waisel 1988; Kadukova *et al.* 2008; Manousaki *et al.* 2007), *in-situ* trials were initiated to establish the potential for the phytoextraction of gold and other elements from a

gold and uranium tailings storage facility, as well as to serve as a long term research site with the key objectives being to assess growth, water-use (Dye *et al*., 2018), cyanide consumption and changes in tree and tailings chemical properties over time since planting in 2010/11 (I.M. Weiersbye, E.M. Bakatula and H. Tutu unpublished data).

As such, this study does not consider the use of compounds to induce gold accumulation *in planta* as the application of such can result in the concomitant mobilization of other elements, a situation that would invalidate the longer term research objectives of the site by affecting the plant survivability and profoundly affecting the tree and tailings chemical properties.

3.3. Methodology

STUDY SITE HISTORY, CHARACTERISATION, PREPARATION AND PLANT SELECTION

Tree trials were conducted on the top of the Anglogold Ashanti Mponeng tailings storage facility situated on the Anglogold Ashanti West Wits mining operation, 70km south west of Johannesburg near the town of Carltonville in South Africa.

The Mponeng tailings facility is an inactive tailings facility consisting of historical tailings that have been reprocessed for additional gold recovery. Deposition at this facility began in 1970's at this location and ended in the early 2000's. The site is at an altitude of 1530 m above sea level with daily temperatures ranging between 14 and 30 ^{o}C in the summer months (November to February) and 0-14 ^{o}C in winter (July to August). The region receives an average of 660mm of rain annually with the majority of rainfall occurring in the mid-late summer

months. Site preparation and planting was performed by anglogold ashanti forestry teams supervised by the university of the Witwatersrand ecological engineering and phytoremediation program (EEPP). Planting consisted of treating the surface of the tailings with municipal sewage sludge (to provide the plants with some organic matter and plant available nutrients) as well as treatment with $Ca(OH)_2$ (to mitigate acid generation potential of the sulphur bearing tailings during the initial planting process). The site was planted in the summer months of 2010/2011 using *T. usneoides* of known provenance (S.G. Mayonde, 2016, unpublished data). Site preparation consisted of digging holes at an emplacement of 1.5m in a row and 3m between rows (1666 trees per hectare). Each hole was dosed with 2l of compost and a further 2l of a 0.1% solution of a water retention gel (potassium polyacrylate). Saplings were then planted in each hole and watered. Site maintenance consisted of regular weeding and two applications of sewage slurry from the mine sewage treatment works.

To compensate for the heterogeneity of substrate particle size and the possible differences in substrate bulk density, pH, EC and redox conditions across the tailings dam (caused by the differential particle deposition during the process used during tailings deposition), four similarly sized trees were selected for harvest at different locations within the plot, where two trees were selected close to the outer edge of the TSF paddock and two trees were selected from the middle of the TSF paddock (Figure 7). In order to control for edge effects, only trees from within at least three rows from the edge of the plot were utilised. Two unplanted control pits with similar characteristics to the sites from where the trees were harvested were selected from areas without trees.

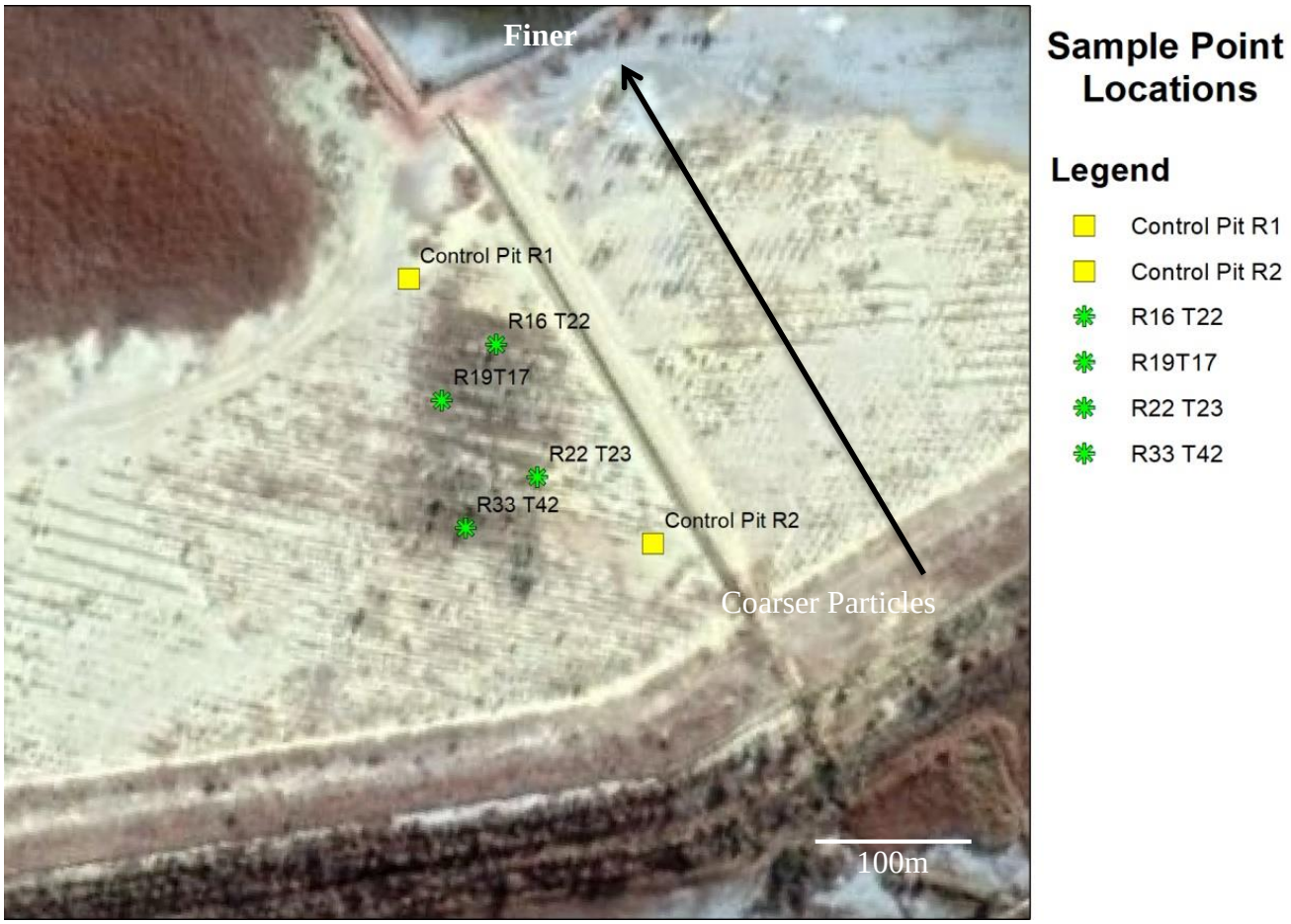

Figure 7: Overview of sample point locations and typical tailings particle size distribution

MATERIAL COLLECTION AND PREPARATION

The entire plant was harvested. Above ground biomass was removed and separated into different size and tissue classes *viz.* leaves, micro twigs (stem diameter ≤2mm), twigs (Stem diameter ≈ 2mm-4mm), branches (Stem diameter ≥ 4mm) (Figure 8). Below ground biomass was harvested using an excavator with a backhoe. The excavator first dug a 1m deep trench 1.5m from the tree on all four sides. Tailings material from different depths were then placed in separate heaps and sieved to separate tree roots from the tailings. The backhoe was then used to remove the root ball and this was trimmed of all roots. Roots were separated according to diameter and placed in sealed plastic bags. The categories for the root diameter were as follows: fine roots (diameter ≤2mm), medium roots (diameter ≈ 2mm-4mm) and coarse roots (diameter ≥ 4mm). After harvest the plant material was washed using deionised (DI) water to remove adhered tailings. The material was then packed into plastic bags, sealed and weighed for fresh mass and stored at 4 ^{o}C. Prior to further sample preparation for elemental analysis, the material was re-rinsed in DI water, followed by gently scrubbing with a soft plastic brush and a final double rinsing with ultrapure (MilliQ) water. The branch and twig material were dissected into bark, cortex and stele sections and root material was separated into epidermis, cortex and stele sections. The tissue was then placed into plastic bags, sealed and stored for 3 days at -17°C prior to dehydration with a freeze drier for 3 days at -85°C (Labconco FreeZone 4.5l freeze dry system). Once dehydrated the samples were homogenised in a ceramic mill until the samples were a fine powder.

Tailings samples were collected from one of the sidewalls of each pit using a plastic auger. Samples for soil profiling were removed at the following depths: 0-2cm, 2-10cm, 10-20cm, 20-30cm, 50-60cm and 70-80cm. The tailings samples were sieved using a 0.5mm plastic

mesh sieve. The samples were then homogenised and two 20g subsamples were removed per sample. One of each of the 20g subsamples was then placed in a sample bottle and semi-sealed with perforated parafilm. This was then dehydrated for 3 days at -85°C (Labconco FreeZone 4.5l freeze dry system) and further subsampled for elemental analysis by ICP-MS and XRF. The second subsample was mixed with 5ml of ultrapure (MilliQ) water and analysed for pH (Probe: WTW SenTix41), oxidation- reduction potential (ORP) (Probe: WTW SenTix ORP) and electroconductivity (Ec) (Probe: WTW Tetra Con®325).



Figure 8: Examples of Stems (A) Twigs (B), Micro-twigs (C), and Leaf shoots biomass collected from selected trees growing *in-situ* trials on the Mponeng tailings storage facility.

The samples were analysed for a range of elements including gold using a Spectro XEPOS desktop electron dispersive x-ray detector (ED- XRD) by the Ecological Engineering and Phytotechnology laboratory, School of Animal, Plant and Environmental Sciences, at the University of the Witwatersrand. A certified reference material (CRM) sample was included in all tests. Gold concentrations were found to be below detection limit by XRF, thus additional analyses were performed by the Central Analytical Facility at the University of Stellenbosch, South Africa. These samples were microwave-digested in a mixture of 5ml of nitric acid and 2 ml of hydrochloric acid (Wu *et al*., 1997) and subsequently diluted to a volume of 50ml with de-ionised water. The samples were then assayed for gold using inductively coupled plasma mass spectrometry (ICP-MS). Machine analytical error or drift was corrected for by comparing the ICP-MS reading with blank digestions and with the gold concentrations of certified reference material as well alongside gold spiked (0.014 and 0.14 mg/kg) certified reference material (National Bureau of Standards Orchard Leaf No. 1571) (see Appendix A Table 14 for the recovery % from the spiked CRM samples). The concentration of gold detected within the diluted subsample was then adjusted using the dilution factor (derived from sample mass and digestion volume) for that specific sample to produce a final gold concentration in mg/kg for the original dried sample. Concentrations that were below instrument detection limits were calculated according to the following formula:

Concentration (mg/kg) = Instrument detection limit (mg/kg)/3

Percentage recovery of elements was calculated for each of the certified reference materials (See Appendix B, Table 25 and Table 26 for the % recoveries for each of the selected elements). Only elements with an 80% recovery or greater were included in further analysis

and discussion. This limited the results to the following elements S, Mg, P, S, Cl, K, Ca, Mn, Fe, Cu, Zn, Rb, Sr, Pb, Th, Au and U.

DATA ANALYSIS

A variety of statistical analytical methods were employed and focused on the elemental concentrations for each of the locations within the sample pit profile as well as for each of the sample tissue types. A translocation factor (%) for each element within each tissue was calculated by determining the elemental concentration ratio between each tissue within the tissue translocation series and calculated according to the following formula:

Translocation factor (%) = (current tissue concentration/ previous tissue concentration) *100

For tissue series as follows:

Fine roots > Root Epidermis > Root Cortex >Root Vascular > Branch Vascular > Twig Vascular > Branch bark > Twig Bark > Micro-Twigs > Leaves. The translocation factor for fine roots and the epidermal tissue was calculated by dividing the tissue concentration by the concentration within the tailings, thus reflecting the transfer from tailings to the immediately adjacent tissue. As fine roots were less than 1mm in diameter the entire root was used as a unit of measure as quantitively analyzing the different tissue types of these small sections was not possible within the time frame allocated to harvesting and sample preparation.

Data were checked for normality using a Shapiro-Wilk test (Shapiro & Wilk, 1965). As the data proved to be non-normal, differences in concentration between the sample groups were

determined using Kruskall wallis tests (Kruskal & Wallis, 1952). Student's t-tests were used to determine if there were any differences in the pH, Eh, and Ec associated with the control and sample pits (Student, 1908).

Summary statistics for the elemental concentrations for the tailings samples and the plant tissue samples are presented in Appendix B Table 29 and Table 30 respectively

Biomass elemental concentration, translocation factor as well as Na/K, Mg/Ca and S/Cl ratios were determined utilising a hierarchical clustering analysis using Wards method (Murtagh & Legendre 2011) to generate dendrograms of observation clusters. This allowed for the behaviour of elements across tissues to be modelled as well as for similar tissues to be grouped and the optimal number of clusters per dendrogram was calculated using the average silhouette width method (See appendix B Figure 24 and Figure 25 for silhouette width charts of optimal number of clusters).

3.4. Results and Discussion

SITE CHEMICAL CHARACTERISTICS

There were no differences in the soil ORP or Ec between the control pits and the sample pits, however there was a difference in pH, where the pH values of the sample pits were higher than the control pits at depths of 10-60cm (Table 4).This suggested that the trees may have ameliorated the rhizosphere conditions by raising pH (Table 7) (Nye, 1981). Tailings containing significant quantities of pyrite are typically acidic (Table 7) as during the weathering process sulphuric acid is generated from sulphide bearing minerals (Johnson and Hallberg, 2005). As members of the genus *Tamarix* such as *T. aphylla* have been documented to accumulate

significant quantities of sulphur (Storey & Thomson, 1994), it is likely that in *T. usneoides*, pH adjustment in the rhizosphere was a result of the action of taking up excess $SO4^{2-}$ ions. $SO4^{2-}$ uptake is via a high affinity H^+ co-transport process which would also result in a decrease in H^+ ion transport (Hawkesford *et al*., 2003). These findings are in agreement with those of Weiersbye and Joubert (2019, in prep) who established that *T. usneoides* trees rooting in acid tailings or acid-mine drainage polluted soils and gold tailings were significantly better at the amelioration of acid pH than other tree species (*Searsia lancea, Searsia pendulina*, Eucalyptus spp).

Table 7: Mean and p-value for pH, EC and Eh (ORP) for each tailings sample depth collected from the control pits and sample pits from the Mponeng Tailings facility

Measure	Depth	Control	Tree	p-value
pH [H^+]	0-2cm	3.72	4.70	0.12
	2-10cm	3.79	4.62	0.15
	10-20cm	3.62	5.00	**0.03**
	20-30cm	3.49	5.31	**0.02**
	50-60cm	3.45	3.76	**0.01**
	70-80cm	3.52	4.49	0.17
EC (S/m)	0-2cm	1980	1495.25	0.40
	2-10cm	1447	1965.5	0.34
	10-20cm	1476.5	1820.75	0.43
	20-30cm	1565.5	2162.75	0.24
	50-60cm	1493	1125	0.49
	70-80cm	1277.5	1380	0.54
ORP (V)	0-2cm	417	388.57	0.28
	2-10cm	422.1	396.7	0.08
	10-20cm	409.45	384.77	0.65
	20-30cm	441.7	384.97	0.07
	50-60cm	369.95	409.5	0.25
	70-80cm	422.75	425.02	0.86

When control pits were compared with the sample pits, differences were found between the different elements, with Zn, Rb, Mn, Mg, K, Fe, Cu, Cl and Ca concentrations being significantly higher in the sample pits than in the control pits, whereas Na and S concentrations were higher in the control pits (Table 8). The reasons for the elevated elemental concentrations in sample pits are potentially twofold. Firstly, the differences could be due to differences in the parent geology that was being mined, resulting in differing geochemical characteristics between the control and sample pits, or secondly the action of tree roots and root exudates had affected the rhizosphere chemistry, lowering the elemental solubility in the rhizosphere through processes such as pH adjustment and phenolic excretion, thereby lowering the rates that elements were leached from the surrounding tailings (Heim *et al*., 2001). The more likely scenario in this instance is the latter option, as the deposition of tailings occurs as a slurry which settles out on the surface of the TSF in very fine layers. This results in differences in the

geochemical characteristics of the tailings facility being associated with depth in the tailings facility than with geospatial location on the TSF surface.

Table 8: Mean Concentration for selected elements for control and sample pits, mean elemental concentration for sample pit depths and p-values for statistical measures

	Test p-value			Median Concentration mg/kg							
Element	Shapiro-Wilk normality test (all data)	Wilcoxon rank sum test (control vs Sample)	Kruskall wallis (Sample depths)	Sample	Control	0-2cm	2-10cm	10-20cm	20-30cm	50-60cm	70-80cm
Na	**0.01**	0.16	0.12	27310	28055	27310	2434	19905	20530	28825	29475
Mg	0.06	**0.001**	0.13	18740	13945	20765	20410	18725	19420	14830	17940
P	**<0.0001**	0.13	0.07	465.3	500.4	591.05	473.4	444.8	411.75	425.55	460.4
S	**<0.0001**	**0.007**	0.72	3604.5	5370	3833	4038	3388.5	3238	3022.5	3642
Cl	**0.001**	**0.0003**	0.07	213.1	70.05	167.6	299.05	333.45	269.95	96.4	155.05
K	**0.001**	**<0.0001**	0.32	15095	11745	15815	15200	14920	18405	12985	14685
Ca	**0.001**	**0.01**	0.10	4953.5	4073	5287	5740	4756	5132.5	3816	4853
Mn	**<0.0001**	**<0.0001**	0.12	530.25	361.25	530.25	602.35	574.9	1238.5	427.85	460.7
Fe	0.15	**0.0005**	0.21	38610	33100	37845	39150	37485	45595	36370	41680
Cu	**0.0001**	0.09	**0.03**	100.5	74	131.6	86.05	83	140.15	87.15	101.05
Zn	**<0.0001**	**<0.0001**	0.17	168.8	75.7	220.25	187.9	158.95	541.4	109.15	164.35
Rb	**0.01**	**0.0007**	0.12	77.5	58.8	75.55	79.55	74	104.45	68.45	89.45
Sr	**0.01**	**0.007**	0.09	52.05	45.05	58.5	52.05	49.35	58.85	45.7	53.45
Sn	**<0.0001**	0.6	0.52	3.1	4.65	6.05	3	16.25	9.5	3.05	6.3
Pb	0.07	**0.005**	0.39	109.2	94.45	111	116.75	103.35	114.55	111.4	107.8
Th	0.06	0.52	0.66	9.65	9.2	9.65	9.5	9.85	9.3	10.15	8.85
U	**<0.0001**	**0.0003089**	**0.0289**	30.85	11.8	80	42.55	23.3	62.95	25.45	26.05

Within the sample pits, U was the only element where there were differences in concentration associated with location within the tailings profile, the U concentrations were highest in the 0-2cm depth profile (80 mg/kg) and lowest within the 10-20cm depth profile (23.3 mg/kg, p-value = 0.0289) (Table 8). Gold concentrations within the tailings facility were very low, with concentrations ranging between 0.81mg/kg and 0.034mg/kg. This is likely due to the fact that the tailings on the TSF are tailings that have been reprocessed using modern techniques which are more efficient at gold extraction. No significant differences in gold

concentration were found between the control pits and the sample pits, nor were there any differences in the concentration of gold associated with pit depth (See Appendix B, Table 33).

PLANT ELEMENTAL UPTAKE

Elemental concentrations were compared between tailings, belowground biomass and aboveground biomass categories (Table 9). Cu, Fe, K, Mg, Mn, Na, Pb, Rb, Th and U concentrations were higher in tailings than in the biomass. This was either due to the elemental concentration in the tailings being higher than is required for plant biological processes (particularly for the macro-nutrients K and Mg, and the micronutrients Cu, Mn and Fe) resulting in *T. usneoides* excluding them from uptake at the root level, or that the elements were not in a form that was bio-available for uptake (Ryan *et al*., 2001). The Ca, Cl, P, S and Sr concentrations were higher in the belowground biomass than in the tailings and the concentrations for elements Cl, Cu, Fe, Mg, Na, P, Rb and Zn were higher in aboveground biomass than belowground biomass (Table 9).

Significant differences in elemental concentration between the different tissues types were found for all the elements that were selected for analysis (Table 10) with the exception of gold which was below detection limit for all tissues except leaf tissue where the mean concentration was 0.0094 mg/kg) (See Appendix B, Table 32). Within belowground biomass, fine roots had the highest concentrations of K, Na, P; the root epidermal tissue had the highest concentrations of Cu, Fe, Mg, Pb, Rb, Th, U and Zn; the cortex tissue had the highest concentrations of Ca, Cl, S and Sr while the vascular tissue did not exhibit elevated elemental concentrations (Table 10). Analyses of the tissue translocation factor (Table 10) showed that the fine roots had the highest translocation factor for Mn, P, U and Zn; the root epidermal

tissue had the highest translocation factor for the elements Cu, Fe, Mg, Na, Rb and Th; the cortex tissue had the highest translocation factor for Ca, Cl, K, S and Sr and the root vascular tissue had the highest translocation factor for Pb.

Table 9: Median Concentration values (mg/kg) for samples grouped into tailings, aboveground and belowground biomass categories

Summaries	Ca	Cl	Cu	Fe	K	Mg	Mn	Na	P	Pb	Rb	S	Sr	Th	U	Zn
Aboveground	11610	5164	26.8	733	8320	11880	257.6	10730	669.6	3.6	9.5	20730	69.5	0.8	1.9	161.8
Belowground	22890	4166	16.3	531.1	8795	7356	287.5	10540	488	3.7	8.1	26880	90.6	1.1	9.4	96.1
Tailings	4648	145.75	94.35	37640	14175	18060	497.45	27435	473.4	107.65	75.25	3956	49.45	9.55	25.45	146.4

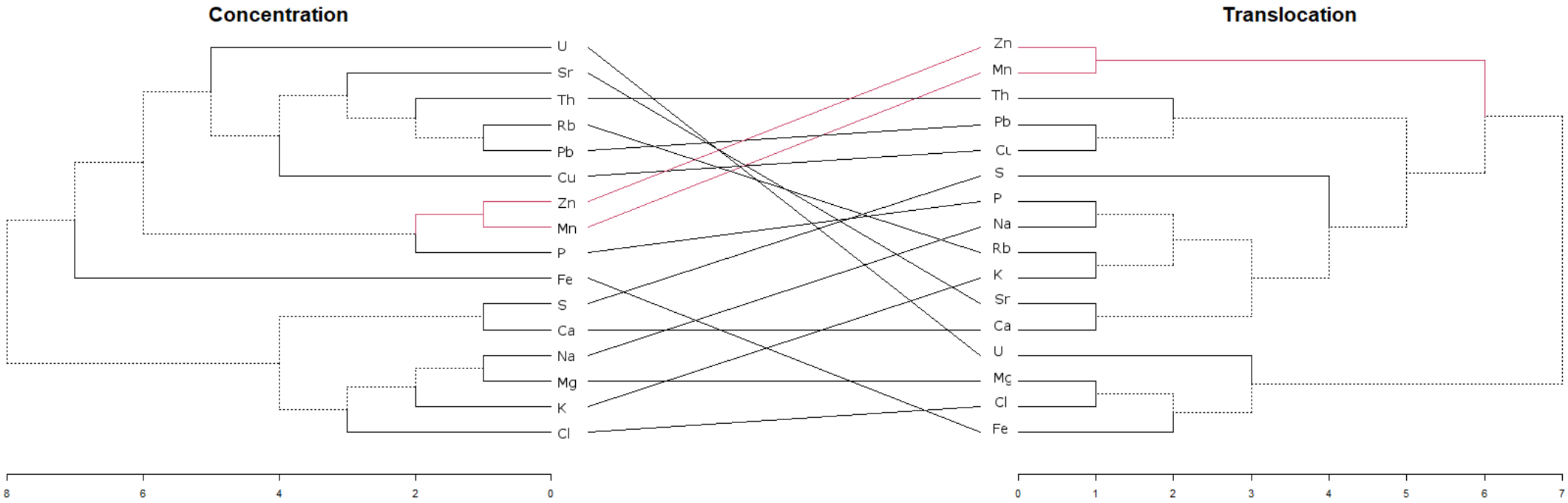

Figure 9: Dendrogram of elemental groupings based on their concentration and translocation factors. The dendrogram was generated using hierarchical clustering analysis (Wards method) to generate a hierarchy of similarity between different elements concentration and translocation factors. Elements with similar groupings for translocation and concentration are likely to have similar physiological response by the plant. As such this dendrogram can be used to determine and relate patterns of uptake for multiple elements.

Table 10: The median elemental concentration (mg/kg) and median translocation factors for belowground plant tissues of *T.usneoides* collected from the Mponeng Tailings facility. Associated p values are also presented.

		Median Concentration mg/kg				Median Translocation factor %			
Element	p-value	Roots Fine	Root Epidermis	Cortex	Root Vascular	Roots Fine	Root Epidermis	Cortex	Root Vascular
Ca	<0.0001	16270	6927	27120	22890	302	42	437	65
Cl	<0.0001	4530	3799	4874	3207	2110	83	1166	85
Cu	0.0006	181	532	12	9	184	294	7	94
Fe	0.001	719	1908	329	530.5	2	265	5	58
K	0.0001	11850	7639	8972	5205	75	64	87	58
Mg	<0.0001	7336	9063	8145	4273	40	123	67	52
Mn	<0.0001	673	487.05	270	193	89	72	46	82
Na	0.0001	11500	9725	11165	8810	45	84	77	79
P	<0.0001	674	412	498	468	140	61	108	91
Pb	0.006	19	30	3	3	17	155	4	164
Rb	<0.0001	11	25	8	5	13	235	20	63
S	<0.0001	18885	14105	34835	26880	510	74	584	77
Sr	<0.0001	61	57	116	90	108	93	207	74
Th	0.03	3	9	1	1	35	255	8	84
U	0.0004	396	1298	7	5	739	327	7	69
Zn	<0.0001	475	550	81	73	170	115	26	94

Hierarchical clustering analysis showed that elements within the tissues can be broadly classified into three groups according to their concentration (Figure 9), with Ca and S Falling into one group; Na, Mg, K and Cl falling into group 2 and U, Sr, Th, Rb, Pb, Zn, P and Fe falling into the third group. However, elemental groupings based on their translocation factors did not yield similar results, with translocation factors falling into three groups, with group one consisting of Th, Cu, Pb, S, Ca, Sr, Na, P, K and Rb, group 2 consisting of Mn and Zn and group 3 comprising U, Fe, Cl and Mg (Figure 9).

High translocation factors for a particular tissue are indicative of increased rates of elemental loading into that tissue (Chen *et al.*, 2009). Such information allows for inferences to be drawn on the mechanisms by which the plant tolerates and transports the ions it accumulates (See Antoniadis *et al.,* 2017 for a comprehensive review). The accumulation of Cl and other

elements with similarly high concentration and translocation factors within the cortex tissue is likely due to elements being parcelled into cytoplasmic vesicles and vacuoles for intra-cellular transport past the Casparian strip (Hodge *et al.*, 2009). Once past the Casparian strip the solutes are unloaded into vascular tissue whereupon it is rapidly transported in solution via the xylem tissue to the aboveground biomass and in the case of excess Ca, Cl and S, excreted. Elements in solution in the xylem tissue are relatively dilute when compared with cortex tissue concentrations as the elements are transported as part of the same process that water is transported to the rest of the plant (Chen *et al*., 2010; Ksouri *et al.*, 2007). Calcium is a macronutrient which is used extensively as a structural or regulatory component in macro-molecules (Wallace *et al.*, 1966) so it was not surprising to detect elevated levels being actively transported in the cortex tissue of *T. usneoides*. In this regard, the Ca may have accumulated as part of the uptake process of SO_4^{2-} ions, where uptake of Ca^{2+} ions would maintain charge balance (Hawksford *et al.*, 2003).

Sulphur concentrations in the root cortex were similarly elevated (Table 10), however unlike for chlorides the tissue with the lowest S concentration was the root epidermis. This was likely a result of *T. usneoides* actively transporting sulphur from the root epidermis and because the surrounding rhizosphere sulphur concentrations were lower, the sulphur in the root epidermis was depleted faster than it could be replenished (Table 10). These findings were similar to those observed in *Tagetes patula* by Makjanic *et al.,* 1988, however those authors did not supply any potential reasons for their observations. Sulphur is utilised in a variety of functions in plant biochemistry, ranging from amino acid synthesis to maintaining protein structure and stability. Importantly, sulphur is utilised in the production of cysteine, an important precursor to the production of metallothioneins which play an integral role in

maintaining ion homeostasis (Joshi *et al.*, 2016). Additionally, Storey & Thomson, 1994 reported that the salt glands of *T. aphylla* contain intracellular calcium sulphate crystals and there is evidence of calcium sulphate excretion by *T. usneoides* (Weiersbye unpublished data; Dennis 2008). Thus, it is likely that sulphur accumulation by *T. usneoides* plays an integral role in maintaining homeostasis and there is a high demand for sulphur in the aboveground biomass, resulting in local depletion of sulphur from the plants roots.

The data showed that the concentrations of the different elements varied with tissue. Typically, most of the elements tested had the lowest concentration in vascular tissue, while the highest concentrations were either found in the cortex or root epidermis. The reasons for this could be related to physiological and biochemical processes which limited the influx of solutes to the rest of the plant in order to prevent ion toxicity (Baxter and Dilkes, 2012). Concentrations of ions within the root cortex tissue that exceed the ambient geochemical concentrations are indicative of active uptake by specific transporter proteins within the membranes of the cortex cells (Baker, 1981). As transporter proteins in cell membranes can only exhibit a certain degree of ion specificity, it is possible that non-nutritive ions can be accidently accumulated (Peralta-Videa *et al*., 2009) and in order to prevent a build-up of these ions, they are rapidly transported to shoot tissue to be excreted (Ding *et al.*, 2010).

Radial ion transfer from the root epidermis to the root xylem tissue is proposed to occur either via the symplasm, via an apoplastic transport route or via a coupled transfer route (Baberon &Geldner, 2014). In apoplastic transport, ions move down a concentration gradient towards the Casparian strip whereupon they are actively transferred into the endodermis (Hodge *et al.*, 2009). Symplastic transport occurs where ions are actively accumulated into

the symplasm of the plant's epithelial cells, transferred via plasmodesmata into the cortex cells and deposited into the endodermal cells where they are transferred to the xylem tissue. This also evidence for a coupled transportation pathway, where polarised transmembrane proteins are localised on an acquisition side of the cell and on an efflux side of the cell, such that the efflux side of one cell corresponds with the acquisition side of another. The transmembrane proteins thus co-ordinate the ion-transfer towards the endodermis via a process of facilitated diffusion down a charge gradient (See Baberon & Geldner, 2014 for a review of the process). The transportation of ions within the root tissue of *T. usneoides* likely follows a combination of the three processes, with ions that are being transported within the cortex tissue at concentrations that exceed ambient geochemical conditions likely following a symplastic or coupled apoplastic-symplastic transport model as a number of elements were accumulated within the root cortex at concentrations that were significantly higher than the root rhizosphere (Table 10).

The differences in the ionic concentration between the epidermal, cortex and vascular tissue of the roots suggested that *T. usneoides* regulates elemental concentration within its roots. As such, elements that were accumulated into the vascular tissue were either actively taken up by the plant, or were accidently taken up as a result of having a similar charge or ionic radius as another element that is required for cellular processing (Clemens, 2006). Of the elements assessed in this study, the only non-nutritive element which was accumulated to any significant concentration within the root vascular tissue was Sr (Table 10) and that was at a concentration that was higher than root epidermal tissue or tailings concentrations. As Sr is a non-nutrient element with a similar charge to Ca, it is likely that it was accidently taken up as part of the cellular processes required for Ca uptake. Similarly, in aboveground biomass

(Table 11), the only element where the highest concentration was found in branch vascular tissue was Sr, while twig vascular tissue and twig bark did not exhibit a similar trend. The loading of vascular tissue with Sr with little evidence of Sr accumulation within other tissues may be due to Sr being bound to the cell walls of the vascular tissue.

Branch bark had the highest Fe concentrations, micro-twigs had the highest concentrations of Pb and leaves had the highest concentrations of Ca, Cl, Cu, K, Mg, Mn, Na, P, Rb, S, U and Zn (Table 11). These trends are presumably the result of the loading of ions into leaf tissue prior to their excretion. Translocation factors followed a different trend, where branch vascular tissue had the highest translocation factor for Cu; twig vascular tissue and micro-twigs did not exhibit high translocation factors for any elements; branch bark had high translocation factor values for Cl, Fe, Mg, Pb, Rb, Th and U; twig bark had the highest translocation factor for K, P, S; and leaves had the highest translocation factor for Ca, Mn, Na, Sr and Zn (Table 11). For the most part, the tissue with the highest concentration of all elements was the leaf (Table 11), with the exception of Sr and Th which were highest in vascular tissue. The tissue with the lowest elemental concentrations varied considerably between the different elements, with Cl, Cu, Fe, K, Mg, Mn, Na, P, Pb, Rb and U having the lowest concentration in wood tissue, while Ca, Sr and Zn had the lowest concentration in bark tissue (Table 11) and S concentration was lowest in twig vascular tissue and Th concentration was lowest in leaf tissue. Dennis, 2008 detected significant concentrations of elements including Ca, Mg, Mn and Cu within the salt exudates of *T. usneoides*, therefore the accumulation of elements within leaf tissue is most likely due to maintenance of homeostasis through the excretion of excess solutes from the salt glands (Ding *et al.*, 2010) whereby solutes are accumulated in leaf tissue prior to excretion (Ding *et al.*, 2010, Wilson *et al*., 2017).

The translocation factors showed a similar trend to elemental concentrations (Table 11). Cl concentrations were significantly higher than S translocation factors for branch bark, micro-twigs and leaf tissue. This indicated that *T. usneoides* actively selects Cl for translocation, despite the fact that in many cases the chloride concentrations of the surrounding tailings were lower than the S concentrations and that *T. usneoides* accumulated significant quantities of S (Table 11). These findings, as well as the differences in the accumulation of metal ions, suggested that there was a certain degree of ion-specificity in the uptake and transportation of bio-available ions.

Table 11: Median elemental concentrations (mg/kg) and median translocation factors for aboveground *T. usneoides* tissues collected from the Mponeng Tailings facility. The associated p values are also presented.

		Median Concentration mg/kg						Median Translocation factor %					
Element	p-value	Branch Vascular	Twig Vascular	Branch Bark	Twig Bark	Micro-twigs	Leaves	Branch Vascular	Twig Vascular	Branch Bark	Twig Bark	Micro twigs	Leaves
Ca	<0.0001	19960	13390	9714	11305	11155	20025	84	124	64	86	100	176
Cl	<0.0001	1524	2486	6344	6111.5	4991	12365	54	39	408	246	81	250
Cu	0.009	15	21	17	26	29	46	184	92	111	118	113	145
Fe	<0.0001	101	239	1031	750	730.05	856	23	12	1057	327	97	113
K	<0.0001	6023	6978	7660	9217	8405	9876	112	93	111	134	90	116
Mg	<0.0001	3058	4452	12055	12485	9077	17100	84	37	381	311	72	180
Mn	<0.0001	160	179	254	279	339	1500	92	76	152	154	107	430
Na	<0.0001	6990	8040	10555	10795	10775	20725	85	79	143	136	100	189
P	<0.0001	478	545	560	725	717	865	113	95	117	131	99	118
Pb	<0.0001	2	3	2	4	5	4	69	65	222	138	123	99
Rb	<0.0001	6	7	9	10	10	13	122	79	150	144	91	147
S	<0.0001	19150	15225	21735	25475	19705	26410	76	69	136	171	76	133
Sr	<0.0001	97	72	56	69	68.85	88	96	118	76	98	98	128
Th	0.002	1	1	1	1	1	0	57	94	112	93	106	32
U	<0.0001	1	1	2	2	2	3	13	10	1825	214	96	133
Zn	<0.0001	135	161	109	161	220	932	210	152	80	94	138	393

Grouping tissue based on elemental concentrations showed that the tissues fell into 2 groups and 2 stand-alone classes (Figure 10). The first group consisted of twig bark, micro – twigs and branch bark and the second group comprised the vascular tissue types and cortex tissue. The root epidermis and leaves did not cluster with any of the other groups and were thus considered as stand-alone classes. When tissue was grouped according to the tissue translocation factor, fine roots and cortex tissue formed a group, root vascular and root epidermis formed a second group, twig bark and twig vascular, micro-twigs and branch vascular tissue and leaves formed a third group, and branch bark was considered a stand-alone class (Figure 10). The groupings of the tissues for the elemental concentration ranges indicate that similar ranges are present within those tissues. Leaf tissue represented the upper concentration range for the majority of the elements analysed, while root epidermis represented the lower bounds with some exceptions for the elements Cu, Fe, Pb, Rb, Th and U. The grouping of twig bark, micro-twigs and branch bark into one group and the grouping of the vascular tissue types and cortex tissue are most likely due to similar elemental loadings being present within those tissues. However, the fact that those tissues did not form similar groupings in terms of their translocation factors is noteworthy as this implied that the physiological processes utilised to achieve those concentrations are not similar between the tissues.

Analysis of the elemental ratios between the different tissues showed that there were changes in the elemental allocation between the tissues (

Table 12). Mg/Ca ratios were highest in root epidermis and lowest in cortex tissue. As the root epidermal tissue Mg concentrations were lower than that of the surrounding tailings, it is

possible that the Mg/Ca ratios in the epidermal tissue were a result of Mg binding to the epidermal tissue. The low vascular and cortex Mg/Ca ratios suggested that the Ca was being transported in preference to Mg. The Na/K ratios were relatively constant in the root tissue, with the exception of fine root tissue which had a lower Na/K ratio than the surrounding tissues, suggesting that K allocation in the fine root tissue was higher than that of the other tissues where Na was actively selected for over K. Halophyte species are well documented to regulate the accumulation of Na and so it is likely that while Na was being accumulated at greater rates than K, it was unlikely to result in toxicity (Zhu, 2001). S/Cl ratios in root tissues showed an increase in the amount of S that was allocated into each tissue type, with the lowest value being found in the root epidermis and the highest in the root cortex. This was interesting as the translocation factors for S in these tissues were considerably lower than those for Cl. The most likely explanation for these observations was that Cl concentrations within the surrounding tailings were low and thus despite actively selecting for Cl, considerably higher quantities of S were accumulated as it was more readily available.

In the aboveground biomass, Mg/Ca ratios were highest in the bark tissue and lowest within leaf tissue. This suggested that Mg was being preferentially transported to bark tissue and Ca transported into leaf tissue where it was most likely excreted out via the salt glands. Na/K ratios were lowest within the branch vascular tissue and highest within leaf tissue which also suggested that the plant was actively loading Na into its leaf tissues. Conversely, for S/Cl ratios, the tissue with the highest value was the vascular tissue, while the lowest value is the leaf tissue, suggesting again that *T. usneoides* has a preference for the transportation of chlorides into leaf tissue. In plants, excess Na^+ is frequently cited as the underlying cause of toxicity associated with salinity stress. The Na^+ toxicity is a result of inhibition of enzyme activity due to competition between K^+ and Na^+ for enzyme binding sites (White & Broadley,

2001). This inhibition can occur within the cytosol as well as at the plasmalemma of root cells resulting in decreased total K^+ uptake, reducing the efficacy of processes such as enzyme activation (Mengel, 2016). The Cl^- component of NaCl has been documented as having limited toxicity, only affecting some members of the genera *Citrus* and *Vitis* for example (White & Broadley, 2001).

Studies into the toxicity of sulphate over chloride by Reich *et al*., 2017 showed an increased toxicity of sulphate over chloride in *Brassica rapa.* The presence of sulphate ions in the growth medium down-regulated expression of genes associated with primary sulphate uptake, while genes encoding for the vacuolar sulphate transport were upregulated. This suggests that the influx of sulphate ions is limited by sulphates within the rhizosphere, while sulphate transportation and sequestration *in planta* are increased. In the glycophyte *Nicotiana tabacum* chlorides were shown to play a role in leaf elongation, turgor pressure maintenance and moderating leaf water balance parameters (Franco-navarro *et al*., 2015). Those authors proposed that uptake and accumulation of Cl^- responds to adaptive functions improving water homeostasis in higher plants. Accumulation of Cl^- as well as a range of organic molecules has been shown to play a role in the maintenance of turgor pressure in guard cells and mature plant cells, thus limiting water loss through the stomata, which could further serve to explain the elevated chloride concentrations present within the leaves of *T. usneoides*. This trait would be particularly useful considering the hot arid environments that the species typically inhabits, where water availability is sporadic.

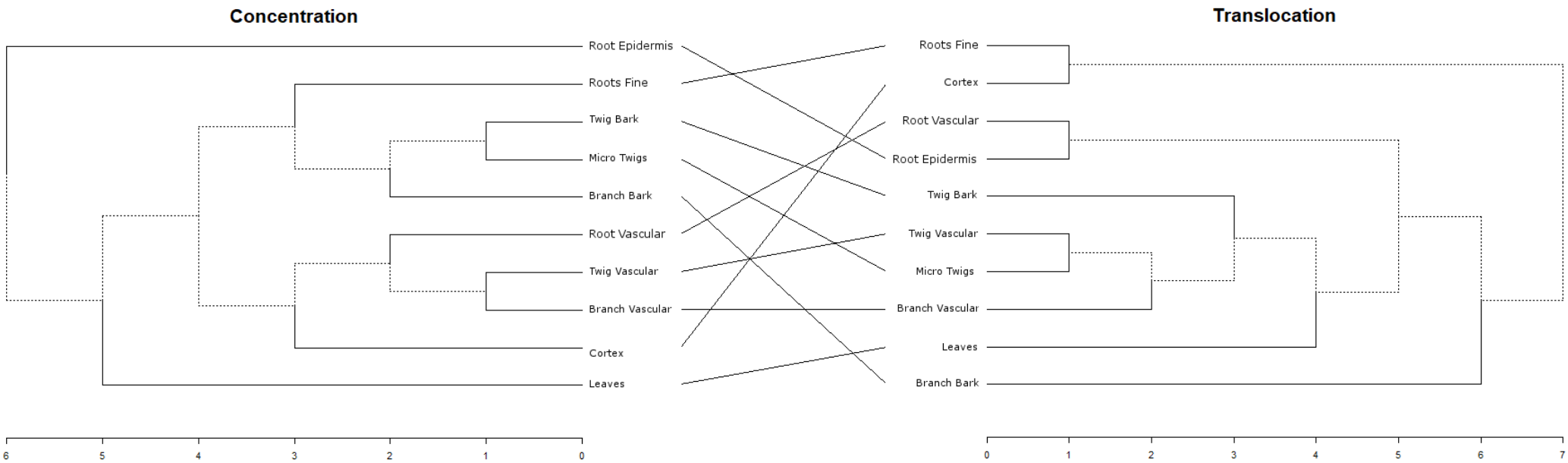

Figure 10: Dendrogram showing tissue groupings for tissue elemental concentration (mg/kg) and the translocation factor (%) derived from multi-factoral unsupervised hierarchical cluster analysis (Wards method) to determine similarities in elemental concentrations and translocation for the different tissue types..

Table 12: Median elemental concentration ratio and p-value from Kruskall - Wallis test for tissue samples collected from trees harvested from the Mponeng tailings facility

		Median Elemental concentration ratio									
Ratio	p-value	Roots Fine	Root Epidermis	Root Vascular	Cortex	Branch Vascular	Branch Bark	Twigs Vascular	Twig Bark	Micro twigs	Leaves
Mg/Ca	<0.0001	0.450867	1.308799	0.173629	0.301413	0.175451	1.207953	0.332218	1.104862	0.811913	0.848845
Na/K	0.01328	0.970664	1.272906	1.528733	1.226162	1.160551	1.307533	1.153841	1.170119	1.280506	2.112559
S/Cl	0.0003623	4.168921	3.712954	6.773884	7.146345	6.517501	3.050448	6.639534	4.138436	4.059805	2.136826

SOLUTE ACCUMULATION IN *TAMARIX USNEOIDES*

Plants which inhabit desert riparian environments are adapted to a wide range of ion concentrations and changes in osmotic pressure as a result of the fluxes in solute concentration that occur during periods of inundation and subsequent evaporation (Horton *et al*., 2003). High solute concentration in the rhizosphere causes a number of disruptions to a plants' ability to prevent dehydration and accumulate nutrients, as the action of accumulating water is largely reliant on the osmotic gradient provided by dissolved solutes in the cytoplasm of the cells of the plant (Kronzucker & Britto, 2011). Thus, in an environment where the solute concentrations of the rhizosphere are significantly higher than those that would typically be found in environments inhabited by glycophytes, halophytes such as *T. usneoides* have adaptations to conventional physiological processes which allow them/it to maintain an osmotic gradient in order to prevent dehydration (Ksouri *et al.,* 2007). The high elemental concentrations that were found in the root epidermal and cortex tissue (S, Cl and Ca ions), could be used to maintain an osmotic gradient to facilitate water flow into root cortex tissue (Table 10) and as such would be an example of this halophytes adaptation to its environment. Furthermore, the high cortex concentrations suggested that the movement of solutes into the cortex was a result of active transport into the symplasm of the cortex cells (a process whereby ions are transported across the plasmalemma against a concentration gradient utilizing energy (Barabash and Stefanovska, 2016)) as passive uptake processes such as apoplastic transport rely on diffusion, solute concentrations in the root cortex would not have exceeded those of the surrounding tailings.

This study has demonstrated that despite accumulating significant quantities of Au *in vitro*, there is limited uptake of gold *in-situ* by *T. usneoides* from gold tailings facilities with

geochemical characteristics such as those found on Mponeng. There are a number of possible explanations for these observations. Firstly, it may be that *T. usneoides* is not capable of rendering gold bio-available for uptake in the manner of other plant species (e.g. cyanogenic species) (Anderson *et al.*, 1999). Gold dissolves under strong acid conditions and as *T. usneoides* raises tailings pH it is unlikely that gold in its native form and will be bioavailable. This finding is supported by the results of the *in vitro* gold accumulation study which showed that the plantlets are capable of gold accumulation at the pH range that is found on a tailings facility when the gold is in a form that is readily bioavailable. Secondly, it is possible that all free gold was removed during the metallurgical process and as a result, the gold that does remain in the tailings facilities is encapsulated within pyrite minerals and thus not easily accessible to the plant for uptake (Filmer, 1982) as the upper limit of gold concentration on the tailings facility (0.8mg/kg) exceeded that of the lower limit where gold was detected *in vitro* (0.5mg/kg) it is likely that the gold on the tailings facility was simply in a form that was inaccessible to the plants for uptake. A third possibility for the reduced uptake *in-situ* when compared with the *in vitro* studies is that the ion channels which are capable of Au uptake may be inhibited due to the presence of other ions in the tailings of similar ionic radius such as U (Mäser *et al.*, 2002). U concentrations in root epidermal tissue and the fine root tissue were considerably higher than tailings concentrations suggesting that the plant was actively taking up uranium into these tissues. If ion competition for binding sites on root tissues were occurring it would effectively explain the lack of gold within the plant.

Studies into gold biogeochemistry have shown that the action of certain bacteria and fungi facilitates the bio-oxidation and complexation of gold (Reith *et al*., 2007). In environments poor in organic matter (such as tailings facilities), the action of lithoautotrophic bacterial populations favours the production of gold thiosulphate. In areas where organic matter is

present, formation of gold cyanide complexes are favoured, while in saline environments bacterial communities favour the production of gold chloride complexes (Southam *et al.*, 2009). This suggests that in environments such as those found on gold tailings facilities the primary forms of microbially induced gold complexes will be gold thiosulphate for the majority of the tailings facility and gold cyanide in the areas where microbes have access to organic matter in the form of leaf detritus and root exudates. The finding of little to no gold accumulation *in planta* in this study is thus likely due to the inherently low gold concentrations of bioavailable gold in the surrounding tailings.

Collectively, the data suggest that it is unlikely that *T. usneoides* is a viable species for use in the phyto-extraction of gold from TSF's without the addition of amendments to increase gold bio-availability as the types of gold from these sites are both derived from gold that was left-over after the metallurgical process has removed the bulk of the gold from tailings (Fashola *et al*., 2016). Sites with differing geochemical characteristics such as metallurgical waste streams or constructed wetlands may have differing geochemical characteristics and so it is recommended that additional studies be performed to assess gold accumulation potential from sites with alternative geochemical conditions. Additionally, *T. usneoides* can be usefully applied for its ability to tolerate highly saline environments and to ameliorate soil conditions through the phytoextraction of sulphates and rhizosphere pH amelioration which would reduce contaminant mobility. A point that is worthwhile noting is that the values which are reported in this study represent 'a moment in time' in the plants physiological processes and it is possible that the flux of elements will change depending on the different environmental factors as well as season. In this regard Galeas *et al.,* 2007 demonstrated that concentrations of S and Se vary depending on season for accumulators and non-accumulator species and as plant elemental accumulation is largely driven a variety of physiological processes. It is likely

that this applies to all elements that are accumulated. Thus, additional studies should attempt to determine the effect of these fluxes and try to develop a model for elemental accumulation in *T. usneoides.*

3.5. Conclusion

Tamarix usneoides exerts tight control on the types of ions that it accumulates, however in this study it did not seem to be able to mobilise gold for uptake. Investigations into the role of site geochemistry on uptake and assessments of the potential for induced gold uptake through the addition of soil ameliorants need to be considered. However, in terms of accumulation of elements such as magnesium, phosphorous, sulphur, chlorine and calcium, there is potential for the use of *T. usneoides* in phyto-extraction, as these elements are accumulated to concentrations that are significantly higher than ambient geochemical background concentrations. The accumulation and excretion of Sulphur in the form of calcium sulphate is a useful trait as it reduces the amount of Sulphur available to Sulphur utilizing bacteria, thus reducing the acid generation potential of an area planted with *T. usneoides* Furthermore, the present data show that *T. usneoides* is capable of significantly altering soil geochemistry, where by raising the rhizosphere pH, it will also reduce the mobility of other metal ions. This implies that *T. usneoides* is particularly suited to the control of shallow contaminant plumes from areas such as unlined return water dams and constructed wetlands where the mobility of solutes in the soil needs to be reduced and the rhizosphere chemistry needs to be altered and the pH raised (phyto-stabilisation, Mendez & Maier, 2008). The removal of elements such as Sulphur and chlorine would also be beneficial within this context. A potential liability to the use of the species for remediation of soils, is that through the action

of excretion of excess solutes from leaf tissue, there is subsequent deposition of these solutes on the soil surface via the salt glands, which can potentially inhibit the growth of other plant species (Di Tomaso, 1998).

3.6. Acknowledgements

This study was supported by AngloGold Ashanti and the Technology for Human Resources for Industry Programme (THRIP) award no. TP13080525596 from the Department of Trade and Industry and the National Research Foundation of South Africa to I.M. Weiersbye and E.T.F. Witkowski.References

3.7. References

Anderson C. W. N., Brooks R. R., Chiarucci A., LaCoste C. J., Leblanc M., Robinson B. H., Simcock R. & Stewart R. B., (1999). Phytomining for nickel, thallium and gold. *Journal of Geochemical Exploration*, 67(1), 407-415.

Antoniadis V., Levizou E., Shaheen S.M., Ok Y.S., Sebastian A., Baum C., Prasad M.N., Wenzel W.W. and Rinklebe J., (2017). Trace elements in the soil-plant interface: Phytoavailability, translocation, and phytoremediation–A review. *Earth-Science Reviews*, *171*,621-645.

Baker A. J., (1981). Accumulators and excluders-strategies in the response of plants to heavy metals. *Journal of plant nutrition*, 3(1-4), 643-654.

Barceló J. U. A. N. & Poschenrieder C. (1990). Plant water relations as affected by heavy metal stress: a review. *Journal of plant nutrition*, 13(1), 1-37.

Baxter I. & Dilkes B. P. (2012). Elemental profiles reflect plant adaptations to the environment. *Science*, *336*(6089), 1661-1663.

Bettger W. J. & O'Dell B. L. (1981) A critical physiological role of zinc in the structure and function of biomembranes. *Life sciences*, 28(13), 1425- 1438.

Blight G. M. (1983). The behaviour of mine tailings during hydraulic deposition. *Journal of the Southern African Institute of Mining and Metallurgy*, 83(4), 87-91.

Chaney R. L., Angl, J. S., Broadhurst C. L., Peters C. A., Tappero R. V. & Sparks D. L. (2007). Improved understanding of hyperaccumulation yields commercial phytoextraction and phytomining technologies. *Journal of Environmental Quality*, *36*(5), 1429-1443.

Chen W., Li, L., Chang A. C., Wu L., Chaney R. L., Smith R., & Ajwa H. (2009). Characterizing the solid–solution partitioning coefficient and plant uptake factor of As, Cd, and Pb in California croplands. *Agriculture, ecosystems & environment*, *129*(1-3), 212-220.

Clemens S, (2006). Toxic metal accumulation, responses to exposure and mechanisms of tolerance in plants. *Biochimie*, 88(11), 1707-1719.

Dennis, A.M (2008). Salt glands and elemental concentrations in leaves of *Tamarix usneoides* E.Mey ex Bunge (*Tamaricaceae*) grown on seepage from Highveld gold mines, unpublished Honours Project.

Di Tomaso J. M. (1998). Impact, biology, and ecology of saltcedar (*Tamarix* spp.) in the southwestern United States. *Weed technology*, 326-336.

Ding F., Yang J. C., Yuan F., Wang B. S., (2010) Progress in mechanism of salt excretion in recretohalopytes. *Frontiers in Biology*, 5(2), 164-170.

Dunn O. J., (1961) Multiple comparisons among means. *Journal of the American Statistical Association* 56, 52–64.

Dye P.J., Jarmain C., Oageng B., Xaba J. and Weiersbye I.M. (2008). The potential of woodlands and reed-beds for control of acid mine drainage in the Witwatersrand Gold Fields, South Africa. In *Mine Closure 2008: Proceedings of the Third International Seminar on Mine Closure* (pp. 487-497).

Dye P. J., Jarmain C., Clulow A. D., Everson C. S., Mengistu M. G. & Weiersbye I. M. (2018). Evapotranspiration from mine-affected riparian sites along the Vaal River in central South Africa. *South African Geographical Journal*, *100*(1), 62-81.

Fashola M. O., Ngole-Jeme V. M. & Babalola O. O. (2016). Heavy metal pollution from gold mines: environmental effects and bacterial strategies for resistance. *International journal of environmental research and public health*, *13*(11), 1047.

Filmer A. O. (1982). The dissolution of gold from roasted pyrite concentrates. *Journal of the Southern African Institute of Mining and Metallurgy*, 82(3), 90-94.

Franco-Navarro J. D., Brumós J., Rosales M. A., Cubero-Font P., Talón M., & Colmenero-Flores J. M. (2015). Chloride regulates leaf cell size and water relations in tobacco plants. *Journal of experimental botany*, *67*(3), 873-891.

Galán E., Gómez-Ariza J. L., González I., Fernández-Caliani J. C., Morales E. & Giráldez I. (2003) Heavy metal partitioning in river sediments severely polluted by acid mine drainage in the Iberian Pyrite Belt. *Applied Geochemistry*, 18(3), 409-421.

Galeas M. L., Zhang L. H., Freeman J. L., Wegner M., & Pilon-Smits E. A. (2007). Seasonal fluctuations of selenium and sulfur accumulation in selenium hyperaccumulators and related non-accumulators. *New Phytologist*, *173*(3), 517-525.

Gardea-Torresdey J.L., Parsons J.G., Gomez E., Peralta-Videa J., Troiani H.E., Santiago P., Jose & Yacaman,M. (2002). Formation and growth of Au nanoparticles inside live alfalfa plants. *Nano Letters*, 2, 397–401.

Girling, C. A., & Peterson, P. J. (1980). Gold in plants. *Gold bulletin*, *13*(4), 151-157.

Hagemeyer, J., & Waisel, Y. (1988). Excretion of ions (Cd^{2+}, Li^{+}, Na^{+} and Cl^{-}) by *Tamarix aphylla*. *Physiologia plantarum*, *73*(4), 541-546.

Hawkesford, M. J., Buchner, P., Hopkins, L., & Howarth, J. R. (2003). Sulphate uptake and transport. In *Sulphur in Plants* (pp. 71-86). Springer Netherlands.

Heim, A., Brunner, I., Frey, B., Frossard, E., & Luster, J. (2001). Aluminium resistance of Norway spruce: Root exudation versus immobilisation in roots. In *Plant Nutrition* (pp. 450-451). Springer, Dordrecht.

Hodge A., Berta G., Doussan C., Merchan F., & Crespi M. (2009). Plant root growth, architecture and function, *Plant and soil*, 321(1-2), 153 – 187.

Horton, J. L., Hart, S. C., & Kolb, T. E. (2003). Physiological condition and water source use of Sonoran Desert riparian trees at the Bill Williams River, Arizona, USA. *Isotopes in Environmental and Health Studies*, 39(1), 69-82.

Johnson D. B., & Hallberg K. B. (2005). Acid mine drainage remediation options: a review. *Science of the total environment*, 338(1), 3-14.

Joshi R., Pareek A., &Singla-Pareek S.L. (2016). Plant Metallothioneins: classification, distribution, function and regulation. In *Plant Metal Interaction* (pp. 239 -261) Elsevier.

Kadukova J., Manousaki E. & Kalogerakis N. (2008). Pb and Cd accumulation and phyto-excretion by salt cedar (*Tamarix smyrnensis* Bunge). *International Journal of Phytoremediation*, 10(1), 31-46.

Kleinkopf G. E. & Wallace A. (1974). Physiological basis for salt tolerance in *Tamarix ramosissima*. *Plant science letters*, *3*(3), 157-163.

Kronsukker H.J. & Britto D.T., (2011). Sodium transport in plants: a critical review, *New Phytologist*, 189,54–81.

Kruskal W. H. & Wallis W. A. (1952). Use of ranks in one-criterion variance analysis. *Journal of the American statistical Association*, *47*(260), 583-621.

Ksouri R., Megdiche W., Debez A., Falleh H., Grignon C. & Abdelly C., (2007). Salinity effects on polyphenol content and antioxidant activities in leaves of the halophyte *Cakile maritima*. *Plant Physiology and Biochemistry*, 45(3), 244-249.

Kuppusamy S., Palanisami T., Megharaj M., Venkateswarlu K., & Naidu R. (2016*). In-situ* remediation approaches for the management of contaminated sites: a comprehensive overview. In *Reviews of Environmental Contamination and Toxicology Volume 236* (pp. 1-115). Springer, Cham.

Lintern M., Anand, R., Ryan, C. & Paterson, D. (2013). Natural gold particles in *Eucalyptus* leaves and their relevance to exploration for buried gold deposits, *Nature Communications*, 4, 2274.

Makjanic J. R. D., Vis A. F., Groneman F. J., Gommers & Henstra S. (1988). Investigation of P and S Distributions in the Roots of *Tagetes patula* L. using Micro-PIXE. *Journal of experimental botany.* 39(11), 1523-1528.

Manousaki E., & Kalogerakis N. (2011). Halophytes—an emerging trend in phytoremediation. *International Journal of Phytoremediation*, 13(10), 959-969.

Marschner H. (2011). Marschner's mineral nutrition of higher plants. Academic press.

Marshall A. T., Haverkamp R. G., Davies C. E., Parsons J. G., Gardea-Torresde, J. L. & van Agterveld D. (2007). Accumulation of gold nanoparticles in *Brassic juncea*. *International journal of phytoremediation*, *9*(3), 197-206.

Mäser P., Gierth M. & Schroeder J. I. (2002). Molecular mechanisms of potassium and sodium uptake in plants. *Plant and soil*, 247(1), 43-54

Mayonde S.G., Cron G., Gaskin J.F. & Byrne M.J. (2015). Evidence of *Tamarix* hybrids in South Africa, as inferred by nuclear ITS and plastid trnS–trnG DNA sequences. *South african journal of botany*. 96, 122-131.

McGrath S.P. & Zhao F.J., (2003). Phytoextraction of metals and metalloids from contaminated soils. *Current Opinion in Biotechnology*, 14(3), 277-282.

Mendez M. O. & Maier R. M. (2008). Phytostabilization of mine tailings in arid and semiarid environments—an emerging remediation technology. *Environmental health perspectives*, 116(3), 278.

Mengel K. (2016). Potassium. In *Handbook of plant nutrition*(pp. 107-136). CRC Press.

Murtagh F. & Legendre P. (2011). Ward's hierarchical clustering method: Clustering criterion and agglomerative algorithm. *arXiv preprint arXiv:1111.6285*.

Naicker K., Cukrowska E. & McCarthy T.S. (2003). Acid mine drainage arising from gold mining activity in Johannesburg, South Africa and environs, *Environmental Pollution*, 122, 29–40.

Nye P. H. (1981). Changes of pH across the rhizosphere induced by roots. *Plant and soil*, *61*(1-2), 7-26.

Peralta-Videa J. R., Lopez M. L., Narayan M., Saupe G., & Gardea-Torresdey J. (2009). The biochemistry of environmental heavy metal uptake by plants: implications for the food chain. *The international journal of biochemistry & cell biology*, 41(8), 1665-1677.

Reich M., Aghajanzadeh T., Helm J., Parmar S., Hawkesford M. J., & De Kok L. J. (2017). Chloride and sulfate salinity differently affect biomass, mineral nutrient composition and expression of sulfate transport and assimilation genes in *Brassica rapa*. *Plant and soil*, *411*(1-2), 319-332.

Reith F., Lengke M. F., Falconer D., Craw D. & Southam, G. (2007). The geomicrobiology of gold. *The ISME Journal*, *1*(7), 567.

Ryan P. R., Delhaize E., & Jones D. L. (2001). Function and mechanism of organic anion exudation from plant roots. *Annual review of plant biology*, 52(1), 527-560.

Shapiro S. S. & Wilk M B (1964). An analysis of variance test for normality (complete samples) (Doctoral dissertation), Rutgers, The State University

Sheoran A. S. & Sheoran V. (2006) Heavy metal removal mechanism of acid mine drainage in wetlands: a critical review. *Minerals Engineering*, 19(2), 105-116.

Southam G., Lengke M. F., Fairbrother L., & Reith F. (2009). The biogeochemistry of gold. *Elements,* 5(5), 303-307.

Barabash, M., & Stefanovska, A. (2016). Model of membrane-potential fluctuations.

Storey R. & Thomson, W. W. (1994). An X-ray microanalysis study of the salt glands and intracellular calcium crystals of *Tamarix*. *Annals of Botany*, *73*(3), 307-313.

Student. (1908). The probable error of a mean. *Biometrika*, 1-25.

Thomson W. W., Berry W. L. & Liu L. L. (1969). Localization and secretion of salt by the salt glands of *Tamarix* aphylla. *Proceedings of the National Academy of Sciences*, *63*(2), 310-317.

Tutu H., McCarthy T. S. & Cukrowska E. (2008) The chemical characteristics of acid mine drainage with particular reference to sources, distribution and remediation: The Witwatersrand Basin, South Africa as a case study. *Applied Geochemistry*, 23(12), 3666-3684.

Tutu H., Camden-Smith B., Cukrowska E. M., Bakatula E. N., Weiersbye I. M., & Sutton M. S. (2011) Mineral efflorescent crusts as sources of pollution in gold mining environments in the Witwatersrand Basin. Mine Water – Managing the Challenges", *IMWA* 2011.

Wallace A., Frolich E., & Lunt O. R. (1966). Calcium requirements of higher plants. *Nature*, 209(5023), 634-634.

Weiersbye I.M. & Witkowski E.T.F (1998) The structure, diversity and persistence of naturally-colonizing and introduced vegetation on gold tailings and tailings-polluted soils. *Plant Ecology & Conservation*, 8, 224.

Weiersbye I.M., Witkowski E. T. F., & Reichardt M., (2006) Floristic composition of gold and uranium tailings dams, and adjacent polluted areas, on South Africa's deep-level mines, *Bothalia*, 36(1), 101-127.

White P. J., & Broadley M. R. (2003). Calcium in plants. *Annals of botany*, 92(4), 487-511.

Wilson H., Mycock D., & Weiersbye I. M. (2017). The salt glands of *Tamarix usneoides* E. Mey. ex Bunge (South African Salt Cedar). *International journal of phytoremediation*, 19(6), 587-595.

Winde F. (2010). Uranium pollution of the Wonderfonteinspruit, 1997-2008 Part 1: Uranium toxicity, regional background and mining-related sources of uranium pollution. *Water Sa*, 36(3), 239-256.

Wu S., Feng, X., & Wittmeier A. (1997). Microwave digestion of plant and grain reference materials in nitric acid or a mixture of nitric acid or a mixture of nitric acid and hydrogen peroxide for the determination of multi-elements by inductively coupled plasma mass spectrometry. *Journal of Analytical Atomic Spectrometry*, *12*(8), 797-806.

Zhu Z.J., Wang H., Yan B., Zheng H., Jiang Y., Miranda O.R., Rotello V.M., Xing B. & Vachet, R.W. (2012). Effect of surface charge on the uptake and distribution of gold nanoparticles in four plant species. *Environmental science & technology*, 46(22), 12391-12398.

4. The salt glands of *Tamarix usneoides* E. Mey. ex Bunge (South African Salt Cedar)

Hayden Wilson, David Mycock, and Isabel M. Weiersbye

University of the Witwatersrand, Johannesburg, Faculty of Science, School of Animal, Plant and Environmental Sciences, +27 (11) 717 6403, Private Bag 3 Wits 2050, South Africa.

Hayden.Wilson@students.wits.ac.za, David.Mycock@wits.ac.za,

Isabel.Weiersbye@wits.ac.za

The following chapter is presented as the manuscript that was accepted for publication by the International Journal of Phytoremediation Volume 19, 2017 - Issue 6, 587-595 https://doi.org/10.1080/15226514.2016.1244163. As such, the referencing system used in this chapter is different to the rest of the thesis.

4.1. Abstract

Tamarix usneoides is a halophyte tree endemic to south-western Africa. This species is known to excrete a range of ions from specialised glandular structures on its leaves. To understand the mechanisms involved in the transport, sequestration and excretion of ions by the glands, a study was performed on salt gland distribution and ultrastructure.

The glands are vesiculated trichomes, comprised of eight cells *viz*., two basal collecting cells and six excretory cells, partially bounded by a secondary cell wall which, could serve as an impermeable barrier, forcing excess ions to move from the apoplast of the surrounding tissue into the cytoplasm of the basal excretory cells. It was hypothesised that the ions are moved across the excretory cells in endocytotic vesicles that fuse with the plasmalemma or form junctional complexes, allowing ion movement from one excretory cell to the next. In the apical cell, the vesicles fuse with the plasmalemma, releasing the ions into the network of cell wall ingrowths which channel the ions to the outside surface of the cell.

This study shows that there are distinct structural adaptations for the processing of ions for excretion, although the mechanism by which ions enter the cells still needs to be determined.

Keywords: Halophyte; gyspophile; excretion; salinity tolerance.

4.2. Introduction

Halophytes are plants which are able to tolerate high salinity in their growth environment and complete their life cycles under such conditions (Scholander *et al.*, 1962; Berry 1970; Marschner *et al*., 2011). Increased Na^+ concentration in cellular cytoplasm is toxic to plants due to competition between Na^+ and K^+ ions (Kramer, 1983; Kronsucker and Britto, 2011). Thus, halophyte plants have developed a series of adaptations to either reduce Na^+ assimilation at the root level or to excrete excess Na^+ ions from specialised glands thereby maintaining ion homeostasis (Kramer *et al.,* 1977). An example of the latter strategy can be found in the genus *Tamarix* (Tamaricaceae) where salts are excreted from specialised structures on the surface of the leaf known as vesiculated trichomes or "salt glands". In certain halophyte species a range of ions are excreted from the salt-glands (Kadukova *et al*., 2008), implying that the cellular mechanisms for the removal of ions is not Na^+ and Cl^- ion specific but may be used as a method to maintain homeostasis for a number of potentially detrimental ions.

The South African Salt Cedar (*Tamarix usneoides* E. Mey. ex Bunge 1843, Tamaricaceae) is an exo-recretohalophyte species that inhabits environments where saline water is present in the arid to semi-arid western region of Southern Africa. The species has also been introduced to gold, uranium and copper mine tailings dams and polluted soils in central South Africa (Weiersbye *et al.,* 2006; I.M. Weiersbye, unpublished survey, May 2008). Because of its salinity tolerance and ability to hyper-accumulate sulphates from acid mine drainage and excrete gypsum and other compounds (Dennis, 2008; I.M. Weiersbye, 2005 unpublished data), *T. usneoides* is used in phytoremediation of acid mine drainage and other contaminated environments (Weiersbye, 2007). A range of elements (lithium, sodium, magnesium, sulphur,

chlorine, potassium, calcium, manganese, nickel, cobalt, zinc, arsenic, selenium, cadmium, gold, lead and uranium) have been detected in the leaves of *T. usneoides,* its hybrid *T. usneoides* x *T. ramossisima at* concentrations exceeding ambient geochemical backgrounds, with sulphate and chloride minerals, including gypsum, epsomite and halite, detected in excreted salts (Kleinkopf and Wallace, 1974; Hagemeyer and Waisel, 1988; I.M. Weiersbye, 2005, unpublished data; Kadukova *et al.*, 2008; Manousaki *et al.*, 2008; Kendall, 2010). Thus, in order to better understand the mechanisms involved in the transport, sequestration and subsequent excretion of excess ions, an ultrastructural study was performed on the salt excretory tissues of *T. usneoides*.

4.3. Methods

PLANT IDENTIFICATION AND PROVENANCE

Due to the presence of *T. usneoides* hybrids with other *Tamarix* species in South Africa (Weiersbye *et al*., 2006; Mayonde *et al*., 2014), the material described in this report has been confirmed as *T. usneoides* using a combination of vegetative and reproductive characters, and amplified fragment length polymorphism (AFLP) data (G. Mayonde, 2015, unpublished data). The following confirmed clones of *T. usneoides* were used: GMS034, GMS046 and GMS053 (provenance Northern Cape). Voucher specimens are being lodged with the C.E. Moss Herbarium, the University of the Witwatersrand, Johannesburg.

PROPAGATION OF MOTHER STOCK MATERIAL

Stem sections (15 cm in length and 0.80 to 1.20 cm in diameter) were cut and planted during late winter in 750 ml plastic planting bags containing 1:4 parts potting compost and river sand such that 10 cm of the length of the stem was submerged in the growth medium (Wilson,

2010). The cuttings were then established within a glass greenhouse maintained at a temperature of 15-30 ^{o}C and irrigated from overhead systems using potable chlorinated water for a period of 15 minutes every 8 hours. Cutting maintenance consisted of regular weeding as well as treatment with either the systemic fungicide Benlate 500WP (5 ml/l) (active ingredient, benzimidazole [500 g kg^{-1}]) or the systemic fungicide Previcure (1 ml/l) (active ingredient, propamocarb) every 4 weeks, and fertilised with a dilute solution of a commercial plant nutrient solution Nitrosol® (3.33 ml/l) every 6 weeks.

PROPAGATION OF *IN VITRO* MATERIAL FOR MICROSCOPY

In vitro material was derived from 3.0 cm long apical shoots that had been harvested from the mother stock material growing in the greenhouse. Working within a laminar flow cabinet, the apical shoots were surface decontaminated by immersing the material in a 2 % sodium hypochlorite solution for 15 minutes, followed by rinsing the material in sterilised ultrapure water (MilliQ). Material was grown in 2 ml of 25 % Murashige and Skoog (1962) growth medium (1.1 g/l) which was buffered with NaOH to pH 4.8, 5.6 or 7.6, prior to autoclaving at 121 ^{o}C for 20 minutes. The plants were grown in 125 ml borosilicate glass growth vials within a growth chamber which maintained a constant temperature of 25 ^{o}C, and a dark/light cycle of 8/16 hours with light intensity of 100 µmol m^{-2} s^{-1} provided by Philips TLD-58W/33-640 fluorescent tubes.

MATERIAL PREPARATION FOR LIGHT AND ELECTRON MICROSCOPY

Apical shoots and leaves were removed from the plantlets grown *in vitro* for a period of 8 weeks. These were fixed overnight at room temperature (20 – 25 ^{o}C) in 2 % gluteraldehyde in a 0.05 M sodium phosphate buffer, pH 7.2. The material was then rinsed four times in the buffer, post-fixed for two hours in 2 % OsO_4 and then rinsed four times in buffer again. The material was then dehydrated through a 10, 25 and 50 % graded ethanol series before staining

in 1 % uranyl acetate in 75 % ethanol. The material was then rinsed in 75 % ethanol and passed through four sequential dehydrations of 15 minutes each, starting with two in 100 % ethanol and then two in propylene oxide.

The tissue was then infiltrated in a solution consisting of 50 % Spurr epoxy resin (Spurr, 1969) and propylene oxide for 4-5 hours. This mixture was then replaced with pure resin and allowed to infiltrate for 14 hours. The samples were then placed in resin trays and polymerised at 70 ^{o}C for 8-12 hours.

A Reichert ultra-microtome was used to cut 0.1 µm sections for transmission electron microscopy and 1 µm sections for light microscopy.

LIGHT MICROSCOPY

1 µm thick sections were obtained from vaginate and sessile leaf tissues as well as stem tissue. The entire leaf was sectioned from the base through to the apex. The sections were collected on glass slides and stained with toluidine blue (60 ml 1% w/v sodium bicarbonate, 40 ml glycerol and 1 g toluidine blue) by placing a drop of solution onto each section and allowing the stain to infiltrate for 5 minutes at a temperature of 60°C. Excess stain was removed by repeatedly rinsing the slide with ultrapure (MilliQ) water. The sections were then mounted in DPX and viewed using an Olympus BX63 microscope. Salt glands were photographed at a magnification of 1000x. A total of 540 sections from 3 leaves on 3 plantlets (3 replicate clones) were viewed.

TRANSMISSION ELECTRON MICROSCOPY

Vaginate and sessile leaf tissue was sectioned into 0.1µm sections, placed on copper grids and then stained with lead citrate ($(C_6H_5O_7)_2Pb_3 \cdot 3H_2O$). These were then viewed and photographed with an FEI Spirit T12 transmission electron microscope (TEM) at a voltage of 120 kV. A total of 350 sections from 3 leaves on 3 plantlets (3 replicate clones) were viewed.

SCANNING ELECTRON MICROSCOPY

Vaginate and sessile leaf tissue was viewed. After post fixation in a 2% osmium tetroxide solution for two hours and subsequent rinsing in a 0.05M sodium phosphate buffer, the tissue was incubated in a 1% aqueous thiosemicarbazide solution for 10 minutes, followed by a further five rinses with the 0.05M buffer. The samples were then again incubated in a 1% aqueous osmium solution for an hour followed by rinsing in the 0.05M buffer four times for 15 minutes each. The samples were then dehydrated in an ascending ethanol series (10, 25, 50, 75 and 100%) followed by two rinses in propylene oxide. The sample was then immersed in 100% hexamethyldisilazane (HMDS) for three minutes and then transferred into a desiccator containing silica gel. The samples were attached to aluminium stubs with carbon glue and sputter coated with gold palladium using an EMITECH K550 X sputter coater to a thickness of 15 nm. The samples were viewed using an FEI Nova Nanolab 600 Field emission gun scanning electron microscope (SEM) operating at 30 kV and 1000x magnification with a working distance of 4 mm. A total of 15 leaf samples from 3 leaves on 3 plantlets (3 replicate clones) were viewed.

4.4. Results

LEAF STRUCTURE AND MECHANISMS FOR SALT EXCRETION

Salt glands and stomata on the surface of *T. usneoides* leaves are evenly distributed across the leaf surface (Figure 11, A, B). The stomata were visibly smaller than the salt glands and were each situated within a shallow depression on the leaf surface, while the salt glands were sunken into a deep pore, surrounded by either columnar epithelial tissue or by multiple layers of cuboidal cells (Figure 12, A).

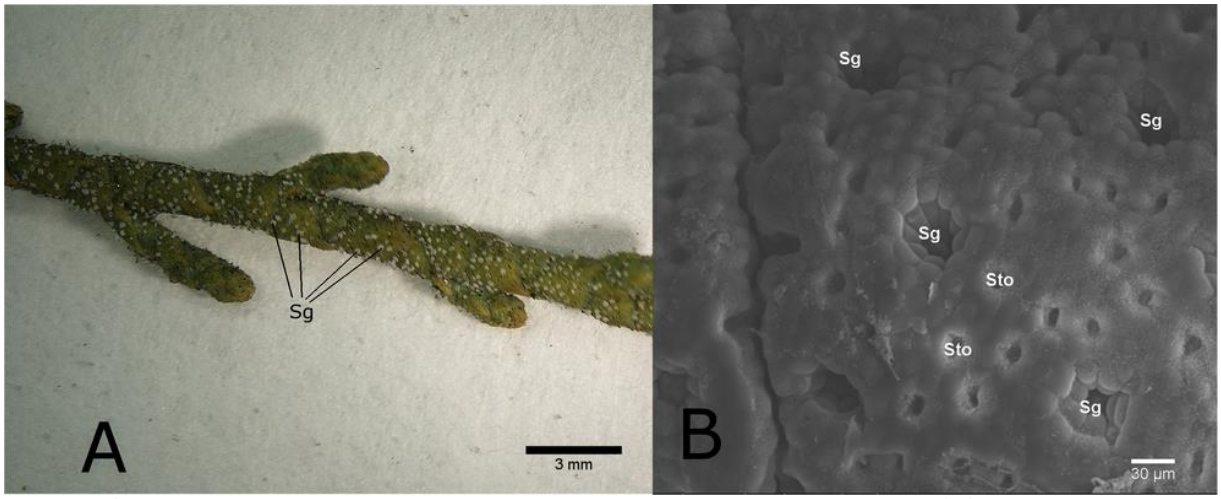

Figure 11 : A) *Tamarix usneoides* stem section showing numerous salt patches from the underlying glands (Sg) situated on small scale like leaves. B) Scanning electron micrograph of the surface of a *Tamarix usneoides* leaf showing salt glands situated within epidermal crypts (Sg) and numerous stomata (Sto) evenly distributed across the leaf surface.

MICROSTRUCTURE OF THE SALT EXCRETORY APPARATUS

The salt gland consists of eight cells, two large collecting cells at the base of the gland and then six excretory cells which are partially bounded by a secondary cell wall (Figure 12, B). The secondary cell wall extends from the leaf surface down the sides of the gland and ends at the junction between the basal excretory cells and the 2 collecting cells (Figure 12, A and Figure 13, A). Similar cell wall structure is also present at the confluence of the two basal collecting cells and the basal excretory cells (Figure 12, A). Sequential sections showed that the latter appears to be a band which runs along the bottom of the excretory cells and is continuous with the secondary cell wall on the outer edge of the excretory cell stack.

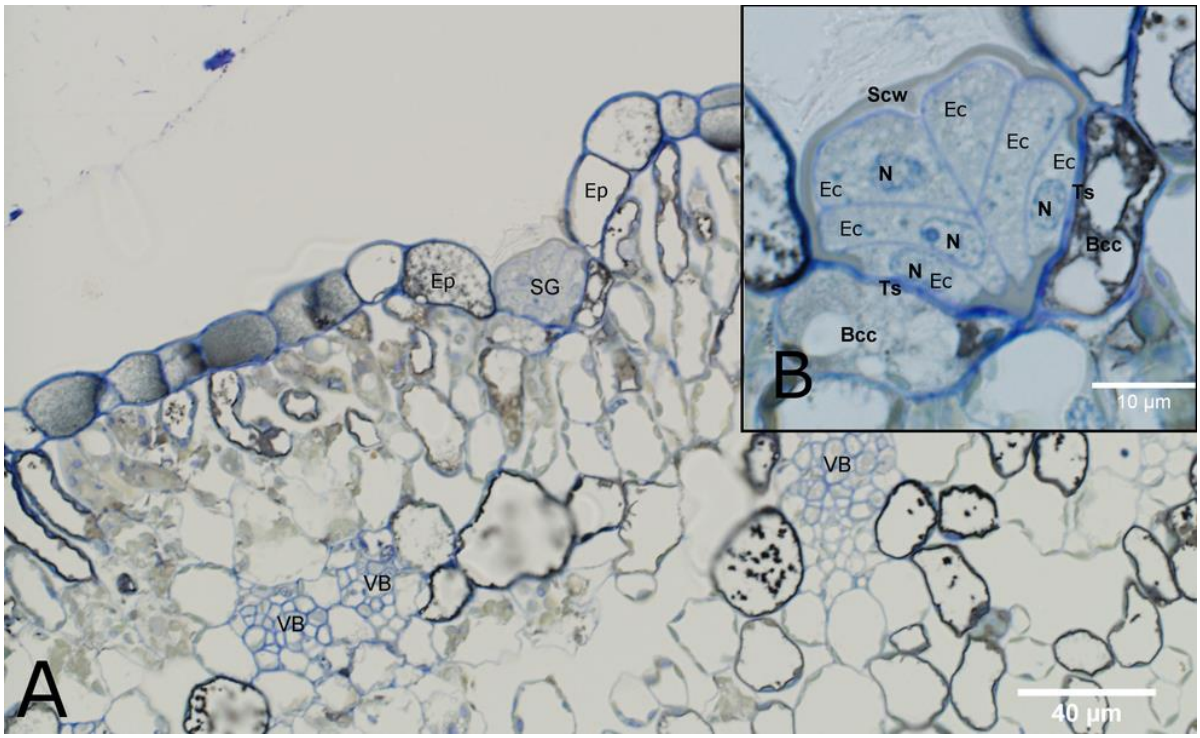

Figure 12: A) Cross section showing how the salt glands (SG) on the adaxial surface of a *Tamarix usneoides* leaf are situated in sunken epidermal crypts and are in close proximity to vascular bundles (VB). B) Cross section through a *Tamarix* salt gland showing basal collecting cells (Bcc) located beneath the stack of excretory cells (Ec) which are surrounded by a specialised secondary cell wall (Scw), This specialised wall is absent at the junction between the basal collecting cell and the lowest excretory cell, this region is often referred to as the transfusion site (Ts).

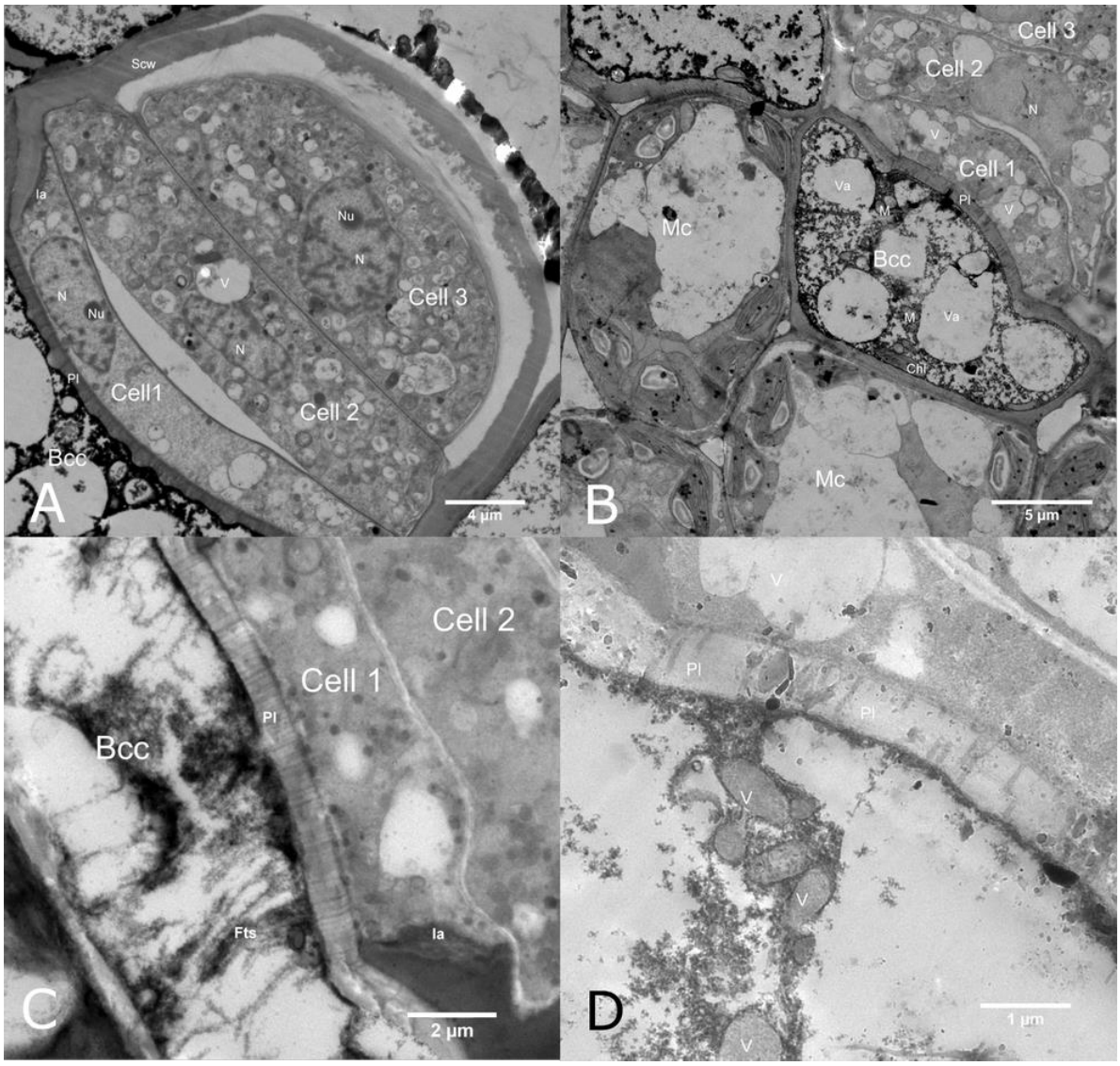

Figure 13: Transmission electron micrographs showing, A) transverse section through a *Tamarix usneoides* salt gland. Note the predominance of plasmodesmata (Pl) between the basal collecting cell (Bcc) and the first excretory cell (Cell 1). The secondary thickening surrounding the excretory cell is clearly defined (Scw). Nucleus (N), Nucleolus (Nu), Secondary Cell wall (Scw), Vesicles (V) and Interfacial apparatus (Ia) are clearly visible. B) Cross section through a basal collecting cell (Bcc) and surrounding mesophyll tissue (Mc) and salt gland (Cells 1-3) showing chloroplasts (Chl) and mitochondria (M) as well as large vacuoles (Va) within the collecting cell, plasmodesmata (Pl) at the transfer site and numerous vesicles (V) and predominant nuclei (N) within the basal excretory cells. C) The transfusion site between the basal collecting cell (Bcc) and the first excretory cell (Cell 1) is characterised by numerous plasmodesmata (Pl). The secondary cell wall of the first excretory cell is subtended by interfacial apparatus (Ia). The vacuoles of the basal cells contain what are suggested to be flocculated tannin strands (Fts). D) The transfusion site between the basal cell (Bcc) and first excretory cell (Cell 1), showing vesicles (V) and numerous plasmodesmata (Pl).

The junction between the two collecting cells and the basal excretory cells is characterised by numerous plasmodesmata and no secondary cell wall (Figure 13, A, C, D). This area has been termed the transfusion site by other authors (Thomson and Liu, 1967, Ding *et al*., 2010) and it is hypothesised that this area is where excess ions are transferred into the salt excretory apparatus.

The two collecting cells at the base of the gland have large vacuoles that are tightly adpressed to the plasmalemma and contain electron dense material, it is hypothesised that this is flocculated tannin or other chelating material. The distribution of the tannins within the vacuole varies, with the majority of the tannins being condensed to the periphery of the vacuole while long thin "strands" appear to traverse from the side opposite to the transfusion area to the transfusion area (Figure 13, C). The cell walls of the collecting cells appear to be similar to the surrounding mesophyll tissue and these collecting cells share a large surface area with the adjacent mesophyll tissue (Figure 13, B). In some sections the central vacuole has been bisected by a series of smaller vesicles that span the cell from the side opposite to the transfusion area to the transfusion area (Figure 13, D). There are few chloroplasts and mitochondria in each basal collecting cell (Figure 13, B).

The six excretory cells have several characteristics which are distinct from the surrounding epithelial cells (Figure 13, A, Figure 14). Firstly, the cytoplasm of the salt excretory cells contain numerous organelles e.g. mitochondria and most particularly the components of the endomembrane system comprising rough endoplasmic reticulum, Golgi bodies and their associated vesicles. Secondly there are structural adaptations such as inner cell wall protuberances/ingrowths that are unique to the salt excretory cells (Figure 14, B, C). These protuberances are very similar in character to cell wall ingrowths such as those described in transfer cells surrounding the xylem tissue of other plant species (Gunning and Pate, 1969).

The plasmalemma of the basal salt excretory cell is closely adpressed to the cell wall at the transfusion site between the collecting cell and the basal excretory cell (Figure 13, C, D). This continues along the sides of the cell until the confluence area between the basal and median salt excretory cells where the plasmalemma pulls away from the cell wall (80% of the salt glands viewed showed this phenomenon) (Figure 13, C). While this may be an artefact of the fixing and sectioning process, other authors have reported similar membrane withdrawal (Thomson and Liu, 1967) and there is no such feature present within the surrounding epithelial tissue or the mesophyll tissue, thus it is likely that this gap is associated in some way with the function of the salt gland.

The salt excretory cells each contain a single nucleus with areas of condensed chromatin (Figure 13, A). All the excretory cells contain large amounts of rough endoplasmic reticulum, Golgi bodies and numerous vesicles, however there is a change in the number and size of the vesicles with location of the cell in the salt gland stack, basal salt excretory cells have fewer, larger vesicles (mean size of 5.5µm) while the apical salt excretory cells have numerous, smaller vesicles (mean size of 1.87µm).

In each of the basal excretory cells of the salt gland, there are two distinctive groupings of organelles, where each group consists of highly condensed endoplasmic reticulum, Golgi bodies, mitochondria and numerous budding vesicles. Each of these groups is located in the area that is immediately adjacent to the transfer site where the secondary cell wall thickening commences (Figure 14, A, B)

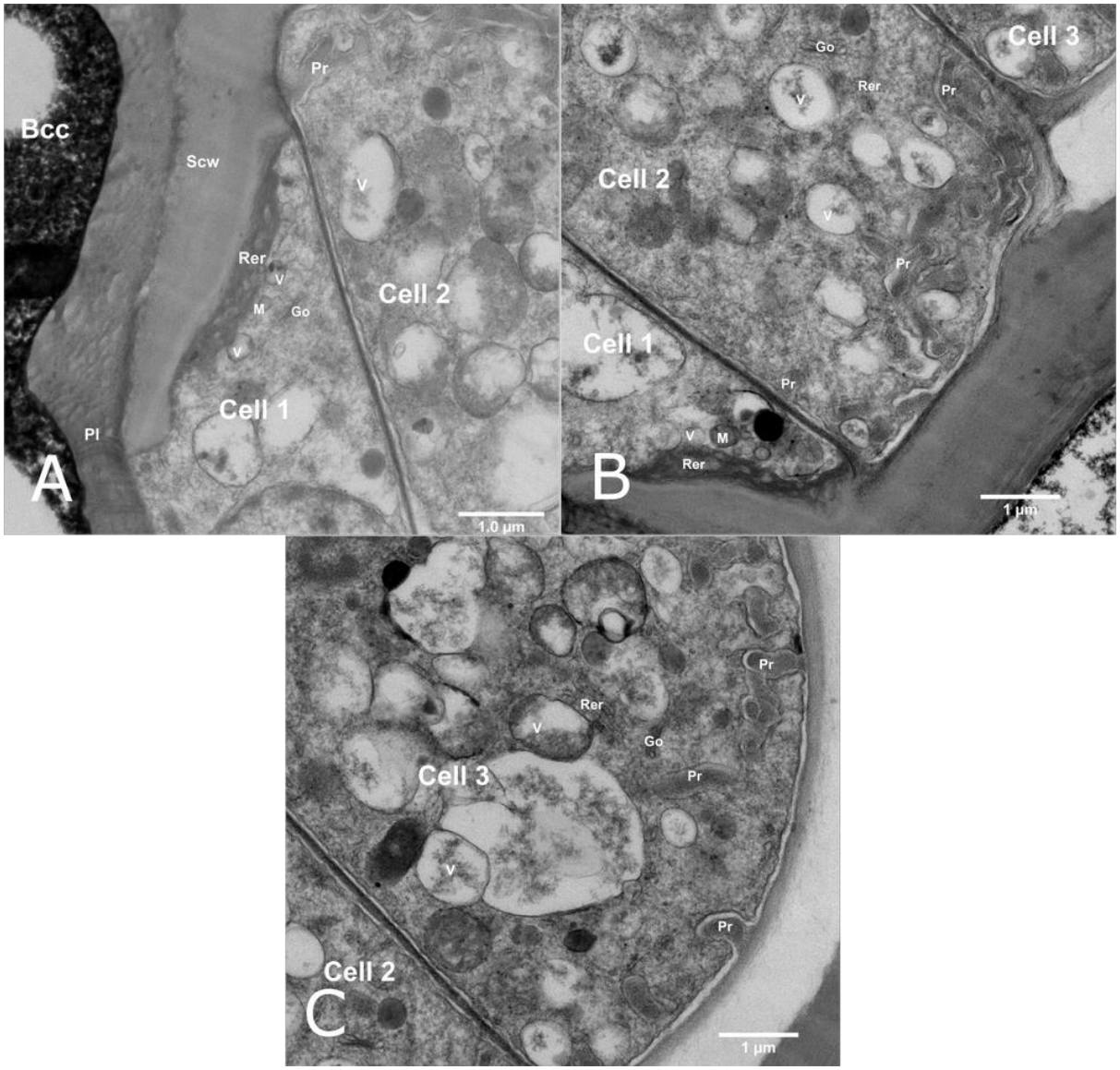

Figure 14: Transmission electron micrographs showing: A.) Cell wall of the basal excretory cell showing interfacial apparatus consisting of budding vesicles (v), Golgi (Go), mitochondria (M) and rough endoplasmic reticulum (Rer) in close proximity to the plasmodesmata (Pl) of the transfer site. Larger vesicles (V) as well as cell wall protuberances (Pr) are present within cell 2. B.) The interfacial apparatus consisting of rough endoplasmic reticulum (Rer), mitochondria (M) and vesicles (V) characterise the first excretory cell (Cell 1) of the stack of cells within the gland and the second excretory cell (Cell 2) is characterised by numerous cell wall protuberances (Pr) as well as larger vesicles (V). C.) Apical excretory cell (Cell 3) of a *T. usneoides* salt gland showing cell protuberances (Pr), rough endoplasmic reticulum, (Rer), vesicles and Golgi (Go)

4.5. Discussion

SALT EXCRETION BY THE LEAVES OF *TAMARIX USNEOIDES*

Tamarix usneoides salt glands exhibit a number of structural adaptations to allow for the transport, 'parcelling' and subsequent removal of excess ions from the plant tissues (Figure 14). Processes to prevent oxidative stress can consist of preventing the excess ions from entering the cytoplasm of the sensitive tissue (such as the photosynthetic tissue) or of intracellular sequestration of the excess ions into vacuoles or vesicles (Figure 13, D; Figure 14). This excludes the ions from the surrounding cytoplasm, thus preventing excess ions from affecting the typical functioning of cellular processes (Ding *et al.*, 2010). Ions travel in solution within the apoplast of surrounding tissue or via vesicles within the symplasm where intercellular transportation of ions can occur via junctional complexes, offloading of excess ions into the plasmodesmata or by transportation through the endoplasmic reticulum networks that are continuous between neighbouring cells i.e. via desmotubules (White and Barton, 2011) (Figure 13, D, Figure 14, A). Moving concentrated ions within the symplasm is an energy expensive process and so it would be more efficient for ions to be transported within the apoplast of the mesophyll cells towards the site of cellular excretion. Transportation of ions via the apoplast of mesophyll cells is a safer process than transporting via the symplasm because excess chloride ions disrupt ion balances as well as osmotic pressure stability (Ding *et al*., 2010). There is evidence that both apoplastic and symplastic pathways for the transport of ions are utilised by *Tamarix* (Thompson and Liu, 1967), as the salt glands of *T. usneoides* are in close proximity to the vascular bundles (within 10 cells distance, Figure 12, A) and the apoplast of the mesophyll tissue between the cells that lie between the salt gland and the vascular bundles share a large contact area (Figure 12). This

enables rapid movement of ions towards the salt excretion site. The vacuoles of the mesophyll tissue that lie between the xylem bundles and the salt gland contain large quantities of polyphenolic compounds which is typical of halophytes e.g. in the leaf tissues of *Avicennia marina* and *Bruguiera gymnorrhyrza* (Mycock *et al.*, 1985, Ksouri *et al.*, 2007) and implies that there is detoxification of excess ions occurring within the cells by complexation with polyphenolic compounds (Ksouri, *et al*., 2008). The rates of excretion which are characteristic of salt glands of the genus *Tamarix* suggest that the process for the transport of excess ions from the xylem to the site of salt excretion is very rapid (Kadukova, *et al.*, 2008). Thus, if ions are being transported from cell to cell via vesicles within the symplasm, there would need to be numerous plasmodesmata at the transfer sites in between the cells involved in ion transport to ensure efficient ion transfer between the cells of the mesophyll tissue. The cells which are involved in the rapid transfer of excess ions are characterised by structural adaptations such as complex cell wall protuberances which increase the surface area of the plasmalemma for excretion (Figure 14, B, C; Fahn, 1988). As neither numerous plasmodesmata, nor cell wall protuberances were in evidence in the mesophyll cells between the xylem vessels and the salt gland, it is more likely that the transfer of excess ions occurs via the apoplast of the mesophyll tissue where ions move down a concentration gradient towards the site of salt excretion. Excess ions that do enter into the mesophyll cells are most likely bound to polyphenolic compounds. The presence of numerous mesophyll cells with large quantities of polyphenolic compounds can be accounted for by the fact that many halophyte species load excess salts into certain cells/tissues and then allow these to senesce as a means to dispose of excess ions (Mycock *et al.*, 1985). Leaf senescence has been observed on *Tamarix* species growing on contaminated mine sites as well as in the population of *Tamarix* grown in the greenhouse at the University of the Witwatersrand that were used to

provide mother stock material for *in vitro* propagation. This suggests that continuous leaf senescence is a characteristic of *T. usneoides* and the presence of polyphenolic compounds in certain tissues within the leaves may serve to isolate excess ions from sensitive photosynthetic tissue

To facilitate the movement of ions from the xylem vessels to the site of excretion there would need to be a mechanism which maintains a concentration gradient where there is a high ion concentration next to the vascular bundles and a low concentration at the salt gland. Presumably the action of excreting excess ions maintains this gradient, however as the excess ions are excreted at very high concentrations (Kadukova, *et al.*, 2008) there also needs to be a mechanism that acts to concentrate the ions within the gland and still maintain the concentration gradient within the surrounding leaf tissue (Echeverría, 2000). This is presumably achieved by actively transporting the excess ions from the collecting cells at the base of the salt gland into the symplasm of the basal excretory cells, thus maintaining an area of low ion concentration in the collecting cell. This can either be achieved by off-loading excess ions into the apoplast of the basal excretory cell at the transfer site between the basal collecting cell and the basal excretory cells, whereupon the ions enter the basal excretory cells via endocytosis or via transporter proteins in plasma membrane (Ding *et al.*, 2010). An alternative mechanism would involve the transport of excess ions via endoplasmic reticulum desmotubules that span neighbouring cells via the plasmodesmata (White and Barton, 2011) This hypothesis is supported by the higher density of plasmodesmata at the transfer site between the basal collecting cell and the basal excretory cells (Figure 13, C) as well as the presence of extensive endoplasmic reticulum on the inner surface of the basal salt excretory cell at the transfer site (Figure 14, A). Ion transport within this type of endoplasmic reticulum can occur in two ways. The first is where vesicles bud off the large central vacuole of the basal

collecting cell and are directly transported via the desmotubules within the plasmodesmata (Figure 13, D). The second is where the vesicles fuse with the endoplasmic reticulum of one cell, whereupon the excess ions are transported across to the neighbouring cell and are offloaded into vesicles by budding off the endoplasmic reticulum in the next cell (White and Barton, 2011). In the present investigation there was no classic evidence of endocytosis occurring at the plasmalemma within the basal collecting cells *viz*. invagination of plasmalemma. There was, however, evidence of transport via the endoplasmic reticulum where vesicles were observed budding off at the plasmodesmata (Figure 12, D). However, there is not enough evidence to rule out any of the former process and it is likely that *T. usneoides* uses a combination of the processes to ensure rapid transport of excess salts away from sensitive tissues.

It is hypothesised that the pathway for the movement of excess ions within the salt gland occurs as follows: As the salt solution moves up the stack towards the exterior surface of the leaf, it is actively concentrated into vesicles (Figure 13, A) (Thomson and Platt-Aloia, 1985). Once at the apex of the excretory cell stack, the solution within the vesicles is moved to the apex of the salt excretory cell where the vesicle fuses with the plasmalemma and the saline solution within the vesicle is expelled to the cell exterior (i.e. exocytosis takes place) (Figure 14, C) (Thompson and Liu, 1967). There are a number of unique structural adaptations within the salt gland which support this hypothesis. Firstly, there is a large secondary thickening which bounds the 6 cells of the excretory cell stack of the salt gland (Figure 12,B, Figure 13, A and Figure 14, A). This secondary thickening possibly serves as an impermeable barrier which isolates the excretory cells from the surrounding tissue, preventing the efflux of concentrated salts from the excretory cells (Fahn, 1988). The differential staining between this wall and that of the other cells of the gland indicate a different wall composition, perhaps being

impermeable to further movement in the apoplast (Figure 12, A and B). The absence of secondary cell wall thickening and the numerous plasmodesmata at the transfusion site between the two collecting cells and the two basal excretory cells (Figure 13, C and D), combined with the large numbers of budding vesicles as well as the interfacial apparatus on the periphery of the transfer site implies that there is active transport occurring at the transfusion site (Echeverría, 2000). This is possibly the parcelling of excess salts from the vacuole of the basal collecting cell and the subsequent unloading of these salts into the basal excretory cells. The action of unloading the excess salts into the excretory cells of the salt gland will maintain a concentration gradient by causing a localised area of low salt concentration to occur at the transfusion site. This gradient will facilitate the movement of excess salts that have been unloaded from the vascular bundles towards the salt glands, thus if the salt glands maintain a sufficiently high rate of excretion it is possible to maintain the salt concentration of the surrounding sensitive photosynthetic tissue below the threshold where salinity stress occurs (Campbell and Thomson, 1975, Flowers and Colmer, 2008).

Maintenance of a high ion transfer rate at the transfusion site implies that there are adaptations which allow for the rapid parcelling of excess salts from both the apoplast as well as the symplasm of the surrounding collecting cells. The presence of numerous vesicles moving across the symplasm of the collecting cells to the transfusion site and the fact that the transfusion site has numerous plasmodesmata supports this hypothesis (Figure 13, A) (Thompson *et al*, 1969, Echeverría, 2000). It is hypothesised that the direct sequestration of excess salts into vesicles serves to isolate the salts from the surrounding cytoplasm/tissue (Echeverría, 2000), thus preventing salinity stress while also allowing the salts to be transported to the site of transfusion. This process is repeated within the salt excretory cells

where the energy for the transportation of the vesicles is supplied by the numerous mitochondria within the salt excretory cells. Movement of the vesicles within the cytoplasm of the salt excretory cells requires that the vesicles are processed by both the endoplasmic reticulum and labelled by the Golgi before it is moved to the transfer site to the next excretory cell, where the salts are further concentrated or moved into the space in between the plasmalemma and the cell wall where they move by diffusion to the surface of the salt gland (Thompson and Liu, 1967).

As there is direct contact between the apoplast of the excretory cells at the top of the salt gland and the neighbouring excretory cells, during the process of offloading excess ions to the leaf surface it is possible for some salts to move back into the apoplast and down towards the original excretory cell (Figure 2, B). This allows for possible backflow of salts into the leaf tissue. This backflow is presumably partially prevented by the secondary cell wall which surrounds the cell; however it is possible for the excess salts to escape at the transfusion site (Figure 2, B, Figure 3, A) (Thompson and Liu, 1967). The interfacial apparatus at the periphery of the transfusion site which consists of highly condensed E.R, vesicles, Golgi and mitochondria could be an adaptation which actively transports salts which are moving in the apoplast of the salt excretory cells and forces the salts back into the vesicles of the basal excretory cell (Figure 4, A, Figure 4, B). Furthermore, the excess salts which escape at the transfusion site could be moved into the symplasm of the basal collecting cells (Figure 3, B, C), whereupon the salts are detoxified by secondary metabolites such as soluble phenolics or anthrocyanins (Ksouri, *et al*., 2008) and are then moved into the large central vacuole of the collecting cell. This mechanism could also serve to buffer fluctuations in the rates of salt uptake and excretion, where excess salts are temporarily bound to secondary metabolites

and then later processed during periods when salt uptake rates are lower or salt excretion rates are higher.

It is likely that the structural adaptations to increase surface area of the dorsal surface of the cells of the salt excretory cell stack maintain the high rates of salt excretion that are required to maintain a sufficient concentration gradient (Fahn, 1988). These adaptations consist of the complex network of cell wall protuberances which are present on the dorsal surface of the apical excretory cells (Figure 4, B). The network of cell wall protuberances increase the surface area of the plasmalemma, allowing for rapid movement of the salts from the vesicles to the exterior surface of the cell. The area of high salt concentration within the cell wall protuberances would facilitate the passive movement of water down the osmotic potential gradient (Levering and Thomson, 1971). This influx of water could potentially exert enough pressure to cause the movement of ions to the exterior surface of the cell, whereupon the water evaporates leaving salt crystals on the surface of the leaf (Figure 1). However, as *Tamarix* is adapted to water limited (saline) environments, the prevention of excess water loss is a priority, hence the small and overlapping leaves with a thick waxy cuticle which surrounds the leaf (Figure 2, A). Salt excretion would be limited by the presence of the cuticle and as such no cuticle is present over the salt glands (Figure 2, B). Thus salt glands represent an area where there is a high potential for evaporative water loss. This water loss is partially reduced by lowering the salt glands within epidermal crypts below the leaf surface (Figure 1, B, Figure 2, A.). Furthermore, salt excretion can slow the rate of water loss, where the salt crystals left over from the evaporated brine serve to create a barrier, slowing evaporation rates at the site of salt excretion and shielding the cells from direct sunlight and the effects of wind. Dye *et al*. (2015) observed very low leaf water potentials from salt-encrusted shoots of *T. usneoides* during the winter dry season. Research on the diurnal and seasonal patterns of

tree water-use by *T. usneoides* suggests that this species is a facultative phreatophyte, performing best in riparian sites, but able to survive where water availability is limited or saline (Dye *et al*., 2015).

The findings of this study support the vacuole-like vesicle mediated transport system as proposed by Thomson and Lui, 1967 and Blumwald and Gelli, 1989 who suggested that the salts within the excretory cells are transported within vesicles that then fuse with the plasmalemma. Alternatively, the vesicles are transported to the plasmalemma where transport channels between the tonoplast of the vesicle line up with the transport channels of the plasmalemma, allowing movement of excess ions to the outside of the cell (Ding, 2010). However, there is also observational evidence at the transfer site between the collecting cells and the basal excretory cells which supports the vesicle/ endoplasmic reticulum transportation system via the plasmodesmata as suggested by White and Barton, 2011.

4.6.Conclusions

The findings of this study have shown that *T. usneoides* has a number of physiological adaptations which could allow for the removal of excess ions from its tissues. The range of ions that are excreted by *T. usneoides* as well as the ultrastrucutural adaptations observed in this study suggest that the methods for the excretion of excess ions and homeostasis maintenance are complex and require further study. These studies will need to focus around the mechanisms by which ions are transported from the surrounding soil medium into the plant, as well as the route *in planta* to the site of salt excretion.

4.7. Acknowledgements

This study forms part of the doctoral research of the first author, and was supported by AngloGold Ashanti and the Technology for Human Resources for Industry Programme (THRIP) award no. TP13080525596 from the Department of Trade and Industry and the National Research Foundation of South Africa to I.M. Weiersbye and E.T.F. Witkowski.

4.8.References

Baum BR. 1978. The genus Tamarix. Jerusalem, The Israeli Academy of Sciences and Humanities.

Berry WL, 1970. Characteristics of salts secreted by *Tamarix aphylla*. American Journal of Botany, 1226-1230.

Campbell CJ, Strong JE, 1964. Salt gland anatomy in *Tamarix pentandra* (Tamaricaceae). The southwestern naturalist, 232-238.

Campbell N, Thomson WW, 1975. Chloride localization in the leaf of *Tamarix*. Protoplasma, *83*(1-2), 1-14.

Ding F, Yang JC, Yuan F, Wang BS, 2010. Progress in mechanism of salt excretion in recretohalopytes. Frontiers in Biology, 5(2), 164-170.

Echeverría E, 2000. Vesicle-mediated solute transport between the vacuole and the plasma membrane. Plant physiology, 123(4), 1217-1226.

Fahn A, 1988. Secretory tissues in vascular plants. New phytologist,108(3), 229-257.

Flowers TJ, Colmer TD, 2008. Salinity tolerance in halophytes. New Phytologist, 179(4), 945-963.

Gunning BES, Pate JS, 1969. “Transfer cells” plant cells with wall ingrowths, specialized in relation to short distance transport of solutes—their occurrence, structure, and development. Protoplasma, 68(1-2), 107-133.

Hagemeyer J, Waisel Y, 1988. Excretion of ions (Cd^{2+}, Li^{+}, Na^{+} and Cl^{-}) by *Tamarix aphylla.* Physiologia plantarum, 73(4), 541-546.

Kadukova J, Manousaki E, Kalogerakis N, 2008. Pb and Cd accumulation and phyto-excretion by salt cedar (*Tamarix smyrnensis* Bunge). International journal of phytoremediation, 10(1), 31-46.

Kleinkopf GE, Wallace A, 1974. Physiological basis for salt tolerance in *Tamarix ramosissima*. Plant science letters, *3*(3), 157-163.

Kramer D, 1983. Genetically determined adaptations in roots to nutritional stress: correlation of structure and function. In Genetic Aspects of Plant Nutrition (pp. 33-39). Springer Netherlands.

Kramer D, Läuchli A, Yeo AR, Gullasch J, 1977. Transfer cells in roots *of Phaseolus coccineus*: ultrastructure and possible function in exclusion of sodium from the shoot. Annals of Botany, 41(5), 1031-1040.

Krämer U, Talke IN, Hanikenne M. 2007. Transition metal transport. FEBS Lett 581(12–25):2263–2272.

Kronzucker HJ, Britto DT, 2011. Sodium transport in plants: a critical review. New Phytologist, 189(1), 54-81.

Ksouri R, Megdiche W, Debez A, Falleh H, Grignon C, Abdelly C, (2007). Salinity effects on polyphenol content and antioxidant activities in leaves of the halophyte *Cakile maritima*. Plant Physiology and Biochemistry,45(3), 244-249.

Levering CA, Thomson WW, 1971. The ultrastructure of the salt gland of *Spartina foliosa*. Planta, 97(3), 183-196.

Manousaki E, Kadukova J, Papadantonakis N, Kalogerakis N, 2008. Phytoextraction and phytoexcretion of Cd by the leaves of *Tamarix smyrnensis* growing on contaminated non-saline and saline soils. Environmental research, 106(3), 326-332.

Marschner H, 2011. *Marschner's mineral nutrition of higher plants*. Academic press.

Mayonde SG, Cron G, Gaskin JF, Byrne MJ. 2015. Evidence of Tamarix hybrids in South Africa, as inferred by nuclear ITS and plastid trnS–trnG DNA sequences. S Afr J Bot 96:122–131.

Murashige T, Skoog F, 1962. A revised medium for rapid growth and bio assays with tobacco tissue cultures. Physiologia plantarum, 15(3), 473-497.

Mycock DJ, Frankland CA, Berjak P, 1985. Some effects of fluoride on the establishment and growth of propagules of *Bruguiera gymnorrhiza* and *Avicennia marina*. South African Journal of Botany, 51, 439-47.

Scholander PF, Hammel HT, Hemmingsen E, Garey W, 1962. Salt balance in mangroves. Plant Physiology, 37(6), 722.

Spurr AR, 1969. A low-viscosity epoxy resin embedding medium for electron microscopy. Journal of ultrastructure research, 26(1), 31-43.

Storey R, Thomson WW. 1994. An X-ray microanalysis study of the salt glands and intracellular calcium crystals of *Tamarix*. Ann Bot 73(3):307–313.

Thomson WW, Liu LL, 1967. Ultrastructural features of the salt gland of *Tamarix aphylla* L. Planta, 73(2), 201-220.

Thomson WW, Berry WL, Liu LL, 1969. Localization and secretion of salt by the salt glands of *Tamarix aphylla*. Proceedings of the National Academy of Sciences, 63(2), 310-317.

Thomson WW, Platt-Aloia K, 1985. The ultrastructure of the plasmodesmata of the salt glands of *Tamarix* as revealed by transmission and freeze-fracture electron microscopy. Protoplasma, 125(1-2), 13-23.

Weiersbye IM, Witkowski ETF, Reichardt M, 2006. Floristic composition of gold and uranium tailings dams, and adjacent polluted areas, on South Africa's deep-level mines. BOTHALIA-PRETORIA, 36(1), 101.

White RG, Barton DA, 2011. The cytoskeleton in plasmodesmata: a role in intercellular transport? Journal of experimental botany, *62*(15), 5249-5266.

5. Ion uptake and compartmentalisation in the leaves of the recretohalophyte *Tamarix usneoides*

Hayden T. Wilson, David J. Mycock and Isabel M. Weiersbye
University of the Witwatersrand, Johannesburg, Faculty of Science, School of Animal, Plant and Environmental Sciences, +27 (11) 717 6403, Private Bag 3 Wits 2050, South Africa.
Hayden.Wilson@students.wits.ac.za, David.Mycock@wits.ac.za, Isabel.Weiersbye@wits.ac.za

The following chapter is in scientific manuscript format as such there is some repetition of contextualising information and background information that was included in previous chapters.

5.1. Abstract

Halophyte plant species such as *Tamarix usneoides* have applications in the remediation of contaminated environments due to their ability to tolerate saline soils. Studies into the mechanisms of tolerance in *Tamarix* have shown that the vesiculated trichomes of the plant are capable of excreting a range of ions and that ion compartmentalisation within the salt glands of the plant likely occurs via a vesicle mediated transport system. The aim of this study was to investigate the processes involved in the uptake of gold and other elements by *T. usneoides in vitro* in order to understand how elements are transported *in planta* and corroborate the observations that were gathered regarding the ultrastructural and tissue adaptations, thus determining how the species allocates elements within root, stem and leaf tissues. Root, stem and leaf sections from *in vitro T. usneoides* plantlets dosed with gold chloride, gold potassium cyanide and gold thiosulphate at a pH of 5.6 to a concentration of 25mg/kg were processed and analysed by collecting optical photographs and scanning electron microscopy by means of both conventional scanning electron microscopy (SEM) imaging as well as back scattered electron (BSE) imaging and Transmission electron microscopy (TEM). Electron dispersive spectroscopy (EDS) spectra were gathered at different locations in the tissues in order to determine the range the range of elements that were present and elemental maps of the specific areas of interest were created using wavelength dispersive x-ray spectroscopy (WDS). The findings of the analyses showed that *T. usneoides* utilises a range of processes to maintain homeostasis. These include exclusion of a number of elements at the root endodermis, differential sequestration of excess ions into specific tissues in aboveground biomass, ion detoxification through the action of metallochaperones such as polyphenolic compounds and finally, though processes such as excretion of excess ions from the salt glands on the leaf surface.

Keywords: Accumulation, Metallochaperone, Polyphenol

5.2. Introduction

Tamarix usneoides is capable of accumulating gold *in vitro,* when it is bio-available for uptake (Wilson et al., 2019 manuscript, Chapter 3 of this thesis) and under field conditions it is capable of accumulating significant quantities of elements such as Mg, Ca, K, Cl, P, S, Mn, Fe and Zn (Wilson et al., 2019 manuscript, Chapter 4 of this thesis). A number of elements such as Pb, Rb, Th and U are excluded from uptake, while other elements are stored within specific tissues prior to their excretion from salt glands.

The movement of ions in aboveground tissues has been hypothesised to follow two potential transportation pathways (Wilson *et al*., 2017). One where the excess ions were transported to the excretory cells via an apoplastic transport route down a concentration gradient and a second where the excess ions were transported via a symplastic transport route, complexed with polyphenolic compounds and sequestered within vacuoles (Wilson *et al*., 2017). The recent evidence for coupled apoplastic and symplastic ion transportation within root tissue (Bao *et al*., 2019) provides a potential third pathway for solute transport within leaf tissue to occur, where polarised ion channels on an influx face of a cell direct ions within the apoplast of the leaf into the symplasm, the ions are then transported across the cell to the efflux face of the cell where upon they are discharged back into the apoplast prior to their subsequent influx into the neighbouring cell (Bao *et al*., 2019).

The strategies utilised by plants for the maintenance of homeostasis under ionic stress are diverse and can consist of a number of processes e.g.

- immobilisation of ions within the rhizosphere by adjusting rhizosphere oxidation states (Violante *et al.*, 2010),
- binding of elements within root epidermal and cortex tissue (Nishizono *et al.*, 1987)

- reduction of bypass flows (Flam-Sheperd et al., 2018)
- uptake and sequestration of ions within aboveground tissues (Baker, 1981) and
- excretion of excess ions (Ding *et al.*, 2010).

These strategies can occur concurrently and plants often utilise a range of mitigation processes to tolerate diverse growing conditions (Conn & Gilliham, 2010). Plant strategies to increase nutrient mobility can also affect the mobility of other metal cations in soils (Wong, 2003). For example, *Brassica napus* and *Lupinus albus* secrete organic anions such as citrate and malate into the surrounding rhizosphere (Ryan *et al.*, 2001). These organic acids compete with phosphate ions at binding sites in the soil which serves to increase phosphate mobility (Souza *et al.*, 2014). Similarly, organic ligand-chelates increase the cation exchange capacity of the substrate and bind strongly to potentially toxic ions such as Al^{3+}, reducing Al^{3+} mobility in the rhizosphere (Ryan *et al.*, 2001; Michalak, 2006). The secretion of organic anions has also been shown to stimulate the activity of microbes within the rhizosphere and adjust the composition of soil microbe communities. These alterations result in conditions that are favourable for the break-down of organic matter (Hamilton and Frank, 2001) and the reduction of metal contaminants (Khan, 2005) which serves to reduce toxic element mobility. The process of ion selection for uptake primarily occurs within the root cortex and at the root endodermis, where elements bind to the apoplastic surface of cell membrane ion transport proteins and are transferred across the membrane into the cytoplasm (Clemens *et al.*, 2016). Due to the fact that there is a degree of ion specificity by the high affinity ion transporters, not all ions are transported from the apoplast into the cytoplasm of these cells (Clemens *et al.*, 2002). This results in an accumulation of ions within the apoplast space which in turn limits the uptake of ions with a similar charge or ionic radius (Antoniadis *et al.*, 2017). However, a number of ion transporters do not differentiate between ions with similar valency or ionic

radius. Consequently, uptake of transition elements such as Cd^{2+} can occur during the accumulation of essential nutrient ions such as Ni^{2+} and Zn^{2+} (Clemens, *et al.,* 2002). Unrestricted uptake can also occur at the root apex where undifferentiated cell growth allows for a small influx of unwanted ions into root tissue (Marschner, 2012). Thus, there is an additional requirement for adaptations to prevent ion toxicity from occurring within aboveground biomass.

Metal ionic stress in plant tissue can manifest in a number of different ways, for example, through the generation of reactive oxygen species (ROS) (Ovečka and Takáč, 2014). Metal ions in plants can cause oxidative stress through the promotion of monoelectron transfers, as transition metals with unpaired electrons can freely accept electrons from, or donate electrons to, O_2, which facilitates the formation of H_2O_2 or O_2^- (Deitz, *et al*., 1999). Furthermore, metal ions can facilitate the creation of ROS through the disruption of regulatory processes. For example, the disruption of electron transport processes within thylakoid membranes of chloroplasts and the inner membrane of mitochondria which results in the creation of free radicals (Michalak, 2006). Metal ions also bind to anti-oxidant enzymes causing their dysfunction and deplete local pools of low molecular weight anti-oxidants which reduces the plant's capacity to control the formation of ROS (Yadav, 2010). Secondly, uptake of metals with a similar valency or ionic radius can affect plant cellular processes as non-nutritive ions can replace key ions in enzyme function which in turn can affect the performance of that enzyme (Hedrich, 2012). An example of this occurring is the replacement of Fe^{2+} ions by hydrated Zn^{2+} ions within chlorophyll which results in reduced chlorophyll function, chlorosis and ultimately loss in photosynthetic capacity (Marschner, 1986).

In order to mitigate the effects of excess ions within the aboveground tissues, plants have developed strategies to chemically isolate the excess elements thereby reducing the chance of ionic stress or elemental toxicity (Michalak, 2006). These include binding the elements to secondary metabolites such as polyphenolic compounds, which reduces the mobility of excess ions by forming chelates between the carboxyl and hydroxyl groups of the phenolic compound (Michalak, 2006), or through the loading of the excess elements into certain tissues and organs which isolates them from surrounding tissues (for example, *Anthyllis vulnenaria* loads excess elements into aging tissues and organs, Siedlecka *et al*., 2001). Additionally, some plants allow tissues loaded with excess elements to senesce, effectively eliminating unwanted elements (Barceló & Poschenrieder, 1990). This process can be coupled with strategies, such as the excretion of excess ions from a tissue via glandular structures (Ding *et al*., 2010).

Observations of flocculated polyphenolic compounds within the mesophyll tissue of *T. usneoides* leaves (Wilson *et al*., 2017), as well as the elevated concentrations of sulphur and chlorine within its leaves (Wilson *et al.,* 2018 Manuscript, Chapter 4 of this thesis) suggests that the differential sequestration of elements within the mesophyll tissue likely plays a role in *T. usneoides* elemental tolerance and excretion processes.

The present study qualitatively investigates the processes involved in the uptake of gold and other elements by *T. usneoides in vitro.* The aim was to understand how the species allocates elements within root, stem and leaf tissue and to corroborate the observations that were gathered regarding the ultrastructural and tissue adaptations and their role in element transport *in planta.*

5.3.Methods

PROPAGATION OF *IN VITRO* MATERIAL

Three cm long apical shoots were harvested from the mother stock material maintained in the University of the Witwatersrand greenhouse. Apical shoots were surface decontaminated in 2% sodium hypochlorite for 15 minutes and rinsed in sterilised deionised water (MilliQ) prior to being added to 10ml borosilicate growth vials containing 2ml of sterilised quarter strength Murashige and Skoog (1962)(MS) growth medium buffered to a pH of 5.6 with NaOH. Vials were incubated in a growth chamber at a constant temperature of 25°C and photoperiod of 16L/8D hours supplied by fluorescent lights producing approximately 2000 lumens of output. Only explants that exhibited no tissue browning or phenolic production were selected for the subsequent gold treatments.

DOSING OF *IN VITRO* PLANTLETS WITH AU

Working aseptically, four clones of 36 six week old plantlets with developed roots and shoots were transferred to sterilised 10ml borosilicate growth vials containing 2ml of quarter strength MS liquid basal growth medium buffered to a pH of 5.6.Each of the vials was dosed with one of three gold compounds (gold (III) chloride ($HAuCl_4$), gold sodium thiosulphate ($Na_3Au(S_2O_3)_2{\cdot}2H_2O$) and gold potassium cyanide (C_2AuKN_2), resulting in final Au concentrations of 25mg/kg (Quarter strength MS used to prevent ion toxicity, See appendix A Table 13 for calculations on tissue culture media ion concentrations). 25mg/kg Au was used in these trials as Au concentrations that exceeded 25mg/kg had an increase in tissue browning and polyphenolic production for the C_2AuKN_2 trials. The vials were agitated every 3 days by gently swirling for 5 seconds. Explant position within the growth chamber was randomised

every 3 days. Explants were incubated under growth chamber conditions for 2 weeks prior to harvest.

ANALYTICAL MICROSCOPY

After exposure to the gold compounds for 2 weeks, plantlets were harvested, with 3 plantlets from each trial being dissected into 10mm long root and stem sections. A subsample of the material consisting of 3 sets of 10mm long apical, median and basal stem sections as well as root sections where harvested from each of the plantlets for the purposes of scanning electron microscopy (SEM) and electron dispersive spectroscopy (EDS) in order to determine the range of concentrations present within the different tissues and positions in the plantlet (12 samples total). The samples were mounted on aluminium stubs using carbon tape and dehydrated in a SiO_2 desiccator prior to carbon coating to a thickness of 10nm layer using an EMITECH K550 X sputter coater. The samples were viewed using a FEI Nova Nanolab 600 Field emission gun SEM operating at 30 kV and 1000x magnification with a working distance of 4 mm.

The remaining materials, root, stem and leaf tissue from each of the plantlets were prepared for analytical microscopy according to the protocol defined in Wilson *et al.* (2017) where the material was fixed overnight at room temperature (20 – 25 ^{o}C) in 2 % gluteraldehyde in a 0.05 M sodium phosphate buffer, pH 7.2. The material was then rinsed four times in buffer, post-fixed for two hours in 2 % OsO_4 and then again rinsed four times in buffer. The material was then dehydrated through a 10, 25 and 50 % graded ethanol series before staining in 1 % uranyl acetate in 75 % ethanol. The material was then rinsed in 75 % ethanol and passed through four sequential dehydrations of 15 minutes each, starting with two in 100 % ethanol and then two in propylene oxide. The tissue was then infiltrated in a solution consisting of 50 % Spurr

epoxy resin (Spurr, 1969) and propylene oxide for 4-5 hours. This mixture was then replaced with pure resin and allowed to infiltrate for 14 hours. The samples were then placed in resin trays and polymerised at 70 ^{o}C for 8-12 hours.

For optical microscopy, samples were sectioned to a thickness of 1 µm thick. Sections were collected on glass slides and stained with toluidine blue (60 ml 1% w/v sodium bicarbonate, 40 ml glycerol and 1 g toluidine blue) by placing a drop of solution onto each section and allowing the stain to infiltrate for 5 minutes at a temperature of 60°C and rinsed off using ultrapure (MilliQ) water. The sections were then mounted in DPX and viewed using an Olympus BX63 microscope. A total of 156 sections were viewed using optical microscopy and these sections were used to identify regions of interest for elemental analysis.

For Transmission electron microscopy, leaf tissue was sectioned into 0.1 µm sections, placed on copper grids and then stained with lead citrate ($(C_6H_5O_7)_2Pb_3 \cdot 3H_2O$). These were then viewed and photographed with a FEI Spirit T12 transmission electron microscope (TEM) at a voltage of 120 kV.

A combination of optical microscopy, SEM, EDS and Wavelength dispersive x-ray spectroscopy (WDS) was performed using a CAMECA SX5-FE EPMA. Samples were sectioned to a thickness of 5 µm, placed on glass slides and carbon coated to a thickness of 10nm layer using an EMITECH K550 X sputter coater. 24 sections were selected for elemental analysis which consisted of first collecting photographs using the optical microscope built into the CAMECA SX5-FE EPMA, followed by creating images using the EPMA's SEM capabilities, using both conventional SEM imaging as well as imaging using back scattered electrons (BSE) which are

well suited to providing additional depth of field as well as for highlighting areas that are mineralised (Harding, 2002). EDS spectra were gathered at different sample locations in order to determine the range of elements that were present within the different tissues. These elemental ranges were then used to select the configuration parameters for elemental mapping. Elemental maps of the specific areas of interest were created using WDS.

5.4. Results and Discussion

MATERIAL QUALITY AS A RESULT OF PROCESSING FOR MICROSCOPY.

Material prepared for SEM did exhibit some shrinkage during the desiccation process, however for the purposes of determining surface elemental concentrations it was deemed adequate as no other method available would prevent the dislodgement of surface elemental accretions.

The process utilized for TEM and EPMA preparation did not result in visible damage to cellular structures (shrinkage or dislodgment of cellular structures) in aboveground biomass, however there was evidence of the preparation methods affecting root tissue where desiccation resulted in shrinkage of the root cortex and epidermal tissue. One of the inherent problems with the methodologies utilized for material preparation used in this stud y is that there is potential that elements may have been relocated to other tissues during the process of fixing and embedding. However due to the constraints in the available instruments (no Cryogenic facilities were available) the study had to rely on more conventional methods for fixing and embedding.

DESCRIPTION OF THE ROOT, STEM AND LEAF STRUCTURE OF *T. USNEOIDES*

The *in vitro* roots of *T. usneoides* plantlets have a convoluted epidermal layer with a loosely arranged cortex layer but the endodermis and vascular tissue were clearly (Figure 15, A).

The vaginate leaves (Figure 15, B) and the sessile leaves (Figure 15, D) share several structural similarities, *viz*. a single cell epidermal layer of approxmately 22µm thick as well as vascular bundles consist of large primary bundles that run down the centre of the leaf, with a series of smaller vascular bundles being present towards the leaf edge . The tissue surrounding the primary bundles often contains a large amount of phenolic material while the cells surrounding the secondary vascular tissue contained comparatively little.

In vaginate leaves (Figure 15, B), the epidermal layer extends around the entire leaf and is characterised by cells containing phenolic compounds that are dispersed within the cell, a large number of stomata as well as salt glands are also present. Intracellular air spaces are larger below the stomata. Within the leaves there is a distinctive palasade layer subtended by the spongy mesophyll tissue. The inner (abaxial) leaf epidermis is in tight juxatposition to the epidermis of the stem. These epidermal layers stains darker than the surrounding tissue. The stem comprises an epidermal layer subtended by a few layers of cortex tissue and a series of vascular bundles surrounding the pith in the centre of the stem. Flocculated and dispersed forms of polyphenolic compounds are scattered through both the leaf and stems (Figure 15, B, C).

In sessile leaves (Figure 15, D), below the adaxial epidermal layer there is a photosynthetic mesophyll tissue, this layer also contains cells where the tannins were either dispersed or flocculated (Figure 15, D). Towards the edges of the leaves the photosynthetic palisade layer becomes less distinguished and more mesophyl like subtended by numerous stomata. In the

more central portion of the leaves the palisade is more tightly packed (there are fewer intracellular air spaces), there are fewer stomata present but is in the region that the salt glands predominate(Figure 15, D). Below the palisade is typical spongy mesophyll which also contained cells filled with flocculated and dispersed tannins. Generally there were fewer stomata present on the abaxial surface of the leaf except towards the edge of the leaf.

The stem is surrounded by an epidermal layer, under which lies a layer of chlorenchyma tissue (Figure 15, D). Within this tissue there is a large amount of intracellular space, however comparatively few stomata were observed. Between the layer of chlorenchyma tissue and the vascular tissue there is a layer of parenchyma tissue containing cells with both flocculated and disperse polyphenolic compounds. The vascular tissue at the centre of the stem is interspersed with parenchyma tissue containing both types of phenolic compound (Figure 15, C).

Towards the leaf tip of the sessile leaf there is a distinct change in the anatomy of the leaf (Figure 15, E). There is little to no difference in the thickness of the epidermal and cuticular layers on the abaxial and adaxial surface and salt glands were present on both ad and abaxial surfaces. The distinct palisade layer is no present with the photosynthetic tissues being more spongy mesophyl like. There are also fewer areas characterised by tannin filled cells associated with the salt glands. Salt glands are evenly distributed amongst the photosynthetic tissue.. There is also only one vascular bundle present within the leaf apex and there are no tannin laden cells adjacent to the vascular bundles. Stomata are present on both the ad- and abaxial surfaces of the leaf and are subtended by large intercellular air spaces.

ROOT ELEMENTAL UPTAKE.

Analysis of the exterior of the washed and dehydrated root tissue of the plantlets that were grown in the gold chloride trial showed distinct spectral peaks associated with gold, chlorine, potassium, sulphur, calcium and magnesium (Figure 16). The elemental concentrations were not evenly distributed over the surface of the material, with gold concentrations being higher in spectrum 2 than in spectrum 1 and calcium concentrations being higher in spectrum 1 (Figure 16, spectrum 1 and 2).

Elemental maps showed that gold accumulation was very low in root tissue (Figure 17, C). Chloride concentrations were elevated in root tissue, with the majority of chlorides being found in the apoplast of the root cortex and epidermal tissue (Figure 17, B). The accumulation and transportation of elements from the rhizosphere into the vascular system prior to translocation to above ground biomass is mediated by the Casparian strip (Cunningham and Berti 1993). Suberisation of the cell walls of the Casparian strip ensures that the cells are impermeable (Chen *et al.*, 2011 Chen *et al.*, 2011). Therefore, for elements to be taken up by the plant they need to enter the vascular bundles via the symplasm of the cells of the cortex tissue. The elements are transported via active processes through the membrane of the cells of the Casparian strip and then via the symplasm into the vascular tissue (Ryan *et al.*, 2001). The advantages of restricting uptake in this way, is that it allows the plant selective control of the elements that are accumulated in the above-ground tissue, thus preventing elemental toxicity (Chen *et al.*, 2011). The low concentration in vascular tissue are potentially due to the transport of elements through the vascular tissue to the aboveground biomass for utilisation (and if necessary sequestration and excretion), alternatively, it could be due to preparation methods, where sectioning of the *in vitro* material prior to fixing and embedding could have

allowed the contents of the vascular tissue to drain out. However, the former explanation is supported by the low elemental concentrations found in vascular tissue from samples collected *in-situ* (Wilson *et al.*, 2019 manuscript, chapter 4 of this thesis) (Figure 17)

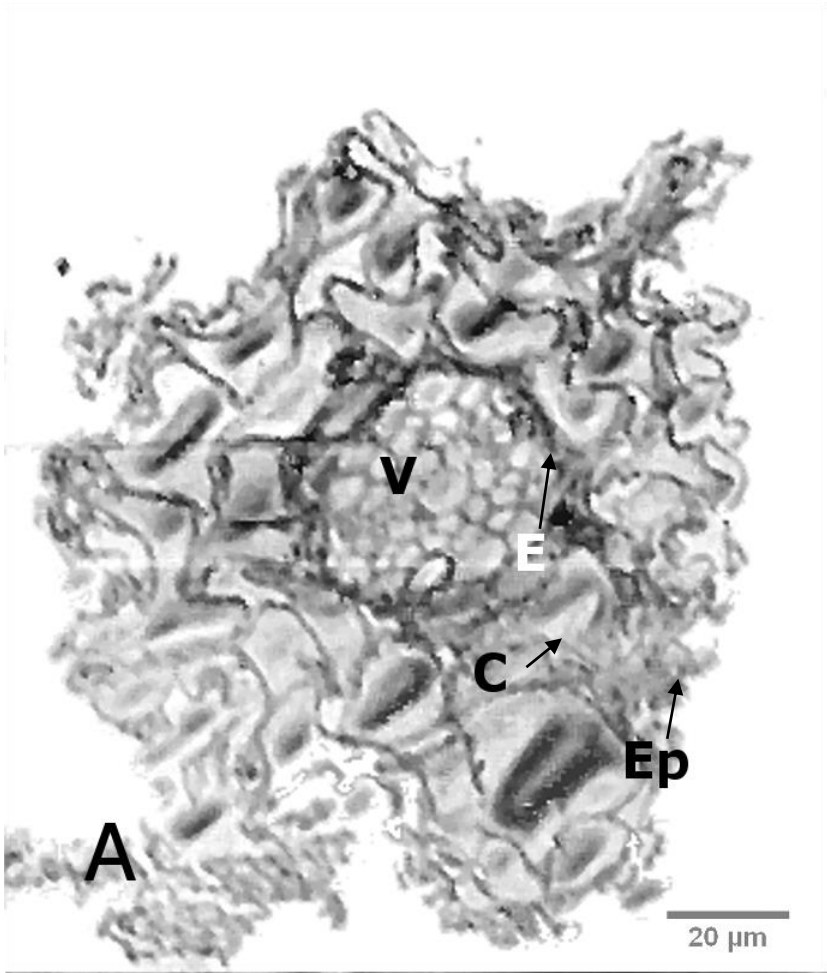

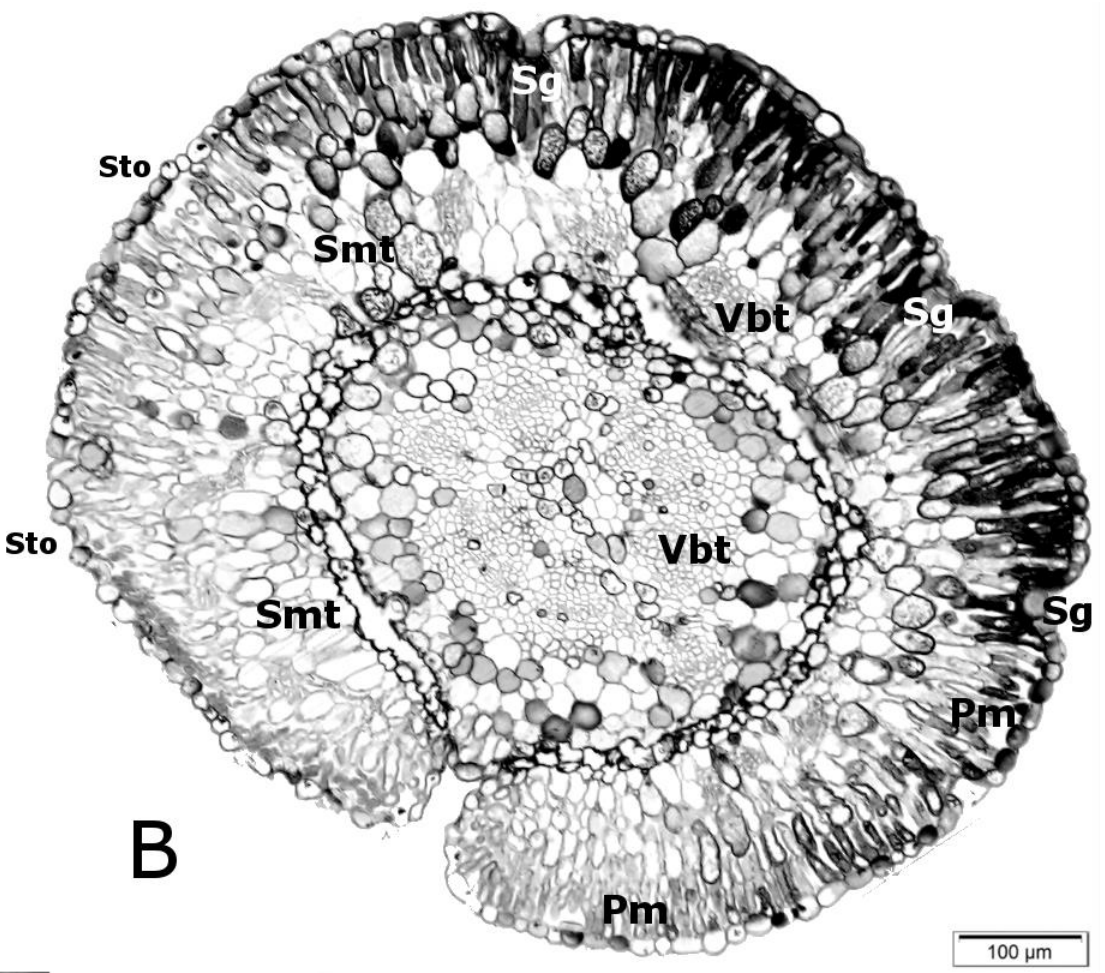

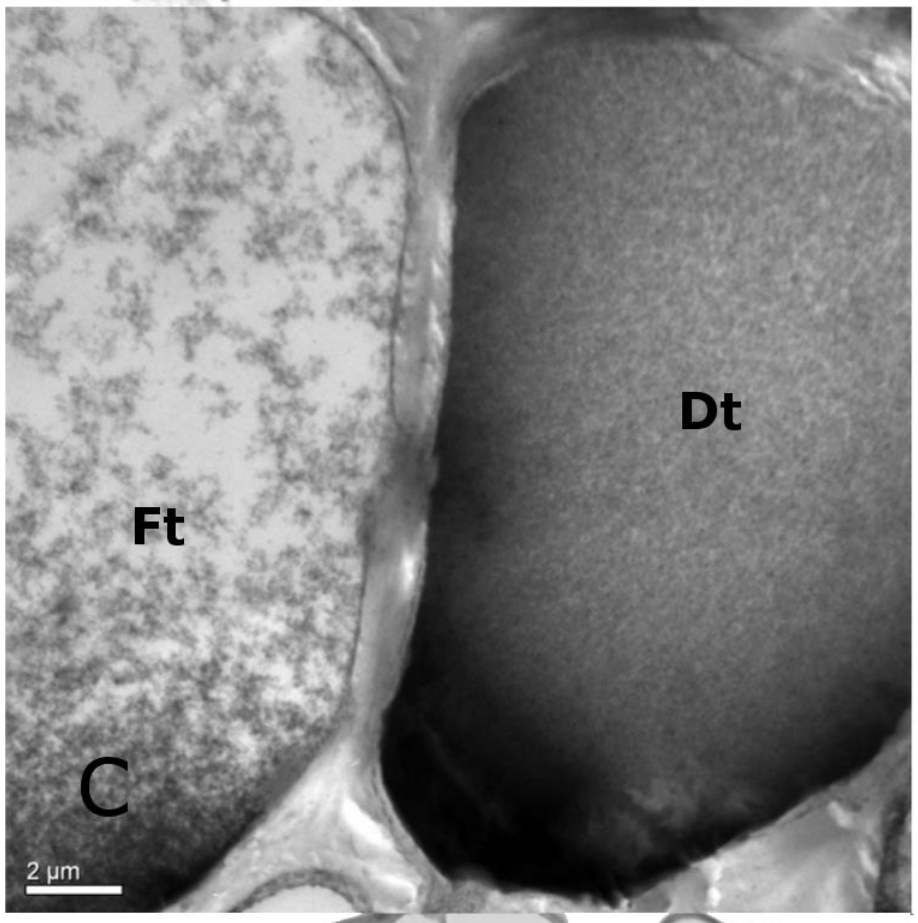

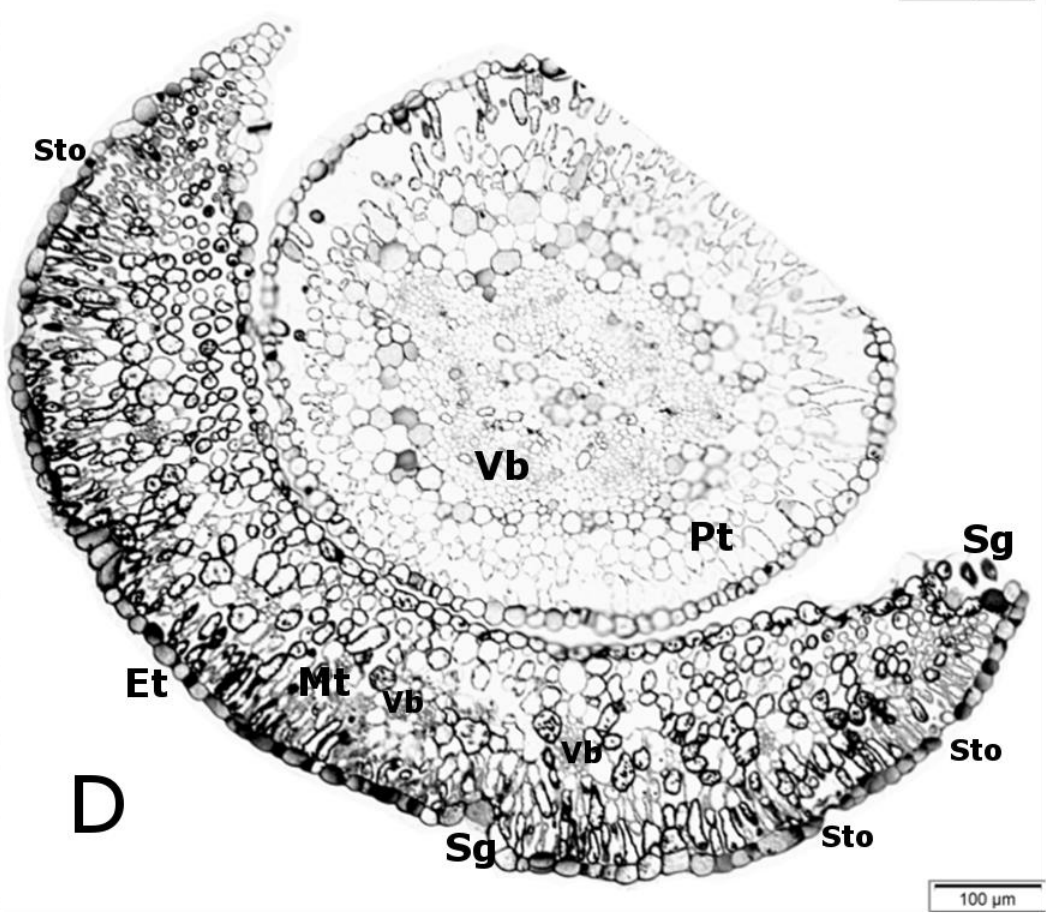

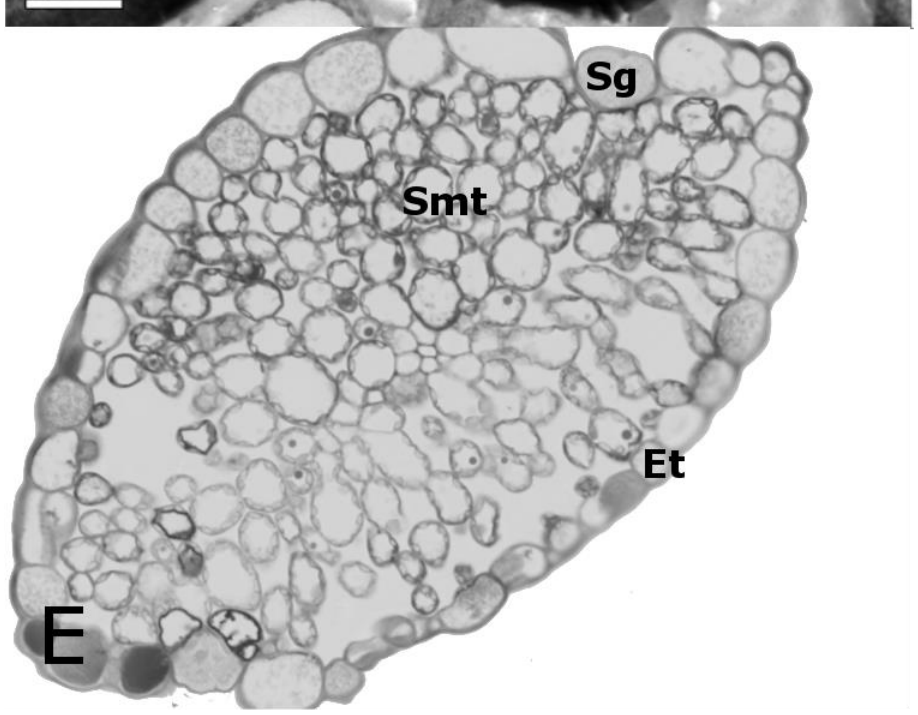

Figure 15: Cross section through *T. usneoides* tissues collected from material grown *in vitro* in 1/4 strength MS at a pH of 5.6 and dosed with AuCl at a concentration of 25mg/kg Au. A.) Root Tissue Showing: (E) endodermis, (V) Vascular tissue, (C) Cortex tissue. B.) : vaginate leaf showing: Palisade mesophyll (Pm), Spongy mesophyll tissue (Smt), salt glands (Sg), Vascular bundle tissue (Vbt), Flocculated polyphenolic compounds (Flph), Stomata (Sto) and Polyphenolic compounds (Ph). C.) Cross section through two parenchyma cells showing flocculated tannins (Ft) and disperse tannins (dt). D.) Cross section through a Sessile leaf and stem showing Showing salt glands (Sg), Epidermal tissue (Et), Mesophyll tissue (Mt), Vascular tissue (Vt), Vascular bundles (Vb), Parenchyma tissue (Pt) and stomata (Sto). E.) median section of a sessile leaf showing stomata (Sto), Epidermal tissue (Ep), Single Vascular bundle (Vb), Spongy mesophyll tissue (Smt) and Salt glands (Sg).

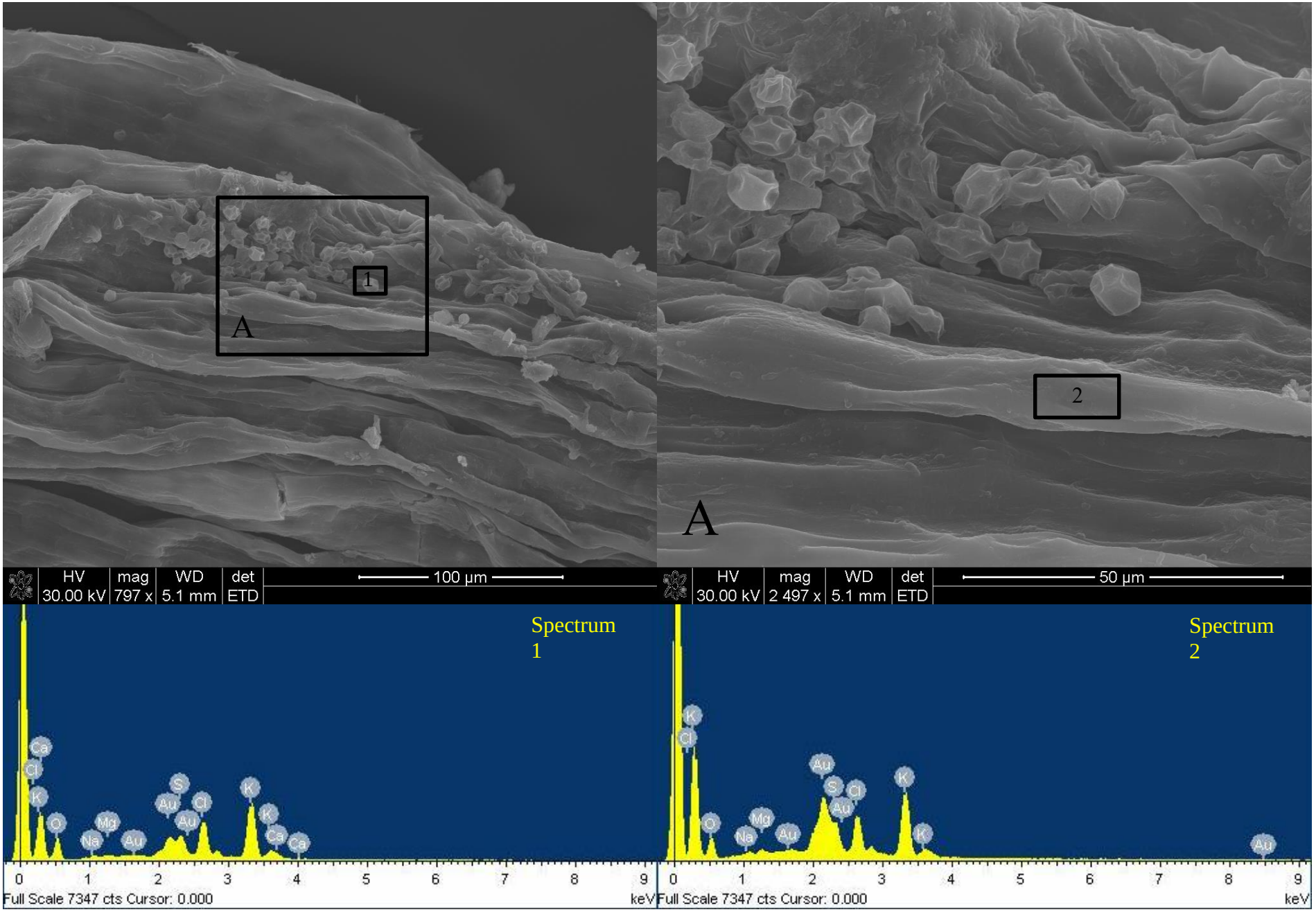

Figure 16: SEM images and 2 EDS spectra of *in vitro T. usneoides* root tissue from material grown in ¼ strength MS and treated with 25mg/kg gold chloride

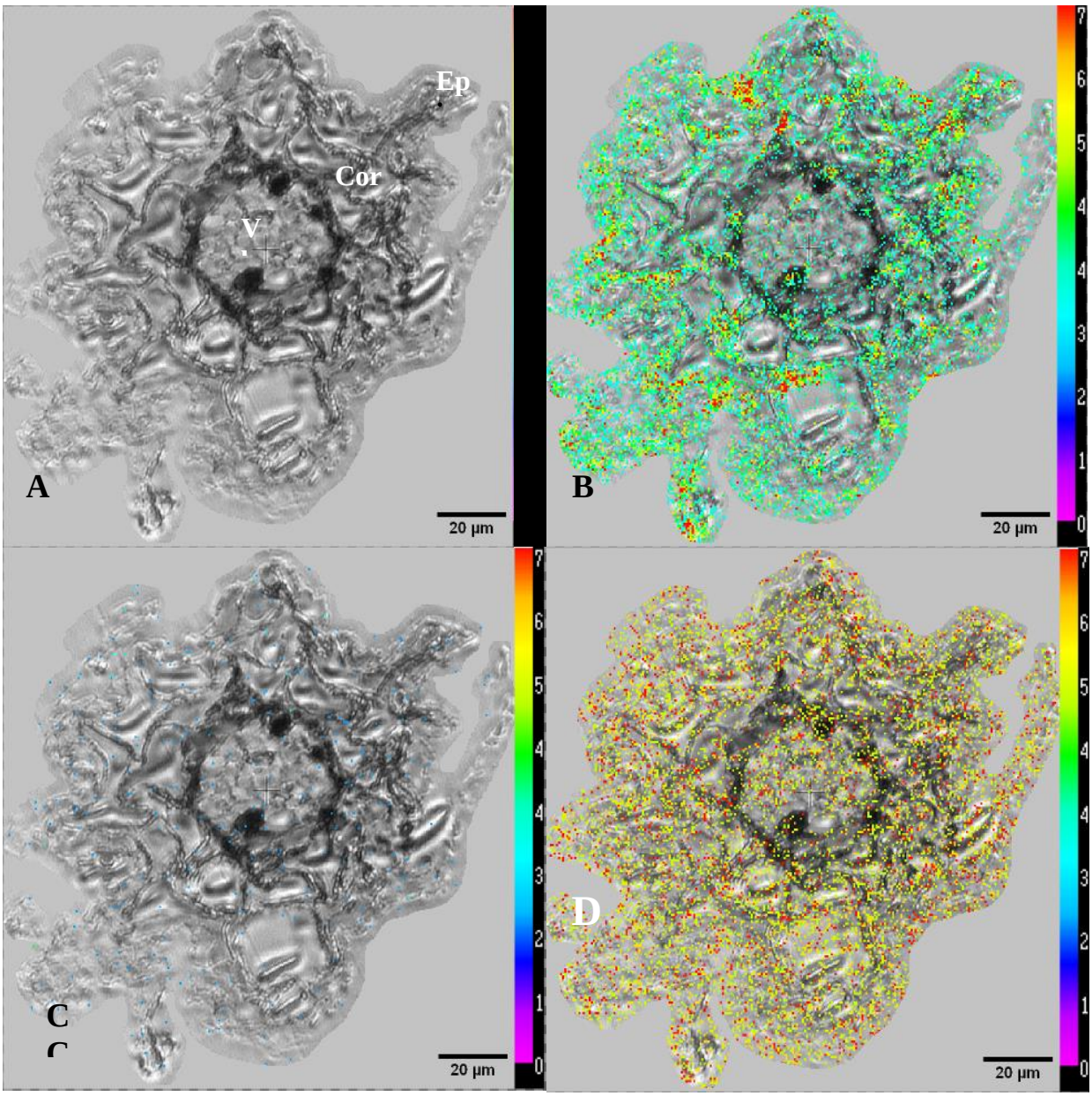

Figure 17: Cross Section (A) through root tissue from of explants grown in gold chloride at a concentration of 25mg/kg showing Vascular bundles (vb), Casparian Strip (Cs), Cortex (Cor) and Epidermis. Overlaid with WDS elemental maps and count values for B) Chlorine C) Gold D) Sodium.

SHOOT TISSUE ELEMENTAL ACCUMULATION AND TRANSFER

When using back scattered electrons (BSCE) SEM images of the exterior of the leaf and stems of *T. usneoides* showed that there was accumulation of sulphur(Figure 18 A, S) but that chloride concentrations were generally low (Figure 18, B). No gold was detected on the surface of the leaf tissue (Figure 18, C) which suggested that it was not being excreted in the same manner as the sulphates (Figure 18, D).

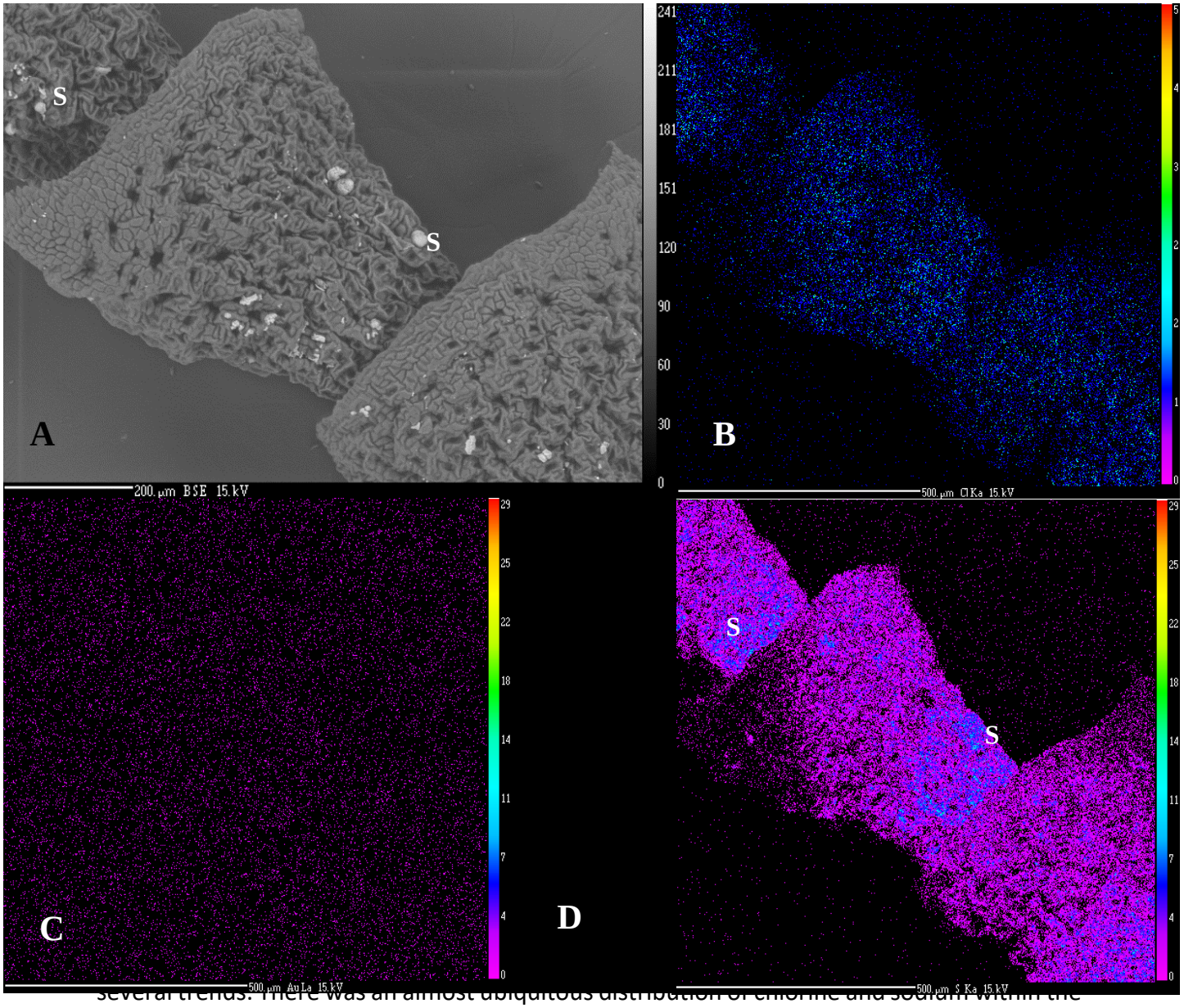

several trends. There was an almost ubiquitous distribution of chlorine and sodium within the

Figure 18: Back scattered electron SEM image (A) showing excreted sulphur (S) and WDS elemental Maps for B.) Cl, C.) Au and D.) S for a stem section from a *T. usneoides* plantlet treated with gold chloride at a concentration of 25 mg/kg

concentrations of sodium and low concentrations for chlorine (Figure 19, Figure 20, Figure 21). In some locations, where there were high concentrations of polyphenolics and sodium, there was exclusion of chlorine from that cell (Figure 19). In the tissue surrounding the salt glands, there was very little accumulation of sodium or chlorides. This observation is significant as the plant is a recretohalophyte and as such one of the primary mechanisms for the maintenance of homeostasis is the secretion of chloride salts from its salt glands (Zhou *et al*., 2001). If active excretion were occurring at that site there would be a resulting accumulation of sodium and chlorine within the gland as well as within the surrounding tissue. The reason for this observation is either due to the elemental concentrations within that tissue being below that at which the regulatory mechanisms involved in elemental excretion are activated (Maggio *et al*., 2007), or the rates of excretion from that tissue were rapid enough to deplete the area local to the salt glands of excess elements, thus maintaining a state with low elemental concentrations (I.M. Weiersbye unpublished data). In this regard, Hagemeyer & Waisel (1988) observed rapid excretion rates in the closely related *T. aphylla*. It is more likely that the first hypothesis is correct, as there is observational evidence of elemental accumulation within other tissues of those sections (i.e. gold and sodium, Figure 19), which implies that there are already regulatory processes involved in maintaining cellular homeostasis, which could potentially be sufficiently effective in preventing ion toxicity. A further observation which supports this hypothesis is the mesophyll tissue surrounding the salt glands contained relatively few cells with significant polyphenolic concentrations (Figure 19), while the cells of stem tissue contain polyphenolics. As polyphenols play a role in maintaining plant homeostasis during ionic stress (Michalak, 2006), it is likely that tissue with low observed concentrations of polyphenols are not experiencing metal stress.

A further observation that was notable was the general lack of sulphur accumulation within the majority of the cells (Figure 19, Figure 20) with the exception of one observation (Figure 21, A) where sulphur accumulation occurred within a parenchyma cell containing flocculated polyphenolics. The exclusion of sodium from that cell suggested that differential ion sequestration may be a mechanism that *T. usneoides* uses in order to maintain homeostasis. Within the sessile leaf tissue, there was comparatively little gold accumulation, while within the stem tissue, gold accumulation primarily occurred within the epidermal tissue and within the parenchyma tissue (Figure 19).

Areas with elevated gold concentrations were typically found within the parenchyma tissue and xylem tissue of the plantlet stem, with greater concentrations closer to the epidermis (Figure 20, B). These areas of elevated gold concentration were associated with flocculated polyphenolic compounds (Figure 20), however, not all areas with flocculated polyphenols had elevated gold or other elements. This was expected as polyphenols may not only be associated with elemental concentration but may be associated with other biological processes such as removal of ROS (Michalak, 2006).

When treated with gold chloride trial *T. usneoides* plantlet leaf tissue showed calcium and sodium accumulation within the palisade tissue (Figure 22). Calcium and sodium were also present within the salt glands in particular in the basal collecting cells of the gland. Again, these areas of elemental accumulation were associated with flocculated polyphenolic compounds. There was however, an even distribution of chlorine throughout the tissues with little of chlorine accumulation associated with a salt gland. This observation may be attributed to the fact that *T. usneoides* is a halophyte and the chloride concentrations within the growth medium may not have been elevated enough to trigger an excretory response.

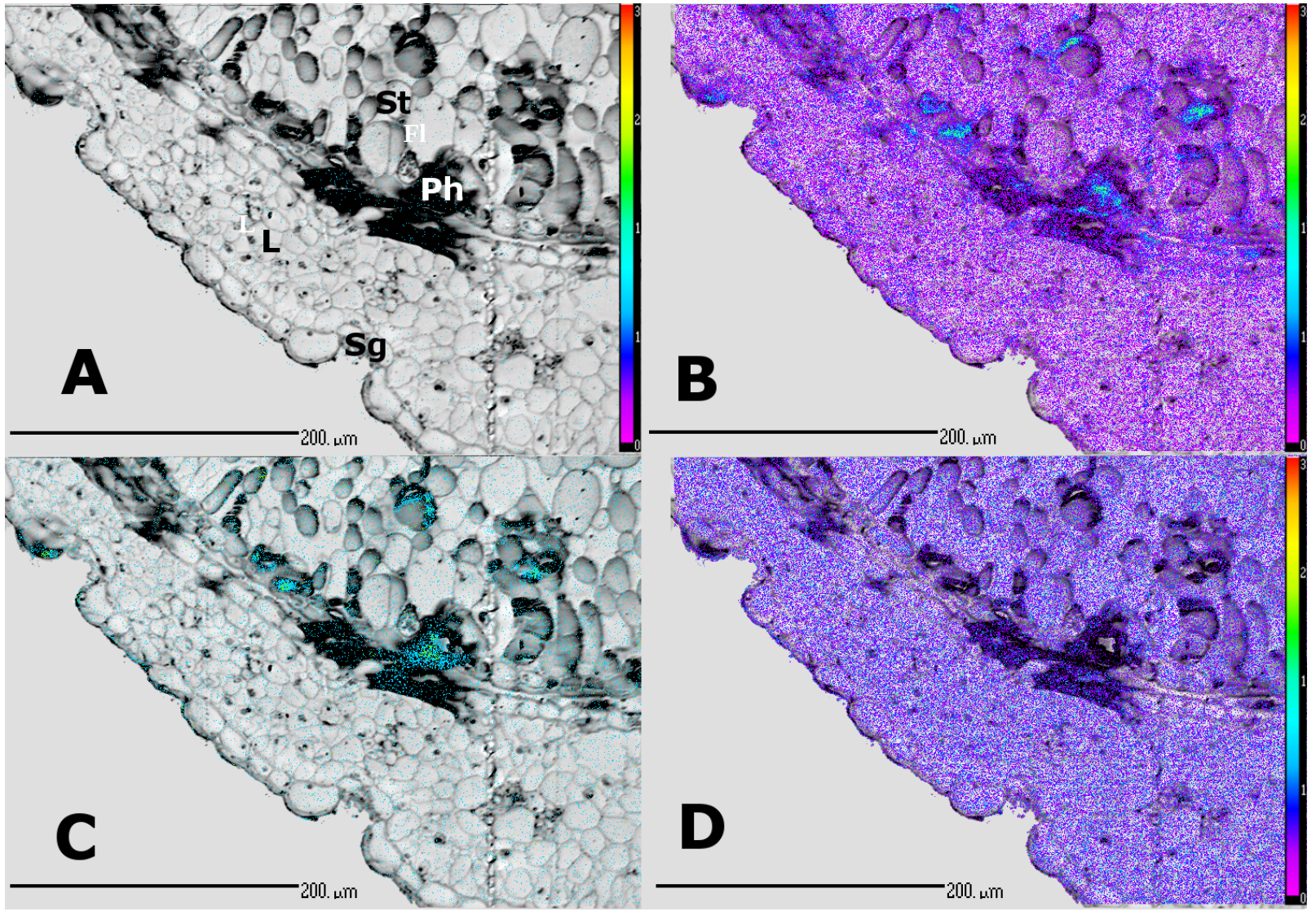

Figure 19: Cross section through a portion of stem (epidermis and subtending parenchyma tissue) (St) and leaf tissue (L) from a *T. usneoides* plantlet grown in a solution of gold thiosulphate at a concentration of 25mg/kg overlaid with WDS elemental maps and counts. A.) Sulphur, B.) Sodium, C.) Gold and D.) Chlorine.

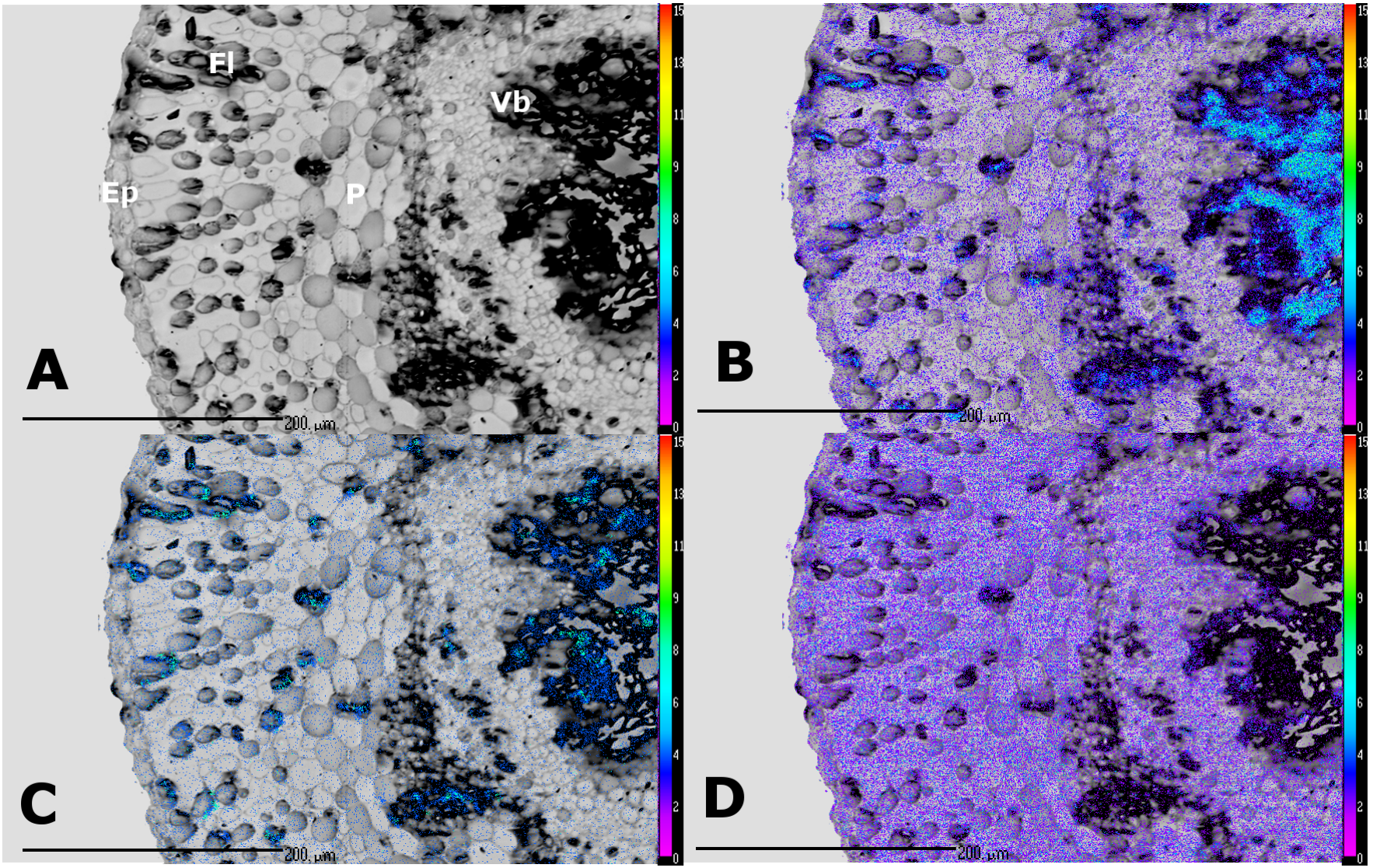

Figure 20: : Cross section througha stem showing Parenchyma tissue (P) with flocculated polyphenolic compounds (Fl) Stem Vascular tissue (Vb) and stem epidermis (Ep) from a *Tamarix usneoides* plantlet grown in a solution of gold thiosulphate dosed to a concentration of 25mg/kg Au, overlaid with WDS elemental maps and counts for A.) sulphur B.) Chlorine, C.) Gold and D.) Sodium.

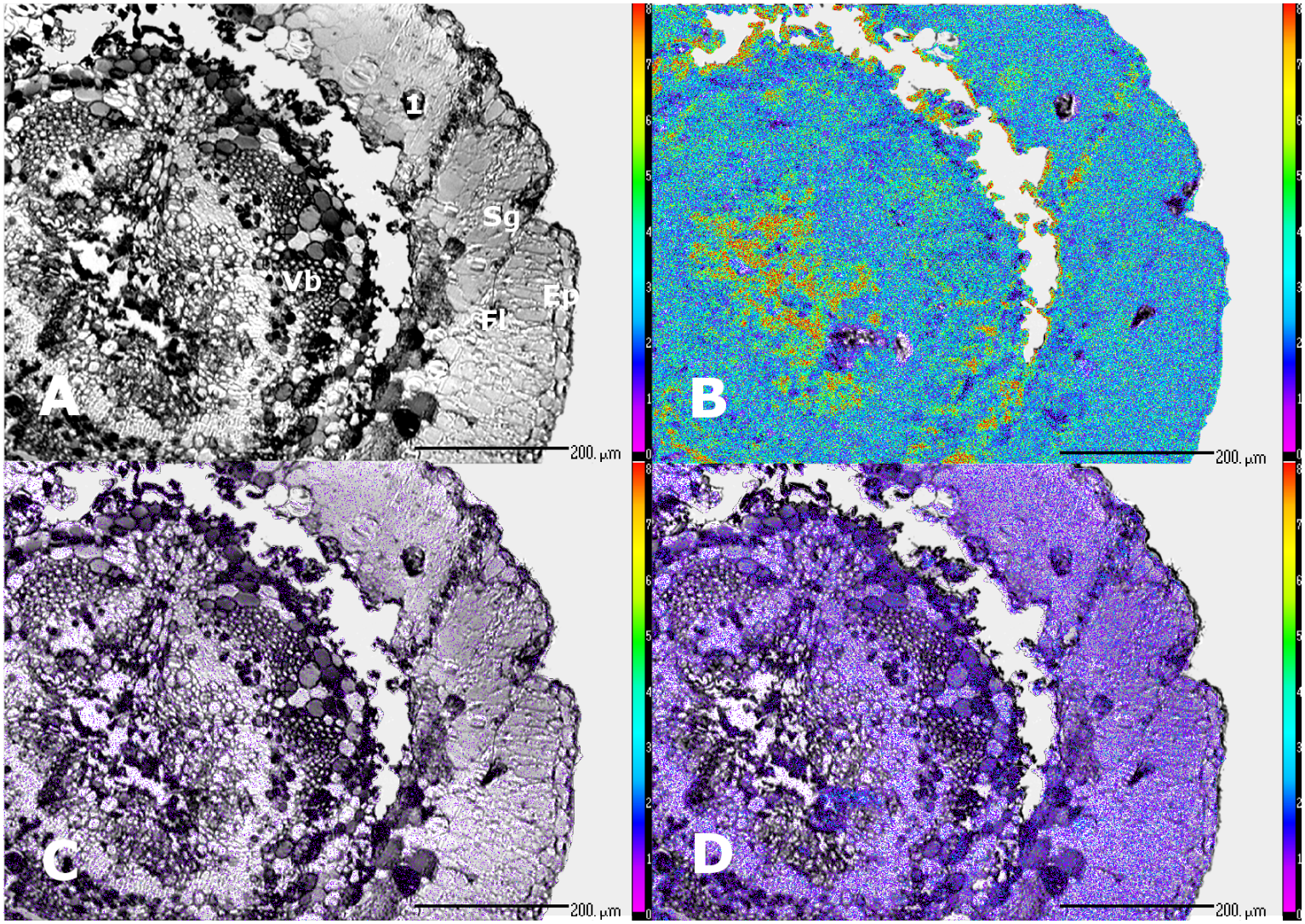

Figure 21: A torn cross section through a vaginate *Tamarix usneoides* leaf from a plantlet grown *in vitro* dosed with Gold Thiosulphate to a concentration of 25mg/kg showing Bascular bundles (Vb), Salt gland (Sg), Epidermal tissue (Ep), overlaid with WDS elemental maps and counts for A.) Sulphur, B.) Sodium, C.) Gold and D.) Chlorine (1) Evidence of elemental exclusion where sulphur is accumulated but sodium is excluded from cells with flocculated polyphenolic compounds (Fl)

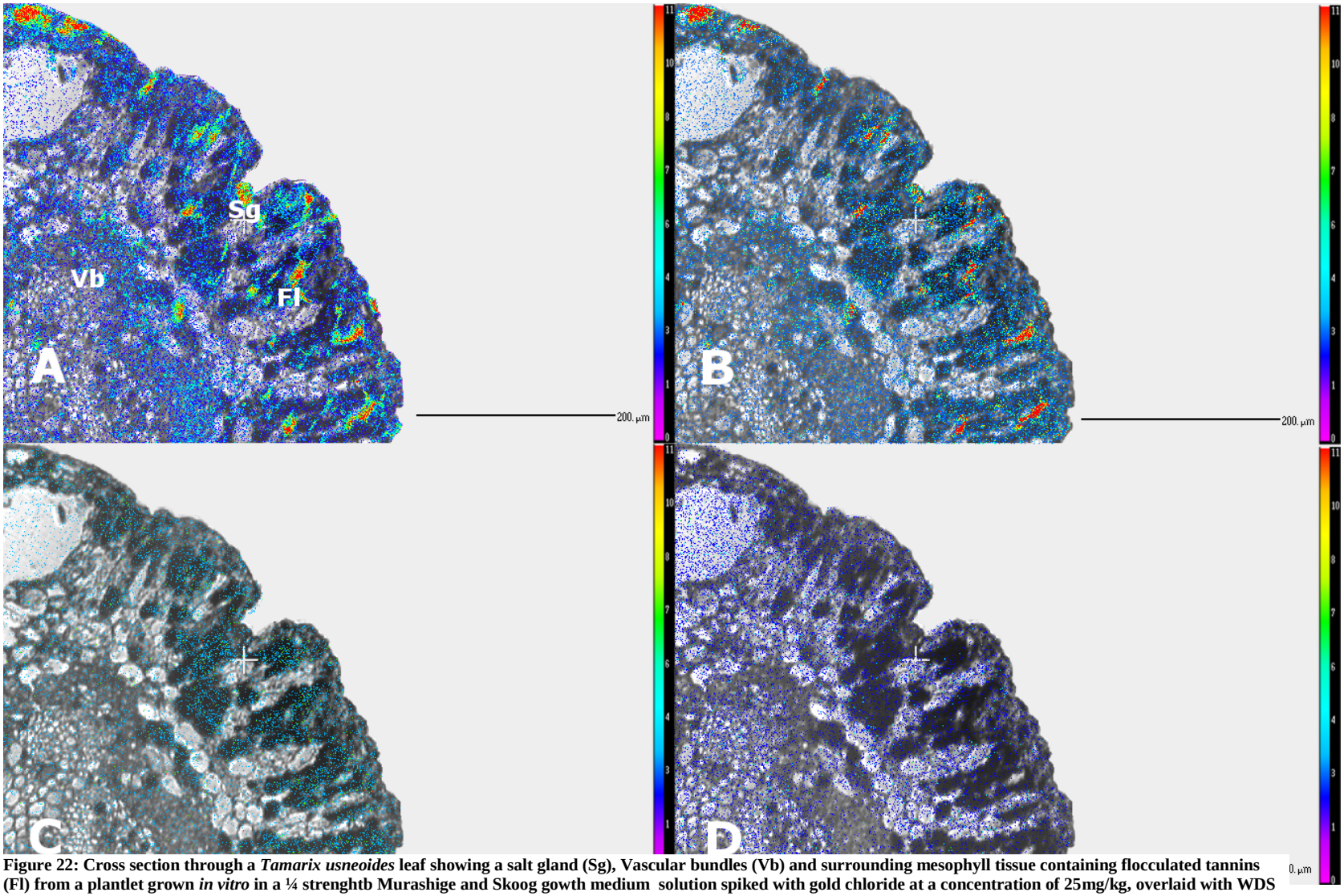

Figure 22: Cross section through a *Tamarix usneoides* leaf showing a salt gland (Sg), Vascular bundles (Vb) and surrounding mesophyll tissue containing flocculated tannins (Fl) from a plantlet grown *in vitro* in a ¼ strenghtb Murashige and Skoog gowth medium solution spiked with gold chloride at a concentration of 25mg/kg, overlaid with WDS elemental maps and counts for A.) Calcium, B.) Sodium, C.) Gold and D.) Chlorine

TISSUE ELEMENTAL TRANSFER

The maintenance of homeostasis and prevention of ionic stress during the process of ion uptake, transport, sequestration and excretion by *T. usneoides* occurs via a number of different processes. The evidence of elemental exclusion from the cytoplasm of the cells of the root cortex tissue (Figure 17, B) suggested that control of the ion balances within its root tissues is part of the suite of traits that the plant exhibits in order to tolerate the extreme elemental concentrations of the saline habitats that it typically inhabits.

Plants have a ubiquitous potassium requirement; however, as potassium concentrations within the soils are typically lower than the concentrations within the plant cytosol, there is a need for the active uptake of potassium (Mäser *et al*., 2002). This poses a problem for plant function as some membrane transporters cannot differentiate between the Na^+ and K^+ ions (Rodríguez-Navarro & Rubio, 2006). This can result in potentially dangerous accumulation of Na^+, or if complete exclusion of Na^+ occurs, severe K^+ deficiencies. Halophyte plants circumvent this by having a higher tolerance for cellular sodium, which they typically achieve by sequestering the excess Na^+ ions within vacuoles, or in the case of recretohalophytes, through the excretion of excess ions from their salt glands (Zhou & Zhao, 2001).

The accumulation of sodium within the aboveground biomass of *T. usneoides*, particularly around the vascular tissue (Figure 20), as well as within cells of the parenchyma tissue around the stem cortex (Figure 20), suggested that sodium could potentially be utilised by the plant in order to control osmolarity of the different tissues, thus maintaining turgor pressure in aboveground biomass (Wakeel *et al.*, 2011). This strategy is similar to that utilised by *Populus euphratica,* where elevated Na^+ concentrations within leaf tissue were associated with increased foliar osmotic pressure (Ottow *et al.,* 2005). However, the evidence from the

elemental maps showed elevated sodium concentrations within vascular tissue as well as in specific localities within the parenchyma tissue of the stem cortex, which is different to the processes utilised by *P. euphratica*, where sodium accumulation occurred within the apoplast of the leaf tissue (Ottow et al., 2005) (Figure 22). This suggested that *T. usneoides* preferentially sequesters sodium within specific cells within the tissue, thus protecting the surrounding chlorenchyma tissue from the toxic effects of excess sodium (Zhou & Zhao, 2001). The evidence of sodium as well as other ions within the tissue surrounding the salt gland suggested that the types of processes utilised for the sequestration and excretion of sodium can apply to a range of other cations, which serves to explain the range of ions observed in other studies (See calcium and sodium concentrations within Figure 22 as well as the sodium and gold concentrations for Figure 19, Dennis, 2008; I.M. Weiersbye, unpublished data). This was likely due to the same families of membrane ion transporters, particularly the active transporters such as cation exchange channels being involved in the processes of elemental sequestration within the tissues (Hedrich, 2012). The observation that *T. usneoides* loads sulphur and sodium into separate cells, suggested that there is ion discrimination that occurs during the process of elemental sequestration. Similarly, differential ion sequestration was clearly visible in Figure 21 where the areas with elevated concentrations of sodium had almost no chlorine present.

The observation of accumulated sulphur on the surface of the plant stem sections (Figure 18) despite low tissue concentrations (Figure 19) and the sulphur localisation in specific cells of the mesophyll tissue (Figure 21, A) implies that the excess sulphur in the in vitro trials was rapidly processed and excreted, resulting in very little build up within the leaf tissue. This supports the observations of rapid excretion of sulphates with little sulphate accumulation as observed in Wilson et al., 2019 manuscript, (chapter 4 table 11 of this thesis).

The elemental maps of *T. usneoides* (Figure 19 and Figure 22) showed that gold accumulation primarily took place within the mesophyll and epidermal tissue of the leaves and within the parenchyma tissue of the stem cortex, with the majority of gold being accumulated in tissues that also contain flocculated polyphenolic compounds. TEM and high magnification EPMA were inconclusive in providing evidence of gold nano-particles (data not shown). It is possible that gold ions or gold nano-particles were being complexed with polyphenolic compounds as has been observed with other metal ions (Figure 20, Michalak, 2006).

It has been hypothesised that flocculated polyphenolic compounds such as tannins play a role in ion detoxification and control of ionic stress in plants (Michalak, 2006). The observations of flocculated polyphenolic compounds in certain cells of the parenchyma tissue are suggestive of a symplastic ion transport route. The polyphenolic compounds potentially form chelates between the different elements that were being transported (Hider *et al.*, 2001) and acted as metallochaperones as described by O'Halloran & Culotta, 2000, where metallochaperones assist in the delivery of transition metal ions to the diverse locations where metalloenzymes require transition metals as co-factors. This process prevents the ions from binding to other enzymes or disrupting cellular processes through the generation of ROS and free radicals (Michalak, 2006). The metal chelation ability of polyphenols, as well as the ability to act as anti-oxidants suggests that the observations of dense polyphenolic compounds in particular tissues may be part of *Tamarix* ion tolerance mechanisms. The increased sodium and calcium concentrations in cells with heavily flocculated polyphenols (Figure 22) in addition to the evidence of gold accumulation in cells with flocculated polyphenols (Figure 19 and Figure 22) as well as in areas with high concentrations of sulphur (Figure 21) suggested that polyphenolic compounds are utilised in the maintenance of homeostasis in *T. usneoides.*

Thompson and Liu (1967) proposed that members of the genus *Tamarix* utilised both an apoplastic as well as a symplastic transportation route for the excretion of excess ions. Observations of the physiology of the tissue surrounding the salt excretory cells support that theory (Wilson *et al.,* 2017, Chapter 5). The apoplastic transfer of ions from the vascular tissue to the salt gland relies on the maintenance of a concentration gradient between the source of ions (vascular tissue) and the salt gland. This was supported by the observed elemental distributions as there was no accumulation of ions within the apoplast of the mesophyll tissue (Figure 19 and Figure 22). The rapid excretion rates, combined with the observations of sulphur accumulation in specific cells as well as the ion accumulation in cells containing flocculated polyphenolics are indicative of a range of differing strategies to maintain ion homeostasis, with certain elements being rapidly excreted (i.e. sulphur (Figure 18)) while other elements such a sodium, calcium and gold (Figure 20 and Figure 22) are sequestered within vacuoles of parenchyma tissue.

5.5.Conclusion

The findings of this chapter suggest that elemental excretion is only a piece of a broader suite of tolerance mechanisms that are utilised by *T. usneoides* to maintain homeostasis. The observations of differential patterns of elemental accumulation suggested that there are a number of distinct processes involved in ion tolerance, ranging from ion exclusion and sequestration within root tissue, to the loading of excess ions into specific cells within parenchyma tissue, to the binding of elements to polyphenols which could potentially serve as metallochaperones, to elemental exclusion in specific tissues and finally, ion excretion from salt glands. The most likely transport pathways are symplastic where excess ions are

ultimately bound within vacuoles and detoxified via phenolics and other metallochaperones which in turn minimises potential interactions between the excess ions and cellular processes that are susceptible to ion toxicity (Ding *et al.*, 2010). Gold accumulation was observed to follow a similar trend to other elements where it was sequestered into parenchyma cells which contained significant quantities of polyphenolic compounds.

The evidence of ion sequestration and differential ion distribution within the tissue of *T. usneoides* collectively suggests that the mechanisms which the plant uses to maintain homeostasis are reliant on the use of ion specific exchange proteins in the cell membranes in order to sort and differentiate between different ions (Clemens *et al.*, 2002). Thus, the range of ions which has been observed in the excretion of members of the genus *Tamarix* as well as the range of elements that have been documented to accumulate within the tissues of *T. usneoides* is likely as a result of the well described actions of ion transporter proteins (Ding *et al.*, 2010).

5.6. Acknowledgements

This study forms part of the doctoral research of the first author, and was supported by AngloGold Ashanti and the Technology for Human Resources for Industry Programme (THRIP) award no. TP13080525596 from the Department of Trade and Industry and the National Research Foundation of South Africa to I.M. Weiersbye and E.T.F. Witkowski.

5.7.References

Antoniadis V., Levizou E., Shaheen S.M., Ok Y.S., Sebastian A., Baum C., Prasa, M.N., Wenzel W.W. and Rinklebe J.,(2017). Trace elements in the soil-plant interface: Phytoavailability, translocation, and phytoremediation–A review. *Earth-science reviews*, *171*, pp.621-645.

Baker A. J., (1981) Accumulators and excluders-strategies in the response of plants to heavy metals. *Journal of plant nutrition*, 3(1-4), 643-654.

Bao Z., Bai J., Cui H., & Gong C. (2019). A missing link in radial ion transport: ion transporters in the endodermis. *Frontiers in Plant Science*, *10*.

Barceló J. U. A. N., & Poschenrieder C. (1990). Plant water relations as affected by heavy metal stress: a review. *Journal of plant nutrition*, 13(1), 1-37.

Chen T., Cai X., Wu X., Karahara I., Schreiber L. & Lin J. (2011). Casparian strip development and its potential function in salt tolerance. *Plant signaling & behavior*, *6*(10), 1499-1502.

Clemens S., Palmgren M. G. & Krämer U. (2002). A long way ahead: understanding and engineering plant metal accumulation. *Trends in plant science*, 7(7), 309-315.

Clemens S., & Ma J. F. (2016). Toxic heavy metal and metalloid accumulation in crop plants and foods. *Annual review of plant biology*, *67*, 489-512.

Conn S., & Gilliham M. (2010). Comparative physiology of elemental distributions in plants. *Annals of botany*, 105(7), 1081-1102.

Cunningham S. D. & Berti W. R. (1993). Remediation of contaminated soils with green plants: an overview. *In vitro Cellular & Developmental Biology-Plant, 29*(4), 207–212.

Dietz K. J., Baier M., & Krämer U. (1999). Free radicals and reactive oxygen species as mediators of heavy metal toxicity in plants. In *Heavy metal stress in plants* (pp. 73-97). Springer Berlin Heidelberg.

Ding F., Yang J. C., Yuan F. & Wang B. S. (2010) Progress in mechanism of salt excretion in recretohalopytes. *Frontiers in biology*, 5(2), 164-170.

Hagemeyer J. & Waisel Y. (1988). Excretion of ions (Cd^{2+}, Li^{+}, Na^{+} and Cl^{-}) by *Tamarix aphylla*. *Physiologia plantarum*, 73(4), 541-546.

Hamilton E. W., & Frank D. A. (2001). Can plants stimulate soil microbes and their own nutrient supply? Evidence from a grazing tolerant grass. *Ecology*, 82(9), 2397-2402.

Harding D. P. (2002). Mineral identification using a scanning electron microscope. *Mining, Metallurgy & Exploration*, *19*(4), 215-219.

Hedrich R. (2012). Ion channels in plants. *Physiological reviews*, 92(4), 1777-1811.

Hider R. C., Liu Z. D. & Khodr H. H. (2001). Metal chelation of polyphenols. In *Methods in enzymology* (Vol. 335, pp. 190-203). Academic Press.

Kadukova J., Manousaki E. & Kalogerakis N. (2008). Pb and Cd accumulation and phyto-excretion by salt cedar (*Tamarix* smyrnensis Bunge). *International journal of phytoremediation*, 10(1), 31-46.

Khan M. A., Ungar I. A. & Showalter A. M. (2000). Effects of salinity on growth, water relations and ion accumulation of the subtropical perennial halophyte, *Atriplex griffithii* var. *stocksii*. *Annals of botany*, 85(2), 225-232.

Khan A. G. (2005). Role of soil microbes in the rhizospheres of plants growing on trace metal contaminated soils in phytoremediation. *Journal of trace elements in medicine and biology*, 18(4), 355-364.

Kleinkopf G. E. & Wallace A. (1974). Physiological basis for salt tolerance in *Tamarix* ramosissima. *Plant science letters*, 3(3), 157-163.

Krämer U., Talke I. N., & Hanikenne M. (2007). Transition metal transport. *FEBS letters*, 581(12), 2263-2272.

Maggio A., Raimondi G., Martino A., & De Pascale S. (2007). Salt stress response in tomato beyond the salinity tolerance threshold. *Environmental and experimental botany*, 59(3), 276-282.

Manousaki E., Kadukova J., Papadantonakis N., & Kalogerakis N. (2008). Phytoextraction and phytoexcretion of Cd by the leaves of *Tamarix* smyrnensis growing on contaminated non-saline and saline soils. *Environmental research*, 106(3), 326-332.

Marschner H. (1986) Mineral nutrition of higher plants. Academic Press, London, p 674

Marschner H. (2011). Marschner's mineral nutrition of higher plants. Academic press.

Mäser P., Gierth M. & Schroeder J. I. (2002). Molecular mechanisms of potassium and sodium uptake in plants. In *Progress in Plant Nutrition: Plenary Lectures of the XIV International Plant Nutrition Colloquium* (pp. 43-54). Springer, Dordrecht.

Michalak A. (2006). Phenolic compounds and their antioxidant activity in plants growing under heavy metal stress. *Polish Journal of environmental studies*, 15(4).

Murashige T. & Skoog F., (1962). A revised medium for rapid growth and bioassays with tobacco tissue cultures. *Physiol. plant*, 15, 473-97.

Nishizono H., Ichikawa H., Suziki S., & Ishii F. (1987). The role of the root cell wall in the heavy metal tolerance ofAthyrium yokoscense. *Plant and soil*, *101*(1), 15-20.

O'Halloran T. V. & Culotta V. C. (2000). Metallochaperones, an intracellular shuttle service for metal ions. *Journal of biological chemistry*, 275(33), 25057-25060.

Ottow E.A., Brinker M., Teichmann T., Fritz E., Kaiser W., Brosché M., Kangasjärvi J., Jiang X. & Polle, A. (2005). *Populus euphratica* displays apoplastic sodium accumulation, osmotic adjustment by decreases in calcium and soluble carbohydrates, and develops leaf succulence under salt stress. *Plant physiology*, *139*(4), 1762-1772.

Ovečka M. & Takáč T. (2014). Managing heavy metal toxicity stress in plants: biological and biotechnological tools. *Biotechnology advances*, *32*(1), 73-86.

Pardo J. M. & Quintero F. J. (2002). Plants and sodium ions: keeping company with the enemy. *Genome biology*, 3(6), reviews1017-1.

Rodríguez-Navarro A. & Rubio F. (2006). High-affinity potassium and sodium transport systems in plants. *Journal of experimental botany*, 57(5), 1149-1160.

Ryan P. R., Delhaize E. & Jones D. L. (2001). Function and mechanism of organic anion exudation from plant roots. *Annual review of plant biology*, 52(1), 527-560.

SIEDLECKA A., TUKENDORF A., SKÓRZAŃSKAPOLIT E., MAKSYMIEC W., WÓJCIK M., BASZYŃSKI T., KRUPA Z. Angiosperms. [in] Metals in the environment. *Analysis of biodiveristy*. Prasad M.NV (red) Marcel Dekker, Inc. New York, Hyderbad India, pp 171-217, 2001

Souza M. F. D., Soares E. M. B., Silva I. R. D., Novais R. F. & Silva M. F. D. O. (2014). Competitive sorption and desorption of phosphate and citrate in clayey and sandy loam soils. *Revista brasileira de ciência do Solo*, *38*(4), 1153-1161.

Spurr A.R., (1969). A low-viscosity epoxy resin embedding medium for electron microscopy. *Journal of ultrastructure research*, 26(1), 31-43.

Thomson W.W., Berry W.L., Liu L.L. (1969). Localization and secretion of salt by the salt glands of *Tamarix aphylla*. *Proc Natl Acad Sci* USA 63 (2):310–317.

Violante A., Cozzolino V., Perelomov L., Caporale A. G. & Pigna M. (2010). Mobility and bioavailability of heavy metals and metalloids in soil environments. *Journal of soil science and plant nutrition*, *10*(3), 268-292.

Wakeel A., Farooq M., Qadir M. & Schubert S. (2011). Potassium substitution by sodium in plants. *Critical reviews in plant sciences*, 30(4), 401-413.

Wong M. H. (2003). Ecological restoration of mine degraded soils, with emphasis on metal contaminated soils. *Chemosphere*, 50(6), 775-780.

Yuan F., Leng B., & Wang B. (2016). Progress in studying salt secretion from the salt glands in recretohalophytes: how do plants secrete salt? *Frontiers in plant science*, 7, 977.

Yadav S. K. (2010). Heavy metals toxicity in plants: an overview on the role of glutathione and phytochelatins in heavy metal stress tolerance of plants. *South African journal of botany*, *76*(2), 167-179.

Zhou S., Han J. L. & Zhao K. F. (2001). Advance of study on recretohalophytes. *Chinese journal of applied and environmental biology*, 7(5), 496-501.

6. Salinity tolerance, metal accumulation and gold phytoextraction by *Tamarix usneoides*

6.1.Introduction

Salinity tolerance in halophytes is a complex trait with a polyphyletic origin (Flowers *et al*, 1977). Some 345 halophyte species have been identified spanning 58 families, with the order Caryophyllales (of which the genus *Tamarix* belongs) counting 21.4% (Flowers *et al*., 2015). Multiple mechanisms are employed in order to achieve salt tolerance, for example, of the nine salt tolerant families within the Caryophyllales, five use salt glands to excrete excess salt from the leaves, while other families achieve salt tolerance through mechanisms such as ion sequestration *in planta* (Shabala & Mackay, 2011). The mechanisms which confer salinity tolerance are not necessarily limited to sodium and chlorine, but may confer tolerance to a suite of other elements (Van Ooosten & Maggio, 2015). Studies into gold accumulation in plants initially focused on the use of plants as biomarkers for mineral exploration (Dunn, 1986) and later moved on to investigate the potential for using plants for biomining gold (Anderson *et al.*, 2005). Subsequent studies have focused on the role of soil amelioration in increasing gold mobility for uptake (Sheoran *et al*., 2013), or have investigated the uptake, translocation and possible phyto-toxicity of gold nano-particles (Iram *et al*., 2014).

In order to better understand the underlying biological processes that *T. usneoides* uses to accumulate gold this final chapter will explore the similarities in the physiological processes utilised by both halophytic and metallophyte plants to achieve their respective tolerances by proposing a model for elemental transport in *T. usneoides*. It will then relate those to the findings of this thesis.

6.2. A model for ion transfer and elemental tolerance in *T. usneoides*

The previous data chapters in this thesis showed that *T. usneoides* has a number of different response strategies for maintaining homeostasis within its tissues while still accumulating ions prior to their excretion. An overview of this model is presented in **Error! Reference source not found.**.

In order for a plant to be able to accumulate ions, the ions in question need to be in a form that is bio-available for uptake. Conversely, the toxic effects of ions can be mitigated through reducing an elements mobility within the rhizosphere by raising or lowering the rhizosphere pH. Rhizosphere pH adjustment is achieved through the action of proton pumps located in the plasmalemma and the secretion of low molecular weight organic compounds from root cells (Kramer et al., 2007). Soil pH adjustment was evident in the *in-situ* uptake trials where pits that had established trees had a significantly higher pH than the control pits (pH of the tailings samples collected from the pits that had trees ranged from 4.4 – 5.7 whereas the control pits had a pH that ranged from 3.4 – 4.2)(Table 7). This suggests that *T. usneoides* may regulate the rhizosphere pH in order to adjust the chemical mobility of the rhizosphere, thus limiting the range of elements that are bio-available for uptake (Figure 23, 1).

The second strategy is the immobilization of elements through binding them to the root epidermal tissue. In the *in situ* study, Cu, Fe, Mg, Pb, Rb, Th, U and Zn had higher mean concentrations on the root epidermis than in the surrounding tailings or in the surrounding root tissue (Table 11). This suggested that the elements were immobilised by binding to the root epidermal tissue surfaces (Figure 23, 2). Elemental maps of root tissue from the *in vitro* samples showed that chlorine accumulated on the surface of the root tissue, while sodium was ubiquitous through the tissues which suggested that sodium exclusion is not a strategy that *T. usneoides* utilises for salinity tolerance, but exclusion may be used for Rb, Th and U (Figure 17).

The accumulation of elements within the root cortex as well as the low translocation factors for root vascular tissue for certain elements (Table 10) suggests that an additional strategy for reducing the effects of excess ions in aboveground biomass is the prevention of translocation of ions to the aboveground biomass. This occurs when certain elements are bio-available for uptake into root tissue, however they are prevented from being transported into aboveground biomass (Clemens, 2006). Ion transportation in *T. usneoides* likely utilises a combination of apoplastic and symplastic transport routes for the uptake, sequestration and excretion of excess ions. Ions are initially transported via the apoplast of the root epidermal and cortex tissues where some ions may become bound to ligands associated with the intercellular spaces (Table 10). Elements (freely available) which are required for cellular function are then actively taken into the symplasm of the root cortex tissue (Figure 23, 3), whereupon they are moved past the Casparian strip (Figure 23, 4) and loaded into the vascular tissue (Table 10) (Figure 23, 5).

The upward movement of ions is facilitated by the action of transpirational pull (Figure 23, 6). Once the elements have reached the leaf vascular tissue, they are offloaded from the xylem vessels into stem parenchyma tissue and the leaf mesophyll tissue (Figure 22)(Figure 23, 7). Ions can then move to the salt gland down a concentration gradient within the apoplast of the mesophyll tissue, or they can be transported from cell to cell symplastically to the basal collecting cells of the salt gland (Figure 12) (**Error! Reference source not found.**, C, Blue). During periods of high transpiration and thus rapid loading of the leaf tissue with excess ions, the excess ions can be transferred into the symplasm and sequestered into vacuoles (Mendoza-Cózat et al., 2011) where they are complexed with polyphenolic compounds (Michalak, 2006). Analyses of the ultrastructure of the *T. usneoides* salt glands and surrounding tissues showed accretions of polyphenolic compounds within the mesophyll cells surrounding the vascular bundles and within micro-vesicles of the salt glands. This finding was corroborated by the tissue elemental mapping where the tissues with the highest concentrations of

Na, Ca, S and Au typically co-occurred with cells containing the polyphenolic compounds (Figure 20) (Figure 23, 9a, b). This suggests that metal chelation and sequestration are key processes in the range of mechanisms that *T. usneoides* utilises to maintain homeostasis during the process of transportation to the salt gland for subsequent excretion. Phytochelatins can be derived from glutathione (Yadav, 2010) or polyphenolic compounds (Michalak, 2006). Sequestration occurs via ionic transfer into vacuoles (Gao et al., 2011) and may occur in conjunction with the aforementioned processes. Phyto-chelation has the added benefit of balancing redox reactions which reduces the creation of ROS within the cytosol. The chelation of excess ions within the vacuole of the stem parenchyma tissue or the leaf mesophyll tissue could serve as a long-term ion storage mechanism. Alternatively it could form part of the intercellular ion transport mechanism, as supported by the observation of flocculated polyphenols between the leaf vascular bundles and the salt glands (Figure 12), as well as the observations of 'strands' of polyphenols spanning the basal collecting cells (Figure 13). The vacuoles of *Tamarix hispida* under salinity and heavy metal stress exhibited upregulation of H+ ATPase (Gao et al., 2011), showing that the process by which *T. hispida* is sequestering ions within its vacuoles is an active process.

A coupled apoplastic and symplastic ion transportation model as proposed by Bao et al., 2019 may also include the complexation of ions with polyphenols as the temporary binding of the ions could provide a way to transfer the ions across the cell in a manner that isolates the ions from cellular function. The observations of low levels of polyphenolic as well as the presence of chloroplasts in some of the chlorenchyma tissue surrounding the salt glands support this hypothesis (Figure 13) (Figure 23, red).

The evidence of differential ion sequestration in *T. usneoides* (Figure 20) also implies ion specificity on the part of the transmembrane transporter proteins of the tonoplast of the vacuole. The processes involved in phyto-chelation and binding to polyphenolic compounds are in some instances reversible

(Hilder et al., 2001) and as such it is possible that the accumulation of elements within the vacuoles of parenchyma tissue and leaf mesophyll tissue as observed in this study (Figure 20, Figure 22) are used as a temporary store for a particular element prior to the elements utilisation in cellular process or prior to its excretion. Alternatively, as leaf and stem senescence has been observed in *T. usneoides* (pers. obs.) it is possible that elements are permanently sequestered within certain cells until that tissue senesces, effectively eliminating excess elements (Barceló & Poschenrieder, 1990). It is likely that a combination of these two strategies are utilised and the degree to which each one is used by the plant to maintain homeostasis will depend on the nature and concentration of the elements present. It is also possible that the chelation and sequestration of metals is dependent on other processes such as transpiration rates. During periods of rapid transpiration (during the day) the transportation of excess elements to the leaf material may exceed the excretion rates of the plant, thus the plant may temporarily store the excess elements in vacuoles prior to their excretion from the salt glands (perhaps at night).

After ions have been transported to the basal collecting cells (Figure 23, 10), they are transferred via the plasmodesmata to the basal excretory cell (**Error! Reference source not found.**, 11) where they are sequestered into microvesicles and transported to the leaf surface for subsequent excretion (Chapter 5) (Figure 23, 12).

The elemental mapping of *T. usneoides* tissue was not capable of determining the mechanisms by which *T. usneoides* moves excess elements to the microvesicles of the salt glands (via endocytosis or excreted via exocytosis, or if the microvesicles form junctional complexes as proposed by Ding et al., 2010). However, the evidence of differential ion sequestration and excretion suggested that the processes that *T. usneoides* utilises for ion transport are reliant on the action of a mechanism that allows for ion differentiation, thus it is likely that ion transport occurs via a range of different cation transporters (See Finazzi et al., 2015) as well as the SULTR, TaALMT1 and SLAC1 anion channels suggested by Hedrich and Geiger (2017).

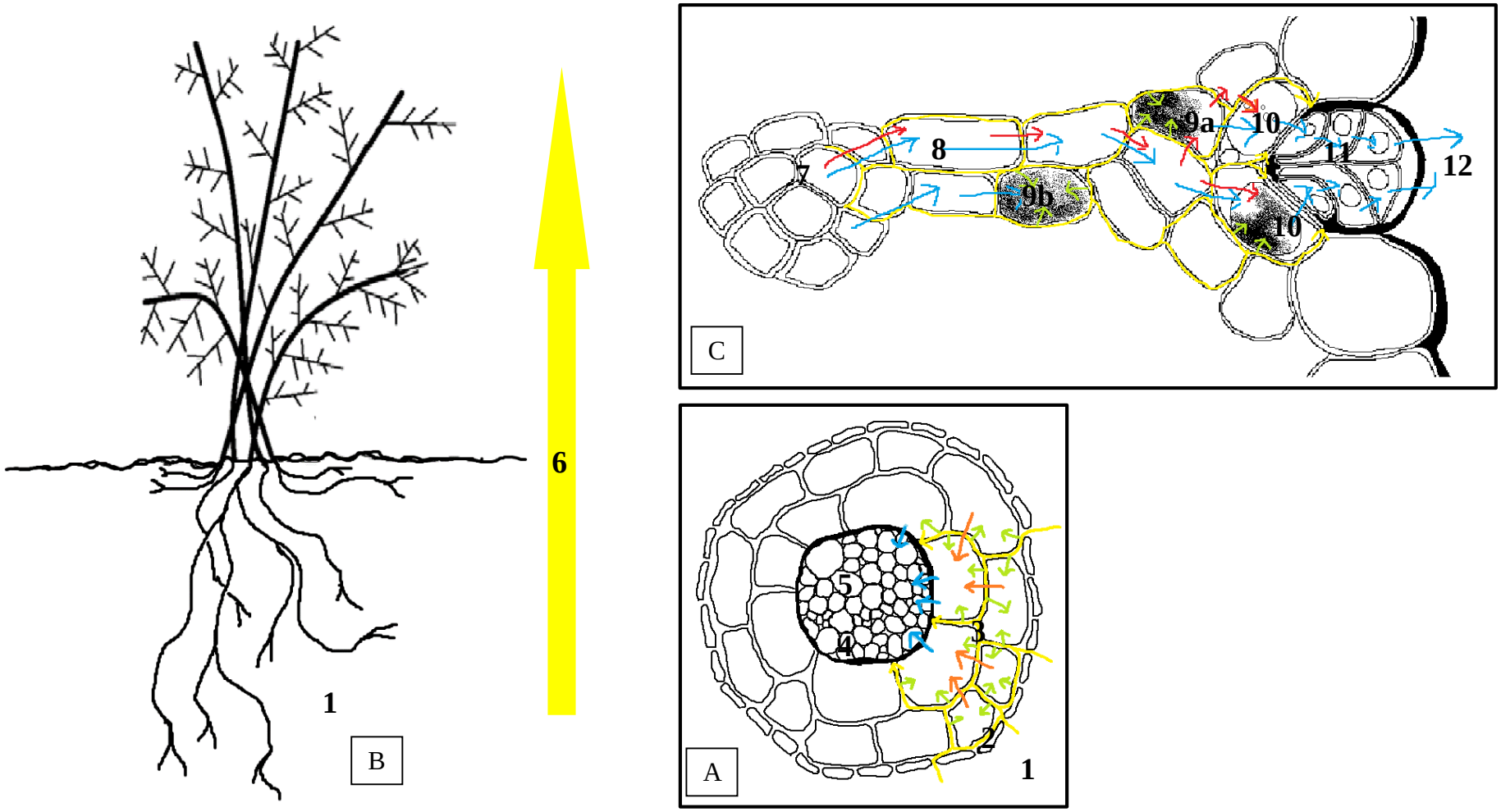

Figure 23: Model of proposed pathways for ion transport from the rhizosphere to the leaf surface. The components of the proposed pathway are: 1) rhizosphere 2) Root Epidermis 3) Root Cortex 4) Casparian strip 5) Root Vascular Tissue 6) Transpirational pull 7) Leaf Vascular tissue Tissue 8) Parenchyma Tissue, 9a) Flocculated Polyphenol, 9b) Dispersed polyphenols 10) Basal Collecting Cells 11) Salt Gland 12) Leaf surface. The pathways are A.) Yellow- Apoplastic transport within the root cortex tissue, Green – Loading of ions into the cortex via active transport Red Intercellular transport in the cortex via a coupled apoplastic and symplastic transport path Blue – Ion transportfrom the cortex tissue into the vascular tissue past the Casparian strip. B) Yellow – Transportation up the vascular tissue via transpirational pull. C) Yellow- Apoplastic transport from the vascular bundles of the leaf to the salt gland Blue- Symplastic transport utilising plasmodemata and vesicle transport Red- Coupled apoplastic-symplastic transportation Green – Ion Sequestration within parenchyma tissue containing flocculated and disperse polyphenolics.

6.3. Ecophysiological reasons for ionic stress tolerance in *Tamarix usneoides*

Salinity causes stress in plants due to reductions in water access (as the osmotic gradient between the rhizosphere is lowered under saline conditions, reducing water absorption rates) (Sairam & Tyagi, 2004) or due to accumulation of Na^+ or Cl^- ions within the plant tissue to the point of toxicity (Bose *et al*., 2014), causing oxidative stress, resulting in the generation of Reactive Oxygen Species (ROS) or due to disturbances in nutrient balance (Flowers *et al*., 2015). Tolerance to elevated concentrations of toxic ions in the rhizosphere is common to both halophyte and metallophyte species (Manousaki *et al*., 2010) and there are similarities between the processes utilised by both classes of plant to: A) exclude the ions from uptake by root tissue (Flowers & Colmer, 2008, Baker *et al*., 1994); B) isolate/sequestrate the ions that are taken up so that they are no longer available to cellular processes (Ma *et al*., 2004, Yang *et al.*, 2005) and C) limit the harmful side effects associated with elevated elemental concentrations (Bose *et al*., 2014, Sobrino-Plata *et al*., 2013).

Excess Na^+ is frequently cited as the underlying cause of toxicity associated with salinity stress, with the Cl^- component only affecting some members of the genera *Citrus* and *Vitis* (White & Broadley, 2001). As such, studies into salinity tolerance have typically focused on the uptake, translocation, sequestration and excretion of Na^+. In particular Na^+ toxicity in the cytosol occurs as a result of inhibition of enzyme activity due to competition between K^+ and Na^+ for enzyme binding sites (Maathuis and Amtmann, 1999, Flowers *et al*., 2015). Competition for binding sites also occurs in the transport proteins located in the plasmalemma of root cells, resulting in decreased total K^+ uptake (Wang *et al.*, 2007) and ultimately increased cytosolic Na^+ concentrations, however some transporters are capable of ionic differentiation (for example, HKT Proteins, Platten *et al*., 2006).

Metal ions cause toxicity via disruption of a number of different cellular processes. Firstly, transition elements such as iron generate reactive oxygen species (ROS) via Haber–Weiss and Fenton reactions (Kehrer, 2000). ROS can cause lipid perioxidation which in turn affects enzyme activity through uncontrolled hydrophobic interactions e.g. in the electron transport chains found in the inner membrane of the mitochondria and the thylakoid membranes of chloroplasts (Farmer & Mueller, 2013). ROS can also impact nucleic acid integrity. Secondly, metal ions can cause toxicity through direct interaction with enzyme and protein activity as well as through displacement of cations at specific binding sites (Sharma & Dietz, 2009). This occurs in a process similar to the competitive inhibition between K^+ and Na^+ and can result in deficiencies in essential nutrients as well as the inhibition in enzyme activity, affecting the function of metalloprotiens in functions like signal transduction, and stabilization of DNA and proteins (Dudev & Lim, 2014).

For both salinity and metal ions, tolerance mechanisms begin with ion exclusion at the root, thus preventing uptake into the plants tissues. Na^+ exclusion in halophytes is a mechanism that has been reported by a number of authors (for example Munns, 2002; Tester & Davenport, 2003; Colmer *et al*., 2006; Munns & Tester, 2008; Plett & Møller, 2010) and exclusion has also been documented in the metallophyte species *Agrostis tenuis, Armeria maritima, Thlaspi caerulescens* to name a few (Baker *et al*., 1994, Dahmani-Muller *et al.*, 2000).

The accumulation of ions within the cytosol is a process that requires regulation in order to prevent ions from reaching toxic concentrations. Transmembrane ion uptake of sodium has been suggested by a number of authors (See Kronzucker and Britto, 2010 for a detailed review) to occur via the action of voltage insensitive non-specific cation exchange channels (VI-NSCC's). These channels have been demonstrated to act as influx and efflux pathways *in planta* for sodium (Nieves-Cordones *et al*., 2016). Voltage insensitive non-specific cation exchange channels are capable of transporting a range of cations, however there is preference in the permeability of these channels for certain ions, for

example in *A. thaliana*, (values reported are relative to Na^+) K^+ (1.49) > $NH4^+$ (1.24) > Rb^+ (1.15) > Cs^+ (1.10) > Na^+ (1.00) > Li^+ (0.73) (Demidchik & Tester, 2002). The ability of both metallophyte and halophyte plants to accumulate nutrient ions such as K^+ despite the inhibitory effect of other cations such as Na^+ on the action of cation exchange channels is a shared trait. Anion uptake has been documented to occur via anion channels such as TaALMT1 and SLAC1 channels (Hedrich and Geiger, 2017).

There are a number of benefits that *T. usneoides* accrues from its ability to tolerate the elevated ion concentrations within its rhizosphere and accumulate elements in its aboveground biomass. Firstly, it allows the plant to exploit an environment where there is very little competition for resources as there are very few species (other than other halophytes) that can tolerate similar conditions (Wendelberger and Richards, 2017). Secondly, accumulation of elements in its above ground biomass can potentially assist it with water access (Wakeel et al., 2011). Desert riparian areas are prone to salinization as during the brief periods of inundation, salts and other elements are leached out of the surrounding rock and accumulate in pools and depressions in the environment (Watson, 1985). During periods of inundation these salts can be transported into the non-perennial streams, dry river beds and paleo-channels that *T. usneoides* inhabits. Inundation periods will have a relatively high osmotic potential as the salt concentration within the water will be low, however as that water begins to evaporate, the salt concentration will increase which in turn would hinder Tamarix ability to maintain turgor pressure and transport nutrients. Maintenance of cellular ionic concentrations at a level that exceeds the concentrations found in the rhizosphere would provide an osmotic gradient which would assist with keeping the plant hydrated while limiting water lost to evapotranspiration (Bradford & Hsiao, 1982). Studies have also shown that accumulation of chlorine plays a role in maintaining a plant's water balance, where chlorides are involved in leaf elongation, turgor pressure maintenance and moderating leaf water balance parameters (Franco-Navarro et al., 2015). Additionally, accumulation of certain elements in its aboveground biomass discourages herbivory (Boyd et al., 2002).

6.4.Gold accumulation within the tissues of *T. usneoides*

Tissue elemental mapping showed that gold accumulation occurred primarily within epidermal and mesophyll tissue of *T. usneoides* stems and leaves (Figure 19). The gold in the root tissues was below detection limits by WDS (Figure 17) however, the *in vitro* tissue concentrations detected by ICP-MS (Table 1) showed significant gold accumulation within the root tissue. It is thus likely that the elevated gold concentrations *in vitro* are a result of gold that is bound to the external root surface, which was potentially lost during the process of fixing and embedding the material for microscopy. The findings of the *in vitro* studies showed that there were significant differences between the gold concentration in root and shoot tissue that varied according to the gold compound present within the growth medium. Studies into gold accumulation by plants have suggested that gold is reduced to Au(0) prior to uptake and translocation to aboveground biomass (Toma *et al.,* 2010). Uptake of Au(0) is likely in the form of gold nano-particles (Gardea-Torresdey *et al*., 2002) and there is evidence that the gold nano-particle type and surface charge play a role in uptake and translocation. Gold nano-particles with positive charge are typically accumulated to a greater extent than nano-particles with a negative charge. However, in studies performed by Zhu *et al.,* 2012, it was shown that the uptake and translocation of nano-particles depended on the nanoparticles surface charge, with nano-particles with a negative charge being preferentially transported to aboveground biomass, while positively charged nano-particles had greater accumulation in root tissue (Zhu *et al.*, 2012). The findings of significant differences between the gold concentrations in the aboveground biomass of *T. usneoides* thus suggested that if the gold is accumulated as Au(0) nano-particles, then the gold compound type present within the rhizosphere likely affects the final gold nano-particle size and shape. No gold nano-

particles were detected in this study, but this does not imply that they were not present within the tissue.

Alternatively, the gold was accumulated in ionic form as anions, as when the gold compounds used in the *in vitro* study dissociate in water they form $[Au(CN)_2]^-$, $[AuCL_4]^-$, $[AuCl_3(OH)]^-$, $[Au(CN)]^{2-}$ and $[Au(S_2O_3)_2]^{3-}$ ions, or if organic molecules are present they form aqueous gold(I/III) thiosulphate and chloride complexes (Boyle 1979; Vlassopoulos & Wood 1990; Vlassopoulos *et al*. 1990, Habashi, 1967, Lengke *et al*., 2006, Southam *et al.*, 2009). Thus if the gold is simply accumulated in the same form as when it initially dissociates in solution, it is likely that gold accumulation occurs via the action of anion channels such as TaALMT1 which has been shown to be permeable to anions such as malate and chloride, NO_3^- and to a lesser extent SO_4^{2-} (Pineros *et al.*, 2008).

As the chemical composition of a contaminated site varies depending on the age of the site (Tutu *et al.*, 2005), chemical composition of the parent ore and the processing methods initially utilised in gold extraction (Ackil, 2002), it is likely that the gold accumulation capabilities of *T. usneoides* will vary depending on the site geochemical characteristics as well as the processes used for gold extraction during the metallurgical process. In the *in vitro* studies, gold concentration did affect uptake where bioconcentration values decreased with an increase in the concentration of gold within the growth medium. However, whether or not this was limited due to a maximum rate for the uptake of gold by *T. usneoides* or by metal toxicity lowering uptake rates is unknown. The only *in vitro* trials which exhibited the symptoms of stress were the gold potassium cyanide trials but it is more likely that this was

as a result of the toxic effects of the cyanide as the gold concentration range for the three different gold compounds tested were identical.

Gold uptake rates *in vitro* were different from the *in-situ* field trial and this was attributed to a range of different factors: Firstly, the *in vitro* plantlets were grown in a sealed container which maintained high humidity, evapotranspiration rates were consequently lowered which could potentially result in a reduction in the rate of nutrient transfer from the root to the shoot (Leuschner, 2002). However, this study also used juvenile material in the form of clonal plantlets and it is possible that the regulatory mechanisms associated with a mature plant were not fully functional in the *in vitro* plantlets, which w/could result in elevated gold uptake ratios (Clemens *et al.*, 2002). The uptake values in the *in vitro* study reflected the uptake of gold that was already bioavailable, whereas in a field situation, the solubility of the gold would be dependent on soil chemistry as well as the ability of *T. usneoides* to secrete chelates to increase gold mobility. One of the few documented cases of plants increasing gold bioavailability is where cyanogenic plants have been actively mobilising gold (Lintern *et al.* 2013) or where the action of the decomposition of leaf litter has resulted in small amounts of cyanide release into the environment which has increased gold bioavailability (Lintern *et al*., 2013). The gold mining industry in South Africa does use potassium cyanide during the gold extraction process and while the majority of the cyanide is recovered before the tailings are released into the environment a small quantity of cyanide does remain bonded as metal-cyanide complexes (Vorster & Flatman, 2001). However, it is unlikely that cyanide excretion by the plant would be particularly effective as during ore processing, the gold which is available for extraction by cyanide leaching would already have been removed during the metallurgical process, with the remaining gold that is deposited on the tailings facility being

encapsulated in pyrite minerals which would prevent the gold from dissolving in the cyanide solution. The action of weathering on a tailings facility (sulphate reduction by sulphur reducing bacteria (Akcil and Koldas, 2006)) could potentially release the gold encapsulated in sulphate minerals. This would expose the gold to various processes that could potentially result in its extraction. A downside to this weathering process is that it leads to the generation of acid mine drainage and concomitant mobilisation of other metals bound within the tailings facility which may be detrimental to environmental health unless appropriate mitigation measures are put in place (Chapman, 1983). Additionally, this weathering process is typically slow and is dependent on the infiltration of water and available oxygen into the tailings facility (Tutu *et al.,* 2008).

6.5. Conclusion

In the South African context, where contamination is rarely limited to the upper surface of the soil (Tutu, *et al*., 2008), the need for plants to be able to access shallow contaminant plumes limits the range of species that can effectively be used for phytoextraction (Dye, *et al.,* 2008). Furthermore, due to the harsh climatic conditions associated with contaminated mining sites, drought, frost and fire tolerance also need to be considered. *Tamarix usneoides* is ideally suited to such climatic conditions as they naturally occur in the western arid to semi-arid regions of southern Africa (Baum, 1978) which regularly experiences extreme water deficit during times of drought as well as water surplus during times of inundation.

Tamarix usneoides is capable of accumulating significant quantities of sulphates and chlorides, and on a mixed species remediation site it could be utilised in conjunction with a

cyanogenic species. This would allow the accumulation of sulphates, chlorides and gold, with the sulphate and chloride removal possibly serving to adjust the site geochemical characteristics rendering them less hostile for other species which serve the cyanogenic function. In this respect future studies should focus on the potential for *T. usneoides* to accumulate gold and sulphates from older tailings facilities or old tailings spills into contaminated wetland sink sites where the gold encapsulated by pyrite minerals has been weathered. The geochemistry of such sites will be different from those of a TSF, with the decomposition of organic matter potentially releasing cyanide which would serve to mobilise gold and more gold being present within the tailings due to the fact that the metallurgical processes for the older gold tailings being less efficient at gold recovery.

The observations in this thesis suggest that *T. usneoides* has the ability to differentially accumulate and process a suite of elements, which implies that it has a highly complex set of control processes in order to regulate ion transfer *in planta*. Additional studies should aim to identify which transfer proteins are involved in elemental transfer and also map the processes which are used in their regulation. Furthermore, the processes by which gold is accumulated require further study (Au^{+}, Au(0) nano-particles, Au – anion complexes). Studies should focus on further development of a model for the process of gold mobilisation and uptake *in planta* as well as development of an understanding as to the ability for *T. usneoides* to accumulate gold that is not already bioavailable. Finally, the applicability of the addition of soil ameliorants and the role of site geochemistry in gold mobility warrant additional investigation if the species were to be used for environmental remediation.

6.6. References

Akcil A., (2002) First application of cyanidation process in Turkish gold mining and its environmental impacts. *Minerals engineering*, 15(9), 695-699.

Akcil A., Koldas S., (2006) Acid mine drainage (AMD): causes, treatment and case studies. *Journal of cleaner production*, 14(12), 1139-1145.

Anderson C. W. N., Brooks R. R., Chiarucci A., LaCoste C. J., Leblanc M., Robinson B. H., Simcock R., and Stewart R. B., (1999). Phytomining for nickel, thallium and gold. *Journal of geochemical exploration*, 67(1), 407-415.

Baker A. J. M., Reeves R. D. & Hajar A. S. M. (1994). Heavy metal accumulation and tolerance in British populations of the metallophyte *Thlaspi caerulescens* J. & C. Presl (*Brassicaceae*). *New phytologist*, 127(1), 61-68.

Baum B.R. (1978). The genus *Tamarix*. Jerusalem, The Israeli Academy of Sciences and Humanities.

Bose J., Rodrigo-Moreno A., & Shabala S. (2014). ROS homeostasis in halophytes in the context of salinity stress tolerance. *Journal of experimental botany*, *65*(5), 1241-1257.

Boyle R. W. (1979). The geochemistry of gold and its deposits. *Geological survey of canada. bulletin*, *280*, 584.

Bradford K. J. & Hsiao T. C. (1982). Physiological responses to moderate water stress. In *Physiological plant ecology II* (pp. 263-324). Springer, Berlin, Heidelberg.

Chapman B. M., Jones D. R. & Jung R. (1983). Processes controlling metal ion attenuation in acid mine drainage streams. *Geochimica et cosmochimica acta*, 47(11), 1957-1973.

Clemens S., Palmgren M. G. & Krämer U. (2002). A long way ahead: understanding and engineering plant metal accumulation. *Trends in plant science*, 7(7), 309-315.

Clemens S. (2006). Toxic metal accumulation, responses to exposure and mechanisms of tolerance in plants. *Biochimie*, 88(11), 1707-1719.

Colmer T. D., Munns R., & Flowers T. J. (2006). Improving salt tolerance of wheat and barley: future prospects. *Australian journal of experimental agriculture*, 45(11), 1425-1443.

Dakora F. D. & Phillips D. A. (2002). Root exudates as mediators of mineral acquisition in low-nutrient environments. In *Food Security in Nutrient-Stressed Environments: Exploiting Plants' Genetic Capabilities* (pp. 201-213). Springer, Dordrecht.

Demidchik V. & Tester M. (2002). Sodium fluxes through nonselective cation channels in the plasma membrane of protoplasts from Arabidopsis roots. *Plant physiology*, *128*(2), 379-387.

Dennis A.M (2008) Salt glands and elemental concentrations in leaves of *Tamarix usneoides* E.Mey ex Bunge (Tamaricaceae) grown on seepage from Highveld gold mines, unpublished Honours Project.

Ding F., Yang J. C., Yuan F. & Wang B. S. (2010) Progress in mechanism of salt excretion in recretohalopytes. *Frontiers in biology*, 5(2), 164-170.

Dudev T. & Lim C. (2014). Ion selectivity strategies of sodium channel selectivity filters. *Accounts of chemical research*, *47*(12), 3580-3587.

Dunn C. E. (1986). Biogeochemistry as an aid to exploration for gold, platinum and palladium in the northern forests of Saskatchewan, Canada. *Journal of geochemical exploration*, *25*(1-2), 21-40.

Dye P.J., Jarmain C., Oageng B., Xaba J. & Weiersbye I.M. (2008) The potential of woodlands and reed-beds for control of acid mine drainage in the Witwatersrand Gold Fields, South Africa. In *Mine Closure 2008: Proceedings of the Third International Seminar on Mine Closure* (pp. 487-497).

Ebbs S. (2004) Biological degradation of cyanide compounds. *Current opinion in biotechnology*, 15(3), 231-236.

Farmer E. E., & Mueller M. J. (2013). ROS-mediated lipid peroxidation and RES-activated signaling. *Annual review of plant biology*, *64*, 429-450.

Finazzi G., Petroutsos D., Tomizioli M., Flori S., Sautron E., Villanova V., Rolland N. & Seigneurin-Berny D. (2015). Ions channels/transporters and chloroplast regulation. *Cell calcium*, 58(1),86-97.

Flowers T. J., & Colmer T. D. (2008). Salinity tolerance in halophytes. *New Phytologist*, 179(4), 945-963.

Flowers T. J., & Colmer T. D. (2015). Plant salt tolerance: adaptations in halophytes. *Annals of botany*, *115*(3), 327-331.

Flowers T. J., Troke P. F., & Yeo A. R. (1977). The mechanism of salt tolerance in halophytes. *Annual review of plant physiology*, *28*(1), 89-121.

Franco-Navarro J. D., Brumós J., Rosales M. A., Cubero-Font,P., Talón M., & Colmenero-Flores J. M. (2015). Chloride regulates leaf cell size and water relations in tobacco plants. *Journal of experimental botany*, *67*(3), 873-891.

Gao C., Wang Y., Jiang B., Liu G., Yu L., Wei Z., & Yang C. (2011). A novel vacuolar membrane H+-ATPase c subunit gene (ThVHAc1) from *Tamarix* hispida confers tolerance to several abiotic stresses *in Saccharomyces cerevisiae*. *Molecular biology reports*, *38*(2), 957-963.

Gardea-Torresdey J. L., Parsons J. G., Gomez E., Peralta-Videa J., Troiani H. E., Santiago P., & Yacaman M. J. (2002). Formation and growth of Au nanoparticles inside live alfalfa plants. *Nano letters*, *2*(4), 397-401.

Hedrich R., & Geiger D. (2017). Biology of SLAC1-type anion channels–from nutrient uptake to stomatal closure. *New phytologist*, *216*(1), 46-61.

Hider R. C., Liu Z. D., & Khodr,H. H. (2001). Metal chelation of polyphenols. In *Methods in enzymology* (Vol. 335, pp. 190-203). Academic Press.

Iram F., Iqbal M. S., Athar M. M., Saeed M. Z., Yasmeen A., & Ahmad R. (2014). Glucoxylan-mediated green synthesis of gold and silver nanoparticles and their phyto-toxicity study. *Carbohydrate polymers*, *104*, 29-33.

Kehrer J. P. (2000). The Haber–Weiss reaction and mechanisms of toxicity. *Toxicology*, *149*(1), 43-50.

Krämer U., Talke I. N., & Hanikenne M. (2007). Transition metal transport. *FEBS letters*, 581(12), 2263-2272.

Kronsukker H.J., & Britto D.T., (2011). Sodium transport in plants: a critical review, *New phytologist,* 189,54–81.

Lengke M. F., Ravel B., Fleet M. E., Wange G., Gordon, R. A., & Southam G. (2006). Mechanisms of gold bioaccumulation by filamentous cyanobacteria from gold (III)− chloride complex. *Environmental science & technology*, *40*(20), 6304-6309.

Leuschner C. (2002). Air humidity as an ecological factor for woodland herbs: leaf water status, nutrient uptake, leaf anatomy, and productivity of eight species grown at low or high vpd levels. Flora-Morphology, Distribution, *Functional Ecology of Plants*, 197(4), 262-274.

Lintern M., Anand R., Ryan C. & Paterson D. (2013) Natural gold particles in Eucalyptus leaves and their relevance to exploration for buried gold deposits, *Nature communications*, 4, 2274.

Ma X. L., Zhang Q., Shi H. Z., Zhu J. K., Zhao Y. X., Ma C. L. & Zhang H. (2004). Molecular cloning and different expression of a vacuolar Na+/H+ antiporter gene in *Suaeda salsa* under salt stress. *Biologia plantarum*, *48*(2), 219-225.

Maathuis F. J., & Amtmann A. N. N. A. (1999). K^+ nutrition and Na^+ toxicity: the basis of cellular K^+/Na^+ ratios. *Annals of botany*, 84(2), 123-133.

Manousaki E., & Kalogerakis N. (2010). Halophytes present new opportunities in phytoremediation of heavy metals and saline soils. *Industrial & engineering chemistry research*, 50(2), 656-660.

McGrath S.P. & Zhao F.J., 2003. Phytoextraction of metals and metalloids from contaminated soils. *Current opinion in biotechnology*, 14(3), pp.277-282.

Mendoza-Cózatl D. G., Jobe T. O., Hauser F., & Schroeder J. I. (2011). Long-distance transport, vacuolar sequestration, tolerance, and transcriptional responses induced by cadmium and arsenic. *Current opinion in plant biology*, 14(5), 554-562.

Michalak, A. (2006). Phenolic compounds and their antioxidant activity in plants growing under heavy metal stress. *Polish Journal of Environmental Studies*, 15(4).

Pineros M. A., Cançado G. M., & Kochian L. V. (2008). Novel properties of the wheat aluminum tolerance organic acid transporter (TaALMT1) revealed by electrophysiological characterization in *Xenopus* oocytes: functional and structural implications. *Plant physiology*, *147*(4), 2131-2146.

Pilon-Smits E. (2005), Phytoremediation, *Annual Review of Plant Biology*, 56, 15–39.

Reid N., Hill S. M., & Lewis D. M. (2008). *Spinifex* biogeochemical expressions of buried gold mineralisation: the great mineral exploration penetrator of transported regolith. *Applied geochemistry*, *23*(1), 76-84.

Salt D. E., Blaylock M., Kumar N. P., Dushenkov V., Ensley B. D., Chet I., & Raskin I. (1995). Phytoremediation: a novel strategy for the removal of toxic metals from the environment using plants. *Nature biotechnology*, 13(5), 468.

Shabala S., & Mackay A. (2011). Ion transport in halophytes. In *Advances in botanical research* (Vol. 57, pp. 151-199). Academic Press.

Sharma S. S., & Dietz K. J. (2009). The relationship between metal toxicity and cellular redox imbalance. *Trends in plant science*, *14*(1), 43-50.

Sheoran V., Sheoran A. S., & Poonia P. (2013). Phytomining of gold: a review. *Journal of geochemical exploration*, *128*, 42-50.

Sobrino-Plata J., Herrero J., Carrasco-Gil S., Pérez-Sanz A., Lobo C., Escobar C., Millán R. & Hernández L.E. (2013). Specific stress responses to cadmium, arsenic and mercury appear in the metallophyte *Silene vulgaris* when grown hydroponically. *RSC Advances*, 3(14), pp.4736-4744.

Southam G., Lengke M. F., Fairbrother L., & Reith F. (2009). The biogeochemistry of gold. *Elements*, *5*(5), 303-307.

Tester M. & Davenport R. (2003). Na^+ tolerance and Na^+ transport in higher plants. *Annals of botany*, *91*(5), 503-527.

Toma H. E., Zamarion V. M., Toma S. H. & Araki K. (2010). The coordination chemistry at gold nanoparticles. *Journal of the brazilian chemical society*, 21(7), 1158-1176.

Tutu H., Cukrowska E. M., Dohnal V., & Havel J. (2005). Application of artificial neural networks for classification of uranium distribution in the Central Rand goldfield, South Africa. *Environmental modeling & assessment*, 10(2), 143-152.

Tutu H., McCarthy T. S., & Cukrowska E. (2008). The chemical characteristics of acid mine drainage with particular reference to sources, distribution and remediation: The

Witwatersrand Basin, South Africa as a case study. *Applied geochemistry*, 23(12), 3666-3684.

Van Oosten M. J., & Maggio A. (2015). Functional biology of halophytes in the phytoremediation of heavy metal contaminated soils. *Environmental and experimental botany*, *111*, 135-146.

Vlassopoulos D. & Wood S. A. (1990). Gold speciation in natural waters: I. Solubility and hydrolysis reactions of gold in aqueous solution. *Geochimica et cosmochimica Acta*, 54(1), 3-12.

Vorster B. J.n & Flatman S. R., 2001. Cyanide control in the metallurgical process of gold extraction in AngloGold (SA). *Journal of the south african institute of mining and etallurgy* (South Africa), 101(7), 359-365.

Wakeel A., Farooq M., Qadir M. & Schubert S. (2011). Potassium substitution by sodium in plants. *Critical reviews in plant sciences*, 30(4), 401-413.

Wang H., Yan Y., Liu Q., Huang Y., Shen Y., Chen L. & Chai J. (2007). Structural basis for modulation of Kv4 K^+ channels by auxiliary KChIP subunits. *Nature neuroscience*, *10*(1), 32.

Watson A. (1985). Structure, chemistry and origins of gypsum crusts in southern Tunisia and the central Namib Desert. *Sedimentology*, 32(6), 855-875.

Wendelberger K. S., & Richards J. H. (2017). Halophytes can salinize soil when competing with glycophytes, intensifying effects of sea level rise in coastal communities. *Oecologia*, *184*(3), 729-737.

White P. J., & Broadley M. R. (2003). Calcium in plants. *Annals of botany*, 92(4), 487-511.

Yadav S. K. (2010). Heavy metals toxicity in plants: an overview on the role of glutathione and phytochelatins in heavy metal stress tolerance of plants. *South African journal of botany*, *76*(2), 167-179.

Yang X., Feng Y., He Z., & Stoffella P. J. (2005). Molecular mechanisms of heavy metal hyperaccumulation and phytoremediation. *Journal of trace elements in medicine and biology*, 18(4), 339-353.

Zhu Z.J., Wang H., Yan B., Zheng H., Jiang Y., Miranda O.R., Rotello V.M., Xing B. & Vachet R.W., (2012). Effect of surface charge on the uptake and distribution of gold nanoparticles in four plant species. *Environmental science & technology*, *46*(22), pp.12391-12398.

Appendices

Appendix A – Supplementary data for chapter 3

Table 13: Murashige and Skoog Basal growth media constituents modified to include gold potassium cyanide, gold chloride and gold thiosulphate at a concentration of 50mg/kg gold

Ions	Basal M&S (mmol/l)	Modified M&S (Gold(I) potassium Cyanide) (mmol/l)	Modified M&S (Gold(III) chloride trihydrate) (mmol/l)	Modified M&S (Gold Thiosulphate) (mmol/l)
(NO3)-	39.40428162	39.40428162	39.40428162	39.40428162
(NH4)+	20.61160246	20.61160246	20.61160246	20.61160246
Ca2+	2.99291224	2.99291224	2.99291224	2.99291224
Cl-	5.986034625	5.986034625	**6.239880388**	5.986034625
Mg2+	1.5011969	1.5011969	1.5011969	1.5011969
(SO4)2-	1.73115758	1.73115758	1.73115758	1.73115758
K+	20.04688914	**20.3007349**	20.04688914	20.04688914
H2(PO4)-	1.249210058	1.249210058	1.249210058	1.249210058
(B)3+	0.100274947	0.100274947	0.100274947	0.100274947
OH-	0.300824842	0.300824842	0.300824842	0.300824842
(Co)2+	0.000105073	0.000105073	0.000105073	0.000105073
(Cu)2+	0.00010012	0.00010012	0.00010012	0.00010012
(Fe)2+	0.099982018	0.099982018	0.099982018	0.099982018
(Mn)2+	0.09996862	0.09996862	0.09996862	0.09996862
I-	0.004999916	0.004999916	0.004999916	0.004999916
Na+	0.201937594	0.201937594	0.201937594	**0.455783357**
(MoO4)2-	0.001033271	0.001033271	0.001033271	0.001033271
(Zn)2+	0.029909922	0.029909922	0.029909922	0.029909922
(EDTA)2-	0.099935525	0.099935525	0.099935525	0.099935525
Au		**0.253845763**	**0.253845763**	**0.253845763**
$(CN)_2$		**0.253845763**		
H+			**0.253845763**	
S2O3				**0.253845763**

Table 14: % gold recovery from CRM and sample material spiked with gold at set concentrations.

CRM Digestion spike recovery		**Sample spike recovery**			
~ 0.1g Peach leaves CRM spiked with Au before digestion		~ 0.1g sample spiked with Au before digestion			
CRM + 14ppb Au	**CRM + 140ppb Au**	**HW 37 + 4.85 ppb Au**	**HW 25 + 24.25 ppb Au**	**CRM + 48.5 ppb Au**	**HW 13 + 86 ppb Au**
% Recovery	% Recovery	% Recovery	% Recovery	% Recovery	% Recovery
112.34	115.94	72.71	89.62	81.74	70.34

Table 15: Normality test values for root and shoot tissue Au concentration for *T. usneoides* plantlets grown *in vitro*

Tissue	Variable	Shapiro-Wilk normality test	p-value
Root	Tiss_conc	0.58153	< 2.2e-16
Shoot	Tiss_conc	0.65774	< 2.2e-16
Root	Tiss_bioconc	0.89287	2.91E-09
Shoot	Tiss_bioconc	0.77695	1.27E-14

Table 16: Kruskall Wallis tests for Tissue Concentration, Gold Percentage recovery and bioconcentration per Tissue type for *T. usneoides* plantlets grown *in vitro* and spikes with 3 different gold compounds

Tissue	Test	chi-squared	df	p-value
Root	Tis_conc by pH	0.18166	2	0.9132
Root	Rec by pH	3.8431	2	0.1464
Root	Bioconc by pH	1.0613	2	0.5882
Shoot	Tis_conc by pH	2.0491	2	0.3589
Shoot	Rec by pH	4.1803	2	0.1237
Shoot	Bioconc by pH	0.25307	2	0.8811
Shoot	Trans by pH	1.0356	2	0.5958
Root	Tis_conc by as.factor(Au_Comp)	28.171	3	3.34E-06
Root	Rec by as.factor(Au_Comp)	34.371	3	1.65E-07
Root	Bioconc by as.factor(Au_Comp)	33.386	3	2.67E-07
Shoot	Tis_conc by as.factor(Au_Comp)	26.673	3	6.90E-06
Shoot	Rec by as.factor(Au_Comp)	34.919	3	1.27E-07
Shoot	Bioconc by as.factor(Au_Comp)	38.205	3	2.56E-08
Shoot	Trans by as.factor(Au_Comp)	46.713	3	4.00E-10
Root	Tis_conc by Au_Conc	126.21	4	< 2.2e-16
Root	Rec by Au_Conc	41.003	4	2.68E-08
Root	Bioconc by Au_Conc	43.857	4	6.87E-09
Shoot	Tis_conc by Au_Conc	132.86	4	< 2.2e-16
Shoot	Rec by Au_Conc	65.247	4	2.28E-13
Shoot	Bioconc by Au_Conc	63.635	4	4.99E-13
Shoot	Trans by Au_Conc	27.13	4	1.87E-05

Table 17: Kruskall wallis test results for tissue gold concentration, bioconcentration and gold recovery by tissue type and treatment concentration for *T. usneoides* plantlets grown *in vitro* in a media solution spiked with additional gold compounds

Dataset	Test	chi-squared	df	p-value
Root_05mg/kg	Tis_conc by as.factor(Au_Comp)	0.12208	2	0.9408
Root_05mg/kg	Rec by as.factor(Au_Comp)	1.2241	2	0.5422
Root_05mg/kg	Bioconc by as.factor(Au_Comp)	0.12208	2	0.9408
Root_5mg/kg	Tis_conc by as.factor(Au_Comp)	0.10236	2	0.9501
Root_5mg/kg	Rec by as.factor(Au_Comp)	9.6822	2	0.007898
Root_5mg/kg	Bioconc by as.factor(Au_Comp)	0.10236	2	0.9501
Root_25mg/kg	Tis_conc by as.factor(Au_Comp)	6.9825	2	0.03046
Root_25mg/kg	Rec by as.factor(Au_Comp)	11.415	2	0.003321
Root_25mg/kg	Bioconc by as.factor(Au_Comp)	6.9825	2	0.03046
Root_50mg/kg	Tis_conc by as.factor(Au_Comp)	12.196	2	0.002248
Root_50mg/kg	Rec by as.factor(Au_Comp)	10.152	2	0.006243
Root_50mg/kg	Bioconc by as.factor(Au_Comp)	12.196	2	0.002248
Shoot_05mg/kg	Tis_conc by as.factor(Au_Comp)	2.2524	2	0.3243
Shoot_05mg/kg	Rec by as.factor(Au_Comp)	0.67111	2	0.7149
Shoot_05mg/kg	Bioconc by as.factor(Au_Comp)	2.2524	2	0.3243
Shoot_5mg/kg	Tis_conc by as.factor(Au_Comp)	6.7139	2	0.03484
Shoot_5mg/kg	Rec by as.factor(Au_Comp)	8.793	2	0.01232
Shoot_5mg/kg	Bioconc by as.factor(Au_Comp)	6.7139	2	0.03484
Shoot_25mg/kg	Tis_conc by as.factor(Au_Comp)	1.2749	2	0.5287
Shoot_25mg/kg	Rec by as.factor(Au_Comp)	2.4327	2	0.2963
Shoot_25mg/kg	Bioconc by as.factor(Au_Comp)	1.2749	2	0.5287
Shoot_50mg/kg	Tis_conc by as.factor(Au_Comp)	18.17	2	0.0001134
Shoot_50mg/kg	Rec by as.factor(Au_Comp)	10.651	2	0.004865
Shoot_50mg/kg	Bioconc by as.factor(Au_Comp)	18.17	2	0.0001134
Shoot_05mg/kg	Trans ~ as.factor(Au_Comp)	1.3867	2	0.4999
Shoot_5mg/kg	Trans ~ as.factor(Au_Comp)	4.8037	2	0.09055
Shoot_25mg/kg	Trans ~ as.factor(Au_Comp)	9.2749	2	0.009683
Shoot_50mg/kg	Trans ~ as.factor(Au_Comp)	27.195	2	1.24E-06

Table 18: Root Tissue Au Concentration (mg/kg) by pH, Gold Compound and Media gold Concentration

pH	Au_comp	mg/kg	n	mean	sd	min	Q1	median	Q3	max
4.6	AuCl	50	3	13035	9657	2782	8574	14365	18162	21959
5.6	AuCl	50	6	12683	9838	1608	5154	11383	21796	23382
4.6	AuS2O3	50	3	8761	2471	6052	7697	9341	10116	10891
5.6	AuCl	25	3	8222	5931	1953	5462	8970	11357	13744
7.6	AuCl	25	3	9036	6561	3370	5442	7515	11869	16224
7.6	AuCl	50	6	10698	9846	2865	3647	6544	15174	27501
5.6	AuS2O3	50	5	4319	2081	814	4294	4860	5437	6190
7.6	AuS2O3	50	6	4065	4467	1480	1838	2508	3017	13093
4.6	AuCN	5	3	2232	1114	1100	1685	2269	2798	3327
4.6	AuCN	50	2	2233	1963	845	1539	2233	2927	3621
5.6	AuCN	50	6	2318	1450	1011	1082	2128	3111	4467
7.6	AuCN	50	6	3135	2377	1247	1528	2085	4164	7197
5.6	AuS2O3	25	3	2936	2839	649	1347	2045	4080	6115
7.6	AuCN	25	3	2524	1589	1436	1613	1789	3068	4347
4.6	AuCl	5	2	1709	1845	404	1057	1709	2361	3014
7.6	AuS2O3	25	3	1394	576	927	1073	1218	1628	2038
5.6	AuCN	25	3	3076	3409	1049	1108	1167	4089	7012
4.6	AuS2O3	5	3	1622	1046	959	1019	1080	1954	2828
5.6	AuCl	5	5	940	639	321	629	776	975	2000
7.6	AuCN	5	6	1033	731	476	527	724	1288	2336
7.6	AuS2O3	5	6	624	324	217	346	707	880	948
5.6	AuS2O3	5	5	889	717	431	484	645	730	2154
7.6	AuCl	5	6	1876	2476	387	543	639	1941	6706
5.6	AuCN	5	7	570	305	160	456	505	628	1160
4.6	AuCN	0.5	3	211	110	88	168	248	273	298
5.6	AuS2O3	0.5	6	173	150	8	60	142	305	356
7.6	AuS2O3	0.5	6	145	106	38	72	138	165	333
7.6	AuCl	0.5	6	148	105	64	85	120	149	351
5.6	AuCl	0.5	5	121	52	53	93	113	167	177
7.6	AuCN	0.5	6	101	50	38	84	90	109	189
5.6	AuCN	0.5	6	114	70	54	62	86	155	225
4.6	AuCl	0.5	3	68	44	27	45	63	89	115
4.6	AuS2O3	0.5	3	54	40	13	34	55	74	93
7.6	None	0	3	3	3	1	2	3	4	6
5.6	None	0	3	4	5	1	1	1	6	11
4.6	None	0	3	1	1	1	1	1	2	2

Table 19: Root Tissue Au Recovery % by pH, Gold Compound and Media gold Concentration

pH	Au_comp	mg/kg	n	mean	sd	min	Q1	median	Q3	max
4.6	AuCl	0.5	3	20	5	15	18	22	23	24
4.6	AuCl	50	3	31	18	14	21	28	39	51
4.6	AuCl	5	2	37	28	18	28	37	47	57
4.6	AuCN	0.5	3	63	6	57	59	62	66	69
4.6	AuCN	50	2	5	5	2	3	5	7	8
4.6	AuCN	5	3	40	20	22	30	37	49	62
4.6	AuS2O3	0.5	3	18	18	4	8	12	25	39
4.6	AuS2O3	50	3	34	24	20	21	21	41	62
4.6	AuS2O3	5	3	41	51	5	12	19	59	99
4.6	None	0	3	0	0	0	0	0	0	0
5.6	AuCl	0.5	5	24	7	14	19	27	29	30
5.6	AuCl	25	3	34	14	19	29	38	42	45
5.6	AuCl	50	6	27	15	8	14	30	39	42
5.6	AuCl	5	5	20	6	13	14	22	22	28
5.6	AuCN	0.5	6	30	8	22	25	27	36	39
5.6	AuCN	25	3	7	7	3	3	3	9	15
5.6	AuCN	50	6	14	16	2	3	5	26	35
5.6	AuCN	5	7	34	24	4	21	35	42	74
5.6	AuS2O3	0.5	6	35	23	19	21	26	39	80
5.6	AuS2O3	25	3	7	6	3	4	5	9	13
5.6	AuS2O3	50	5	11	11	1	4	5	19	26
5.6	AuS2O3	5	5	14	6	8	11	13	16	23
5.6	None	0	3	0	0	0	0	0	0	0
7.6	AuCl	0.5	6	30	15	17	18	25	35	57
7.6	AuCl	25	3	24	1	23	23	24	25	26
7.6	AuCl	50	6	22	11	10	14	24	29	36
7.6	AuCl	5	6	20	8	9	19	21	21	33
7.6	AuCN	0.5	6	20	11	12	14	15	27	37
7.6	AuCN	25	3	5	1	4	4	5	5	5
7.6	AuCN	50	6	10	12	2	3	5	12	33
7.6	AuCN	5	6	25	14	10	20	23	24	52
7.6	AuS2O3	0.5	6	23	9	11	17	20	29	35
7.6	AuS2O3	25	3	5	1	3	4	5	5	6
7.6	AuS2O3	50	6	15	24	3	4	5	10	63
7.6	AuS2O3	5	6	9	7	3	5	9	10	23
7.6	None	0	3	0	0	0	0	0	0	0

Table 20: Root Tissue Au Bioconcentration factor by pH, Gold Compound and Media gold Concentration

pH	Au_comp	mg/kg	n	mean	sd	min	Q1	median	Q3	max
4.6	AuCl	0.5	3	13651	8773	5451	9026	12600	17751	22902
4.6	AuCl	50	3	26071	19315	5564	17147	28730	36324	43918
4.6	AuCl	5	2	34182	36900	8090	21136	34182	47228	60275
4.6	AuCN	0.5	3	42281	21982	17574	33586	49597	54634	59671
4.6	AuCN	50	2	4465	3926	1689	3077	4465	5853	7241
4.6	AuCN	5	3	44640	22278	21997	33693	45389	55961	66533
4.6	AuS2O3	0.5	3	10711	7943	2660	6796	10932	14736	18541
4.6	AuS2O3	50	3	17523	4941	12105	15393	18682	20232	21781
4.6	AuS2O3	5	3	32447	20924	19176	20387	21597	39082	56567
4.6	None	0	3	0	0	0	0	0	0	0
5.6	AuCl	0.5	5	24154	10358	10627	18648	22614	33468	35410
5.6	AuCl	25	3	32890	23723	7813	21847	35880	45428	54975
5.6	AuCl	50	6	25367	19676	3215	10309	22765	43592	46765
5.6	AuCl	5	5	18803	12773	6412	12585	15521	19500	39995
5.6	AuCN	0.5	6	22727	14053	10703	12368	17183	30940	45003
5.6	AuCN	25	3	12303	13637	4196	4431	4666	16357	28048
5.6	AuCN	50	6	4635	2900	2023	2164	4256	6221	8933
5.6	AuCN	5	7	11406	6108	3204	9115	10103	12558	23191
5.6	AuS2O3	0.5	6	34672	29913	1605	11989	28385	61006	71256
5.6	AuS2O3	25	3	11746	11358	2598	5389	8181	16320	24458
5.6	AuS2O3	50	5	8638	4162	1628	8588	9720	10873	12380
5.6	AuS2O3	5	5	17779	14343	8627	9683	12905	14606	43072
5.6	None	0	3	0	0	0	0	0	0	0
7.6	AuCl	0.5	6	29621	21048	12860	17037	24099	29795	70293
7.6	AuCl	25	3	36146	26243	13482	21770	30058	47478	64897
7.6	AuCl	50	6	21395	19692	5730	7295	13089	30347	55001
7.6	AuCl	5	6	37521	49524	7745	10850	12779	38818	134117
7.6	AuCN	0.5	6	20121	9967	7695	16735	17908	21798	37774
7.6	AuCN	25	3	10096	6355	5745	6450	7156	12272	17389
7.6	AuCN	50	6	6271	4754	2494	3056	4170	8328	14393
7.6	AuCN	5	6	20662	14614	9525	10543	14489	25763	46720
7.6	AuS2O3	0.5	6	29016	21231	7580	14313	27631	32994	66597
7.6	AuS2O3	25	3	5578	2303	3709	4291	4873	6512	8151
7.6	AuS2O3	50	6	8130	8933	2960	3675	5016	6035	26185
7.6	AuS2O3	5	6	12475	6482	4345	6926	14140	17600	18952
7.6	None	0	3	0	0	0	0	0	0	0

Table 21: Shoot Tissue Au Concentration (mg/kg) by pH, Gold Compound and Media gold Concentration

pH	Au_comp	mg/kg	n	mean	sd	min	Q1	median	Q3	max
4.6	AuCl	0.5	3	2	0	2	2	2	2	3
4.6	AuCl	50	3	120	65	48	93	137	156	175
4.6	AuCl	5	2	12	1	12	12	12	12	13
4.6	AuCN	0.5	3	3	0	3	3	3	3	4
4.6	AuCN	50	2	207	150	101	154	207	260	314
4.6	AuCN	5	3	28	15	12	21	31	37	42
4.6	AuS2O3	0.5	3	5	1	4	4	5	5	5
4.6	AuS2O3	50	3	202	254	28	56	84	289	493
4.6	AuS2O3	5	3	33	35	12	13	14	44	74
4.6	None	0	3	0	0	0	0	0	0	0
5.6	AuCl	0.5	5	4	1	3	4	4	5	6
5.6	AuCl	25	3	122	91	48	71	95	159	223
5.6	AuCl	50	6	88	78	9	30	73	122	216
5.6	AuCl	5	5	15	5	8	12	17	18	20
5.6	AuCN	0.5	6	4	3	2	2	3	4	9
5.6	AuCN	25	3	134	49	92	107	122	155	188
5.6	AuCN	50	6	275	185	149	159	212	279	635
5.6	AuCN	5	7	29	20	8	14	20	44	60
5.6	AuS2O3	0.5	6	5	3	1	3	4	6	10
5.6	AuS2O3	25	3	114	78	42	73	104	151	197
5.6	AuS2O3	50	5	111	57	29	95	110	136	185
5.6	AuS2O3	5	5	20	5	12	18	21	24	25
5.6	None	0	3	0	0	0	0	0	0	1
7.6	AuCl	0.5	6	4	2	2	3	3	4	7
7.6	AuCl	25	3	143	140	32	65	98	199	301
7.6	AuCl	50	6	96	24	59	83	102	115	119
7.6	AuCl	5	6	16	7	8	10	18	22	24
7.6	AuCN	0.5	6	5	4	2	2	3	8	10
7.6	AuCN	25	3	166	11	156	160	165	171	178
7.6	AuCN	50	6	337	159	124	223	366	422	551
7.6	AuCN	5	6	38	23	14	23	33	43	79
7.6	AuS2O3	0.5	6	4	2	3	3	3	5	9
7.6	AuS2O3	25	3	102	40	57	86	114	125	135
7.6	AuS2O3	50	6	62	21	43	47	59	66	100
7.6	AuS2O3	5	6	19	15	9	10	14	20	47
7.6	None	0	3	1	1	0	1	1	2	3

Table 22: Shoot Tissue Au Recovery % by pH, Gold Compound and Media gold Concentration

pH	Au_comp	mg/kg	n	mean	sd	min	Q1	median	Q3	max
4.6	AuCl	0.5	3	6	3	4	4	5	7	9
4.6	AuCl	50	3	3	1	2	3	3	3	3
4.6	AuCl	5	2	2	0	2	2	2	2	3
4.6	AuCN	0.5	3	11	7	5	7	10	14	18
4.6	AuCN	50	2	2	0	1	2	2	2	2
4.6	AuCN	5	3	6	2	4	4	5	6	8
4.6	AuS2O3	0.5	3	10	2	8	9	9	11	13
4.6	AuS2O3	50	3	5	6	1	1	2	7	12
4.6	AuS2O3	5	3	3	3	0	2	3	4	6
4.6	None	0	3	0	0	0	0	0	0	0
5.6	AuCl	0.5	5	14	4	9	11	13	17	19
5.6	AuCl	25	3	7	5	2	5	9	10	11
5.6	AuCl	50	6	3	2	0	1	3	3	6
5.6	AuCl	5	5	4	2	2	3	3	5	8
5.6	AuCN	0.5	6	11	7	6	6	7	15	23
5.6	AuCN	25	3	7	1	6	7	8	8	8
5.6	AuCN	50	6	7	3	5	6	7	8	13
5.6	AuCN	5	7	8	4	3	5	6	10	15
5.6	AuS2O3	0.5	6	17	13	3	8	13	21	40
5.6	AuS2O3	25	3	7	6	2	3	5	9	14
5.6	AuS2O3	50	5	3	2	1	2	3	3	7
5.6	AuS2O3	5	5	8	7	2	4	4	8	19
5.6	None	0	3	0	0	0	0	0	0	0
7.6	AuCl	0.5	6	9	6	0	6	8	14	17
7.6	AuCl	25	3	8	6	2	5	8	11	15
7.6	AuCl	50	6	3	1	1	2	3	4	5
7.6	AuCl	5	6	5	4	2	3	4	8	11
7.6	AuCN	0.5	6	12	9	5	7	10	12	29
7.6	AuCN	25	3	9	2	7	9	10	11	11
7.6	AuCN	50	6	7	3	1	6	6	9	11
7.6	AuCN	5	6	8	1	6	7	8	8	10
7.6	AuS2O3	0.5	6	14	11	5	8	9	14	34
7.6	AuS2O3	25	3	4	1	3	3	3	4	5
7.6	AuS2O3	50	6	2	1	1	1	2	2	2
7.6	AuS2O3	5	6	4	2	3	3	4	4	7
7.6	None	0	3	0	0	0	0	0	0	0

Table 23: Shoot Tissue Au Bioconcentration factor by pH, Gold Compound and Media gold Concentration

pH	Au_comp	mg/kg	n	mean	sd	min	Q1	median	Q3	max
4.6	AuCl	0.5	3	440	79	360	402	444	481	518
4.6	AuCl	50	3	241	130	97	186	275	312	350
4.6	AuCl	5	2	243	14	234	238	243	248	253
4.6	AuCN	0.5	3	657	88	574	610	646	698	750
4.6	AuCN	50	2	415	300	202	309	415	521	627
4.6	AuCN	5	3	567	307	236	430	623	733	842
4.6	AuS2O3	0.5	3	943	161	760	886	1012	1035	1059
4.6	AuS2O3	50	3	404	508	56	112	168	578	987
4.6	AuS2O3	5	3	665	708	235	257	278	880	1483
4.6	None	0	3	0	0	0	0	0	0	0
5.6	AuCl	0.5	5	894	256	682	703	800	988	1298
5.6	AuCl	25	3	488	363	193	285	378	635	893
5.6	AuCl	50	6	175	156	19	60	146	243	433
5.6	AuCl	5	5	305	100	161	246	342	366	407
5.6	AuCN	0.5	6	760	503	395	467	630	716	1751
5.6	AuCN	25	3	536	196	369	428	487	619	751
5.6	AuCN	50	6	550	370	298	318	424	557	1269
5.6	AuCN	5	7	582	399	159	283	409	872	1195
5.6	AuS2O3	0.5	6	941	612	152	686	780	1216	1917
5.6	AuS2O3	25	3	458	313	167	292	417	603	789
5.6	AuS2O3	50	5	222	115	57	190	220	272	371
5.6	AuS2O3	5	5	400	106	240	353	427	484	498
5.6	None	0	3	0	0	0	0	0	0	0
7.6	AuCl	0.5	6	755	374	348	612	641	801	1446
7.6	AuCl	25	3	574	562	127	259	391	797	1204
7.6	AuCl	50	6	192	47	119	166	203	229	238
7.6	AuCl	5	6	325	142	158	197	351	436	483
7.6	AuCN	0.5	6	977	710	393	476	625	1501	2000
7.6	AuCN	25	3	665	45	623	642	660	686	712
7.6	AuCN	50	6	674	317	249	446	732	844	1101
7.6	AuCN	5	6	751	462	287	466	653	860	1578
7.6	AuS2O3	0.5	6	863	476	533	570	658	924	1772
7.6	AuS2O3	25	3	409	161	229	343	458	499	540
7.6	AuS2O3	50	6	125	42	87	95	119	132	201
7.6	AuS2O3	5	6	383	291	185	199	276	400	948
7.6	None	0	3	0	0	0	0	0	0	0

Table 24: Shoot Tissue Au Translocation Factor by pH, Gold Compound and Media gold Concentration

pH	Au_comp	mg/kg	n	mean	sd	min	Q1	median	Q3	max
4.6	AuCl	0.5	3	4	3	2	3	3	5	8
4.6	AuCl	50	3	2	3	0	1	1	3	5
4.6	AuCl	5	2	2	2	0	1	2	2	3
4.6	AuCN	0.5	3	2	1	1	1	2	3	4
4.6	AuCN	50	2	20	24	3	11	20	29	37
4.6	AuCN	5	3	2	2	1	1	1	2	4
4.6	AuS2O3	0.5	3	17	19	5	6	7	23	40
4.6	AuS2O3	50	3	2	3	0	1	1	3	5
4.6	AuS2O3	5	3	2	1	1	1	1	2	3
4.6	None	0	3	27	6	21	25	30	31	32
5.6	AuCl	0.5	5	4	1	3	4	4	4	7
5.6	AuCl	25	3	2	1	1	2	2	2	2
5.6	AuCl	50	6	1	1	0	1	1	1	2
5.6	AuCl	5	5	2	2	0	2	2	3	5
5.6	AuCN	0.5	6	4	2	1	3	4	5	6
5.6	AuCN	25	3	7	4	3	6	9	10	10
5.6	AuCN	50	6	14	8	5	10	14	15	28
5.6	AuCN	5	7	5	3	2	4	5	6	10
5.6	AuS2O3	0.5	6	5	3	1	3	4	7	10
5.6	AuS2O3	25	3	5	2	3	4	5	6	6
5.6	AuS2O3	50	5	3	1	2	2	3	3	4
5.6	AuS2O3	5	5	3	2	1	3	4	4	5
5.6	None	0	3	16	9	6	13	20	21	22
7.6	AuCl	0.5	6	4	2	0	2	4	5	7
7.6	AuCl	25	3	2	2	0	2	3	3	4
7.6	AuCl	50	6	2	1	0	1	1	3	3
7.6	AuCl	5	6	2	2	0	1	2	3	5
7.6	AuCN	0.5	6	6	5	1	2	5	9	12
7.6	AuCN	25	3	8	4	4	7	10	10	11
7.6	AuCN	50	6	14	8	6	8	12	20	24
7.6	AuCN	5	6	4	2	2	3	3	5	8
7.6	AuS2O3	0.5	6	5	3	1	2	5	6	10
7.6	AuS2O3	25	3	7	2	6	6	7	8	9
7.6	AuS2O3	50	6	3	2	0	1	3	4	5
7.6	AuS2O3	5	6	5	7	1	2	2	4	20
7.6	None	0	3	38	7	30	35	41	42	43

Appendix B – Supplementary data for chapter 4

Table 25: Percentage recovery for selected elements from tailings certified reference material as analysed using the XEPOS XRF

Element	Na	Mg	P	S	Cl	K	Ca	Mn	Fe	Cu	Zn	Rb	Sr	Pb	Th	U
CRM_GSD1				55.	82.	92.	91.	89.	98.	97.	91.	95.		91.	87.	44.
2	12.7	49.6	60.8	2	9	6	5	8	9	2	9	3	100	5	7	8
CRM_GSD1				57.	82.	93.	92.	90.	96.	98.	92.	95.	96.	91.	83.	52.
2	12.9	49.7	63.1	7	0	1	0	0	4	2	6	3	3	7	5	5
CRM_GSD1				56.	83.	92.	91.	89.	98.	97.	92.	95.	96.	92.	84.	64.
2	12.7	49.5	61.0	6	6	0	5	5	6	0	2	2	7	0	9	1
CRM_GSD1				66.	92.	91.	90.	88.	95.	97.	92.	95.	96.	93.	75.	84.
2	12.3	51.0	61.8	1	8	5	9	7	9	6	0	2	7	0	0	6

Table 26: Percentage recovery of selected elements from biomass certified reference material as analysed using the XEPOS XRF

CRM	Na	Mg	P	S	Cl	K	Ca	Mn	Fe	Cu	Zn	Rb	Sr	Pb	Th	U
	96.	67	85	75	90	76	77	63	62	64	77		87			
banana seed	4	.9	.2	.2	.2	.3	.9	.3	.6	.1	.4		.9	Below detection		
orchard			92	72	75	80	82	63	76	67	75	89	90		below	below
leaves 1571		77.0	.0	.6	.6	.2	.3	.3	.7	.6	.3	.8	.9	95.71	detection	detection
spinach	56	70.	80	72		80	73	64		70	82	80	83	below	below	below
leaves	.8	0	.5	.7		.6	.8	.3		.6	.8	.9	.1	detection	detection	detection
dandelion	51	81.	87	69	79	65	58	42	55	52	67	98	93			
roots	.0	7	.6	.4	.6	.1	.9	.7	.7	.1	.9	.4	.6	80.83		

Table 27: Summary Statistics for pH, EC and Eh for tailings samples collected from the control pits and sample pits from the Mponeng Tailings facility

	Sample	n	mean	sd	min	Q1	median	Q3	max	p-value
pH	control	12	3.600833	0.263075	3.35	3.395	3.475	3.7175	4.09	<0.0001
	tree	24	4.650417	0.800057	3.49	3.89	4.51	5.29	6.36	
Ec	control	12	1539.917	368.1997	1122	1185.5	1560	1750.25	2360	0.4666
	tree	24	1658.208	589.5318	926	1225.5	1396.5	1939.75	2820	
Eh	control	12	413.825	31.54665	351	397.9	421.45	432.575	455.9	0.145
	tree	24	398.2583	22.3156	352.5	387.5	400.5	413.775	440.6	

Table 28: Summary statistics for pH, EC and Eh at 6 different sampling depths from the sample pits located on the Mponeng tailings facility

	Sample	n	mean	sd	min	Q1	median	Q3	max	p-value
Ph	0-2cm	6	4.375	0.776859	3.4	3.83	4.29	5.065	5.27	
	2-10cm	6	4.346667	0.538838	3.49	4.1625	4.395	4.5525	5.11	
	10-20cm	6	4.545	0.909016	3.38	3.99	4.43	5.1325	5.82	0.4553
	20-30cm	6	4.708333	1.16534	3.35	3.8	4.65	5.455	6.36	
	50-60cm	6	3.66	0.186333	3.45	3.5025	3.675	3.7575	3.93	
	70-80cm	6	4.168333	0.976	3.38	3.525	3.65	4.93	5.49	
EC	0-2cm	6	1656.833	438.8222	1194	1313.5	1635.5	1841.25	2360	
	2-10cm	6	1792.667	661.6095	1147	1322	1570.5	2199.25	2820	
	10-20cm	6	1706	454.3791	1193	1372.5	1705	1874.75	2440	0.4111
	20-30cm	6	1963.667	710.6056	1051	1542.75	1815.5	2575	2820	
	50-60cm	6	1247.667	323.5346	926	1113	1152.5	1256.5	1864	
	70-80cm	6	1345.833	168.584	1163	1236	1326	1397.25	1633	
Eh	0-2cm	6	398.05	26.69065	352.5	393.125	399.3	409.6	433.1	
	2-10cm	6	405.1667	15.95101	381.5	399.75	403.15	412.625	428.8	
	10-20cm	6	393	33.50343	363.2	369.375	381.4	407.9	449.9	0.4608
	20-30cm	6	403.8833	34.74066	359.3	381.925	401.85	422.3	455.9	
	50-60cm	6	396.3167	26.56512	351	389.05	397.2	417.05	422.5	
	70-80cm	6	424.2667	10.72785	413.1	416.275	421.85	430.8	440.6	

Table 29: Summary statistics for elemental concentration (mg/kg) for tailings samples collected at different depths from control and sample pits on the mponeng tailings facility

Element	Location	Depth	n	mean	sd	min	Q1	medean	Q3	Max
Ca	Control	10-20cm	2	3858.5	532.4514	3482	3670.25	3858.5	4046.75	4235
Ca	Control	20-30cm	2	3911	114.5513	3830	3870.5	3911	3951.5	3992
Ca	Control	2-10cm	2	4003	691.5504	3514	3758.5	4003	4247.5	4492
Ca	Control	50-60cm	2	3760.5	188.7975	3627	3693.75	3760.5	3827.25	3894
Ca	Control	70-80cm	4	5119.25	876.3018	4154	4574	5076	5621.25	6171
Cl	Control	10-20cm	2	84.85	74.1755	32.4	58.625	84.85	111.075	137.3
Cl	Control	20-30cm	2	64.9	14.14214	54.9	59.9	64.9	69.9	74.9
Cl	Control	2-10cm	2	87.5	31.53696	65.2	76.35	87.5	98.65	109.8
Cl	Control	50-60cm	2	60.35	2.616295	58.5	59.425	60.35	61.275	62.2
Cl	Control	70-80cm	4	112.975	64.05817	20.5	94.975	135.45	153.45	160.5
Cu	Control	10-20cm	2	77.6	8.061017	71.9	74.75	77.6	80.45	83.3
Cu	Control	20-30cm	2	71.8	3.959798	69	70.4	71.8	73.2	74.6
Cu	Control	2-10cm	2	73.15	20.71823	58.5	65.825	73.15	80.475	87.8
Cu	Control	50-60cm	2	123.85	71.34707	73.4	98.625	123.85	149.075	174.3
Cu	Control	70-80cm	4	123.975	71.70083	53.7	68.4	120.2	175.775	201.8
Fe	Control	10-20cm	2	31260	2107.178	29770	30515	31260	32005	32750

Fe	Control	20-30cm	2	30890	890.9545	30260	30575	30890	31205	31520
Fe	Control	2-10cm	2	32945	2283.955	31330	32137.5	32945	33752.5	34560
Fe	Control	50-60cm	2	36525	4277.996	33500	35012.5	36525	38037.5	39550
Fe	Control	70-80cm	4	36170	6588.945	30080	32607.5	34590	38152.5	45420
K	Control	10-20cm	2	11185	558.6144	10790	10987.5	11185	11382.5	11580
K	Control	20-30cm	2	11650	127.2792	11560	11605	11650	11695	11740
K	Control	2-10cm	2	11860	523.259	11490	11675	11860	12045	12230
K	Control	50-60cm	2	12870	1583.919	11750	12310	12870	13430	13990
K	Control	70-80cm	4	13442.5	3158.959	10710	11767.5	12545	14220	17970
Mg	Control	10-20cm	2	13945	700.0357	13450	13697.5	13945	14192.5	14440
Mg	Control	20-30cm	2	13235	49.49747	13200	13217.5	13235	13252.5	13270
Mg	Control	2-10cm	2	15245	49.49747	15210	15227.5	15245	15262.5	15280
Mg	Control	50-60cm	2	15155	3118.341	12950	14052.5	15155	16257.5	17360
Mg	Control	70-80cm	4	16295	3893.092	12680	13145	16005	19155	20490
Mn	Control	10-20cm	2	335.25	19.02117	321.8	328.525	335.25	341.975	348.7
Mn	Control	20-30cm	2	339.15	20.29396	324.8	331.975	339.15	346.325	353.5
Mn	Control	2-10cm	2	383.7	22.76884	367.6	375.65	383.7	391.75	399.8
Mn	Control	50-60cm	2	379.35	34.57752	354.9	367.125	379.35	391.575	403.8
Mn	Control	70-80cm	4	447.75	98.74784	353	369.275	442.8	521.275	552.4
Na	Control	0-2cm	2	28465	4009.295	25630	27047.5	28465	29882.5	31300
Na	Control	10-20cm	2	27125	1096.016	26350	26737.5	27125	27512.5	27900
Na	Control	20-30cm	2	28015	1873.833	26690	27352.5	28015	28677.5	29340
Na	Control	2-10cm	2	28055	1718.269	26840	27447.5	28055	28662.5	29270
Na	Control	50-60cm	2	30485	3217.336	28210	29347.5	30485	31622.5	32760
Na	Control	70-80cm	2	27780	1329.361	26840	27310	27780	28250	28720
P	Control	10-20cm	2	456.2	51.6188	419.7	437.95	456.2	474.45	492.7
P	Control	20-30cm	2	460.2	29.69848	439.2	449.7	460.2	470.7	481.2
P	Control	2-10cm	2	554.4	65.47809	508.1	531.25	554.4	577.55	600.7
P	Control	50-60cm	2	470.45	180.5244	342.8	406.625	470.45	534.275	598.1
P	Control	70-80cm	4	725.75	386.4924	465.1	515.725	569.45	779.475	1299
Pb	Control	10-20cm	2	87.85	4.737615	84.5	86.175	87.85	89.525	91.2
Pb	Control	20-30cm	2	93.8	9.616652	87	90.4	93.8	97.2	100.6
Pb	Control	2-10cm	2	94.35	0.353553	94.1	94.225	94.35	94.475	94.6
Pb	Control	50-60cm	2	111.65	16.05132	100.3	105.975	111.65	117.325	123
Pb	Control	70-80cm	4	108.075	31.3382	87.7	92.65	94.9	110.325	154.8

Rb	Control	10-20cm	2	55.05	8.131728	49.3	52.175	55.05	57.925	60.8
Rb	Control	20-30cm	2	58.8	2.404163	57.1	57.95	58.8	59.65	60.5
Rb	Control	2-10cm	2	54.05	0.777818	53.5	53.775	54.05	54.325	54.6
Rb	Control	50-60cm	2	67.5	25.59727	49.4	58.45	67.5	76.55	85.6
Rb	Control	70-80cm	4	65.275	17.54107	46.6	57.7	62.8	70.375	88.9
S	Control	10-20cm	2	3803.5	2352.544	2140	2971.75	3803.5	4635.25	5467
S	Control	20-30cm	2	4532	1654.63	3362	3947	4532	5117	5702
S	Control	2-10cm	2	4535	2211.83	2971	3753	4535	5317	6099
S	Control	50-60cm	2	5270.5	621.5469	4831	5050.75	5270.5	5490.25	5710
S	Control	70-80cm	4	7417.25	3274.284	5119	5234.5	6210	8392.75	12130
Sn	Control	10-20cm	2	6.05	4.313351	3	4.525	6.05	7.575	9.1
Sn	Control	20-30cm	2	4.65	2.333452	3	3.825	4.65	5.475	6.3
Sn	Control	2-10cm	2	9.85	9.687363	3	6.425	9.85	13.275	16.7
Sn	Control	50-60cm	2	3	0	3	3	3	3	3
Sn	Control	70-80cm	4	9.95	6.594189	3	7.35	8.95	11.55	18.9
Sr	Control	10-20cm	2	40.75	2.05061	39.3	40.025	40.75	41.475	42.2
Sr	Control	20-30cm	2	40.5	1.697056	39.3	39.9	40.5	41.1	41.7
Sr	Control	2-10cm	2	43.6	4.384062	40.5	42.05	43.6	45.15	46.7
Sr	Control	50-60cm	2	48.35	0.070711	48.3	48.325	48.35	48.375	48.4
Sr	Control	70-80cm	4	56.275	16.34653	43.5	45.825	51	61.45	79.6
Th	Control	10-20cm	2	11.2	2.404163	9.5	10.35	11.2	12.05	12.9
Th	Control	20-30cm	2	8	0.707107	7.5	7.75	8	8.25	8.5
Th	Control	2-10cm	2	8.75	0.212132	8.6	8.675	8.75	8.825	8.9
Th	Control	50-60cm	2	8.4	2.404163	6.7	7.55	8.4	9.25	10.1
Th	Control	70-80cm	4	10.525	3.314991	6.7	8.95	10.35	11.925	14.7
U	Control	10-20cm	2	8.45	8.273149	2.6	5.525	8.45	11.375	14.3
U	Control	20-30cm	2	17.7	14.84924	7.2	12.45	17.7	22.95	28.2
U	Control	2-10cm	2	8.4	0.141421	8.3	8.35	8.4	8.45	8.5
U	Control	50-60cm	2	9.25	10.11163	2.1	5.675	9.25	12.825	16.4
U	Control	70-80cm	4	62.175	96.29023	9.3	13.125	16.45	65.5	206.5
Zn	Control	10-20cm	2	65.2	11.87939	56.8	61	65.2	69.4	73.6
Zn	Control	20-30cm	2	68.95	25.10229	51.2	60.075	68.95	77.825	86.7
Zn	Control	2-10cm	2	72.9	14.84924	62.4	67.65	72.9	78.15	83.4
Zn	Control	50-60cm	2	120.05	82.37794	61.8	90.925	120.05	149.175	178.3
Zn	Control	70-80cm	4	130.7	88.99899	67.3	75.175	97.65	153.175	260.2

Ca	Sample	10-20cm	4	4839.75	473.0316	4441	4453.75	4756	5142	5406
Ca	Sample	20-30cm	4	5239.5	719.235	4491	4863	5132.5	5509	6202
Ca	Sample	2-10cm	4	5955.25	1502.133	4552	4828	5740	6867.25	7789
Ca	Sample	50-60cm	4	4000.5	443.5272	3710	3761.75	3816	4054.75	4660
Ca	Sample	70-80cm	7	4972.286	528.6463	4059	4717.5	5070	5287	5668
Ca	Sample	Depth	1	8296	*NA*	8296	8296	8296	8296	8296
Cl	Sample	10-20cm	4	344.75	75.25541	265.7	309.95	333.45	368.25	446.4
Cl	Sample	20-30cm	4	307.375	172.5385	141	224.325	269.95	353	548.6
Cl	Sample	2-10cm	4	289.275	172.5457	88.4	179.525	299.05	408.8	470.6
Cl	Sample	50-60cm	4	101.55	37.75266	62.9	78.35	96.4	119.6	150.5
Cl	Sample	70-80cm	8	182.8	101.0659	82.5	112.075	155.05	226.9	384.3
Cu	Sample	10-20cm	4	81.3	12.74755	64.2	77.625	83	86.675	95
Cu	Sample	20-30cm	4	151.1	68.3632	87.7	100.6	140.15	190.65	236.4
Cu	Sample	2-10cm	4	86.025	14.48594	70.8	75.375	86.05	96.7	101.2
Cu	Sample	50-60cm	4	88.55	20.63371	68.4	72.675	87.15	103.025	111.5
Fe	Sample	10-20cm	4	37707.5	2165.939	35300	36830	37485	38362.5	40560
Fe	Sample	20-30cm	4	45555	6712.578	38940	40230	45595	50920	52090
Fe	Sample	2-10cm	4	39645	2544.229	37500	37612.5	39150	41182.5	42780
Fe	Sample	50-60cm	4	36820	4598.601	32010	33847.5	36370	39342.5	42530
Fe	Sample	70-80cm	8	39745	3432.508	34530	37597.5	39700	41720	45340
K	Sample	10-20cm	4	14752.5	524.3011	14010	14572.5	14920	15100	15160
K	Sample	20-30cm	4	18377.5	5009.414	12990	14812.5	18405	21970	23710
K	Sample	2-10cm	4	15282.5	1996.52	12990	14220	15200	16262.5	17740
K	Sample	50-60cm	4	13492.5	1727.337	12180	12180	12985	14297.5	15820
K	Sample	70-80cm	8	15943.75	2684.984	12610	14857.5	15300	16375	21750
Mg	Sample	10-20cm	4	18997.5	937.4922	18210	18435	18725	19287.5	20330
Mg	Sample	20-30cm	4	20207.5	4656.081	15610	17335	19420	22292.5	26380
Mg	Sample	2-10cm	4	20207.5	2204.788	17320	19622.5	20410	20995	22690
Mg	Sample	50-60cm	4	15565	2281.001	13840	13967.5	14830	16427.5	18760
Mg	Sample	70-80cm	8	19110	2526.353	14110	18315	19580	21022.5	21640
Mn	Sample	10-20cm	4	629.525	218.332	430.5	512.85	574.9	691.575	937.8
Mn	Sample	20-30cm	4	1132.95	457.1656	524.8	912.7	1238.5	1458.75	1530
Mn	Sample	2-10cm	4	639.4	190.6492	465.2	504.65	602.35	737.1	887.7
Mn	Sample	50-60cm	4	463.3	102.7851	383.3	415.025	427.85	476.125	614.2
Mn	Sample	70-80cm	8	622.575	323.7749	426.4	472.9	517.6	565.95	1404
Na	Sample	0-2cm	4	27255	1047.839	25920	26925	27310	27640	28480

Na	Sample	10-20cm	4	21445	3764.027	18960	19252.5	19905	22097.5	27010
Na	Sample	20-30cm	4	22662.5	5481.024	18880	19375	20530	23817.5	30710
Na	Sample	2-10cm	4	23622.5	5104.484	17860	20057.5	24345	27910	27940
Na	Sample	50-60cm	4	28662.5	829.8343	27510	28492.5	28825	28995	29490
Na	Sample	70-80cm	4	29285	7341.955	20280	25860	29475	32900	37910
P	Sample	10-20cm	4	438.775	44.64739	383.6	412.7	444.8	470.875	481.9
P	Sample	20-30cm	4	420.925	30.6167	396.8	399.5	411.75	433.175	463.4
P	Sample	2-10cm	4	462.9	23.76917	427.4	460.85	473.4	475.45	477.4
P	Sample	50-60cm	4	436.675	73.94527	360.2	396.65	425.55	465.575	535.4
P	Sample	70-80cm	8	528.7625	98.59791	380.2	481.45	533.15	576.675	674.7
Pb	Sample	10-20cm	4	104.05	4.743065	99.3	101.025	103.35	106.375	110.2
Pb	Sample	20-30cm	4	116.35	21.88645	94	100.9	114.55	130	142.3
Pb	Sample	2-10cm	4	116	5.974948	108.2	113.375	116.75	119.375	122.3
Pb	Sample	2-10cm	4	116	5.974948	108.2	113.375	116.75	119.375	122.3
Pb	Sample	50-60cm	4	112.275	5.536169	107.1	108.225	111.4	115.45	119.2
Pb	Sample	70-80cm	8	110.375	13.7425	85	107.75	109.15	114.45	134.7
Rb	Sample	10-20cm	4	73.05	7.216878	63.7	69.625	74	77.425	80.5
Rb	Sample	20-30cm	4	102.8	25.63292	75.5	83.75	104.45	123.5	126.8
Rb	Sample	2-10cm	4	80.85	6.100546	75	77.55	79.55	82.85	89.3
Rb	Sample	50-60cm	4	69.4	10.30631	60.4	60.7	68.45	77.15	80.3
Rb	Sample	70-80cm	8	82.625	13.54714	65.3	74.375	79.55	88.425	109.2
S	Sample	10-20cm	4	3532.75	442.4345	3175	3334	3388.5	3587.25	4179
S	Sample	20-30cm	4	3409.5	994.3901	2554	2611	3238	4036.5	4608
S	Sample	2-10cm	4	3698.75	849.1079	2437	3625	4038	4111.75	4282
S	Sample	50-60cm	4	3122.5	831.9986	2274	2577	3022.5	3568	4171
S	Sample	70-80cm	8	3926.25	1139.151	2516	3438.25	3833	3978.75	6470
Sn	Sample	10-20cm	4	13.7	7.448937	3	11.475	16.25	18.475	19.3
Sn	Sample	20-30cm	4	11.75	10.7109	3	3.075	9.5	18.175	25
Sn	Sample	2-10cm	4	3.55	1.1	3	3	3	3.55	5.2
Sn	Sample	50-60cm	4	7.1	8.13347	3	3	3.05	7.15	19.3
Sn	Sample	70-80cm	8	7.9375	6.805867	3	3	6.05	9.725	22.7
Sr	Sample	10-20cm	4	52.175	8.15981	45.9	47.7	49.35	53.825	64.1
Sr	Sample	20-30cm	4	58.775	10.50409	46	54.1	58.85	63.525	71.4
Sr	Sample	2-10cm	4	51.35	1.859211	48.6	51.15	52.05	52.25	52.7
Sr	Sample	50-60cm	4	46.2	3.273123	42.8	44.525	45.7	47.375	50.6

Sr	Sample	70-80cm	8	57.5	8.251926	46.8	51.8	56.65	61.35	72.5
Th	Sample	10-20cm	4	10.15	1.078579	9.2	9.65	9.85	10.35	11.7
Th	Sample	20-30cm	4	9.8	1.428286	8.7	9.15	9.3	9.95	11.9
Th	Sample	2-10cm	4	9.525	0.694622	8.8	9.025	9.5	10	10.3
Th	Sample	50-60cm	4	9.9	1.71075	7.6	9.325	10.15	10.725	11.7
Th	Sample	70-80cm	8	9.0375	1.023911	7.4	8.55	9.25	9.7	10.4
U	Sample	10-20cm	4	29.95	18.34584	16.2	21.15	23.3	32.1	57
U	Sample	20-30cm	4	113.05	123.1726	30.6	45.15	62.95	130.85	295.7
U	Sample	2-10cm	4	44.2	22.93309	21.7	26.725	42.55	60.025	70
U	Sample	50-60cm	4	24.55	6.219593	16.2	22.425	25.45	27.575	31.1
U	Sample	70-80cm	8	56.4875	28.41038	21.8	27.775	64	76.05	90
Zn	Sample	10-20cm	4	198.825	132.6096	86.8	132.55	158.95	225.225	390.6
Zn	Sample	20-30cm	4	542.325	320.2827	156.7	395.2	541.4	688.525	929.8
Zn	Sample	2-10cm	4	210.625	118.7248	106.6	119.875	187.9	278.65	360.1
Zn	Sample	50-60cm	4	122.475	40.11296	92.2	95.5	109.15	136.125	179.4
Zn	Sample	70-80cm	8	248.8125	166.2356	133.6	157.15	183.5	257.675	635

Table 30: Summary statistics for elemental concentration in tissue samples from trees harvested from the Mponeng tailings facility

Element	Tissue	n	mean	sd	min	Q1	median	Q3	max
Ca	Branch Bark	8	10726.88	2182.284	8933	9211.75	9714.5	11822.5	15200
Ca	Branch Vascular	3	17950	3585.847	13810	16885	19960	20020	20080
Ca	Cortex	4	27495	1248.372	26450	26802.5	27120	27812.5	29290
Ca	Leaves	4	20062.5	193.1105	19890	19920	20025	20167.5	20310
Ca	Micro twigs	8	11407.5	544.7608	10850	11055	11155	11720	12360
Ca	Root Epidermis	2	6926.5	190.2117	6792	6859.25	6926.5	6993.75	7061
Ca	Root Vascular	5	23904	2053.042	22190	22640	22890	24610	27190
Ca	Roots Fine	2	16270	127.2792	16180	16225	16270	16315	16360
Ca	Twig Bark	8	11302.5	420.1275	10760	11030	11305	11552.5	12000
Ca	Twigs Vascular	4	13150	1672.882	10920	12510	13390	14030	14900
Cl	Branch Bark	8	5904.125	2056.506	1591	5819.25	6344.5	6730.75	8053
Cl	Branch Vascular	3	1659	543.2302	1196	1360	1524	1890.5	2257
Cl	Cortex	4	4979.75	475.4958	4522	4783	4874.5	5071.25	5648
Cl	Leaves	4	12350	255.2123	12100	12145	12365	12570	12570
Cl	Micro twigs	8	4934.125	246.3931	4576	4722.25	4991	5145.25	5191
Cl	Root Epidermis	2	3799	55.15433	3760	3779.5	3799	3818.5	3838
Cl	Root Vascular	5	3210.6	950.5105	2187	2338	3207	4155	4166
Cl	Roots Fine	2	4530	8.485281	4524	4527	4530	4533	4536

Cl	Twig Bark	8	6039.375	1092.091	4489	5545.25	6111.5	6687.75	7379
Cl	Twigs Vascular	4	2481.5	447.3824	1979	2187.5	2486.5	2780.5	2974
Cu	Branch Bark	8	22.925	10.14731	13.9	15.125	17.15	34.95	35.3
Cu	Branch Vascular	3	15.46667	0.550757	15.1	15.15	15.2	15.65	16.1
Cu	Cortex	4	12.4	2.892519	9.5	10.775	11.9	13.525	16.3
Cu	Leaves	4	46.175	5.898799	41.1	41.175	45.55	50.55	52.5
Cu	Micro twigs	8	31.9875	5.193798	27.9	28.4	29.3	34.35	40.2
Cu	Root Epidermis	2	531.8	9.33381	525.2	528.5	531.8	535.1	538.4
Cu	Root Vascular	5	40.08	43.53708	7	8.5	9.4	86.3	89.2
Cu	Roots Fine	2	180.55	5.868986	176.4	178.475	180.55	182.625	184.7
Cu	Twig Bark	8	25.75	2.110518	23.2	24.125	25.9	26.85	29.5
Cu	Twigs Vascular	4	21.225	2.165448	18.9	19.65	21.3	22.875	23.4
Fe	Branch Bark	8	1963.213	1707.784	163.6	745.325	1031.5	3922.5	4085
Fe	Branch Vascular	3	119.8	35.05039	97.5	99.6	101.7	130.95	160.2
Fe	Cortex	4	391.95	249.1672	166.4	254.15	329.15	466.95	743.1
Fe	Leaves	4	855.15	24.48135	828.1	837.925	856.45	873.675	879.6
Fe	Micro twigs	8	798.475	264.4431	505.1	672.475	730.05	879.175	1224
Fe	Root Epidermis	2	1908	42.42641	1878	1893	1908	1923	1938
Fe	Root Vascular	5	436.64	301.0006	89.6	190.7	530.5	531.1	841.3
Fe	Roots Fine	2	718.7	18.80904	705.4	712.05	718.7	725.35	732
Fe	Twig Bark	8	763.6	112.9552	626.8	673.575	750.35	847.85	908
Fe	Twigs Vascular	4	239.2	24.71774	217.1	218.15	239.45	260.5	260.8
K	Branch Bark	8	7429.5	923.0004	6152	6524.75	7660	8095.5	8615
K	Branch Vascular	3	6245.667	945.8654	5431	5727	6023	6653	7283
K	Cortex	4	9016.5	305.0885	8738	8780.75	8972	9207.75	9384
K	Leaves	4	9861	646.3549	9262	9322	9876	10415	10430
K	Micro twigs	8	8476.375	690.0925	7645	7993	8405	8780.75	9523
K	Root Epidermis	2	7639	210.7178	7490	7564.5	7639	7713.5	7788
K	Root Vascular	5	6620	2306.489	4507	5130	5205	9095	9163
K	Roots Fine	2	11850	183.8478	11720	11785	11850	11915	11980
K	Twig Bark	8	9258.875	597.3284	8439	8856	9216.5	9607.25	10190
K	Twigs Vascular	4	6807	655.6127	5898	6555	6978	7230	7374
Mg	Branch Bark	8	10887.75	3378.502	2582	11540	12055	12320	12670
Mg	Branch Vascular	3	3030	486.6046	2530	2794	3058	3280	3502
Mg	Cortex	4	8314.5	375.5587	8093	8105.75	8145	8353.75	8875
Mg	Leaves	4	17087.5	2879.703	14500	14642.5	17100	19545	19650
Mg	Micro twigs	8	9439.875	1660.343	7674	8437	9077.5	10002	12230
Mg	Root Epidermis	2	9063.5	111.0158	8985	9024.25	9063.5	9102.75	9142

Mg	Root Vascular	5	4502.6	1433.547	2972	3302	4273	5974	5992
Mg	Roots Fine	2	7335.5	28.99138	7315	7325.25	7335.5	7345.75	7356
Mg	Twig Bark	8	12483.75	424.6322	11880	12297.5	12485	12630	13270
Mg	Twigs Vascular	4	4154	785.499	2993	4045.25	4452	4560.75	4719
Mn	Branch Bark	8	235.125	42.31642	166.9	196.95	254.4	266.25	279.1
Mn	Branch Vascular	3	161.1333	9.720768	151.8	156.1	160.4	165.8	171.2
Mn	Cortex	4	259.75	34.98099	210.1	248.125	270.7	282.325	287.5
Mn	Leaves	4	1500.75	298.7969	1240	1243	1500	1757.75	1763
Mn	Micro twigs	8	350.0875	82.75586	248.4	308.125	338.85	384.975	476
Mn	Root Epidermis	2	487.05	10.39447	479.7	483.375	487.05	490.725	494.4
Mn	Root Vascular	5	227.9	86.34333	134	172.7	193.8	317	322
Mn	Roots Fine	2	673.1	6.081118	668.8	670.95	673.1	675.25	677.4
Mn	Twig Bark	8	281.0125	48.36541	221.9	240.15	279.35	318.075	341.8
Mn	Twigs Vascular	4	180.275	16.72251	162.5	168.95	179.35	190.675	199.9
Na	Branch Bark	8	10003.75	1465.478	7080	9385	10555	11062.5	11290
Na	Branch Vascular	3	7143.333	488.3987	6750	6870	6990	7340	7690
Na	Cortex	4	11155	347.8026	10790	10895	11165	11425	11500
Na	Leaves	4	20852.5	442.5965	20470	20635	20725	20942.5	21490
Na	Micro twigs	8	11080	846.7417	10290	10430	10775	11537.5	12550
Na	Root Epidermis	2	9725	360.6245	9470	9597.5	9725	9852.5	9980
Na	Root Vascular	5	8876	1503.323	6890	8010	8810	10130	10540
Na	Roots Fine	2	11500	127.2792	11410	11455	11500	11545	11590
Na	Twig Bark	8	10711.25	474.0234	10160	10330	10795	10880	11600
Na	Twigs Vascular	4	7962.5	518.4834	7360	7615	8040	8387.5	8410
P	Branch Bark	8	565.5625	48.19034	514.1	527.5	560.35	585.2	649.1
P	Branch Vascular	3	482.5667	22.28011	462.6	470.55	478.5	492.55	506.6
P	Cortex	4	491.775	38.94581	439.6	475.9	498.3	514.175	530.9
P	Leaves	4	859.025	26.5623	822.7	848.125	865.25	876.15	882.9
P	Micro twigs	8	720.95	53.50348	640.5	693.225	716.85	751.5	793.3
P	Root Epidermis	2	412.4	11.73797	404.1	408.25	412.4	416.55	420.7
P	Root Vascular	5	466.68	59.18008	404.7	409.7	468.1	523.1	527.8
P	Roots Fine	2	674.4	3.11127	672.2	673.3	674.4	675.5	676.6
P	Twig Bark	8	721.55	45.61569	657.5	689.05	724.95	763.725	766.3
P	Twigs Vascular	4	548.825	35.95176	514.1	521.45	545.45	572.825	590.3
Pb	Branch Bark	8	4.6125	3.430717	1	2.35	2.6	8.375	9
Pb	Branch Vascular	3	1.666667	0.493288	1.1	1.5	1.9	1.95	2
Pb	Cortex	4	2.45	0.842615	1.5	1.875	2.5	3.075	3.3
Pb	Leaves	4	4.375	0.629153	3.8	3.875	4.3	4.8	5.1

Pb	Micro twigs	8	4.5375	1.113473	3	3.875	4.55	5.225	6
Pb	Root Epidermis	2	29.65	0.070711	29.6	29.625	29.65	29.675	29.7
Pb	Root Vascular	5	4.68	3.12362	1.8	1.9	3.7	8	8
Pb	Roots Fine	2	19.1	0.424264	18.8	18.95	19.1	19.25	19.4
Pb	Twig Bark	8	3.675	0.839643	2.9	3.05	3.5	3.9	5.3
Pb	Twigs Vascular	4	2.85	0.58023	2.4	2.55	2.65	2.95	3.7

Table 31: Comparison of mean Gold concentration (mg/kg) between Control and Sample pits at 6 different depths

Depth	Control	Tree	p-value
0-2cm	0.47	0.2025	0.5754
2-10cm	0.1445	0.0745	0.3505
10-20cm	0.15	0.17775	0.7764
20-30cm	0.1695	0.09025	0.4556
50-60cm	0.17	0.13	0.1201
70-80cm	0.185	0.1325	0.5669

Table 32: Mean Au concentration per tissue type

Tissue	**Concentration (mg/kg)**
Bark (Branch)	0.003333333
Bark (twig)	0.003333333
Coarse Root (Cortex)	0.003333333
Coarse Root (Epidermis)	0.003333333
Coarse root (Vascular)	0.003333333
Leaves	0.009416667
Medium Root (Cortex)	0.003333333
Medium Root (Epidermis)	0.003333333
Medium Root (Vascular)	0.003333333
Roots (Fine)	0.003333333
Twigs (Micro)	0.003333333
Wood (Branch)	0.003333333
Wood (Twig)	0.003333333

Table 33: comparison between mean elemental concentrations (mg/kg) for Control and Sample pits

Element	Control	Sample	p-value
Ca	4295.25	5135.083	0.0163
Cl	87.2583	234.7583	<0.0001
Cu	99.0583	109.0333	0.5618
Fe	33993.3	39869.58	0.00145

K	12408.3	15632.08	0.00049
Mg	15028.3	18866.25	0.00044
Mn	388.825	685.0542	0.00038
Na	28320.8	25488.75	0.0251
P	565.458	469.4667	0.2085
Pb	100.633	111.5708	0.09849
Rb	60.9917	81.89167	0.00041
S	5495.92	3602.667	0.02632
Sr	47.625	53.91667	0.09938
Th	9.56667	9.575	0.9911
U	28.025	54.12083	0.2063
Zn	98.0833	261.9792	0.00141

Table 34: Summary statistics for elemental ratios derived from tissue elemental concentration (mg/kg) from trees harvested from the Mponeng tailings facility

Ratio	Tissue	n	mean	sd	min	Q1	median	Q3	max
Mg/Ca	Branch Bark	8	1.080529	0.386716	0.169868	1.05155	1.207953	1.284967	1.354087
Mg/Ca	Branch Vascular	3	0.170314	0.016082	0.152291	0.163871	0.175451	0.179326	0.183201
Mg/Ca	Cortex	4	0.302946	0.020987	0.279276	0.292458	0.301413	0.3119	0.329681
Mg/Ca	Leaves	4	0.850835	0.13621	0.72901	0.735062	0.848845	0.964618	0.97664
Mg/Ca	Micro twigs	8	0.824245	0.111539	0.691351	0.75149	0.811913	0.885753	0.989482
Mg/Ca	Root Epidermis	2	1.308799	0.019914	1.294718	1.301758	1.308799	1.315839	1.32288
Mg/Ca	Root Vascular	5	0.191759	0.071454	0.121442	0.129838	0.173629	0.264664	0.26922
Mg/Ca	Roots Fine	2	0.450867	0.001745	0.449633	0.45025	0.450867	0.451484	0.452101
Mg/Ca	Twig Bark	8	1.106606	0.070578	1.004167	1.058579	1.104862	1.16857	1.194419
Mg/Ca	Twigs Vascular	4	0.321208	0.080226	0.217831	0.281371	0.332218	0.372056	0.402564
Na/K	Branch Bark	8	1.359959	0.245078	1.112014	1.154763	1.307533	1.487551	1.7263
Na/K	Branch Vascular	3	1.1531	0.093713	1.055884	1.108217	1.160551	1.201708	1.242865
Na/K	Cortex	4	1.237909	0.046907	1.194666	1.217784	1.226162	1.246287	1.304646
Na/K	Leaves	4	2.122965	0.172641	1.966379	1.97937	2.112559	2.256153	2.300364
Na/K	Micro twigs	8	1.319106	0.189617	1.111583	1.195377	1.280506	1.401577	1.610626
Na/K	Root Epidermis	2	1.272906	0.012096	1.264353	1.268629	1.272906	1.277182	1.281459
Na/K	Root Vascular	5	1.409813	0.264749	1.113799	1.150278	1.528733	1.538905	1.717349
Na/K	Roots Fine	2	0.970664	0.0258	0.952421	0.961543	0.970664	0.979786	0.988908
Na/K	Twig Bark	8	1.160934	0.087751	1.018646	1.113332	1.170119	1.22032	1.286882
Na/K	Twigs Vascular	4	1.181651	0.176094	0.998101	1.10205	1.153841	1.233442	1.420821
S/Cl	Branch Bark	7	3.597462	0.73287	2.992673	3.002918	3.050448	4.318264	4.49675

S/Cl	Branch Vascular	1	6.517501	*NA*	6.517501	6.517501	6.517501	6.517501	6.517501
S/Cl	Cortex	4	7.063183	0.873511	5.917139	6.815527	7.146345	7.394001	8.042901
S/Cl	Leaves	4	2.138155	0.045663	2.09467	2.101233	2.136826	2.173747	2.184298
S/Cl	Micro twigs	8	4.019038	0.356839	3.565787	3.754339	4.059805	4.318626	4.388342
S/Cl	Root Epidermis	2	3.712954	0.018541	3.699844	3.706399	3.712954	3.719509	3.726064
S/Cl	Root Vascular	3	8.543426	3.247	6.565584	6.669734	6.773884	9.532347	12.29081
S/Cl	Roots Fine	2	4.168921	0.049954	4.133598	4.151259	4.168921	4.186583	4.204244
S/Cl	Twig Bark	8	4.449897	1.051456	3.454398	3.814387	4.138436	4.756918	6.101582
S/Cl	Twigs Vascular	4	6.456638	1.724039	4.421654	5.349707	6.639534	7.746465	8.125831

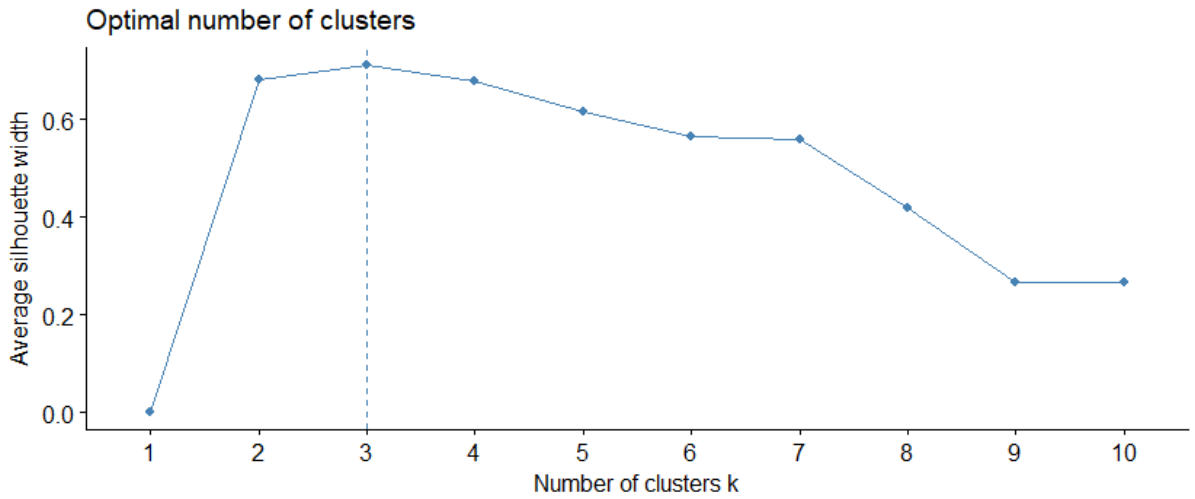

Figure 24: Optimal number of clusters for the elemental concentration dendrogram

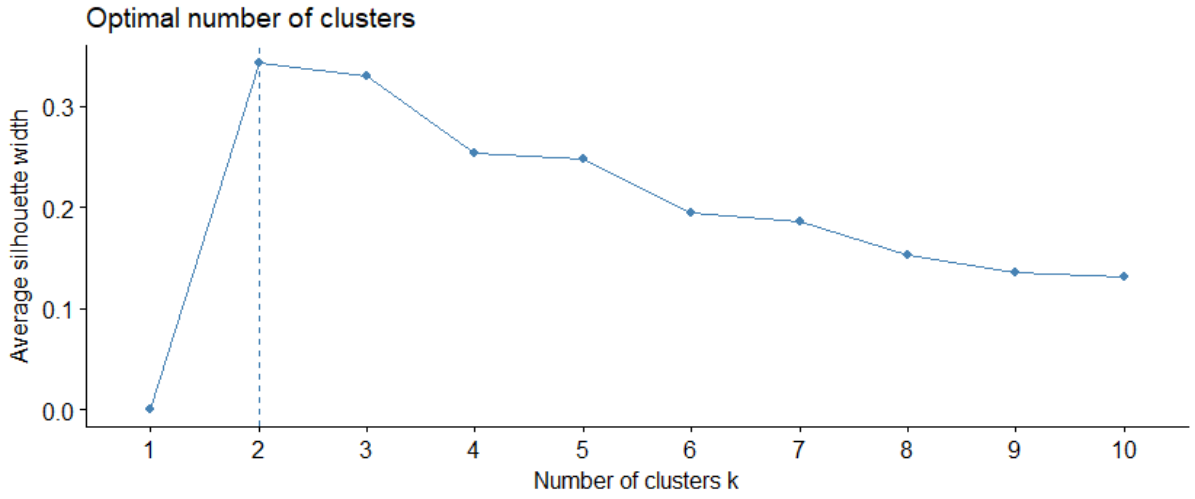

Figure 25: Optimal number of clusters for the elemental Translocation factor dendrogram